

University of Southampton Research Repository ePrints Soton

Copyright © and Moral Rights for this thesis are retained by the author and/or other copyright owners. A copy can be downloaded for personal non-commercial research or study, without prior permission or charge. This thesis cannot be reproduced or quoted extensively from without first obtaining permission in writing from the copyright holder/s. The content must not be changed in any way or sold commercially in any format or medium without the formal permission of the copyright holders.

When referring to this work, full bibliographic details including the author, title, awarding institution and date of the thesis must be given e.g.

AUTHOR (year of submission) "Full thesis title", University of Southampton, name of the University School or Department, PhD Thesis, pagination

UNIVERSITY OF SOUTHAMPTON

Faculty of Engineering, Science & Mathematics

School of Chemistry

Dipyrromethane Based Receptors for Anions

by

Sara Allasia

Doctor of Philosophy

October 2008

UNIVERSITY OF SOUTHAMPTON

ABSTRACT

FACULTY OF ENGINEERING, SCIENCE & MATHEMATICS

SCHOOL OF CHEMISTRY

Doctor of Philosophy

DIPYRROMETHANE BASED RECEPTORS FOR ANIONS

by Sara Allasia

This thesis is principally concerned with the synthesis of a range of dipyrromethane based receptors and their ability to bind anions, in particular carboxylates of amino acid derivatives.

Chapter I provides a general introduction to the field of Supramolecular Chemistry and its applications. In this chapter a series of receptors for anions are presented their properties discussed. A particular attention is given to the aromatic heterocycles based receptors and to enantioselective receptors.

Chapter II describes the synthesis of a series of acyclic receptors which are the results of subsequent modifications of a simple tweezer, based on a dipyrromethane unit coupled with two butyl amines, previously studied by the group.¹ The binding properties with a series of anions are presented and, for the chiral receptors, the binding properties with *N*-protected amino acids were investigated.

Chapter III describes the synthesis and the binding properties of a series of macrocycles obtained by modifications of the tweezer receptors. The binding properties of the macrocyclic receptors with a series of anions and amino acids are also presented.

To Mum and Dad

TABLE OF CONTENTS

PREFACE	IV
ACKNOWLEDGEMENTS	V
ABBREVIATIONS	VI
CHAPTER I	1
INTRODUCTION	1
1.1 Supramolecular chemistry	1
1.2 Molecular recognition	1
<i>1.2.1 Interactional complementarity</i>	2
<i>1.2.2 Steric complementarity and multiple interaction sites</i>	13
1.3 Applications of supramolecular chemistry	16
<i>1.3.1 Supramolecular reactivity and catalysis</i>	16
<i>1.3.2 Supramolecular sensors</i>	18
<i>1.3.3 Transport across membranes</i>	19
<i>1.3.4 Supramolecular Self-Assemblies and Molecular Machines</i>	21
<i>1.4.1 Amide based receptors</i>	24
<i>1.4.2 Urea and thiourea based receptor</i>	27
<i>1.4.2 Ammonium and guanidinium based receptors</i>	30
<i>1.4.3 Aromatic heterocycles as anion receptors</i>	33
<i>1.4.3.1 Pyrrole based receptors</i>	33
<i>1.4.3.2 Indole based receptors</i>	40
<i>1.4.3.3 Carbazole based receptors</i>	42
<i>1.4.3.4 Imidazole based receptor.</i>	44
1.5 Enantiomeric recognition	45
1.6 Aims of the project	50
CHAPTER II	55
ACYCLIC DIPYRROMETHANE BASED RECEPTORS	55
2.1 Synthesis of the dipyrromethane core	55
2.2 Overview of the synthesised receptors	58
2.4 Methods used to analyse the binding properties	67
<i>2.4.1 NMR Titrations</i>	68
<i>2.4.2 UV Titrations</i>	70
<i>2.4.3 Job Plot</i>	72

2.5 Binding properties of dipyrromethane tweezer receptors in DMSO-d₆	73
2.5.1 <i>Conclusions</i>	79
2.5.2 <i>Binding constants with dihydrogen phosphate in DMSO-5% H₂O</i>	80
2.6 Binding properties in CD₃CN	80
2.6.1 <i>Receptors 101, 102, 104 and 107</i>	80
2.6.2 <i>Receptors with polar functionalities</i>	82
a) <i>Hydroxyl vs phenyl ring</i>	82
b) <i>Amide vs Ester</i>	92
c) <i>Receptors with polar functionalities: acetate vs phosphate selectivity</i>	97
2.7 Tweezer receptors bearing substituents on the phenyl ring	101
2.7.1 <i>Anion-π interactions</i>	103
2.7.2 <i>Analysis of receptors bearing substituents on the phenyl ring in CD₃CN</i>	103
2.7.3 <i>Binding studies in DMSO-d₆ -0.5% H₂O</i>	107
2.8 Enantiomeric recognition	107
2.9 Conclusions	113
 CHAPTER III	 115
 MACROCYCLIC DIPYRROMETHANE BASED RECEPTORS	 115
3.1 Chiral macrocyclic dipyrromethane based receptors	115
3.2 Synthesis	115
3.3 Anion template directed macrocyclisation	117
3.3.1 <i>Sulphonamide based macrocycle</i>	117
3.3.2 <i>Dipyrromethane based macrocycle</i>	124
3.4 Dipyrromethane-based chiral macrocycles: binding properties	130
3.4.1 <i>Binding properties in CDCl₃</i>	130
3.4.2 <i>Binding properties in DMSO-d₆</i>	132
3.4 Enantiomeric recognition	136
3.5 Achiral macrocyclic dipyrromethane based receptors	141
3.6 Conclusions	149
3.8 General conclusions	150
 CHAPTER IV	 152
 EXPERIMENTAL	 152
4.1 General Experimental	152
4.2 Instrumentation	152

4.3 Experimental for NMR binding studies	153
4.4 Method used for obtaining binding constants	153
4.5 Synthesis in Chapter II	154
4.6 Synthesis in Chapter III	177
4.7 NMR titrations	189
4.8 UV titrations	240
4.9 NMR Job Plots	242
APPENDIX A	246
REFERENCES	248

Preface

The research contained within this thesis was carried out under the supervision of Professor J. D. Kilburn and Professor P. A. Gale at the University of Southampton between January 2005 and January 2008. No part of this thesis has previously been submitted to this or any other University.

Acknowledgements

In the first place I would like to thank my supervisors for the opportunity they gave me to undertake my PhD in an intellectually stimulant environment such as the School of Chemistry. In particular I would like to thank Professor J. D. Kilburn for his help and for the instructive problem sessions. I would like to thank Professor P. A. Gale for his supervision and for sharing his wide knowledge of Supramolecular Chemistry.

Thanks to Martin Grossel for his contagious enthusiasm and for marking my reports.

I would like to thank all members of the Kilburn group, past and present, particularly Jon Shepherd, Jon Powell, Allison, Luke, Jarya, Ola and Sally.

I wish also to thank all the members of the Gale group past and present, particularly Simon, Gareth, Jenny and Claudia.

A special thank to the Grossel group for being nice labmates for part of my PhD, particularly Georgie, Francesco and Andrew.

Thanks to the staff of the School of Chemistry: especially to Julie, John, Neil, Joan, Karl, Graham, Bev and Bevy.

I also would like to thank Marco, Eugen, Ilaria, Elena and all the others who made my extra-lab hours more pleasant.

I would like to thank my family and my friends from “home” for their help and constant support particularly in the difficult times, particularly to Giulia and Samanta.

And finally, I would like to thank Oscar, my husband, not only for his support, advice, and for goading me (sometimes a bit too much), but also for the nice evenings and weekends.

Abbreviations

Ac acetyl

AcOH acetic acid

Ala alanine

Asn asparagine

Boc *tert*-butoxycarbonyl

Bn benzyl

br broad

Bu butyl

BzO⁻ benzoate

CBS carboxylate binding site

CBPQT⁴⁺ cyclobis(paraquat-para-phenylene)

CDI 1,1'-carbonyldiimidazole

CFTR transmembrane conductance regulator

d doublet

DCM dichloromethane

DIPEA *N,N'*-diisopropylethylamine

DMAP 4-(*N,N'*-dimethylamino)pyridine

DMF *N,N'*-dimethylformamide

DMSO dimethylsulphoxide

DNA Deoxyribonucleic acid

DPPC dipalmitoylphosphatidylcholine

EA ethyl acetate

ee enantiomeric excess

EDC *N*-(3-dimethylaminopropyl)-*N'*-ethylcarbodiimide hydrochloride

EtOH ethanol

EYPC egg-yolk phosphatidylcholine

FT-IR Fourier transform infrared

G guest

H host

HOBt 1-hydroxybenzotriazole

HPLC high performance liquid chromatography
ITC isothermal titration calorimetry
Me methyl
MeOH methanol
NaHMDS Sodium bis(trimethylsilyl)amide
NEMS nanoelectromechanical systems
m multiplet
mp melting point
NMR nuclear magnetic resonance
NP naphthalene
Pd/C palladium on charcoal
PE petroleum ether
PFP pentafluorophenol
Ph Phenyl
Phe Phenylalanine
ppm parts per million
PPR prototypical palindromic [3] rotaxane
pTsOH *p*-toluenesulfonic acid
PyBOP benzotriazole-1-yl-oxy-tris-pyrrolidino-phosphoniumhexafluorophosphate
q quartet
quant. quantitative
quin quintet
s singlet
Ser serine
t triplet
TBA tetrabutylammonium
TFA trifluoroacetic acid
THF tetrahydrofuran
TLC thin layer chromatography
TMS tetramethyl silane
TTF tetrathiafulvalene

Trp tryptophan

Tricarballate propane-1,2,3-tricarboxylate

Trimesoate benzene-1,3,5-tricarboxylate

Tyr tyrosine

UV ultraviolet

Val valine

Chapter I

Introduction

1.1 Supramolecular chemistry

The discovery of crown ethers by Pedersen in the 1960s is generally agreed as the birth of supramolecular chemistry. This was the first time that a neutral synthetic molecule was shown to bind alkali metal ions.² Since this accidental discovery, due in large part to the curiosity of Pedersen, a new field of science has arisen to yield more complex systems and new applications. Supramolecular chemistry was defined by Lehn³ as “Chemistry beyond the molecule”. The main objective of this field of chemistry is to gain control over intermolecular bonds as molecular chemistry does over covalent bonds. As supramolecular chemistry has developed, it has organised concepts that were previously introduced. For example the idea of the *übermolecule* (literally supermolecule) was introduced by Wolf⁴ and “*Corpora non agunt nisi fixata*” by Paul Ehrlich,⁵ who stated that the molecules do not act if they are not bound. Biology and Nature in general, have been fruitful sources for the concepts and ideas of supramolecular chemistry, in particular the study of enzymatic reactions and intermolecular interactions among others. Enzymes, for example, not only contain a binding site, but also possess a reactive function which leads to a chemical transformation.

1.2 Molecular recognition

The concept of molecular recognition has been developed following the observation of enzymatic reactions. The enzyme binding site binds a ligand with high selectivity. This specificity is such that it was illustrated by Fischer with the “Lock and Key” principle in 1894.⁶ The substrate and the receptor, in order to achieve recognition, must have geometrical and interactional⁷ complementarity (figure 1).

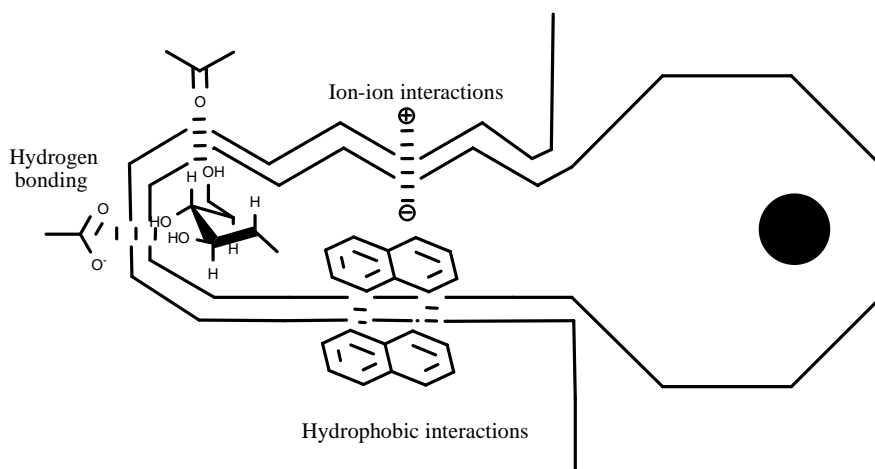


Figure 1 *Lock and Key principle.*

A substrate is selective for a certain receptor if their binding energy is much higher than the one generated by the interaction with any other putative guest. A series of principles can be followed in order to achieve recognition: ⁷

- interactional complementarity
- steric complementarity
- multiple interaction sites
- strong overall binding

By following these principles effective molecular receptors can be designed. A molecular receptor can be defined as an organic structure held together by covalent bonds capable of binding selectively substrates (ionic or molecular) by means of intermolecular interactions, leading to an assembly of two or more species, known as a supermolecule.

1.2.1 Interactional complementarity

The interactional complementarity can be achieved by using non covalent intermolecular interactions. The energy involved in these types of interactions varies from the 2 kJmol⁻¹ in dispersion forces to 250 kJ·mol⁻¹ for an ionic bond. In comparison the range of a typical single covalent bond is around 350 kJ·mol⁻¹ rising up to 942 kJ·mol⁻¹ for the very stable triple bond in N₂. Intermolecular forces can be divided into ion-ion, ion-dipole, dipole-dipole interactions, hydrogen bonding, cation- π , π - π stacking, Van-der-Waals forces and the hydrophobic effect.

Ion-ion interactions

The energy involved in ion-ion interactions ($100\text{--}350\text{ kJ}\cdot\text{mol}^{-1}$) is comparable to the strength of covalent bonding. The classical example of this kind of interaction is the cubic lattice of NaCl, where the cation Na^+ is able to organise six complementary atoms donors around itself in order to maximise non-covalent interactions.

Schmidtchen has used these interactions in the design of a macrotricyclic (1, figure 2) that binds halides in water.⁸

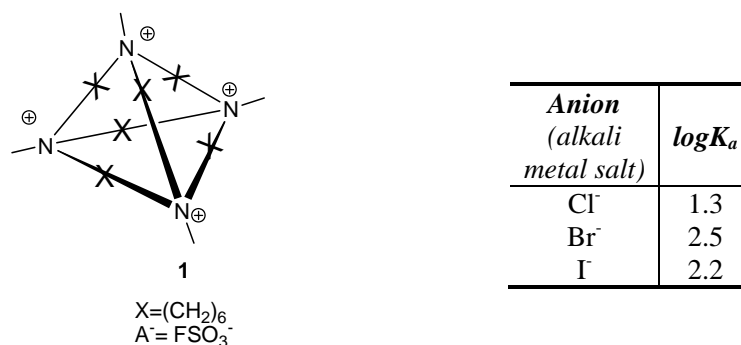


Figure 2 Binding constants of macrotricyclic 1 in H_2O .

Ion-dipole interactions

The energy of this interaction can be between $50\text{--}200\text{ kJ}\cdot\text{mol}^{-1}$ and describes the bonding of an ion and a polar molecule. A classical example is the hydration of sodium cations. The complex formed between crown-ether 2 (figure 3) and Na^+ , as picrate salt, is stabilised by ion-dipole interactions and has binding free energy of $\Delta G^\circ = -35.1\text{ kJ}\cdot\text{mol}^{-1}$.

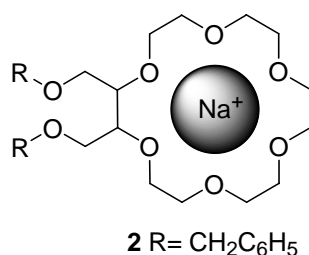


Figure 3 Complex formed between 2 and sodium.

Dipole-dipole interactions

This type of binding occurs when two dipoles are aligned; the energy involved in this interaction is between $5\text{--}50\text{ kJ}\cdot\text{mol}^{-1}$. There are two types of dipole-dipole interactions;

one is generated from matching a single pair of poles on adjacent molecules and the other one from oppositely aligning dipoles (figure 4).

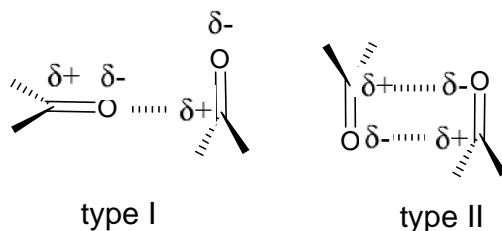


Figure 4 *Dipole-dipole interactions in carbonyls.*

Hydrogen bonding

Energetically this interaction is stronger than a dipole-dipole interaction. For neutral molecules it varies between 10 and 65 kJ·mol⁻¹ and when one of the components is charged it can be up to 190 kJmol⁻¹. This interaction is highly solvent dependent. The hydrogen bond can be visualised as a dative bond or as a purely electrostatic interaction. There are three types of hydrogen bond (Figure 5).⁹

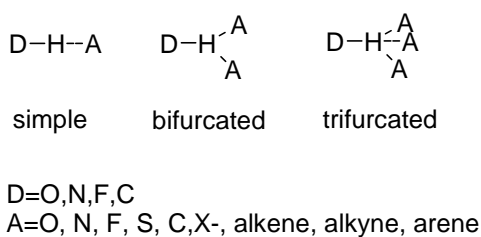


Figure 5 *Types of hydrogen bonds.*

Because of its high directionality it is a powerful tool in the design of receptors. The changes in the overall stability constant induced by the removal of a hydrogen bond has been investigated for biological systems in the duplex formation of DNA pairs.¹⁰ Hamilton has studied the role on the overall binding by adding or removing a hydrogen bond in synthetic molecules.¹¹ A receptor for barbiturates has been designed and its binding properties have been tested. The stability constant is very high ($K_a = 10^5 \text{ M}^{-1}$ in DCM) and it was measured by means of UV titration. In this complex there is high complementarity between the host and the guest and there are six hydrogen bonds (figure 6).

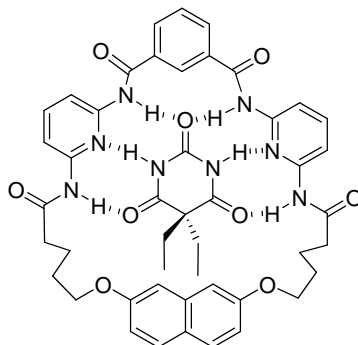


Figure 6 Complex formed by macrocycle **3** and the barbiturate.

Hamilton has completed the study by changing the hydrogen bonds' pattern. The stability constants of the complexes formed by macrocycle **3** and guests **a**, **b** and **c** have been measured by NMR titrations (figure 7).

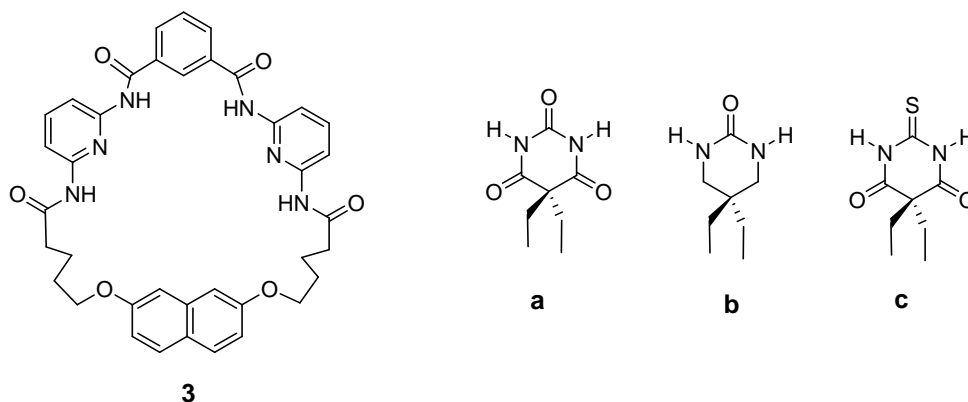


Figure 7 Series of guest chosen by Hamilton to prove the contribute of the hydrogen bonds in the overall binding.

The urea **b** lacks two of the six hydrogen bonding sites therefore the complex formed is much weaker ($K_a = 4 \cdot 10^2 \text{ M}^{-1}$ in CDCl_3). This comparison must be treated with caution because, by removing two carbonyl groups, the acidity of the NHs' is also modified and this can influence the strength of their hydrogen bonds. However, during this study, Hamilton and co-workers have quantified the contribution of this hydrogen bond as $7.54 \text{ kJ} \cdot \text{mol}^{-1}$. By changing the barbiturate **a** into the thiobarbiturate **c** a drop of the binding constant is observed ($K_a = 7.4 \cdot 10^2 \text{ M}^{-1}$ in CDCl_3). The sulphur is a weaker hydrogen bond acceptor than oxygen and its larger size inhibits the binding in the cavity.

Cation- π interactions

This interaction has an energy involved of 5-80 kJmol⁻¹ and it has a predominant electrostatic nature: it occurs when a positively charged cation is in proximity of a π -electron cloud (figure 8).

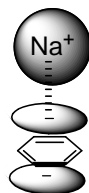


Figure 8 *Example of a cation- π interaction.*

This type of interaction normally is present between a metal cation and a calixarene, and a review has recently been published on this subject.¹² The nature of the cation π interaction in the calixarene has been verified by the crystal structure of the caesium-calixarene complex (figure 9) which was published in the early 1990s.¹³

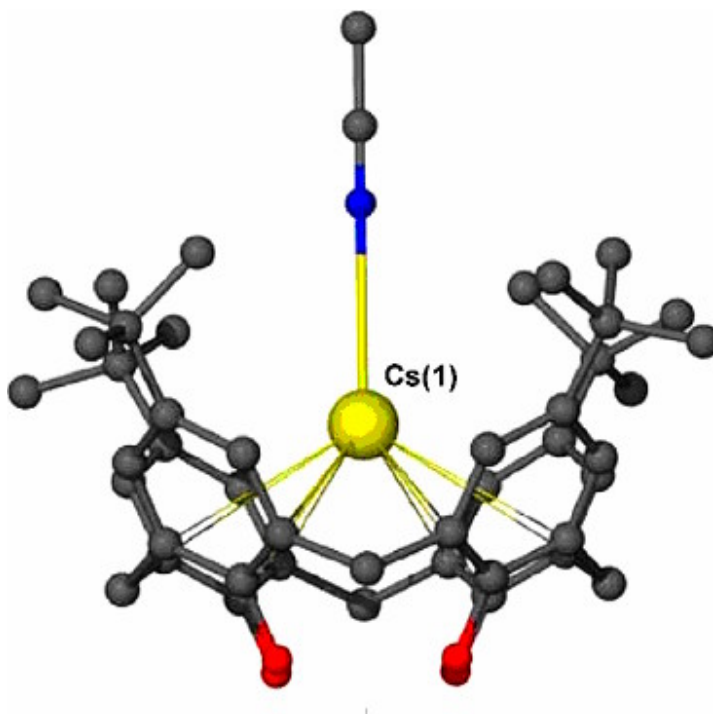


Figure 9 *Crystal structure of the complex Caesium-calixarene*

After the discovery of this interaction some researchers have tried to engineer a three-dimensional structure held by cation- π interactions. Gokel and co-workers have

synthesised a lariat ether with appended side arms that emulate the amino acid tryptophan (**4**, figure 10) and they have studied its binding properties with potassium iodide.¹⁴

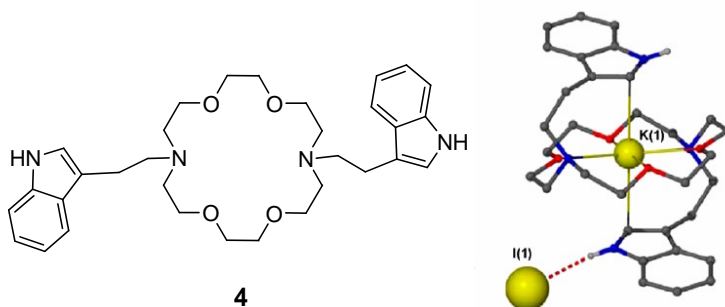


Figure 10 Receptor **4** and crystal structure of the complex between receptor **4** and KI.

The potassium is complexed by the crown ether and interacts with the indole moiety with a cation- π interaction. The structure was verified both by X-ray crystallography and by NMR titration in deuterated acetone at 25 °C. The conclusion was that the system assumes the same structure, both in solid state and in solution.

π - π interactions

Electrostatic interactions may occur between electron rich and electron poor aromatic rings. These interactions have predominantly two geometries, although there is a series of intermediate stages between the two. The face-to-face geometry is the result of an electrostatic interaction as observed in the structure of graphite. The edge-to-face geometry can be envisaged as a weak form of hydrogen bond between the slightly electron deficient hydrogen atom of one aromatic ring and the electron cloud of the other aromatic ring.

Hunter and Sanders¹⁵ consider the electrostatic components of this interaction as shown in figure 11 as a balance between the repulsive and attractive forces between the charges.

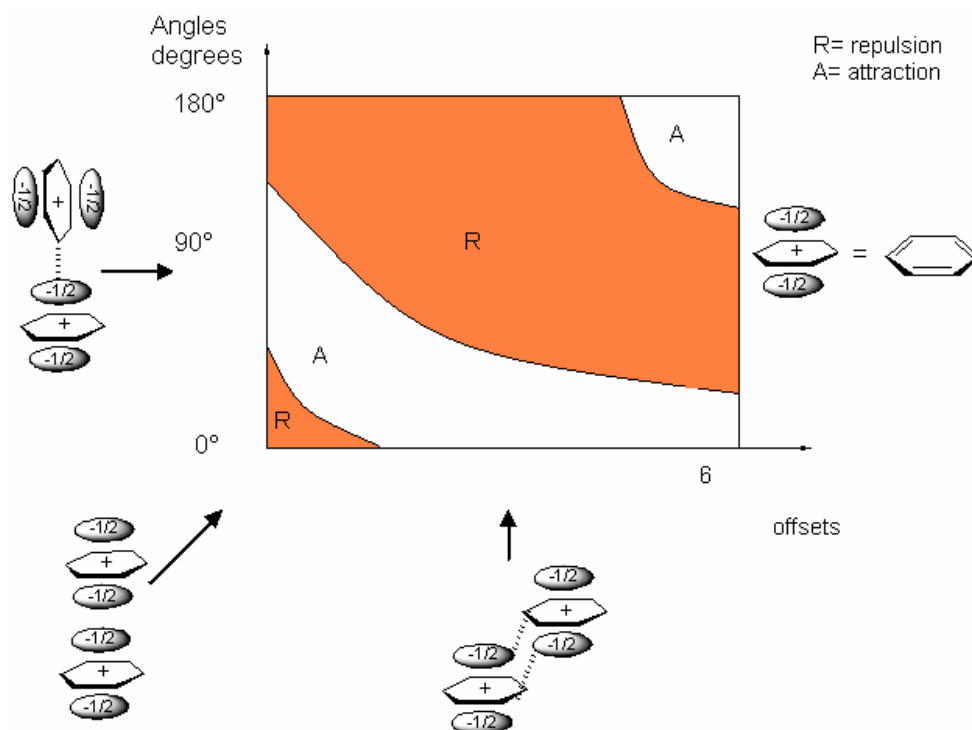


Figure 11 Chart developed by Sanders and Hunter to explain the interaction between two idealized phenyl rings as a function of orientation.

A study by Cozzi¹⁶ corroborates this interpretation. He has studied naphthalene groups substituted with two phenyl rings. Assuming that the position of the phenyl is perpendicular to the naphthalene, the rotational energy of the phenyl rings were measured by means of a high temperature NMR study. The energy was higher in presence of electron withdrawing substituents with the biggest effect was given by the nitro group. A higher rotational activation energy correlates to a higher stability of the face-to-face geometry (table 1).

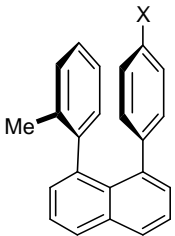
	X	ΔG^\ddagger
I	OMe	58.2
II	Me	69.4
III	H	61.5
IV	Cl	64.9
V	COOMe	70.8
VI	NO ₂	72.4

Table 1 Rotation energy of the phenyl rings. Transition's state ΔG measured in $\text{kJ}\cdot\text{mol}^{-1}$.
¹. The rotation energy has been measured by warming the compound in DMSO-*d*₆.

An analogous study on the edge-to-face geometry by Hunter¹⁷ gives experimental evidences of the purely electrostatic nature of this interaction. The polarisation of the π system by means of the substituents may give an energetic contribution between + $1\text{kJ}\cdot\text{mol}^{-1}$ (repulsive) and – $4.9\text{kJ}\cdot\text{mol}^{-1}$ (attractive). Any other effect had been removed in this experiment by a double-mutant approach. A weak interaction can be evaluated only as a perturbation of a stronger interaction. Their influence is generally evaluated by changing the structure of the complex's components. For example, to evaluate the contribution of the edge-to-face interaction in complex **5** (figure 12), a series of compounds have been analysed where the substituents X, X' and Y were electron donating (NMe₂) or electron withdrawing (NO₂).

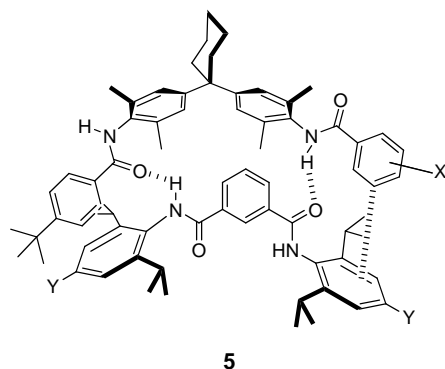


Figure 12 Complexes used by Hunter to evaluate the edge to face interaction.

Any change that affects an interaction may also affect the neighbouring one. A solution found to avoid this error is to apply thermodynamics cycles to structure variations (figure 13).¹⁸⁻²⁰ The choice of a rigid system avoided the problems related to a loss of conformation during the formation of the complex and in this particular system the aromatic rings involved in the interaction are in an edge-to-face conformation.²¹

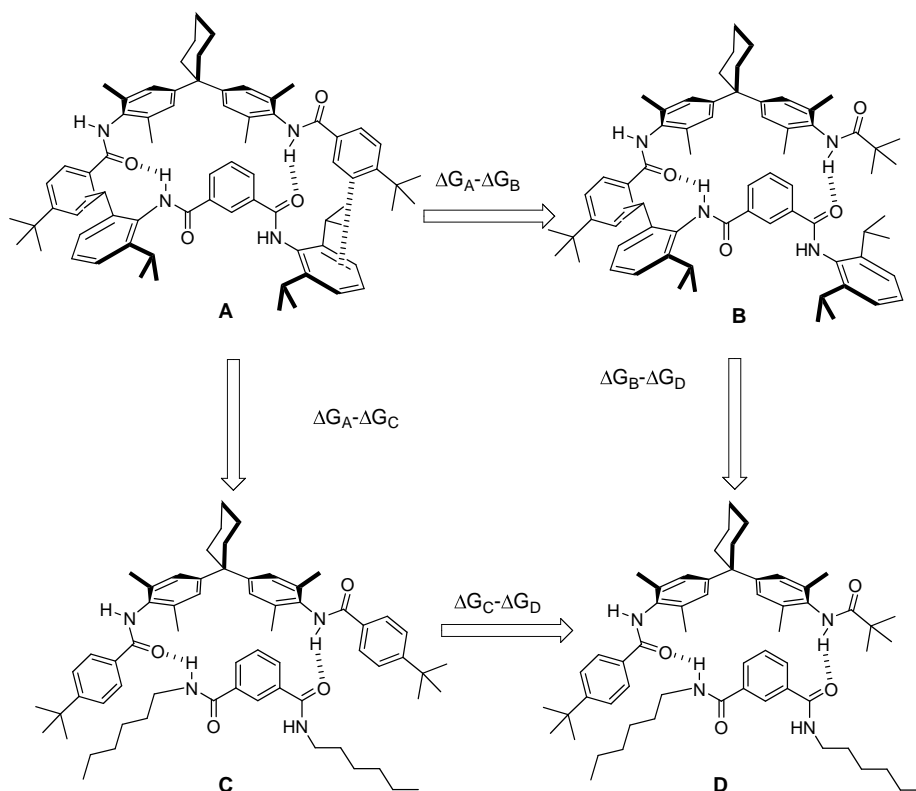


Figure 13 Double mutant cycle for determining the magnitude of the terminal aromatic interaction.

The complexes **A-D** (figure 13) have been synthesised and analysed. The energetic value of the π - π interaction can be evaluated by removing one of the interacting aryl groups as in **C** or **D**. However, by removing this portion of molecule (**A** \rightarrow **B**), also the H bond is affected and not only the aromatic interaction. The CH from the terminal aromatic ring is H-bonding to the amide's oxygen (figure 14).

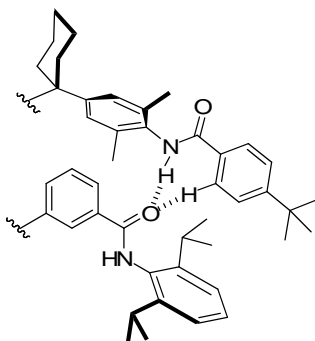


Figure 14 *Secondary H bonding in complex A.*

The loss of this secondary interaction can be evaluated by using the double mutant complex **D**. Thus comparing the complexes **C** and **D** the loss of the secondary interactions is evaluated. Applying the same principles a series of complexes have been evaluated and it was possible to quantify the attractive and the repulsive effect of the substituents.

Hydrophobic effect

The hydrophobic effect describes the affinity of apolar guests for hydrophobic binding sites in aqueous solution. The hydrophobic effect can be pictured as a release of water from the host cavity into the bulk solvent. The energetic components are enthalpic and entropic.

The enthalpic contribution may be favourable if the water has a much stronger interaction with other molecules of water than with the inner cavity of the receptor. The entropic factor is also favourable, as the molecules of water freed from the cavity of the receptor by the formation of the complex will have a greater degree of disorder when released and hence contribute for a more negative ΔG (figure 15).

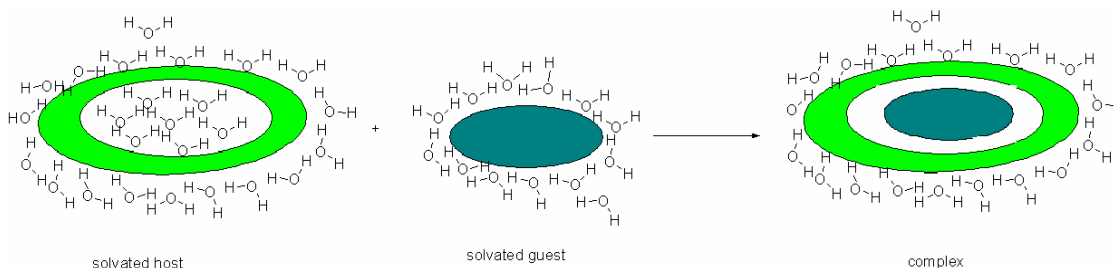


Figure 15 *Schematic representation of the hydrophobic effect.*

An example of hydrophobic effect is the complexation of pyrene by a cyclophane (complex **6**, figure 16).²² The stability constant of complex **6** has been evaluated by Diederich and co-workers in a series of solvents. The highest stability constant has been measured in water and a significant decrease was observed when the polarity of the solvent was decreased ($K_a = 6.0 \cdot 10^6 \text{ M}^{-1}$ in H_2O , $K_a = 4.4 \cdot 10^4 \text{ M}^{-1}$ in methanol and $K_a = 1.2 \cdot 10^1 \text{ M}^{-1}$ in benzene).

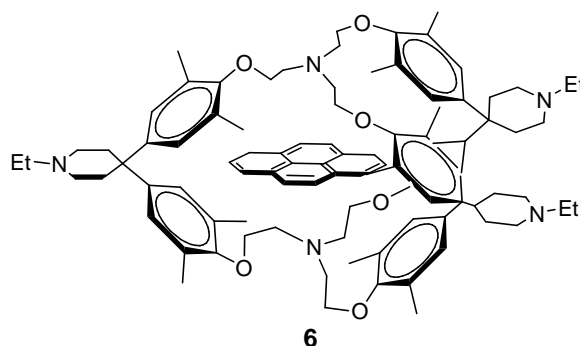


Figure 16 *Complex formed between cyclophane **6** and pyrene.*

Van der Waals forces

The strength of the van der Waals interactions is quantified by the Lennard-Jones potential. The Van der Waals interactions can be attractive or repulsive with the attractive potential generated by the polarisation of the electrons cloud by the presence of an adjacent nucleus giving an attractive interaction. The repulsive component arises from the overlap of electron clouds. Therefore the nature of this kind of interactions lies between the concept of interactional complementarity and steric complementarity.

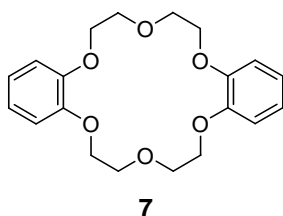
An example of van der Waals forces is the inclusion of small organic molecules in the calixarene cavity.²³

1.2.2 Steric complementarity and multiple interaction sites

Steric complementarity concerns shape and size and is exploited by the presence of convex and concave domains in the correct location in the host and the guest. The steric complementarity depends on a well defined three dimensional structure with correct positioning of the binding sites. There should be a complementarity of both size and shape.

Size

An example of how size is important in the binding process goes back to the early days of the supramolecular chemistry. As Pedersen reports in his Nobel Lecture² the 18-crown-6 unit is selective for potassium ions as the cation just fits into the hole. The radius of the cavity in the dibenzo-18-crown-6 **7** is between 2.6-3.2 Å and therefore the ion that is most efficiently extracted is potassium (25.2%) that has a radius of 2.66 Å. With sodium and caesium the percentage of extraction is much lower because the first is too small and the latter is too large (figure 17).



<i>Cation</i>	<i>Radius(Å)</i>	<i>% extraction (H₂O to DCM)</i>
Li ⁺	1.36	0
Na ⁺	1.94	1.6
K ⁺	2.66	25.2
Cs ⁺	3.34	5.8

Figure 17 Extraction from water into organic phase of cations with Dibenzo-18-crown-6 **7** (radius 2.6-3.2Å).

Preorganisation and Macrocyclic effect

A representation of the binding process is an equilibrium whose stability is expressed as its constant.

$$[\text{Host}] + [\text{Guest}] \leftrightarrow [\text{Complex}] \quad K = \frac{[\text{Complex}]}{[\text{Host}][\text{Guest}]}$$

The equilibrium constant reflects the free energy change which is a combination of enthalpy and entropy.

$$\Delta G = \Delta H - T\Delta S$$

Ignoring the effect of the solvent, the enthalpic factor involves predominantly the interactions between the host and the guest (e.g. hydrogen bond, electrostatic interaction) and the entropic factors are related to the conformational properties.

The association of two molecules is entropically disfavoured because it results in a loss of translational, rotational and conformational freedom. A series of preorganised (e.g. assuming a constricted conformation ready for binding) receptors has been designed in order to illustrate this. Among the receptors for alkali metal ions the comparison between the podand, the coronand and the spherand is a clear example of how the preorganisation plays a key role in enhancing the binding. The binding constant for the podand **8** is lower in comparison with the crown ether **2** and the spherand **10** (figure 18).

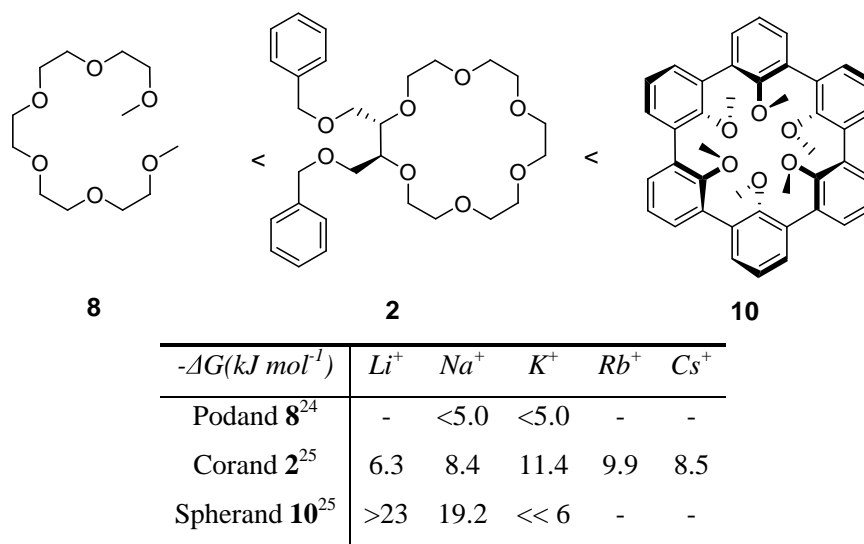


Figure 18 Binding free energies for alkali metal picrates in $CDCl_3$ saturated with D_2O at 298K.

The difference, in stability constants, between a macrocyclic and an acyclic receptor, bearing the same type of binding site, can rise up to four orders of magnitude.²⁶ The gain in stability results from favourable entropic and enthalpic changes upon binding. Macrocyclic molecules are generally less solvated as their surface is less accessible to molecules of solvent, so the enthalpy paid in the desolvation process is usually less than

in acyclic systems. From an entropic standpoint, macrocycles adopt less flexible conformations than acyclic receptors so they lose fewer degrees of freedom upon complexation. This concept was introduced for the first time in 1969 by Cabbiness and Margerum.²⁷ The difference between the corand and the spherand is also due to preorganisation. The crown ethers, for example, are not completely pre-organised: 18-crown-6, in solid state, adopts a crumpled conformation with the methylene groups pointing into the cavity. When it complexes a metal ion the conformation changes to gauche (figure19) with a loss of entropy.

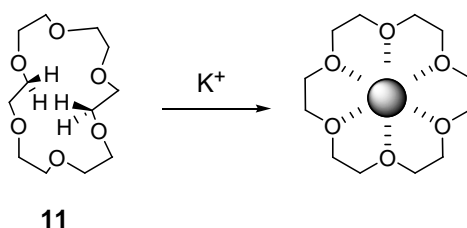


Figure 19 Conformations of crown ether **11** free (in the solid state) and in a complex with K^+ .

Thermodynamic and kinetic selectivity

The goal of host design is selectivity: that is the selective binding of one guest in the presence of other putative guests. In thermodynamic terms the selectivity is the ratio between the binding constant of two different guests with a particular host.

$$Selectivity = \frac{K_{guest1}}{K_{guest2}}$$

This kind of selectivity can be obtained by applying the principles of interactional and structural complementarity. Some binding process can be related to a subsequent transformation: for example in enzymatic catalysis, once the substrate is bound to the binding site, it becomes liable for chemical transformations and then it is released. In this case the binding site is selective not only for the substrate that is more strongly bound, but also for the substrate that reacts faster. This is also called kinetic selectivity. This concept is the basis for supramolecular catalysis, guest sensing and signalling.

1.3 Applications of supramolecular chemistry

The binding between two entities involves a molecular recognition process and, if, in addition to the binding site, the receptor contains reactive group, it may effect a chemical transformation and behave as a supramolecular reagent or catalyst. Synthetic receptors may also act as translocators of the bound units, as in the case of the transport through a membrane, where the substrate is bound, carried and finally released into the arrival solution. If in the substrate there is more than one binding site and the motion of the guest between the two binding sites can be generated by an external stimulus (e.g. light), molecular machines²⁸ can be generated. By applying the principles of supramolecular chemistry, a series of devices (e.g. sensors)²⁹ and materials (e.g. polymers)³⁰ have been designed.

1.3.1 Supramolecular reactivity and catalysis

A major source of inspiration for supramolecular catalysis is the activity of enzymes. The features of enzymatic catalysis are binding, reaction and release of a substrate specific for the enzyme. This is the objective for the chemists who design supramolecular catalysts. In order to be an effective catalyst the receptor should bind the substrate and help it to adopt a conformation close to the transition state and, in this manner, activate the reaction. Furthermore the receptor should release the product in order to react with another molecule of substrate. The supramolecular reagent or catalyst may activate the reaction with a template effect as shown in this example by Rebek³¹ where the reaction rate between the amide and the activated ester is accelerated of a factor of ten by the presence of the templating agent. The structure acts as shown in figure 20. The mechanism has been corroborated by measuring the rate of reactivity in presence of competitors for the binding site.

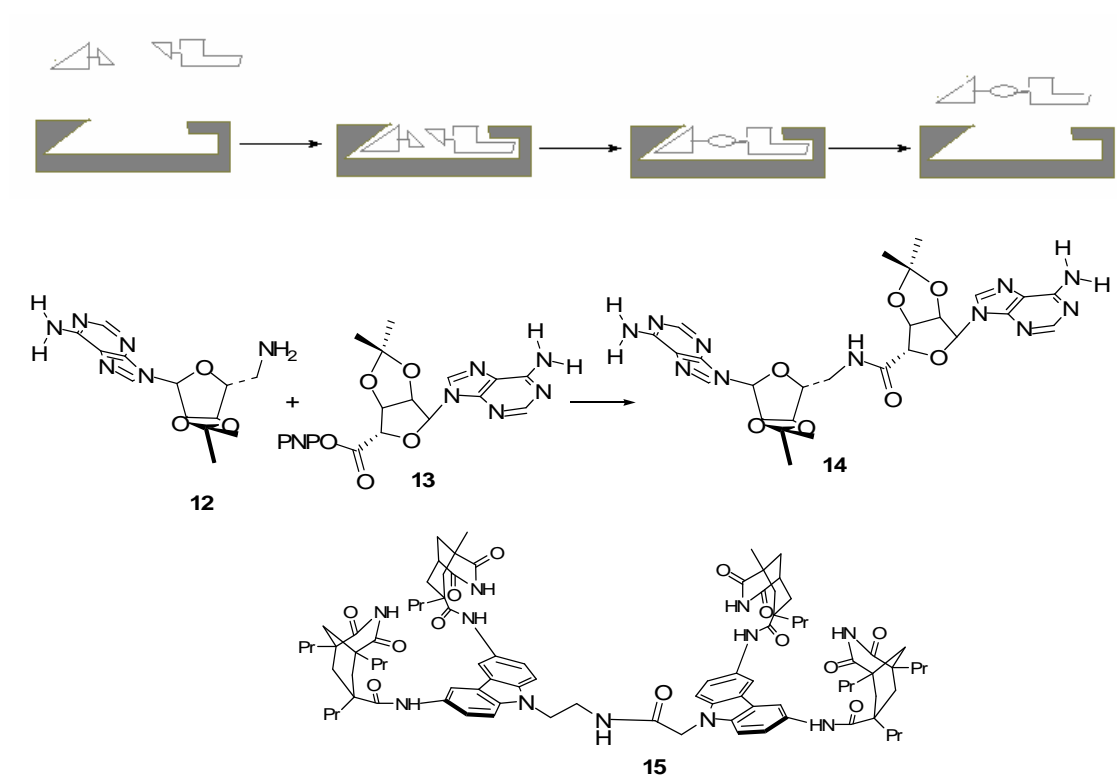
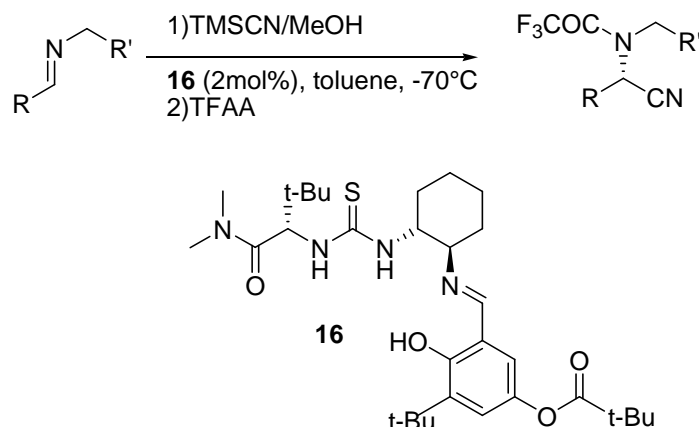


Figure 20 *Templating action of Rebeck's catalyst (15) to promote the reaction between 12 and 13.*

Hydrogen bonding acts not only as a structural motif in preorganising the reactants in the favourable conformation, but it can also activate an electrophile to undergo a nucleophilic attack.³² This property has been exploited in the design of small organocatalysts. Jacobsen and co-workers discovered that the Schiff base thiourea **16**, originally designed as a ligand for a Lewis acid, catalysed the Strecker reaction (scheme 1) with higher enantioselectivity without the presence of the metal.



Scheme 1 *Enantioselective Strecker reactions catalyzed by thiourea Schiff bases*

The catalyst activates the substrate via two hydrogen bonds between the acidic NH and the imine's lone pair: this activates the electrophile for the nucleophilic attack of the cyanide. The mechanism has been investigated by structural modifications, NMR, kinetic and computational studies.³³

1.3.2 Supramolecular sensors

A supramolecular sensor is a device where the complexation generates a change in the properties of the host (e.g. redox potential, fluorescence, phosphorescence). The sensor is composed of a binding site, a linker and an active unit.

In this example by Gale³⁴ the calixpyrrole unit is designed to bind an anion and this event is sensed by the variations of the fluorescence of the pendant anthracene unit (figure 21).

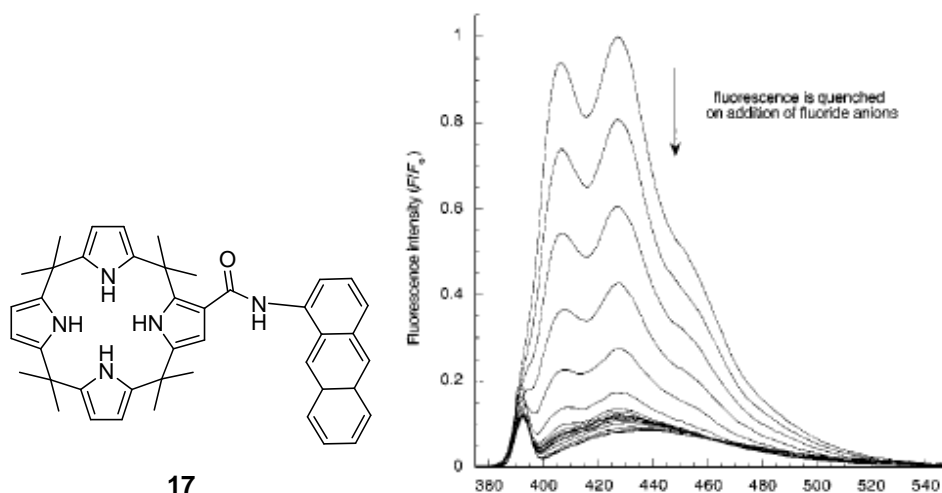


Figure 21 Fluorescence spectra of calixpyrrole **17** in DCM showing the changes upon addition increasing tetrabutylammonium fluoride.

When **17** interacts with anions as chloride, fluoride and dihydrogen phosphate (as tetrabutylammonium salts), the fluorescence of the anthracene is quenched. The data obtained with the fluorescence experiments (figure 21) are comparable to those obtained with H^1 -NMR titrations.

1.3.3 Transport across membranes

There is an increasing interest in the design of receptors able to transport ions through cell membranes. Many biological processes are regulated by the concentration of different species inside and outside the cell. For example the life of the cell depends on the correct concentration gradient of sodium and potassium ions across the lipid bilayer. Therefore an active pump is present in the cell membrane in order to maintain a suitable concentration of the cations inside and outside the cell.³⁵

The design and synthesis of molecules capable of transporting cations and anions across the membrane can be particularly useful for treating diseases caused by the presence or absence of certain ions in the cell. Transport can be performed by a carrier or by a transmembrane channel.

The transport by an active carrier is a stepwise process; the first event is the recognition of the guest by the carrier, then the transport through the membrane and finally the release of the guest. For the efficiency of the process the receptor should be selective for

a certain guest, but the association constant must be low enough to allow an efficient release, when the transport is performed.³⁶

In a recent study Gale, Quesada and Davis³⁷ showed how a well designed simple molecule can act as chloride transporter through a lipid bilayer membrane.

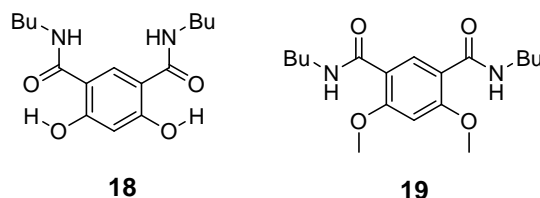
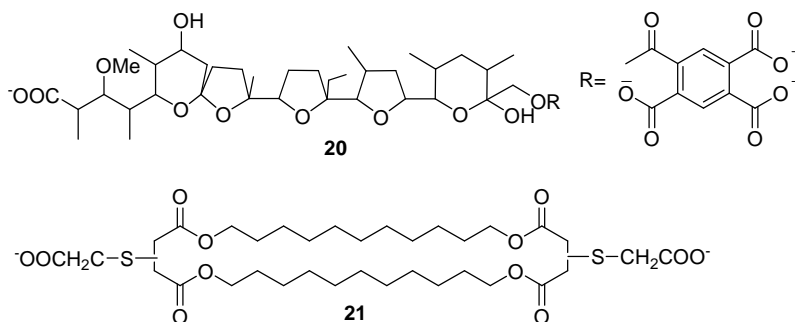


Figure 22 Transporters for chloride through membrane.

In **18** (figure 22) the phenolic groups, via intramolecular hydrogen bonds, preorganise the receptor in the *syn-syn* conformation, keeping the two amides in a convergent conformation. In the negative control compound **19** (figure 22), the methoxy groups receive intramolecular hydrogen bonding from the amide NHs locking the compound in the *anti-anti* conformation, impeding binding. The compounds were studied in solution, and as transmembrane carriers. Compound **18** showed a significant transport of chloride activity across EYPC (egg-yolk phosphatidylcholine) bilayer, while **19** showed neither binding ability nor activity with halides.

Another way of achieving the transport through membranes is with an ion channel. Fuhrhop and Liman designed an ion channel for monolayer lipid membranes,³⁸ which is able to release lithium ion from the vesicles (figure 23).



of **21**. When the experiment was performed using DPPC dipalmitoylphosphatidylcholine bilayer membrane vesicles no leakage of lithium was observed.

1.3.4 Supramolecular Self-Assemblies and Molecular Machines

The evolution of supramolecular chemistry together with analytical techniques led to the design and synthesis of more and more complicated structures. From the inorganic supramolecular structures of the early 1990s such as ladders,³⁹ or helices⁴⁰ consisting of organic moieties assembled around metallic ions, the research led to structures made only by organic frameworks. These structures have become more and more complex, from the supramolecular ribbons⁴¹ to the apple peel,⁴² supramolecular polymers,³⁰ rotaxanes⁴³ and catenanes.⁴⁴

The manipulation of supramolecular assemblies has started a new approach for the development of nanoelectromechanical systems (NEMS). The molecular machines transform chemical, electrical or photochemical energy into controlled molecular motion. A step forward would be represented by the translation of the movement to a macroscopic scale.

This is the objective of the design of the molecular muscle.²⁸ The design of this machine took inspiration from the observation of how the myosin and actin protein's filaments slide relative one to each other giving the origin of muscle contraction. The molecular muscle is composed of a PPR (prototypical palindromic [3] rotaxane) (**24**) linked to a gold surface.

The PPR.8PF₆ unit is formed by a rod (**22**) that incorporates two pairs of complementary TTF (tetrathiafulvalene) and NP (naphthalene) units and a tetracatoinic cyclophane CBPQT⁴⁺ (cyclobis(paraquat-*para*-phenylene)) (**23**, figure 23).

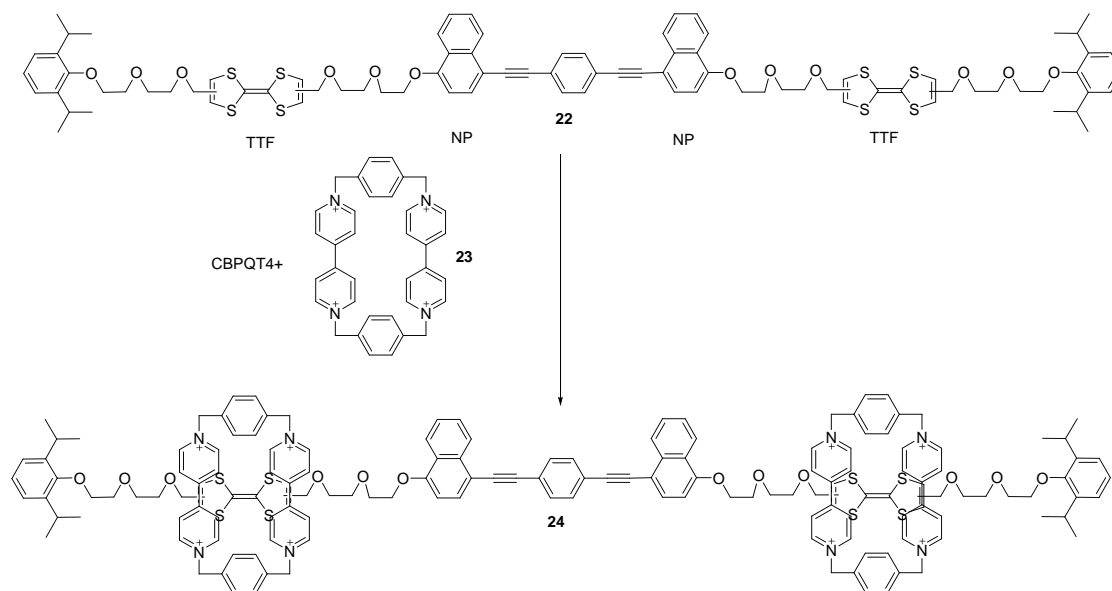


Figure 24 Structure of the PPR.8PF₆ unit (The counter ion PF₆⁻ is omitted for clarity).

This molecular machine is redox driven. The redox active TTF serves as a recognition site for the CBPQT, as a result of the π - π interaction. Therefore the cyclophane has a greater affinity for this unit rather than the competitor NP. When the system is perturbed by the removal of one or two electrons, the TTF is oxidised and the CBPQT ring is repelled by the presence of the positive charge and moves towards the naphthalene unit, as shown schematically in figure 24. The mechanism (figure 25) is completely reversible and can be activated chemically or electrochemically. The mechanism has been proven by NMR and UV-Vis experiments.

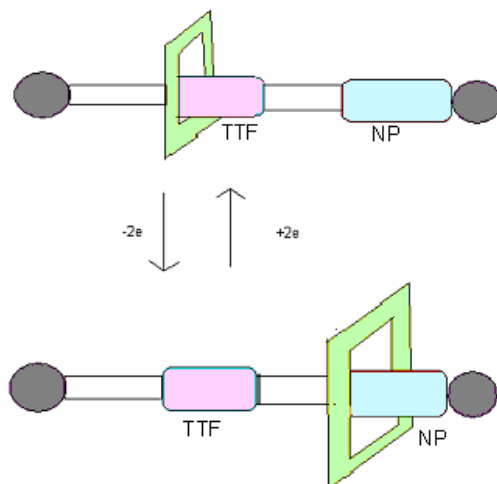


Figure 25 *Schematic behaviour of the basic component molecular muscle.*

By functionalising the two rings with a disulfide tether an anchor for a gold surface has been created, to transfer the mechanical movement to the attached surface. A cantilever beam coated with gold has been chosen as the surface. A cantilever beam is a flexible plank that is held only at one end. A series of randomly oriented six billion molecular muscles produced an upward mechanical bending of the beam; a subsequent reduction released the stress upon the beam which returned to the equilibrium position (figure 26).

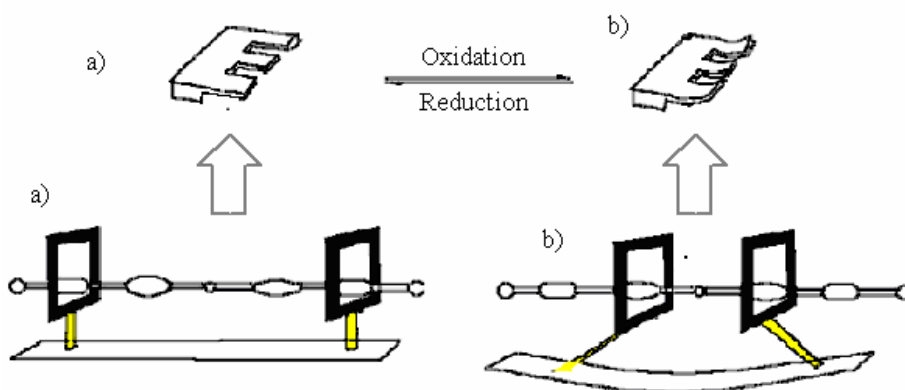


Figure 26 *Molecular muscle schematic mechanism (b) and macroscopic outcome on the cantilever beam.*

1.4 Receptors for anions

Anions play a key role in different biological processes, by regulating processes in the cell life: for example DNA is a polyanion. However anions can also have a deleterious effect. For example the misregulation of chloride concentration is closely related to cystic fibrosis. Chloride channels play a vital role in the cell life: by keeping the optimal concentration of chloride inside and outside the membrane they regulate a series of other events such as the pH, the homeostasis and the stimulus of secretion. Cystic fibrosis is responsible for mutations on the transmembrane conductance regulator (CFTR) chloride channel with a consequent uncontrolled production of sticky mucus leading to progressive disability and multisystem failure.⁴⁵

Some other anions in high concentration are pollutant and can have deleterious effects on the environment. For example phosphate and nitrate are present in agricultural fertiliser and are the cause of eutrophication of lakes and water ways.⁴⁶ In the last twenty five years research in this area has flourished and²⁹ it keeps generating⁴⁷⁻⁴⁹ new receptors to bind anions.

Anions are larger than isoelectronic cations and they exhibit a wide range of geometries: spherical (halides), linear (e.g. N_3^-), planar (e.g. carboxylates), tetrahedral (e.g. phosphates). Anion receptors can be classified according to the functional group that is acting as binding site.

1.4.1 Amide based receptors

The use of secondary amides as hydrogen bond donors to anions has wide application in Nature.⁵⁰ This functional group has been exploited in several synthetic receptors due to its versatility.^{48,49,51,52}

Hamilton designed a rigid and convergent receptor for tetrahedral oxo-anions with a C_3 symmetry which was geometrically optimal for binding tetrahedral anions such as phosphate and sulphate.⁵³ The preorganisation of receptor **25** (figure 27) gives much higher binding constants (e.g. with nitrate $4 \cdot 10^5 \text{ M}^{-1}$ in CDCl_3 -2% $\text{DMSO-}d_6$) than those obtained with the acyclic receptor **26** (e.g. with nitrate 620 M^{-1} in CDCl_3 -2% $\text{DMSO-}d_6$).

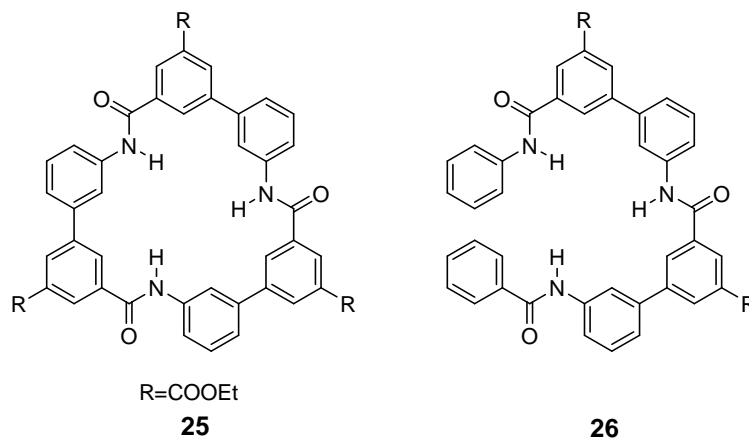


Figure 27 Receptor **25** can bind tosylate with a high binding constant in $CDCl_3$ -2% $DMSO-d_6$, while the bonding constant of **26** were significantly lower with all the anions tested.

A series of a more flexible macrocycles containing amides as H bonding donors has been designed by Jurczak (figure 28).⁵⁴

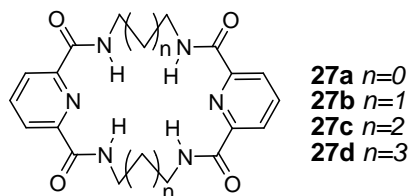


Figure 28 Jurczak's polyamide macrocycles.

In this case there is some preorganisation: the amide is hydrogen bonding with the pyridine locking the receptor in the conformation syn-syn (A, table 2). The evidence of the effectiveness of this type of intramolecular hydrogen bonding pattern was demonstrated by Hunter⁵⁵ who has found that A (table 2) was the energetically favoured conformation of the bis-amido pyridine ($X = N$) building block. This binding site has been widely used in a series of other receptors (e.g. Kilburn⁵⁶ and Gale⁵⁷).

X	A	B	C
N	149 kJmol ⁻¹	174 kJmol ⁻¹	261 kJmol ⁻¹
CH	166 kJmol ⁻¹	144 kJmol ⁻¹	164 kJmol ⁻¹

Table 2 Energies of the conformations A, B and C calculated with the CHARMM force field.

Jurczak also found that the optimal chain length for binding anions in DMSO-*d*₆ was *n* = 1 for any anion. For example receptor **27b** forms a more stable complex (*K*_a = 2283 M⁻¹ in DMSO-*d*₆) with benzoate than receptors **27a** (*K*_a = 220 M⁻¹ in DMSO-*d*₆) and **27d** (*K*_a = 301 M⁻¹ in DMSO-*d*₆), while receptor **27c** was not soluble in DMSO.

Another example of a polyamide macrocycle was reported by Bowman-James (figure 29).⁵⁸ It was demonstrated the contribution of each amide to the binding process, by analysing the complex with fluoride using the NMR spectroscopy. When one equivalent of fluoride was added to a solution of **28** in DMSO-*d*₆, the amide signal moved downfield and its multiplicity changed from a singlet to a doublet with a coupling constant of *J* = 27 Hz. This could be ascribed to a ¹H-¹⁹F coupling as in the case of the complex of sapphyrine with fluoride.⁵⁹ In the ¹⁹F NMR spectrum of tetrabutylammonium fluoride upon addition of **28** the signal was shifted from -97.6 ppm to -111.7 and it appeared as a septet. This multiplicity revealed that the fluoride was coupling with six equivalent protons; the shape of the multiplet demonstrated that in solution the fluoride is encapsulated into receptor **28**, and that interacts with all the six hydrogen bond donors.

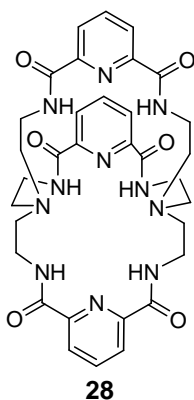


Figure 29 Bowman-James amide macrotricyclic.

1.4.2 Urea and thiourea based receptor

Ureas and thioureas are useful building blocks for the design of receptor for Y shaped anions, because they have two parallel hydrogen bond donors. This tool has been widely used for the design of receptors for carboxylates.⁶⁰

Gale and co-workers have recently published⁶¹ a study comparing the affinity for various anions of a bis-urea based on 1,2-phenylenediamine and an analogous amide (table 3).

Anion (TBA salt)	Receptor $K_a(M^{-1})$		
	29 	30 	31
AcO ⁻	98	251	3210
BzO ⁻	43	113	1330
H ₂ PO ₄ ⁻	149	295	732

Table 3 Stability constants (M^{-1}) measured in DMSO- d_6 at 298K.

A first comparison between receptors **29**, **30** and **31**, shows that **31** forms much more stable complexes with anions (table 3). This was explained by the cooperativity of the four hydrogen bonds in binding one benzoate and by the fact that the bound conformation

can be stabilised by internal interactions. This interpretation is corroborated by the crystal structure (figure 30).

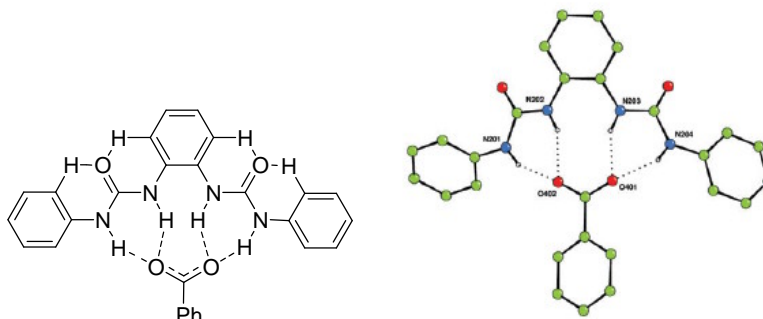


Figure 30 Complex formed between **31** and benzoate.

To investigate the role of each single component they have synthesised two substituted compounds **32** and **33**, with electron withdrawing components in the central and in the pendant rings.

Anion (TBA salt)	Receptor $K_a(M^{-1})$	
	32 	33
AcO ⁻	8079	4018
BzO ⁻	2248	1399
H ₂ PO ₄ ⁻	4724	666

Table 4 Stability constants (M^{-1}) measured in DMSO-*d*₆ at 298K.

The binding constants in solution for **33** were similar to those obtained for **31**, despite an increase in the acidity of two urea's NHs. For **32**, on the other hand, an interesting increment in the binding has been observed. An explanation has been rationalised for this behaviour: the difference cannot be simply explained by the varied acidity of the NH bond, because this would have given the same result on both **32** and **33**. The addition of an electron withdrawing group influences also the acidity of the aromatic CH on the same

ring of the substituent, increasing the strength of the intramolecular interactions with the urea's carbonyl (figure 31). The increase of these interactions in the central ring leads to a better preorganisation, as was demonstrated by receptor **32**.

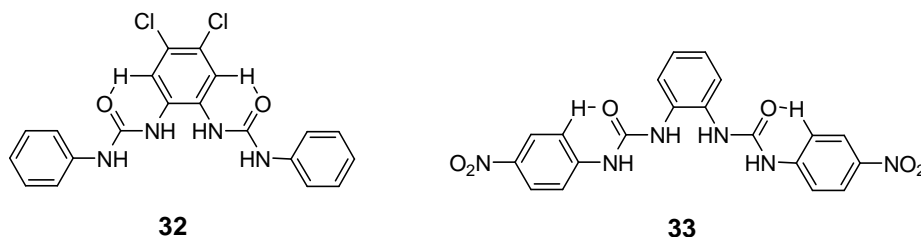


Figure 31 *Effects of the presence of electron withdrawing groups.*

Encouraged with the binding constants obtained they decided to synthesise the thiourea analogues of **30**. Thioureas are more acidic than ureas and normally give higher binding constants.

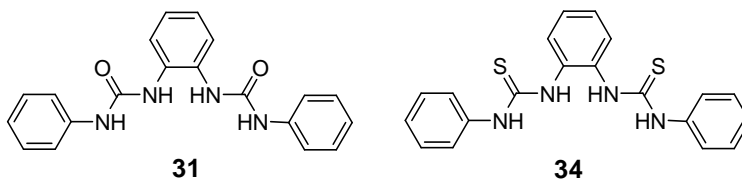


Figure 32 *Thiourea analogous of receptor 31.*

In this case, however, the binding constants measured for carboxylates are one order of magnitude less than those obtained for **31**. Sulfur is bigger than oxygen therefore the geometry of **34** is planar, but distorted and the hydrogen bond donors are not co-planar reducing the affinity of the receptor for anions.

Another interesting example has been introduced by Kilburn and co-workers and is a switchable receptor.⁶² Pyridyl thiourea **34** is selective for acetate at neutral pH, however upon addition of one equivalent of acid it is protonated and changes conformation becoming selective for halides.

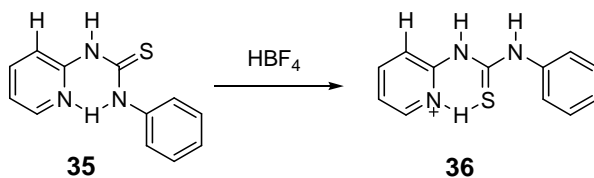


Figure 33 Conformations adopted by a pyridyl thiourea based receptor in neutral and acidic conditions.

The neutral form **35** is stabilised by the presence of an intramolecular hydrogen bond between the nitrogen of the pyridine and the H of the thiourea (figure 33). It binds the acetate with the H of the free thiourea and the CH on the pyridyl group. No changes were recorded upon addition of halides. By adding one equivalent of tetrafluoroboric acid, the acid protonates the pyridine, with a consequent release of the previous internal hydrogen bond and the formation of an H bonding between the pyridinium and the sulfur of the thiourea (figure 33). In this way the binding mode changes and the two NH of the thiourea are parallel and set to bind the first equivalent of anion with a binding constant of 10^4 M^{-1} while a second equivalent of anion binds to the pyridinium with a binding constant of $\sim 100 \text{ M}^{-1}$ (figure 34).

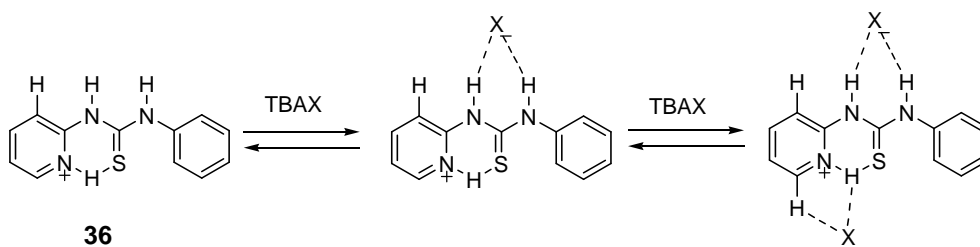


Figure 34 Structure of the complexes formed between the protonated specie and the halides.

1.4.2 Ammonium and guanidinium based receptors

Ammonium and guanidinium based receptors bind anions with a combination of ion-ion interactions and hydrogen bond.²⁹ The first examples of anion receptors are a series of macrobicycles designed by Park and Simmons which are able to encapsulate anions in aqueous media (figure 35).⁶³

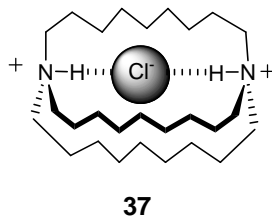


Figure 35 General structure of Park and Simmons macrobicycles.

A recent example of how ammonium species are used as part of a more complex structure is shown in tripodal receptor **38** introduced by Anslyn, Frontera and Morey.⁶⁴ After a series of comparative computational studies receptor **38** has been synthesised and its properties tested with a series of anions. Selectivity for di and tricarboxylates was confirmed by ITC titrations techniques.

Anion	$K_a (M^{-1})$
citrate	$1.1 \cdot 10^5$
tricarballate	$1.5 \cdot 10^5$
trimesoate	$4.5 \cdot 10^4$
glutarate	$2.2 \cdot 10^4$
succinate	$2.8 \cdot 10^2$
isocitrate	$1.5 \cdot 10^4$
acetate	$<1.0 \cdot 10^2$

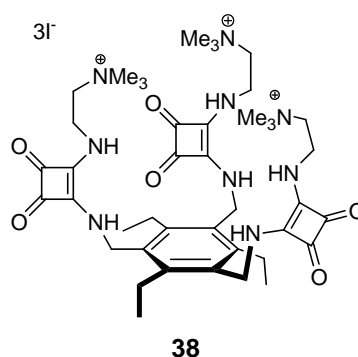
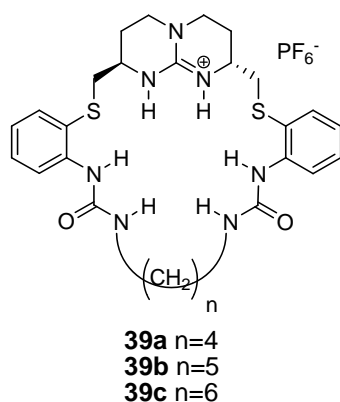


Figure 36 Binding constants measured in EtOH:H₂O 3:1 v/v

Receptor **38** has also been used as sensor for citrate in competition assays with fluorescein.

Guanidinium receptors provide a combination of ion-ion interactions and two parallel H-bonds; it provides a very good pattern to bind Y shaped anions such as nitrates and carboxylates. A recent example by de Mendoza integrates bicyclic guanidinium pattern with two ureas in a macrocyclic structure (figure 37).⁶⁵



Receptor	$K (M^{-1})$ with nitrate
39a	7260
39b	15200
39c	73700

Figure 37 De Mendoza's receptors for nitrate: binding constants measured by ITC titration technique in CH_3CN at 303 K.

Receptor **39c** gave the most stable complexes with nitrate. In this complex both the NHs from the guanidinium and from the ureas form an H-bond with the guest as shown in the crystal structure and in the proposed binding model (figure 38).

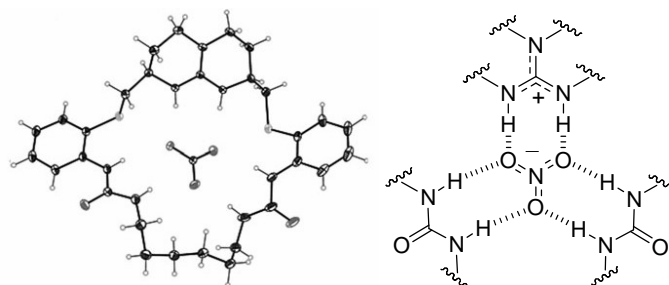


Figure 38 Crystal structure of the complex **39c**• NO_3^- and proposed binding model.

The macrocyclic structure plays a key role in the binding efficacy. Complexes formed by receptors **39a**, **39b**, and **39c** with nitrate have values of binding constants generally higher than those formed by acyclic receptor **40** (figure 39) with nitrate ($K_a = 5380 M^{-1}$).

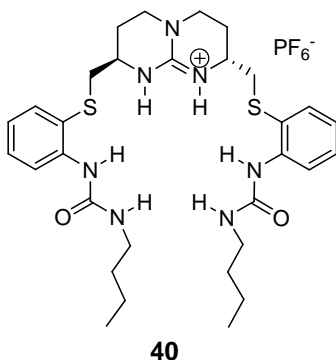


Figure 39 Tweezer analogous of receptor **40**.

1.4.3 Aromatic heterocycles as anion receptors

There is much interest in anion receptors composed of aromatic heterocycles. The heteroatomic unit can act as H bond donor as in the case of the pyrrole NH, or acceptor as the case of the pyridine nitrogen.

1.4.3.1 Pyrrole based receptors

Pyrrole is an ideal group to bind anions because it does not contain a hydrogen bond acceptor that could compete with a putative anionic guest for hydrogen bond formation with the NH group.⁶⁶ It has also been demonstrated that pyrrole itself, at least in solid phase, can form a stable complex with an anion.⁶⁷ In the crystal structure of the pyrrole-TBACl complex there is an H-bonding between the NH and the anion (figure 40).

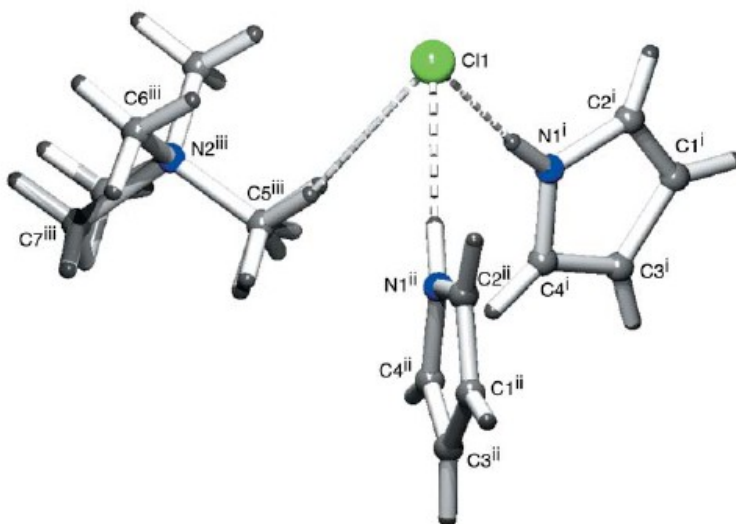
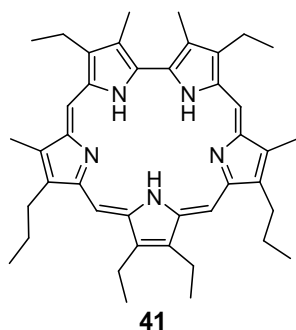


Figure 40 First example of a pyrrole-chloride (TBA) complex

A wide variety of cyclic and acyclic pyrrole based receptors have been developed.

Macrocyclic pyrrole based receptor

The use of pyrrole as anion receptor was pioneered and developed by Sessler. The serendipitous discovery that protonated sapphyrin **41** binds anions introduced the idea of taking advantage of the properties of this moiety.⁶⁸ Protonated sapphyrin binds strongly to halides and is selective for fluoride: particularly receptor **41** forms a complex with HF in DCM so stable that the stability constant can not be reliably evaluated because it is too high.⁵⁹



<i>Anion</i>	<i>Method</i>	41 $K_a(M^{-1})$
F ⁻ ⁵⁹	fluorescence	$>10^8$
Cl ⁻ ⁵⁹	lifetime	$1.8 \cdot 10^7$
Br ⁻ ⁵⁹	lifetime	$1.5 \cdot 10^6$
<i>p</i> -toluate ⁶⁹	¹ H-NMR	$9.5 \cdot 10^3$

Figure 41 Sapphyrin structure and binding properties measured in DCM.

Another important class of pyrrole containing anion receptors are the calixpyrroles. These compounds were synthesised for the first time by Bayer in 1886.⁷⁰ Anions such as chloride and fluoride are complexed at the centre of the cavity by pyrrole NH groups. The electron rich cavity of the complexed calix-4-pyrrole **42** is able to coordinate cations, the result is an efficient receptor for ion pairs as shown in figure 42.⁷¹

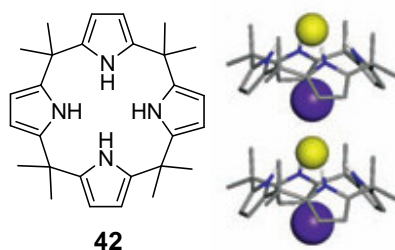


Figure 42 *Crystal structure of the complex formed between a calix-4-pyrrole **42** and CsF. Fluoride is coordinated by pyrrole NHs while Cs sits in the cavity of the calix-4-pyrrole leading to the formation of a crystalline network.*

A variation of this motif has been introduced by Kohnke and coworkers to achieve the larger calix-6-pyrrole **43** (figure 43).⁷² It was found that the bromide is more strongly bound by the calix-6-pyrrole **43** ($K_a = 710 \text{ M}^{-1}$, $^1\text{H NMR}$ in CD_2Cl_2)⁷³ than by calix-4-pyrrole **42** ($K_a = 10 \text{ M}^{-1}$, $^1\text{H NMR}$ in CD_2Cl_2).⁷⁴

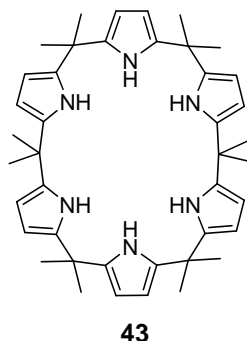
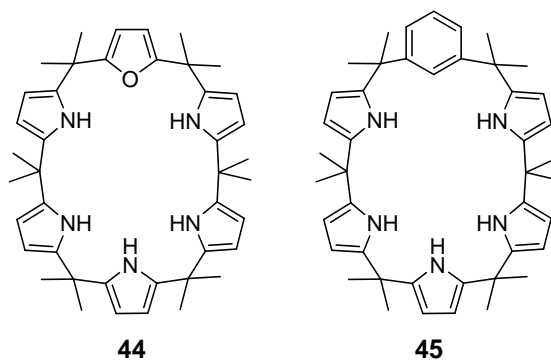


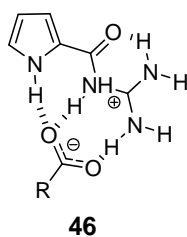
Figure 43 *Calix-6-pyrrole*

Other modifications of this motif are based on the introduction of other aromatic rings into the calix structure: for example a furan⁷³ in the calix-6-pyrrole as in **44** (figure 44) or a benzene⁷⁵ in the calix-6-pyrrole as in **45** (figure 44). The complex formed between receptor **44** and bromide is less stable ($K_a = 69 \text{ M}^{-1}$) than the one formed by **43** ($K_a = 710 \text{ M}^{-1}$) and the same anion in the same conditions (CD_2Cl_2). Also **45** ($K_a = 296 \text{ M}^{-1}$) forms less stable complex with bromide than **43**.

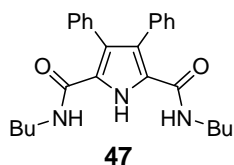
**Figure 44**Acyclic pyrrole based receptor

Two approaches have been undertaken to enhance the binding ability of pyrrole in the design of simple tweezer receptors.

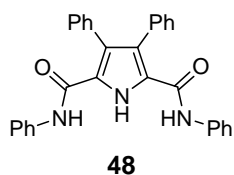
The binding ability of this system is increased by functionalising the molecule in the 2 and 5 positions of the pyrrole ring. Schmuck has produced a variety of receptors by adding a guanidinio-carbonyl moiety to the pyrrole. Experimental results show that guanidinio-carbonyl pyrrole systems bind carboxylates in very polar solvent mixtures of water-DMSO.⁷⁶ For example the complex formed by receptor **46** (figure 45) and the tetramethylammonium salt of *N*Ac-L-AlaO⁻ has a stability constant of 130 M⁻¹ in a very polar mixture of DMSO-*d*₆-40% water.

**Figure 45** Binding mode of receptor **46** with a carboxylate

The approach taken by Gale consists of appending amide groups in position 2 and 5 of the pyrrole ring. Receptors **47** and **48** revealed good affinity with oxo-anions.⁷⁷ Receptor **47** is selective for benzoate in CD₃CN, while receptor **48** is selective for dihydrogenphosphate in DMSO-*d*₆ (figure 46).



Anion (TBA salt) in CD_3CN	Receptor $K_a (M^{-1})$ 47
BzO^-	2500
$H_2PO_4^-$	357



Anion (TBA salt) $DMSO-d_6$ -0.5% water	Receptor $K_a (M^{-1})$ 48
BzO^-	560
$H_2PO_4^-$	1450

Figure 46 Stability constants (M^{-1}) for diamido-pyrrole based receptor in CD_3CN (**47**) and in $DMSO-d_6$ (**48**).

The hydrogen bonding pattern has been elucidated by the crystal structure⁷⁸ of the complex: (figure 47) one oxygen of the benzoate forms a hydrogen bond with the pyrrole proton and one of the amides, and the other one with the other amide.

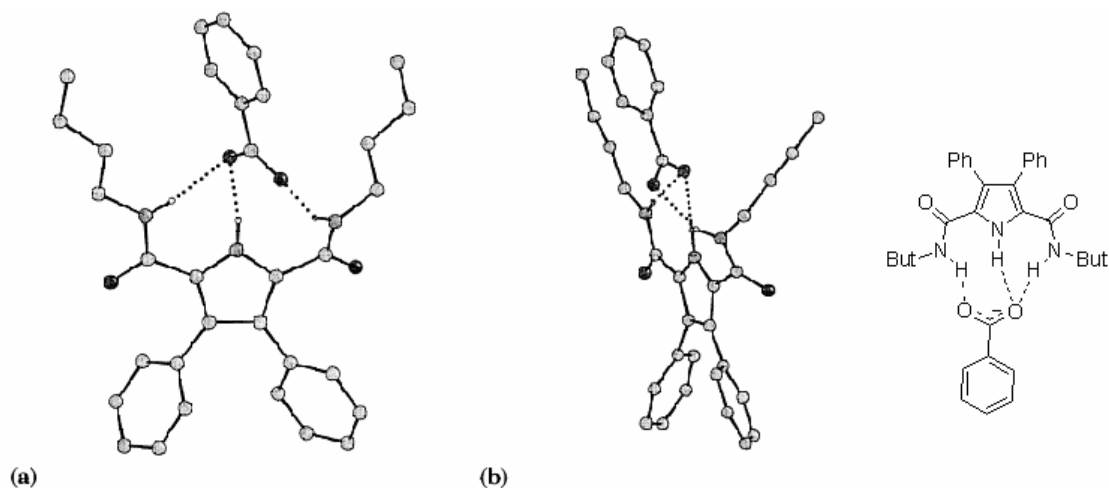


Figure 47 Crystal structure of the complex **47**·benzoate and hydrogen -bond pattern proposed for this complex.

Receptors with increased affinity for anions have been synthesised by adding electron withdrawing substituents on the aniline⁷⁹ (**49-50**, figure 48) and on the pyrrole ring (**51**, figure 48).⁸⁰

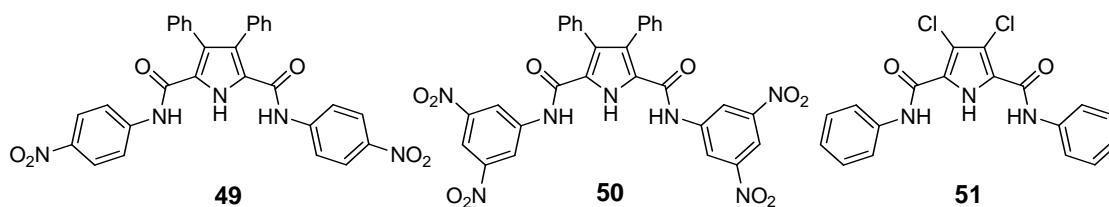


Figure 48 Modification of receptor **48** by the addition of electron withdrawing substituents.

For receptor **49** and **50**, an increment in the stability constants for the complexes with anions has been observed as shown in table 5.

Anion (TBA salt)	Receptor $K_a (M^{-1})$		
	48	49	50
F ⁻	74	1245	- ^a
Cl ⁻	11	39	53
BzO ⁻	560	4150	4200

Table 5 Binding constants (M^{-1}) measured between receptor **48**, **49** and **50** with a series of anions in DMSO- d_6 -0.5% water. ^aData could not be reliably obtained

Upon addition of fluoride to a solution of host **50** all signals from the NHs disappeared and the CH belonging to the nitro-substituted phenyl ring gave a pattern that can be rationalised as a three step process. The first equivalent of fluoride is coordinated by the receptor; the second equivalent promotes a deprotonation process; while the third equivalent is coordinated by the deprotonated receptor, with the aid of the aromatic CHs. Another evidence of the deprotonation is the fact that, when fluoride was added to a solution of **50**, the solution became deep blue, while it was colourless in presence of other anions. In receptor **51** the electron withdrawing chlorine atoms increased acidity of the pyrrole NH that in presence of basic anions such as fluoride or hydroxyl underwent deprotonation leading to the formation of interlocked pyrrole anion dimers (figure 49).⁸¹

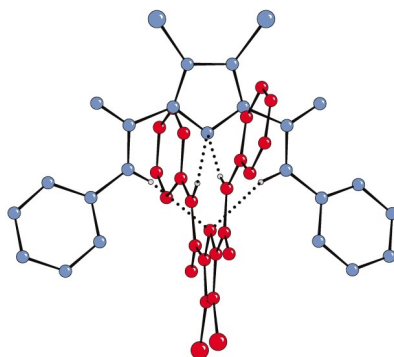
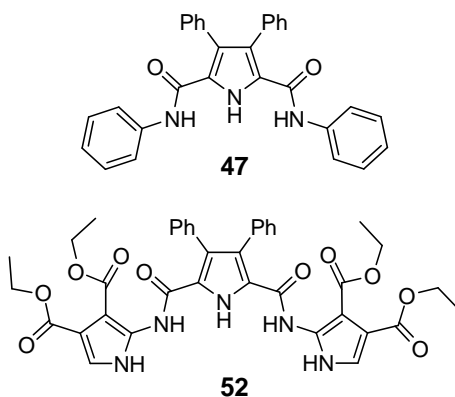


Figure 49 Structure of interlocked pyrrole anion dimers

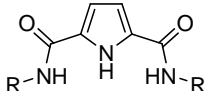
By modifying the appended side-chains of the pyrrole unit with ferrocene units Gale and co-workers designed redox-active receptors for anions.⁸² The versatility of this simple unit gave the opportunity to obtain ion-pair receptors, by adding a crown-ether unit.⁸³ In order to maximise the binding properties of this scaffold two pyrrole units have been appended: a relevant increment of the binding constants has been observed.⁸⁴



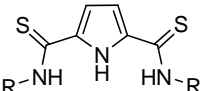
Anion (TBA salt)	Receptor $K_a (M^{-1})$	
	47	52
$H_2PO_4^-$	1450	5500
BzO^-	560	10300

Figure 50 Binding properties ($K_a = M^{-1}$) of receptor **47** and **51** measured in $DMSO-d_6$ -0.5% water.

Jurzack has further modified the structure of the amidopyrroles by transforming the amides into thioamides.⁸⁵ The higher acidity of the thioamides and their lower ability to accept hydrogen bond seemed to be a good hypothesis for achieving higher affinities for anions. However, the differences measured are not so significant: a study using the ITC revealed that, although the thioamides have stronger interaction with the anion (higher enthalpic gain), the binding constants are similar due to enthalpy/entropy compensation (figure 51).



53



54

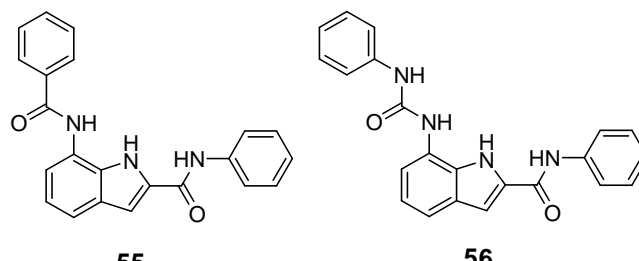
Receptor	$\log K_a$	ΔH (kJmol ⁻¹)	$T\Delta S$ (kJmol ⁻¹)
53	4.34	-14.71	9.90
54	4.40	-16.40	8.54

Figure 51 Jurzack's amides and thioamides general structure. Thermodynamic parameters of binding benzoate by ligand **53** and **54** with $R = Ph$ in CH_3CN at 296 K measured by ITC

1.4.3.2 Indole based receptors

Very few examples of indole based receptors for anions are present in the literature, although this moiety has been exploited in nature (as tryptophan) to bind sulfate in the sulfate binding protein.⁸⁶

In a recent study Gale and Albrecht have presented two new structures based on this moiety.



Anion (TBA salt)	Receptor $K_a (M^{-1})$	
	55	56
$H_2PO_4^-$	310	4950
AcO^-	650	10000
BzO^-	100	4460
Cl^-	<10	380

Figure 52 Gale and Albrecht indole based receptors. Binding constants (M^{-1}) measured in $DMSO-d_6$ -0.5% water.

Receptor **56** is a much stronger binder for anions than **55**. From an analysis of the curves obtained with the different protons two different hydrogen bond patterns can be envisaged.

While **55** forms a cleft type binding site, in **56** the anion interacts mostly with the indole and urea NH, and less with the amide (figure 53).

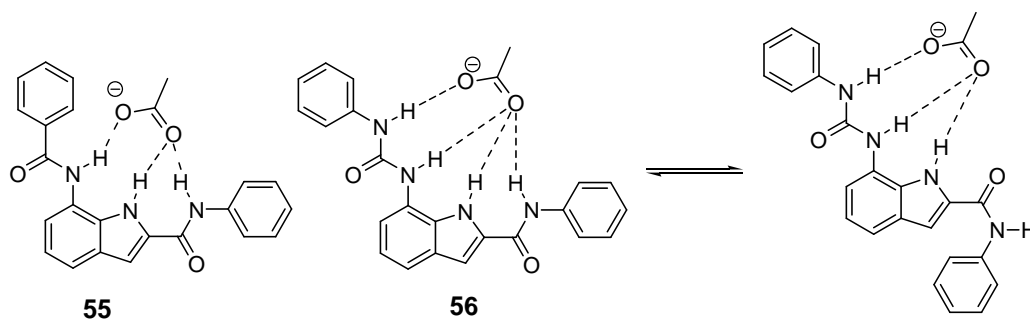


Figure 53 Hydrogen bond pattern of complexes between acetate and receptors **55** and **56**.

A bis-indole receptor **57** has been synthesised by Jeong.⁸⁷ The hydrogen bonding pattern is efficient not only in the binding of simple anions such as phosphate ($K_a = 3.9 \cdot 10^4 M^{-1}$ in

DMSO-*d*₆-0.2% water) and acetate ($K_a = 7.4 \cdot 10^4 \text{ M}^{-1}$ in DMSO-*d*₆-0.2% water) but it also forms highly stable complexes with dicarboxylates (e.g. malonate, $K_a = 1.6 \cdot 10^5 \text{ M}^{-1}$) in very competitive solvents such as mixtures of DMSO-10% methanol.

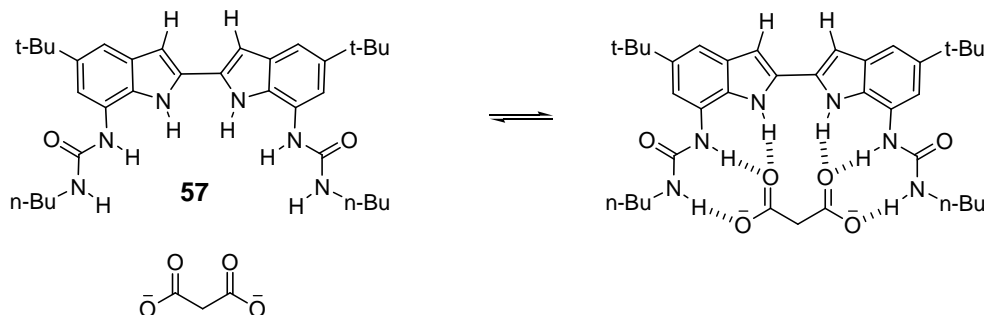
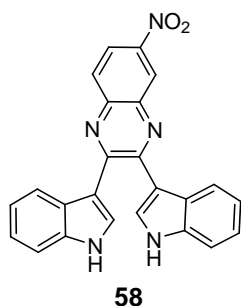


Figure 54 Binding model suggested for the complex between **57** and malonate.

A bis-indole receptor **58** synthesised by Sessler and co-workers⁸⁸ is highly selective for phosphate (figure 55) with colour changes occurring upon the addition of phosphate and fluoride to the receptor solution in dichloromethane.

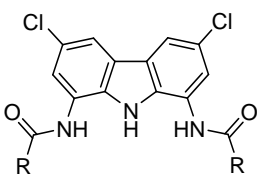


Anion (TBA salt)	Receptor $K_a (\text{M}^{-1})$ 58
Cl^-	470
HSO_4^-	250
BzO^-	2700
H_2PO_4^-	20 000

Figure 55 Receptor **58** and the stability constants ($K_a = \text{M}^{-1}$) of the complex between receptor **58** and anions added to the solution measured by means of UV-vis titrations in dichloromethane.

1.4.3.3 Carbazole based receptors

The carbazole based receptor designed by Jurczak⁸⁹ took inspiration and merged together two pre-existing receptors: the Gale's amidopyrrole⁷⁷ and Umezawa's xanthene scaffold.⁹⁰ The result is a receptor selective for oxo-anions and particularly for phosphates.



59a R=Ph
59b R=Pr

<i>Anion</i> (TBA salt)	<i>Receptor</i> $K_a(M^{-1})$	
	59a	59b
Cl ⁻	13	115
BzO ⁻	1230	8340
H ₂ PO ₄ ⁻	1910	19800

Figure 56 Binding constants ($K_a = M^{-1}$) in DMSO-*d*₆-0.5% water.

Sessler introduced a carbazole group into a calixpyrrole unit, changing the conformation of the cavity from a cone to a saddle.⁹¹ The conformation is confirmed by the crystal structure of the receptor (figure 57).

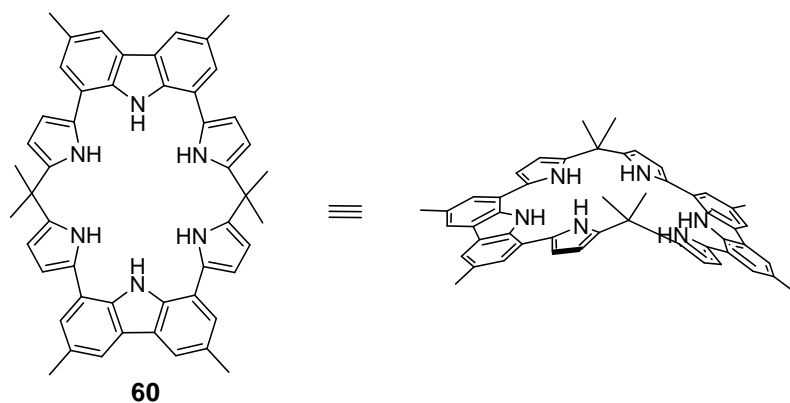


Figure 57 Receptor **60** and its conformation confirmed by crystal structure.

A structure of the complex between benzoate and receptor **60** shows that the aryl residue of the anion is folded in the cavity of the receptor (figure 58).

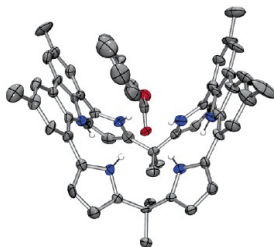


Figure 58 Crystal structure of the complex formed between receptor **60** and benzoate.

1.4.3.4 Imidazole based receptor.

A chemosensor based on a benzimidazole unit is able to indicate the presence of fluoride and acetate.⁹² When fluorescent receptor **61** (figure 59) forms a complex with acetate, in acetonitrile, its fluorescence is switched off.

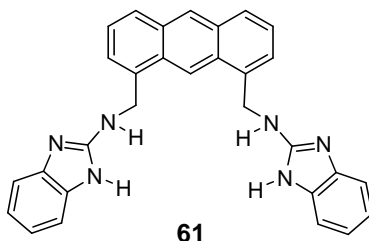


Figure 59 Structure of receptor **61**.

Receptor **62** (figure 59) was developed on a similar structure: the imidazole component acts as hydrogen bond donor to the anion,⁹³ while the nitro-unit increases the binding ability and acts as chromophore. When acetate or phosphate was added to a solution of receptor **62** (figure 60) in CH₃CN-1% DMSO the colour of the solution changed from colourless to bright yellow.

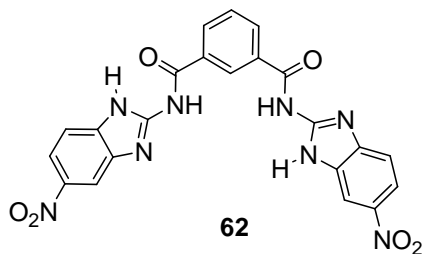


Figure 60 Structure of receptor **62**.

1.5 Enantiomeric recognition

Chirality can play a dramatic role in the biological activity of a substance. There are many examples where, if one enantiomer has therapeutic properties, the other could be inactive, or dangerous for the health. An example widely known is the case of thalidomide.⁹⁴ Therefore, it is more and more important to obtain enantiomerically pure compounds and to have methods able to quantify the enantiomeric purity of a sample. That is why the design of enantioselective receptors is still a vital area of research.⁹⁵

The design of chiral receptors is based on a rule that states: “Chiral recognition requires a minimum of three simultaneous interactions between receptor and one of the enantiomers, with at least one of these interactions being stereochemically dependent”.⁹⁶

Receptors able to discriminate the two enantiomers can be used as sensors,⁹⁷ as stationary phases for HPLC chiral columns⁹⁸ or as carriers through a membrane.⁹⁹

The calixarene based fluorescent receptor **63** (figure 60) designed by He and co-workers¹⁰⁰ is able to discriminate between the two enantiomers of *N*Boc-Ala-OTBA. The fluorescence of receptor **63** (figure 61) is turned off only when the D enantiomer of the *N* protected alanine is present in a DMSO solution of the receptor. When the L enantiomer is added to a solution of the receptor the fluorescence is not affected.

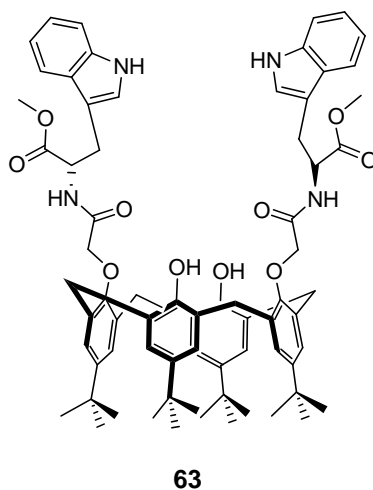


Figure 61 Structure of enantioselective receptor **63**.

A typical example of stationary phase for HPLC columns has been developed by Villani.⁹⁸ By linking macrocyclic receptor **64** (figure 62) to a silica HPLC column

discrimination in the retention times of the two enantiomers of a series of amino acids derivatives has been achieved.

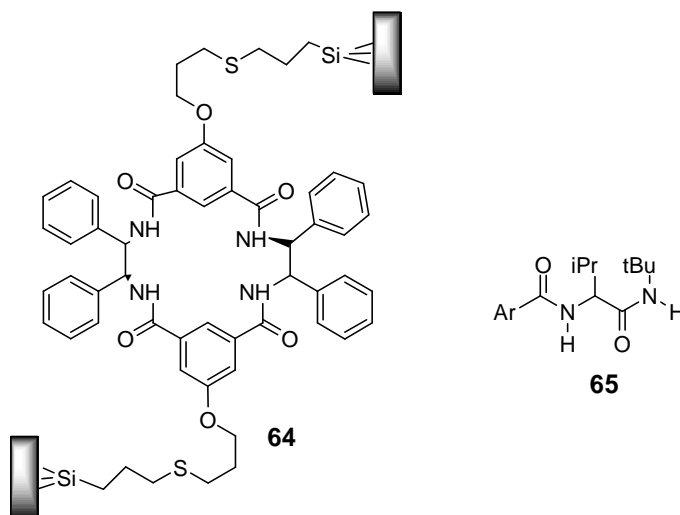


Figure 62 With the stationary phase **64** the derivative **65** from the *D* amino acid is eluted with the solvent, while the derivative from the *L* enantiomer has a retention time of around 30 minutes.

Enantiomeric recognition of carboxylates has been achieved by the use of natural and modified natural receptors, such as cyclodextrins (e.g. receptor **66**)¹⁰¹ and (+)-tubocurarine (e.g. receptor **67**).¹⁰² Receptor **66** (figure 63) forms a more stable complex with the *L* enantiomer of *N*Ac-TrpO[−] ($K_a = 2310 \text{ M}^{-1}$ in D₂O at 25°C) than with the *D* enantiomer ($K_a = 1420 \text{ M}^{-1}$ in D₂O at 25°C). The tubocurarin based receptor **67** (figure 63) binds the *S* enantiomer of compound **68** more strongly ($K_a = 59.5 \text{ M}^{-1}$ in D₂O at 25°C) than the *R* enantiomer ($K_a = 15.8 \text{ M}^{-1}$ in D₂O at 25°C).

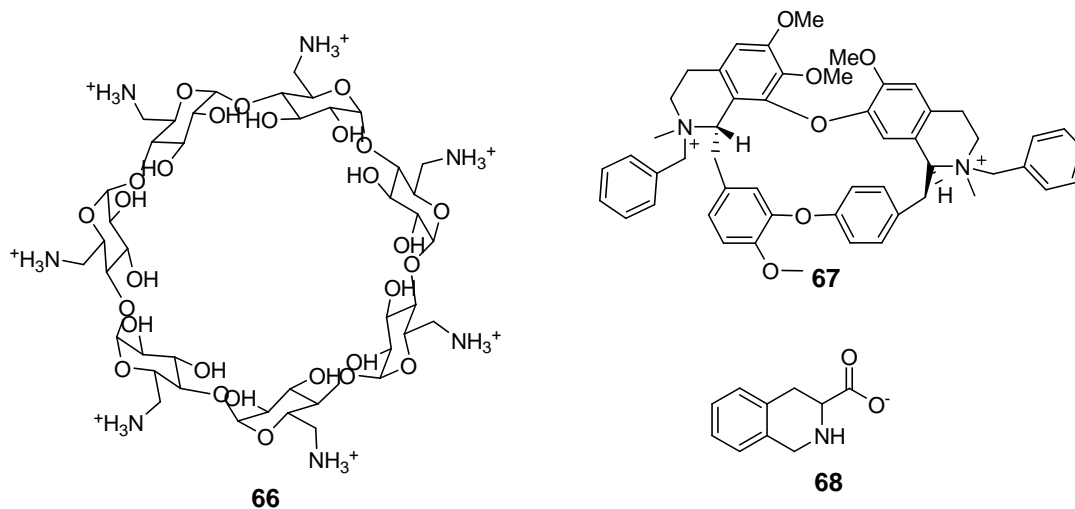


Figure 63 Examples of receptors derived from natural molecules.

Synthetic receptors for anions can be classified according to their principal functional groups. Among the ammonium based macrocyclic receptors a widely used structure is a polyazamacrocycles with chiral substituents. The receptor designed by Lehn and Gotor shows good selectivity for *N*Ac-D-Asp.¹⁰³ Receptor **69** (figure 64) binds the D enantiomer of the tetrabutylammonium salt of *N*Ac-Asp more strongly ($\log K_a = 5.34$ in water) than the L enantiomer ($\log K_a = 4.57$ in water).

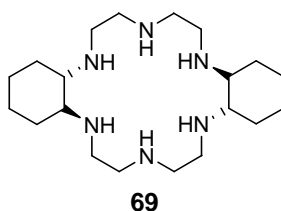


Figure 64 Lehn's receptor for aspartate.

Another widely used moiety is the guanidinium: as mentioned before, it can provide two parallel hydrogen bonding and an ion-ion interaction which are particularly effective for binding Y-shaped substrates such as carboxylates or phosphates.

By modifying a bicyclic structure introduced by Schmidtchen,¹⁰⁴ de Mendoza designed the elegant enantioselective receptor **70** (figure 64) which can transfer, from an aqueous solution of the racemate to an organic solution, the L enantiomer of phenylalanine and tryptophane with a very high ee.⁹⁹

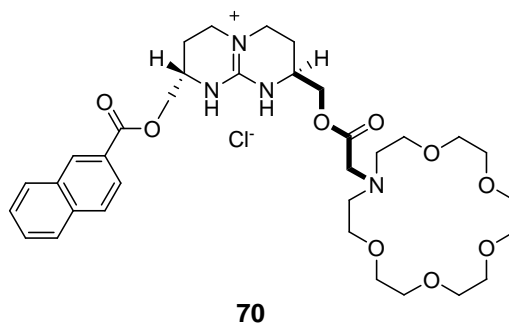
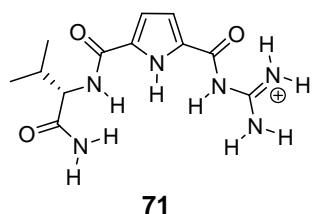


Figure 65 *De Mendoza's receptor for L-Tryptophan*

While the guanidinium unit interacts with the carboxylate of the amino acid, the crown ether complexes the ammonium and the naphthalene unit interacts with the side chain of the tryptophan with hydrophobic and $\pi-\pi$ interactions.

The guanidinium moiety has also been appended to other structures. Schmuck, for example, has modified receptor **46** (§ 1.4.3.1) into **71** (figure 65) by adding an amide and a chiral unit in position five to achieve enantioselectivity towards a series of amino acids in very competitive solvent mixtures as DMSO- d_6 - 40% water.⁷⁶



<i>Guest</i>	<i>Receptor</i> $K_a (M^{-1})$
NAc-Ala	71
L	1610
D	930

Figure 66 *Binding properties of receptor 71*

Davis and co-workers have functionalised a steroid skeleton with a combination of binding sites such as a guanidinium and an amide or urethane and obtained a series of receptors able to extract the L enantiomer of NAc-Ala, NAc-Phe, NAc-Val and NAc-Trp from aqueous solution into chloroform (figure 67).¹⁰⁵

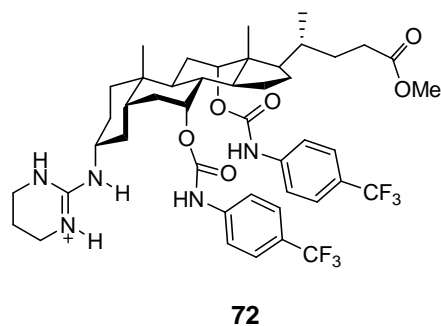


Figure 67 Davis receptor for *N*-protected amino acids.

Other functionalities that form stable complexes with carboxylates are ureas and thioureas. Kilburn and co-workers have developed chiral receptors for carboxylates based on this moiety. The open chain receptor **73** is selective for the L enantiomer of *N* protected amino acids: the highest selectivity is achieved is 1:2 with Asn.¹⁰⁶ The complex formed between receptor **73** (figure 68) and L enantiomer of *N*Ac-Asn-OTBA is more stable ($K_a = 1690 \text{ M}^{-1}$ in CDCl_3) than the complex formed with the D enantiomer ($K_a = 800 \text{ M}^{-1}$ in CDCl_3).

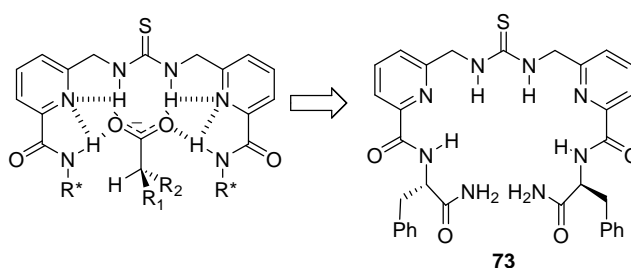
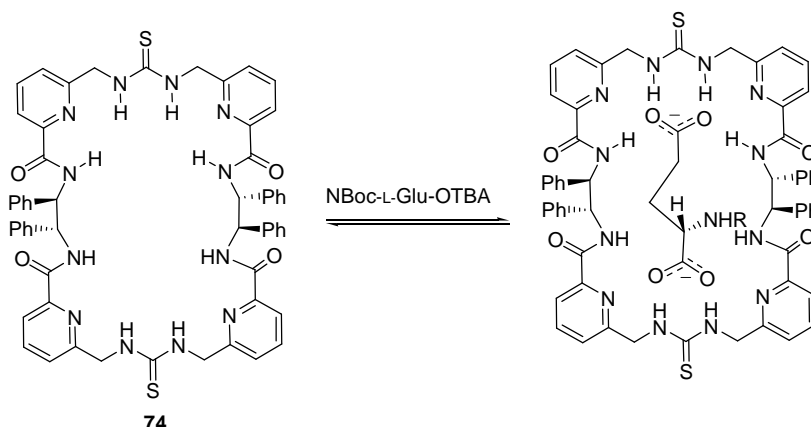


Figure 68 Kilburn acyclic receptor for amino acids

A development of this structure led to the synthesis of a macrocyclic receptor with high enantioselectivity.¹⁰⁷ In acetonitrile, receptor **74** (figure 69) has a strong 1:1 binding with the bis-tetrabutylammonium salt of *N*Boc-L-Glu, while the D enantiomer has a very low 1:1 binding constant and a very high 1:2 binding constant (figure 69).

This suggests that, while the L enantiomer fits nicely in the cavity and the receptor interacts with two carboxylates belonging to the same guest, the D enantiomer does not.

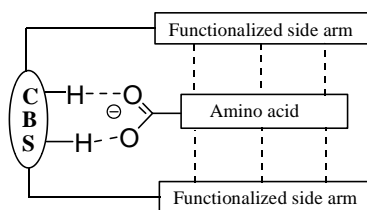


Guest	$K_{1:1} (M^{-1})$	$K_{1:2} (M^{-1})$
NBoc-Glu		
L	$2.83 \cdot 10^4$	-
D	38.4	$4.92 \cdot 10^4$

Figure 69 Calorimetric titrations for receptor **74** with NBoc-Glu bis-TBA salt in acetonitrile

1.6 Aims of the project

Part of this project was part of a wider research program of an EU Network (Enantioselective Recognition: Towards the Separation of Racemates). The universities and the companies involved focused on the separation of amino acids and other racemic carboxylic acid derivatives. The main research interests of the Network are the synthesis of the receptors, the optimisation of the extraction process through membranes, the development of chiral HPLC columns with linked receptors and computational studies of the host-guest interactions. One of the goals of this project is the synthesis and the study of the binding properties of suitable receptors for enantiomeric amino acid recognition. The receptors will have a general structure composed of a CBS (carboxylate binding site) and functionalised side arms (figure 70). While the CBS interacts with the carboxylate, the chiral functionalised side arms will bind the amino acid side chain with secondary interactions. The amino acid is then "surrounded" by a chiral microenvironment providing selectivity.¹⁰⁸

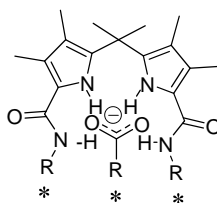


75

CBS = carboxylate binding site

Figure 70 General model for tweezer receptor binding amino acid

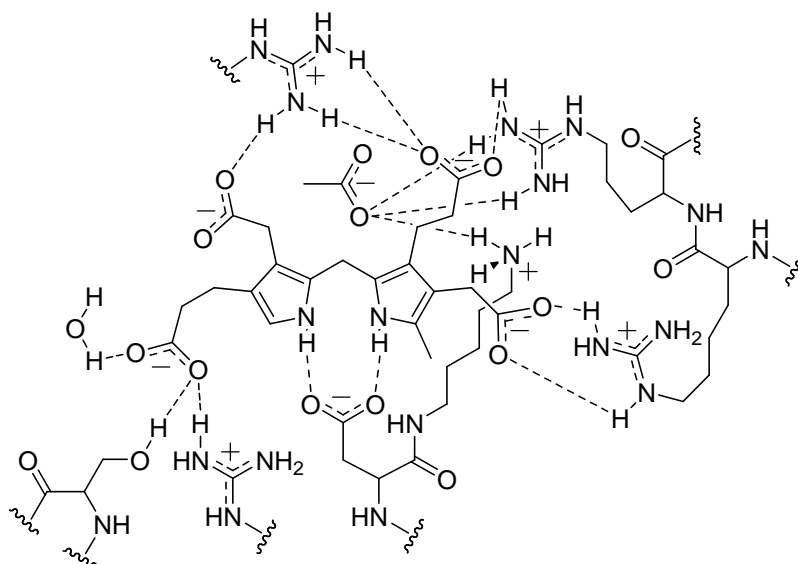
We have been interested in receptors where the CBS was a dipyrromethane unit.



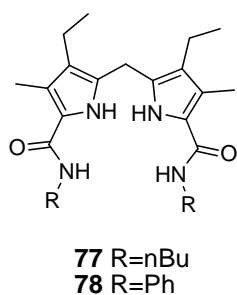
76

Figure 71 General model for chiral- dipyrromethane receptor

This unit occurs as binding motif for carboxylates in Nature. The structure of the binding site of the enzyme porphobilinogen deaminase shows how the NH of the pyrrole hydrogen bonded to a carboxylate (figure 72).¹⁰⁹

**Figure 72** Structure of the active site of the enzyme porphobilinogen deaminase.

Taking inspiration from this crystal structure and encouraged by the binding properties of the 2,5-diamidopyrrole,⁷⁷ Gale and co-workers synthesised a series of dipyrromethane based receptors.^{1,110} Receptor **77** and **78** give very high stability constants with phosphate and fluoride in very competitive solvents as DMSO-25% water (figure 73).

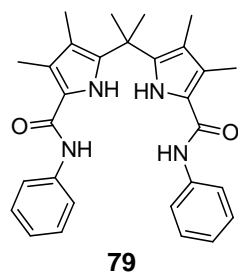


Anion (TBA salt)	Receptor $K_a (M^{-1})$	
	77	78
F ⁻	7560	8990
Cl ⁻	23	43
Br ⁻	13	10
HSO ₄ ⁻	44	128
BzO ⁻	354	424
F ^{-a}	11	114
H ₂ PO ₄ ^{-a}	20	234

Figure 73 Binding properties of receptor **77** and **78** in DMSO-*d*₆-5% water. ^aDMSO-*d*₆-25% water.

Receptors **77** and **78** were not stable. It was found that they were easily oxidised at the methylene position in solution.¹ Therefore it was necessary to synthesize analogous compounds containing two alkyl groups attached to the sp³ hybridized *meso*-carbon. This strategy has been used also to stabilize calixpyrroles.⁷⁰

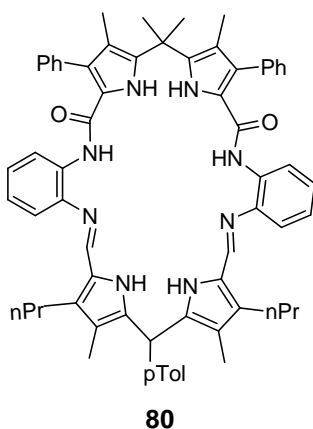
Receptor **79** has a good selectivity for oxo-anions such as carboxylates and phosphate in the competitive solvents mixture DMSO-*d*₆- 5% water (figure 74).



Anion (TBA salt)	Receptor $K_a (M^{-1})$
	79
F ⁻	124
Cl ⁻	<15
BzO ⁻	41
H ₂ PO ₄ ⁻	1092

Figure 74 Binding properties of receptor **79** measured by NMR titration in DMSO-*d*₆ - 5% water

The dipyrromethane unit has been inserted by Sessler and co-workers in a series of Schiff-base macrocycles (figure 75).¹¹¹



Anion (TBA salt)	Receptor $K_a (M^{-1})$
	80
Cl ⁻	4100
AcO ⁻	4100 000 ^a
HSO ₄ ⁻	18700
H ₂ PO ₄ ⁻	850 000

Figure 75 Structure and binding properties of macrocycle **80** in neat acetonitrile by means of UV-Titrations. ^aBinding constants determined from competition studies with dihydrogen phosphate.

On the basis of these results the project will involve the synthesis and the study of the properties of both chiral and achiral dipyrromethane based receptors (figure 76).

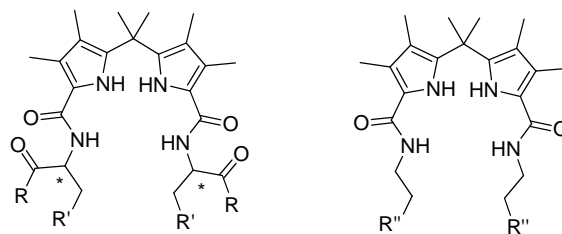


Figure 76 General structure of the acyclic dipyrromethane based receptor

The introduction of two further amide groups and the major preorganisation of the macrocyclic structures (figure 77) should increase the affinity for the anions as well as the enantioselectivity.

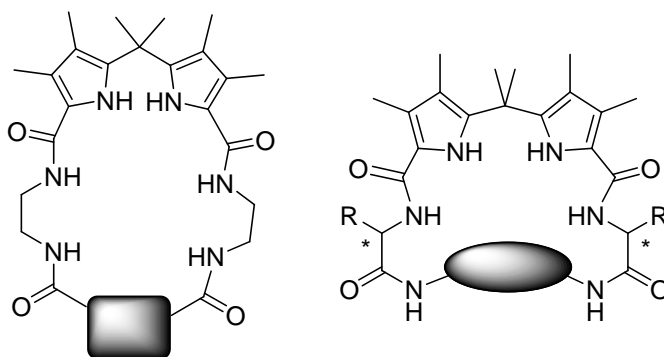


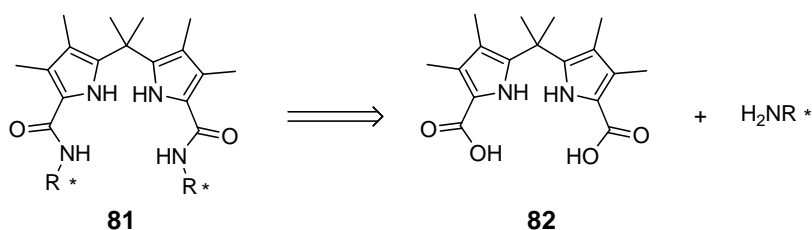
Figure 77 General structure of cyclic dipyrromethane-based receptors

Chapter II

Acyclic Dipyrromethane Based Receptors

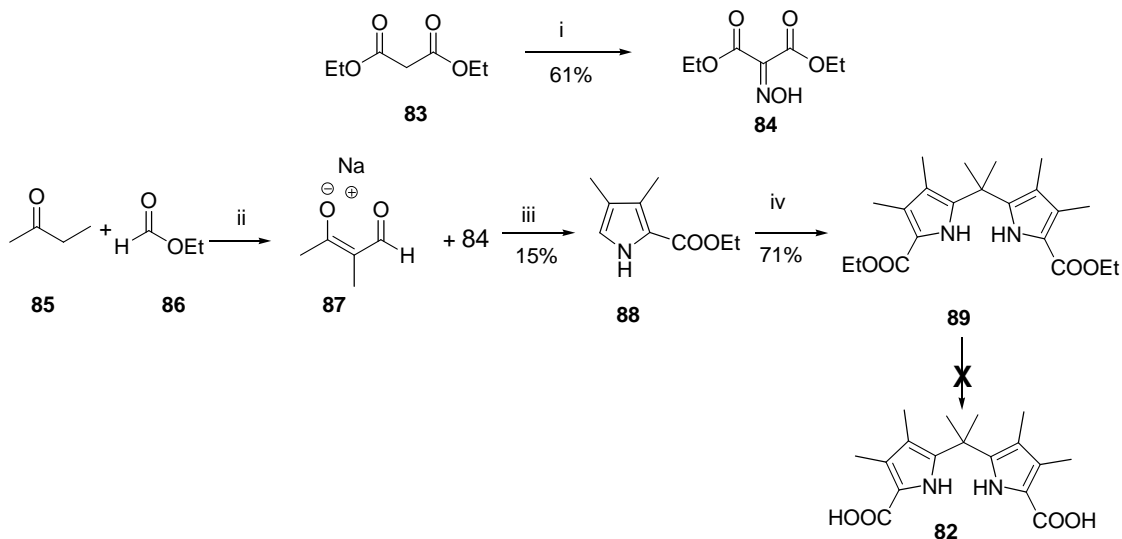
2.1 Synthesis of the dipyrromethane core

Acyclic dipyrromethane based receptors with general structure **81** can be synthesised by coupling diacid **82** with a series of amines, to obtain a wide range of receptors (scheme 2).



Scheme 2

Our first aim was to develop a reliable and efficient way to synthesise diacid **82** on a multigram scale. The route previously used in our group was undertaken first.¹ The key intermediate of this synthesis is 2-carboethoxy-3,4-dimethyl-1*H*-pyrrole **88** (Scheme 3).

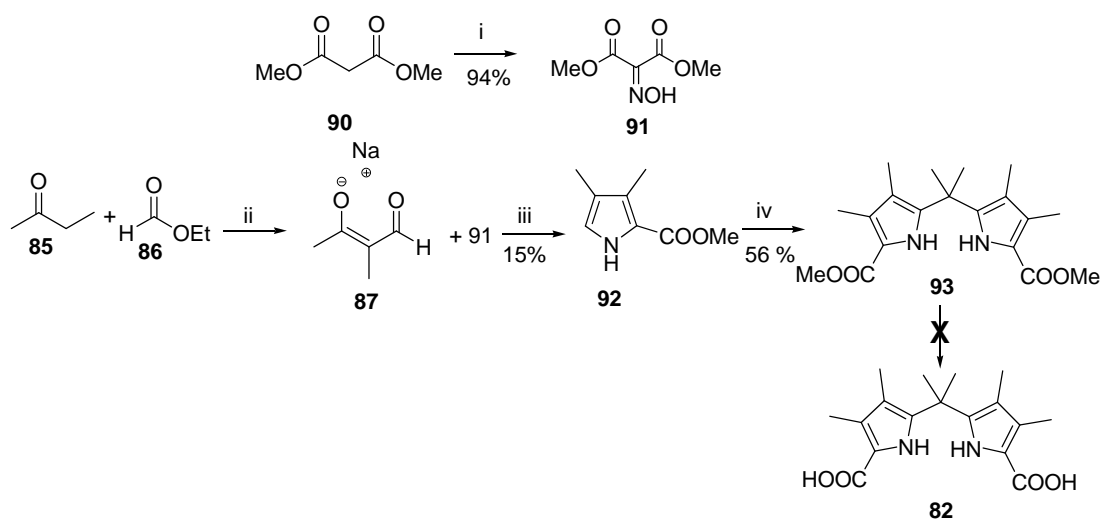


Scheme 3 i) NaNO_2 , NaOH , AcOH ; ii) Na , THF ; iii) Zn , NaOAc , AcOH ; iv) 2,2 dimethoxypropane, $p\text{TsOH}$, DCM .

Ethyl malonate **83** was converted into oximine **84** upon treatment with sodium nitrite under acidic conditions.¹¹² Butan-2-one **85** and ethyl acetate **86** were condensed in the presence of sodium metal to yield salt **87**. A reductive condensation of oximino-malonate **84** and salt **87** in acidic conditions yielded 2-carboethoxy-pyrrole **88** in only 15% yield.^{113,114} This procedure is known as Paal-Knorr pyrrole synthesis.¹¹⁵ The condensation of two pyrrole units in the presence of dimethoxypropane catalysed by *p*-toluenesulfonic acid lead to the formation of dipyrromethane **89**.¹¹⁶ The hydrolysis en route to **82**, however, was capricious giving yields between 0% and 68%. Competing decarboxylation¹¹⁷ was believed to be the main problem in this base mediated hydrolysis. A variety of conditions were attempted (by changing the base and tuning the temperature)¹¹⁸ but none was particularly successful.

As the problem was the hydrolysis of the aromatic diethyl ester **89**, two solutions were considered: the choice of a better leaving group than ethoxy such as methoxy, or the choice of a different reaction. For this purpose a milder method, such as catalytic hydrogenolysis of benzyl ester was envisaged. Both methods were undertaken.

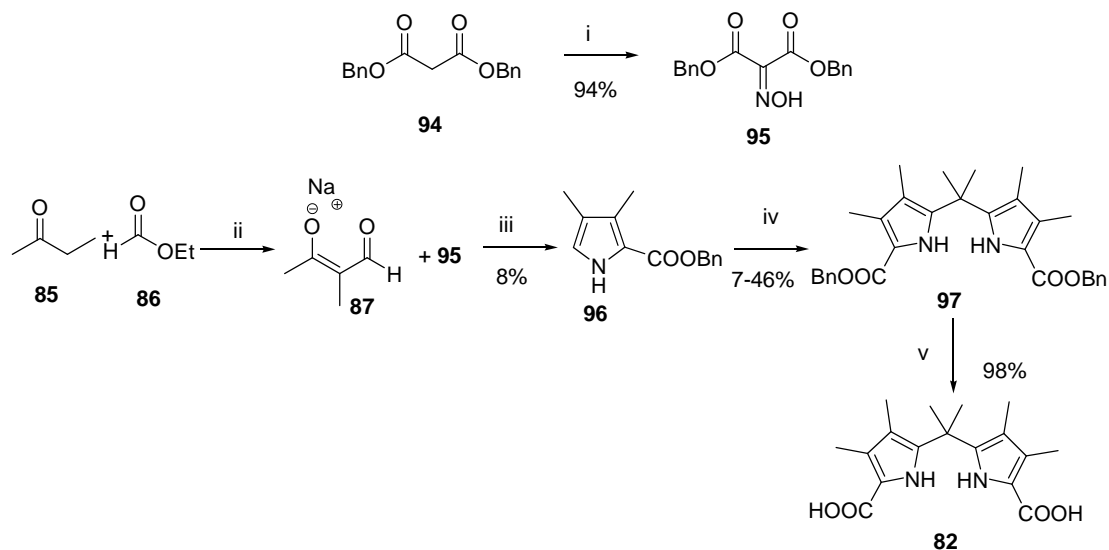
The key intermediate for the synthesis of dimethyl ester **92** was 2-pyrrole methyl ester **92** (scheme 4).



Scheme 4 *i) NaNO₂, NaOH, AcOH; ii) Na, THF; iii) Zn, NaOAc, AcOH; iv) 2,2 dimethoxypropane, pTsOH, DCM.*

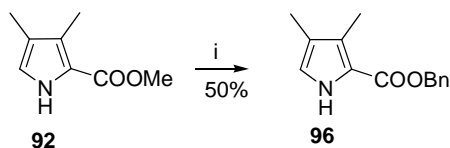
The same protocol used for the synthesis of dipyrromethane **89** was followed. 2-carbomethoxy-pyrrole **92** was obtained with the same yield of **88**, without chromatography. However, despite several attempts hydrolysis of **93** was not successful and diacid **82** was never obtained.

The key intermediate that needed to be synthesised to perform the catalytic hydrogenolysis instead of the hydrolysis was 2-pyrrole benzyl ester **96** (scheme 5)



Scheme 5 i) NaNO_2 , NaOH , AcOH ; ii) Na , THF ; iii) Zn , NaOAc , AcOH ; iv) $2,2\text{-dimethoxypropane}$, $p\text{TsOH}$, DCM , v) Pd/C , H_2 , THF .

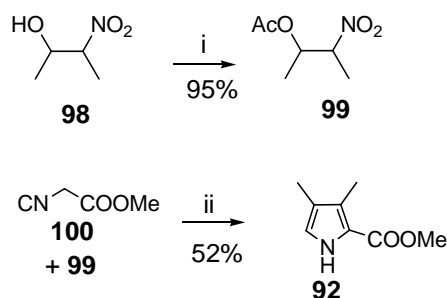
The same protocol used for the synthesis of dipyrromethanes **89** and **93** was followed. Unfortunately, 2-carbobenzoxypyrrole **96** was not obtained with sufficient purity and this affected the following step. However, diacid **82** was smoothly obtained in excellent yield under H_2 atmosphere and in presence of Pd/C . Therefore it was then decided to combine the advantages of each procedure to establish a reliable protocol to obtain diacid **82**, by synthesising 2-carbomethoxy-pyrrole **92** and converting it into 2-benzoxypyrrole **96** by transesterification (scheme 6).



Scheme 6 i) BnOH , NaHMDS .

Methyl ester **92** was thus transesterified in good yield into benzyl ester **96** in presence of benzyl alcohol and NaHMDS.¹¹⁹ Diacid **82** was then prepared smoothly with the protocol previously described (scheme 5).

A further improvement was obtained using the Zard-Barton method^{120,121} (scheme 7), which provided a threefold yield increase and a reaction crude that allowed a more expeditious purification.



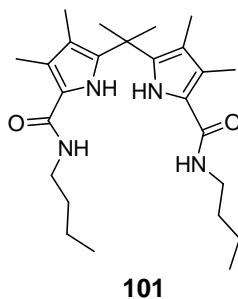
Scheme 7 i) Ac_2O , DMAP, DCM; ii) **99**, THF; DBU.

Commercially available nitrobutanol **98** was acetylated and subsequently condensed with **100** in basic conditions to yield pyrrole **92** in reasonable yield. The protocol to obtain diacid **82** was optimised in due course: the combination of the Zard-Barton method to obtain the pyrrole **92** and the transesterification allowed the efficient preparation of a quantity of diacid **82** sufficient to synthesise and study a variety of receptors.

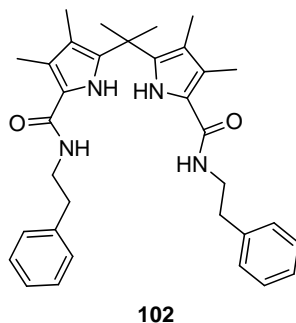
2.2 Overview of the synthesised receptors

Simple achiral tweezer receptors containing a dipyrromethane moiety were recently synthesised and analysed in our group¹ and showed interesting properties in binding oxo-anions such as phosphate and acetate. In this study these structures were modified in order to investigate the role of each single component in binding anions and to synthesise chiral receptors for amino acid recognition.

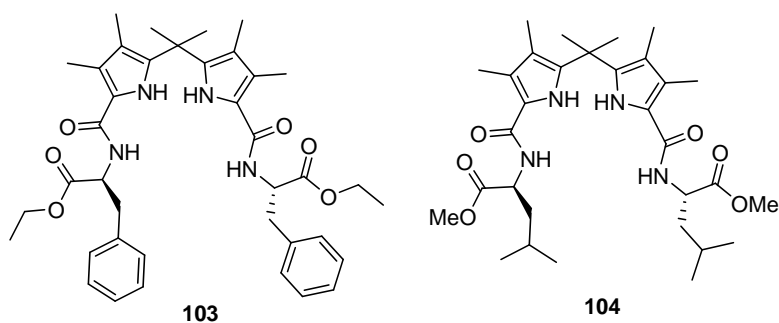
As the goal of our project was to incorporate the chirality by coupling an amino acid to diaacid **82**, the resulting amide would be aliphatic and therefore it was decided to investigate the binding properties of receptor **101** (figure 78) as a model. This receptor was already synthesised and analysed by the group.¹ In this study it was re-synthesised and tested in different solvents.

**Figure 78**

It was then decided to introduce a phenyl ring and receptor **102** (figure 79) was synthesised.

**Figure 79**

A further step consisted of introducing chirality into the system. This objective was achieved by coupling diacid **82** with different amino acid derivatives. Two receptors were then synthesised: **103** bearing an aromatic residue and **104** bearing an alkyl residue (figure 80).

**Figure 80**

To enhance the number of the possible interactions between the receptor and the guest, particularly with an amino acid guest, in order to increase the enantioselectivity, polar

groups were added into the system. This was achieved by substituting phenylalanine with serine (**106** figure 81) and by changing the ester to an amide (**105**). Tweezer **107** was synthesised for a more appropriate comparison with **105**. To check effectively the structure-activity relationship only one change should be made at a time on the molecule.²¹

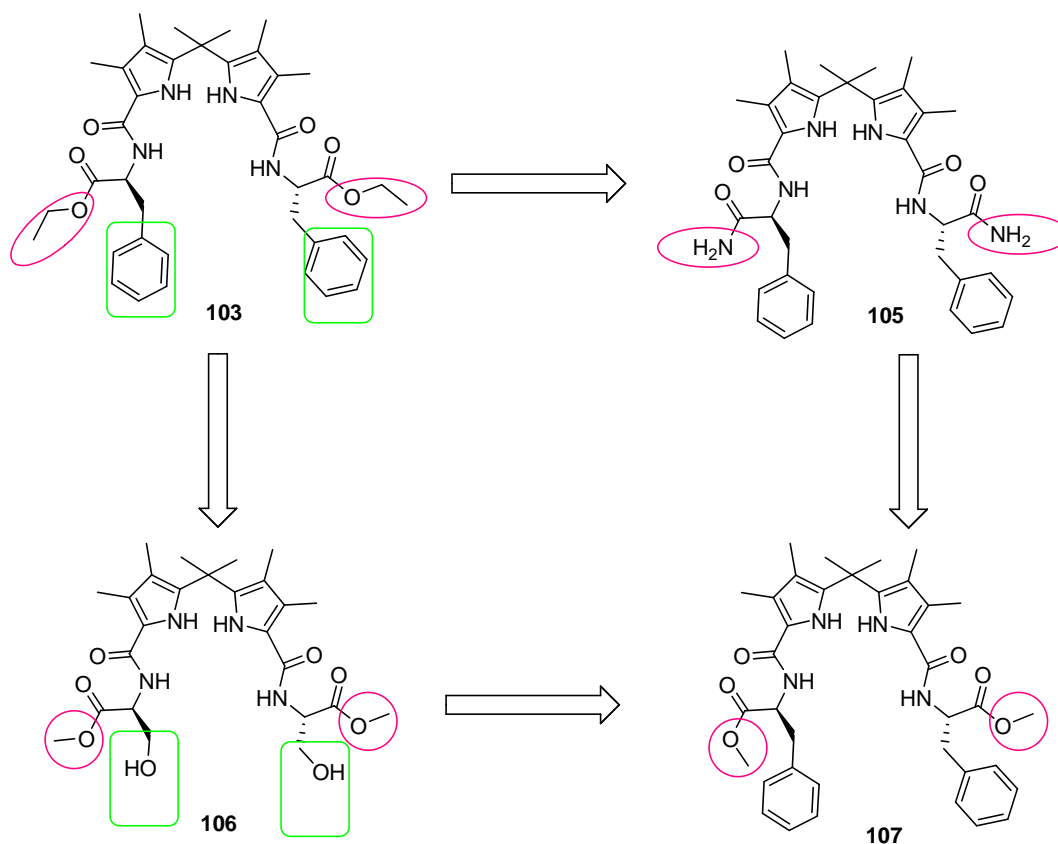
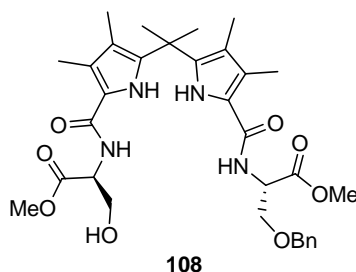
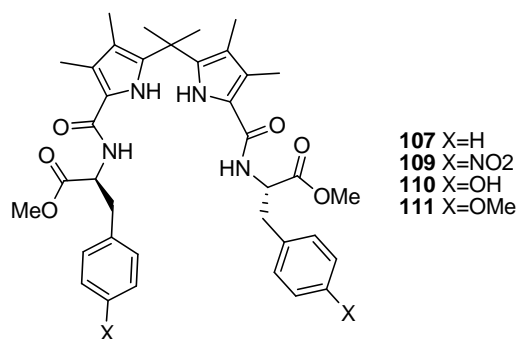


Figure 81

To complete our investigation on the effects of hydrogen bonding donors, tweezer **108**, a partially protected form of receptor **106**, was also synthesised.

**Figure 82**

The possible interactions between the phenyl ring of the phenylalanine and the anionic guest were also investigated by varying the substituents on the phenyl ring. The substituents modulate the π system's electron density and therefore the properties of the whole ring are affected (e.g. it modulates the acidity of the C-H bonds). A receptor bearing an electron donating group (**110** figure 83) and one with an electron withdrawing group (**109** figure 82) were synthesised and their properties were analysed and compared to **107**.

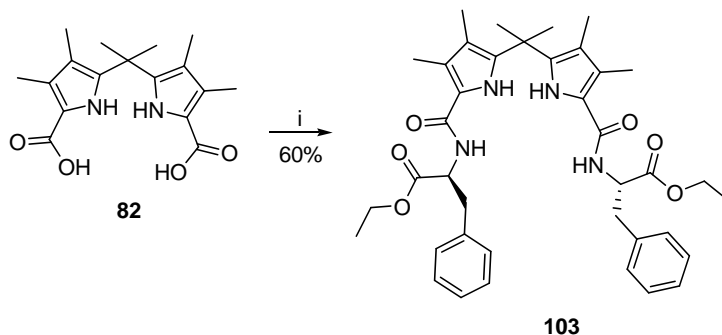
**Figure 83**

As the phenol of **110** could be deprotonated by addition of a basic anionic guest and interfere with the formation of the complex, a methylated version of tweezer **110** was also synthesised.

2.3 Synthesis of the tweezer receptors

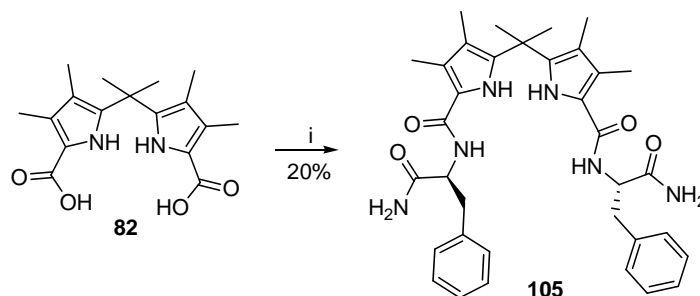
Dipyrromethane-based tweezer receptors were synthesised by coupling diacid **82** with the related amine. The coupling conditions were optimised during the course of this study.

Receptor **103** was synthesised by coupling the dipyrromethane diacid **82** with the ethylester of phenylalanine hydrochloride (scheme 8).



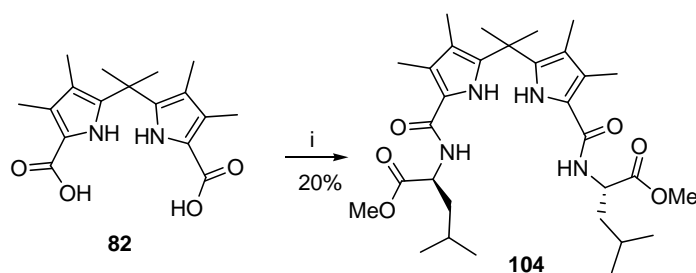
Scheme 8 i) EDC, HOBt, DIPEA, H_2N -L-Phe-OEt.HCl, DCM.

Receptor **103** was obtained in good yield following an EDC/HOBt¹²² mediated coupling. The same conditions were used for the synthesis of receptor **105** (scheme 9).



Scheme 9 i) EDC, HOBt, DIPEA, H_2N -L-Phe-NH₂.HCl, DCM.

Tweezer **105** was obtained in low yields due to poor solubility and purification difficulties. Using a similar procedure receptor **104** was synthesised (scheme 10). In this case the activated ester was formed by using PyBOP as coupling reagent.

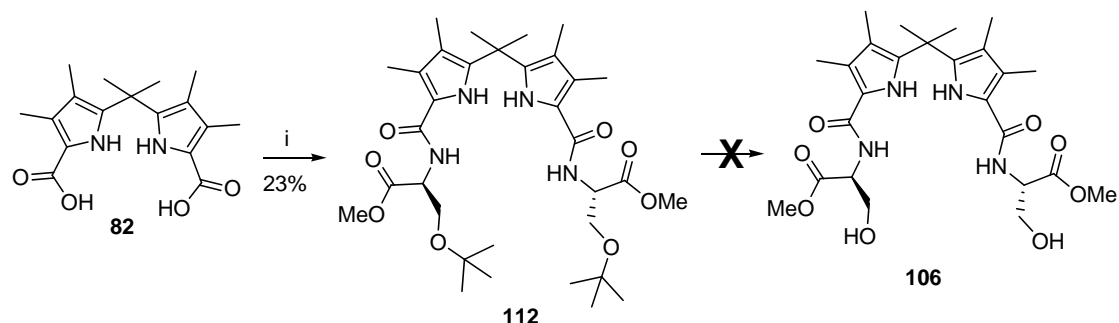


Scheme 10 i) H_2N -L-Leu-OMe.HCl, PyBOP, Et₃N, DCM

Receptor **104** was obtained in poor unoptimised yield.

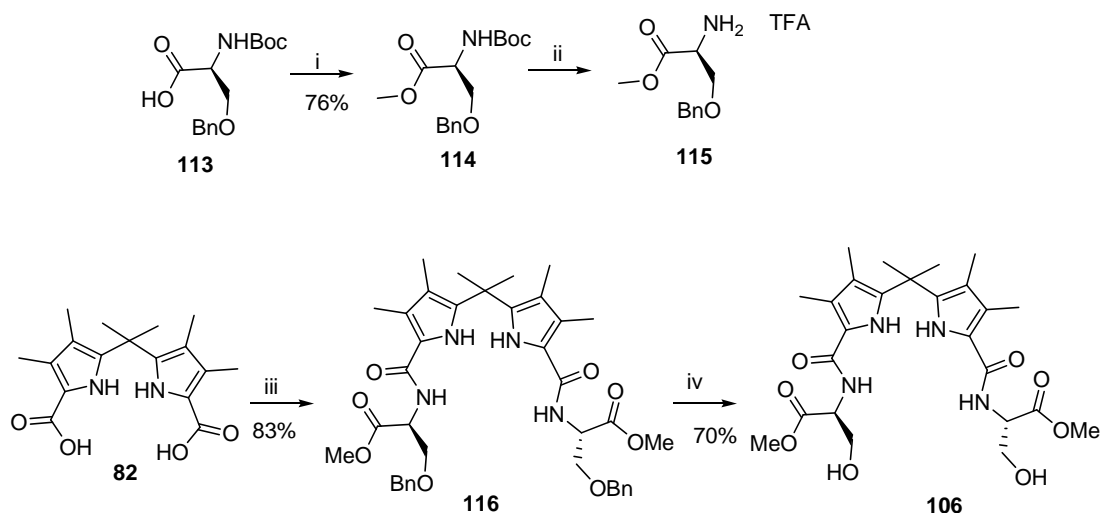
For the synthesis of receptor **106** it was decided to use the serine methyl ester protected on the side chain with a *tert*-butyl group (scheme 11), to increase the solubility of the

tweezer and facilitate its purification. The desired tweezer would then be obtained by deprotection under acidic conditions.



Scheme 11 *i) PyBOP, DIPEA, H₂N-L-Ser(OtBu)-OMe.HCl, DCM.*

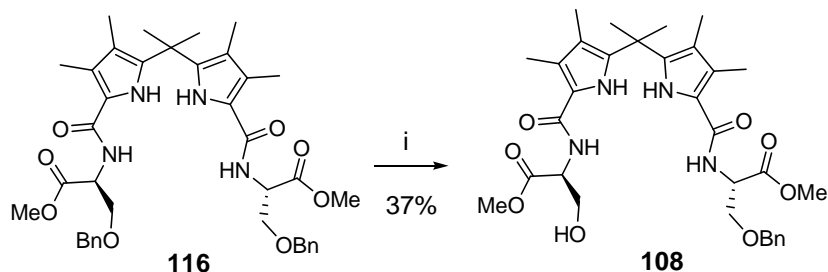
The formation of tweezer **112** proceeded smoothly but in low yield, which was not optimised: however the removal of the *tert*-butyl groups under acidic conditions was surprisingly slow and led to decomposition. Acidity was assumed to be the cause of the decomposition, therefore a protecting group that could be removed in neutral or basic conditions was needed, and, for this reason, benzyl ether was chosen (scheme 12).



Scheme 12 *i) MeI, NaHCO₃, DMF; ii) TFA, DCM; iii) 115, PyBOP, DIPEA, DCM; iv) H₂, Pd/C, THF.*

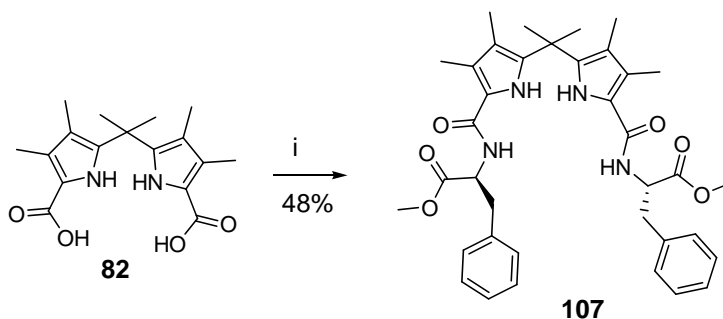
Commercially available serine **113** was methylated using a literature procedure.¹²³ The Boc deprotection of **114** led to the formation of a suitable precursor for tweezer **116**; which was synthesised with a PyBOP¹²⁴ mediated coupling. The cleavage of the benzylether^{125,126} was slow (4 days) but proceeded smoothly and dialcohol **106** was obtained in good yield.

Receptor **108** was obtained by modifying the deprotection conditions (percentage of catalyst and reaction time) of tweezer **116** (scheme 13).



Scheme 13 i) H_2 , Pd/C, THF.

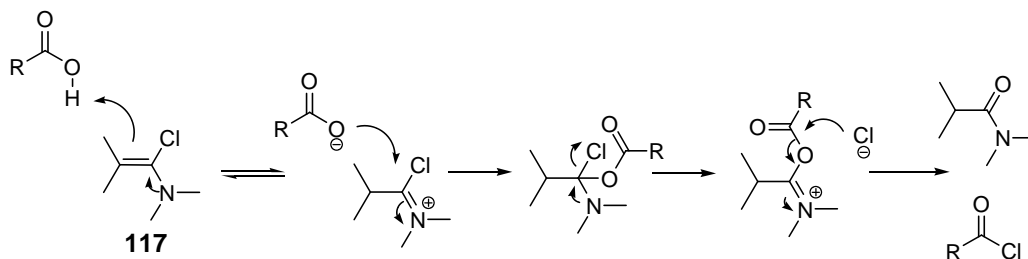
For the synthesis of receptor **107** a study has been done to evaluate which was the best protocol for the peptide coupling of diacid **82** and an amine in terms of yields and purification issues. A preliminary investigation showed that the conversion took place only when PyBOP¹²⁴ or a mixture of EDC and HOBt¹²² was used (scheme 15).



Scheme 14 i) EDC, HOBt, DIPEA, H_2N -L-Phe-OMe.HCl, DCM

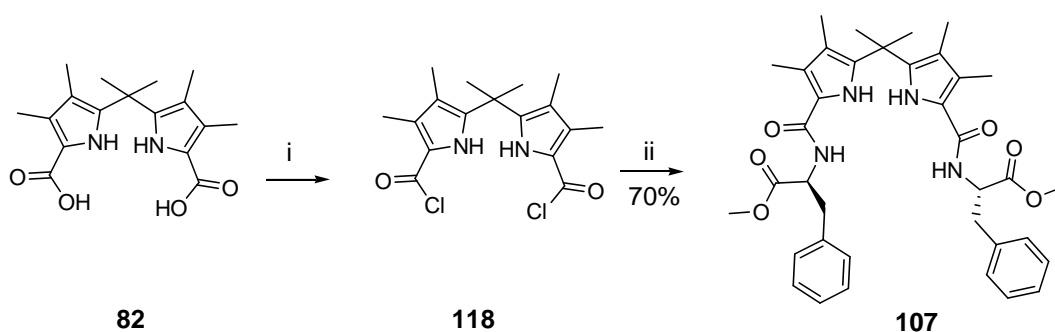
No product was detected when the synthesis was attempted using the activated ester with hydroxysuccinimide,¹²⁷ pentafluorophenol¹²⁸⁻¹³⁰ or CDI.^{131,132}

In order to minimise the purification problems, a general strategy involving acyl chloride of **82** was considered. The acyl chloride mediated coupling was capricious when oxalyl chloride¹³³ was used. This could be attributed to the acid sensitivity of pyrroles, as seen in the deprotection of tweezer **112**, which underwent decomposition in acid conditions, and the HCl generated by oxalyl chloride¹³⁴ might have affected the dipyrromethane system. For this reason the use of the Ghosez¹³⁵ reagent was envisaged. This reagent (1-chloro-*N,N*,2-trimethylprop-1-en-1-amine) is a mild way to obtain acyl chlorides, and no hydrochloric acid is developed during the reaction which works at room temperature (scheme 15).



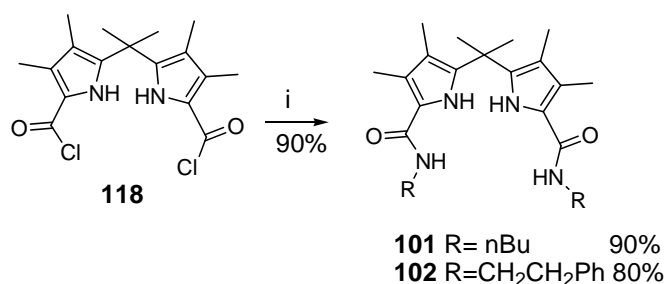
Scheme 15 Mechanism of the formation of acyl chloride with Ghosez reagent¹³⁵

A first test yielded receptor **107** in slightly improved yield in comparison with the EDC/HOBt promoted coupling (scheme 16).



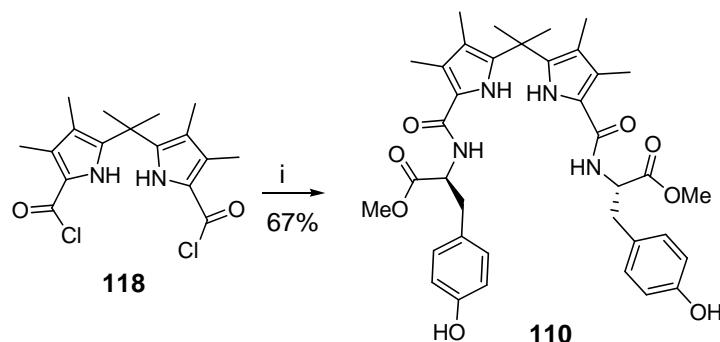
Scheme 16 i) 1-chloro-*N,N*,2-trimethylprop-1-en-1-amine, THF; ii) H_2N -L-Phe-OMe·HCl, Et_3N , DCM. *yield calculated on the crude with NMR.

This protocol was applied to other substrates and tweezers were obtained in good yield. Receptors **101** and **102** were synthesised in excellent yields by coupling acyl chloride **118**, which was formed with the Ghosez reagent, with an excess of the relevant amine (Scheme 17).



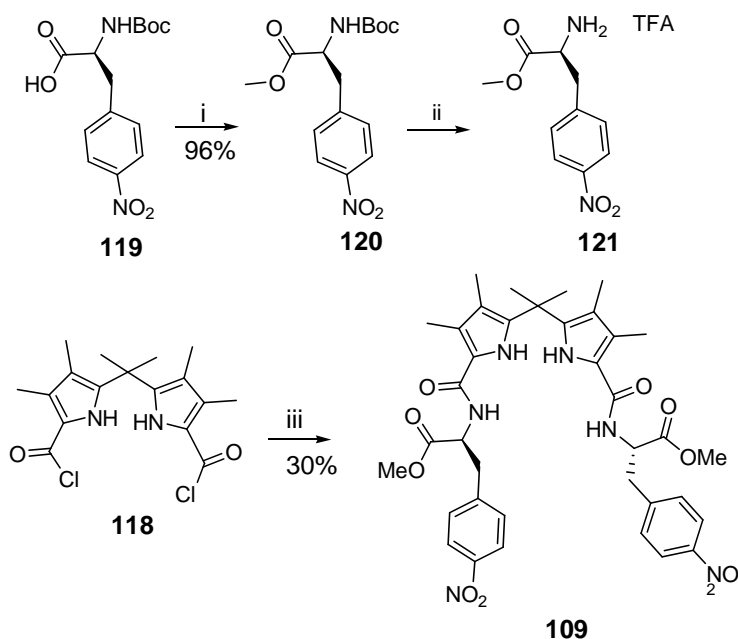
Scheme 17 i) NH_2R , DCM.

A similar protocol was used for the synthesis of tweezer **110** (Scheme 18).



Scheme 18 i) H_2N -L-Tyr(OH)OMe.HCl, Et_3N , DCM.

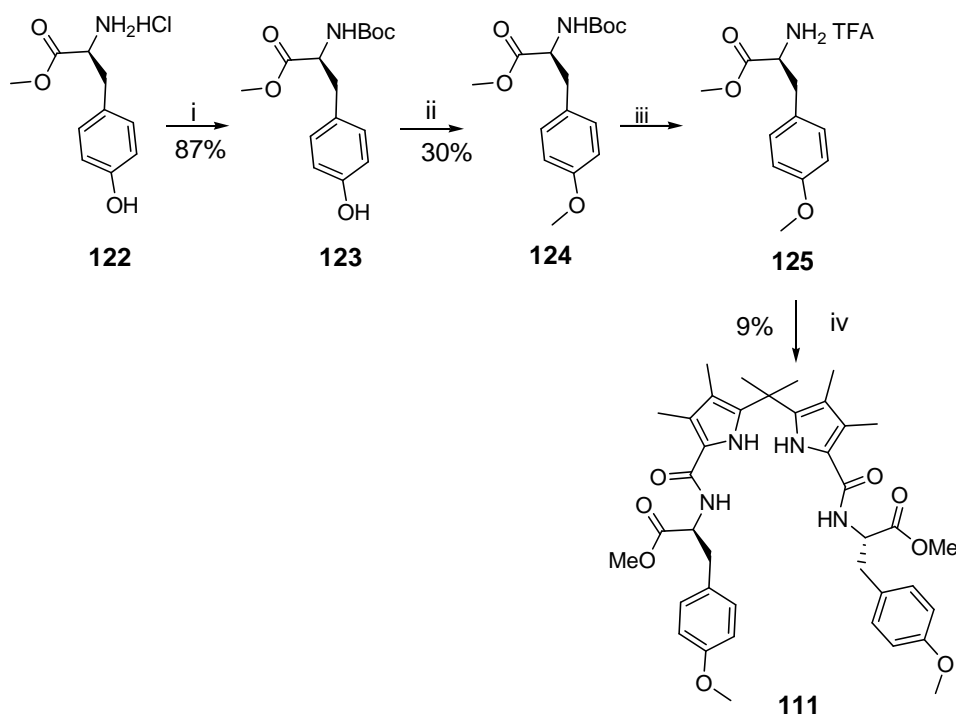
For the synthesis of receptor **109** (scheme 19) and **111** the relevant amines needed to be synthesised by modification of the commercially available amino acids.



Scheme 19 i) TMS-diazomethane, MeOH, toluene; ii) TFA, DCM; iii) **121**, Et_3N , DCM.

Commercially available *p*-nitro phenylalanine **119** was methylated in excellent yield with TMS-diazomethane¹³⁶ to yield methyl ester **120**, which was then deprotected and coupled with acyl chloride **118** to yield tweezer **109** in reasonable yield.

Tweezer **111** was synthesised by coupling the tyrosine derivative **125** (scheme 20) with diacid **82** with a PyBOP mediated coupling.



Scheme 20 i) Boc_2O , NaHCO_3 , THF , MeOH ; ii) K_2CO_3 , MeI , DMF ; iii) TFA , DCM ; iv) PyBOP , DIPEA , **82**, DCM

Tyrosine **122** was protected in good yields following a literature procedure.¹³⁷ The methylation of **123** was more problematic, after a series of attempts it worked only in moderate yields under the conditions described (scheme 21).¹³⁸

The methylated tyrosine **124** was converted quantitatively into TFA salt **125** which reacted with diacid **82** in presence of PyBOP to yield tweezer **111**, in low, unoptimised yield.

2.4 Methods used to analyse the binding properties

The binding process is an equilibrium associated with a thermodynamic binding constant (K) (§1.2.2).



Equation 1 Binding equilibrium and related constant

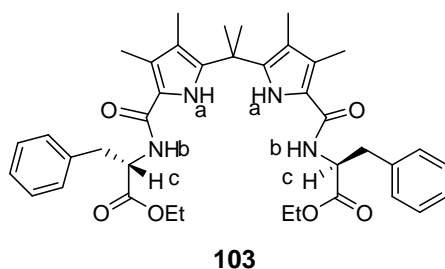
The techniques developed to calculate the binding constant consist of adding small aliquots of a guest stock solution to a solution of host and measuring the properties of the resulting solution. During this study NMR titrations and UV titrations were undertaken.

2.4.1 NMR Titrations

When the complex is formed a change of the chemical shift of the receptor's protons is observed, because, in the complex, the magnetic field around the nucleus is not equivalent to the field in the uncomplexed host. The chemical shift of a proton will be the average signal from the free host and from the host associated with the guest, provided that the exchange is fast on the NMR timescale. By plotting the different chemical shifts versus the equivalents of guest added a curve is obtained.

The titration between tweezer **103** and the tetrabutylammonium salt of *N*Boc-D-Phe in CD₃CN will be taken as an example.

Upon addition of the guest to a solution of receptor **103** the pyrrolic (*a*, figure 84) and amidic (*b*) protons shifted 2 ppm downfield, which is the typical behaviour of a proton involved in a hydrogen bond interaction. The signal belonging to the amino acid's CH (*c*) had a small ($\Delta\delta \approx 0.2$ ppm) upfield movement, this proton was not directly involved in the hydrogen bond but its change in chemical shift was a consequence of the binding process.



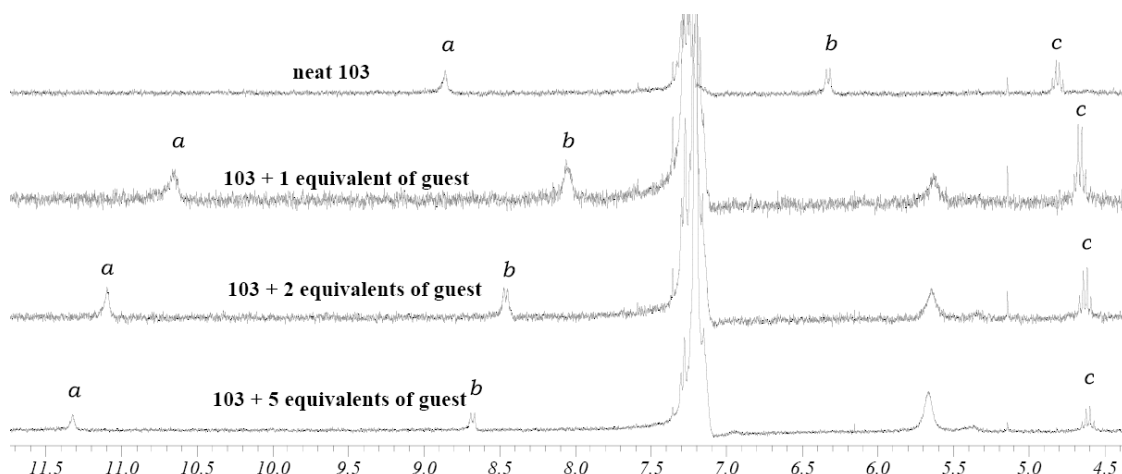


Figure 84 Changes observed in the chemical shift of the pyrrolic (a) amidic (b) and CH (c) protons upon addition of the tetrabutylammonium salt of NBoc-D-Phe-O to a solution of **103** in CD_3CN .

The changes in the chemical shift were then plotted against the guest concentration and a curve was then formed. For example the chemical shift of the pyrrole proton was plotted (figure 85).

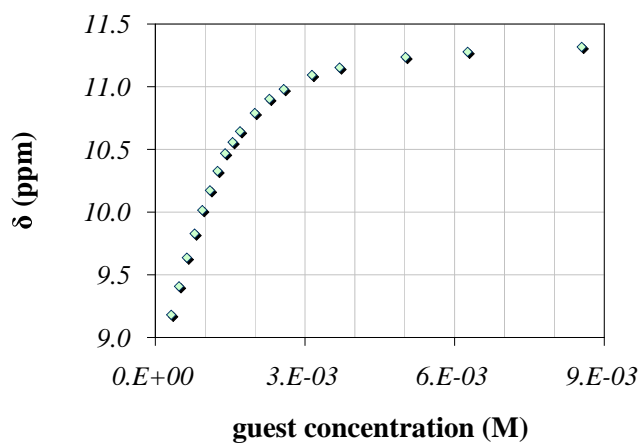


Figure 85 Curve obtained by plotting the chemical shift of the pyrrole (a) proton upon addition of guest against the concentration of guest in solution

The binding constant is calculated from the curve with a curve fitting software such as titNMR provided by Chris Hunter.¹³⁹ This program can calculate the binding constant according to the predefined binding model. In this case, the shape of the curve suggested

that the undergoing process was a 1:1 host: guest complexation and it was calculated with titNMR. The values obtained by the calculation of the binding constant measured from each proton, in theory, should be the same because the binding constant is a macroscopic effect that describes the behaviour of the system.

In this case the value of the 1:1 binding constant calculated from every proton is similar (table 6) and the stability constant of the complex between tweezer **103** and the tetrabutylammonium salt of NBoc-D-Phe gave an average value of $4.95 \cdot 10^3 \text{ M}^{-1}$.

	Protons monitored		
	a	b	c
$K_a(\text{M}^{-1})$	4790	5140	4910

Table 6 Values obtained fitting in a 1:1 model the curves obtained by monitoring the pyrrole (a), amidic (b) and (c) CH proton of tweezer **103** in the titration with NBoc-D-PheOTBA in CD_3CN .

The NMR titrations have some limitations, but they are generally reliable for association constants in the range of $10\text{-}10^4 \text{ M}^{-1}$. A higher binding constant can be measured accurately only when the solutions have a concentration in the μM range and the NMR is not sensitive enough to detect a product at such a low concentration.¹⁴⁰

2.4.2 UV Titrations

The Ultraviolet-visible spectrophotometric titration is a very sensitive technique that allows detection at very low concentrations. It has, however, some limitations: the host and the complex must be UV active and they must absorb at different wavelengths.

The UV titration method is also used to understand the stoichiometry of the binding. By superimposing all the spectra obtained by a UV titration, keeping constant the concentration of the host, the presence or the absence of an isosbestic point can give some information about the stoichiometry of the binding. An isosbestic point is the point of common adsorption intensity for all spectra of a titration.¹⁴¹ If an isosbestic point is present it can be concluded that only two stoichiometric species are present in solution, therefore only one complex is formed. So the stoichiometry should be 1:1.¹⁴¹ For example the UV titration between receptor **107** and tetrabutylammonium acetate was performed by adding small aliquots of acetate to a solution of tweezer **107** in CH_3CN . After each

addition, a UV spectrum of the resulting solution was recorded. Upon addition of acetate the absorption band at 289 nm was decreasing, while an absorption band at 271.5 nm was formed. By superimposing the spectra of the titration (figure 86) an isosbestic point was observed, which was an indication that the binding stoichiometry was 1:1.

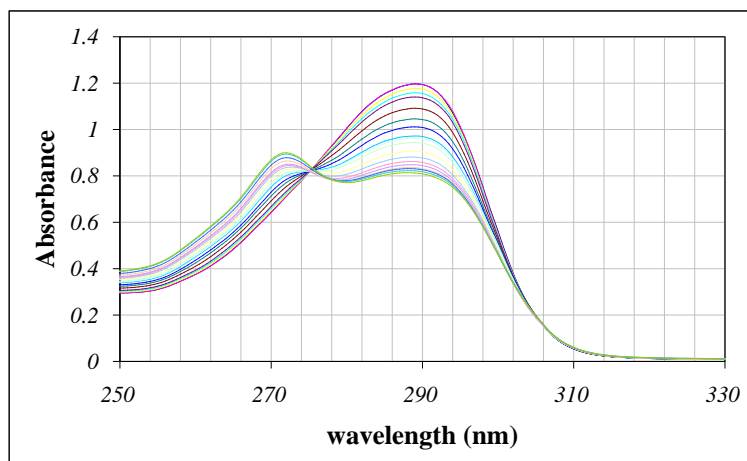


Figure 86 Superimposed absorption spectra obtained from the titration of **107** with tetrabutylammonium acetate in CH_3CN .

The binding constant could be calculated by monitoring the changes on the absorbance at a certain wavelength (e.g. at 289 nm, figure 87) against the concentration of the guest and treating the curve with a curve fitting software program.

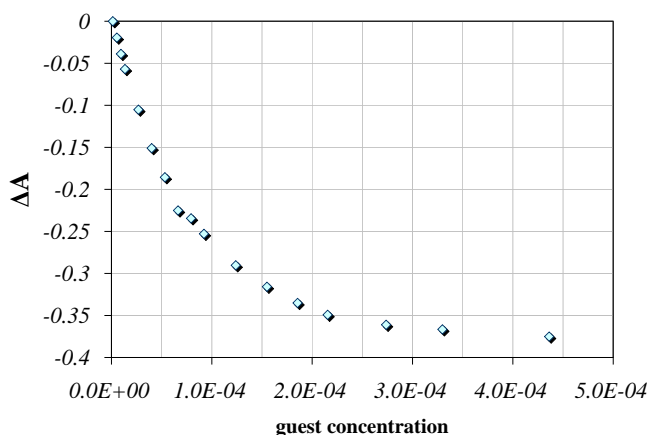


Figure 87 Curve obtained by plotting the difference of absorbance (ΔA) at 289 nm observed upon addition of guest to a solution of **107** in CH_3CN against the concentration of tetrabutylammonium acetate.

The binding constant calculated according the binding model 1:1 host:guest was $K_a = 15300 \text{ M}^{-1}$.

2.4.3 Job Plot

The stoichiometry of the binding can also be evaluated by an NMR technique called a Job Plot. A Job Plot, also called the method of continuous variation, consists of preparing a series of solutions of substrate and receptor where the total mole fraction of the host and the guest is constant. A spectrum is recorded for each solution. By plotting the value obtained by multiplying the difference of the chemical shift for the molar fraction of the guest ($\Delta\delta \cdot \chi_H$) against the mole fraction of the host,¹⁴⁰ a parabola will be represented and the position of the maximum indicates the stoichiometry of the binding.

If the maximum is at 0.5 the complex formed is a 1:1 host:guest. If on the other hand the maximum is at 0.33 the stoichiometry of the binding will be 1:2 host:guest, in the case of the maximum at 0.66 the major binding process would be 2:1 host:guest.

The Job Plot of the complex between receptor **107** and tetrabutylammonium acetate was performed (figure 88).

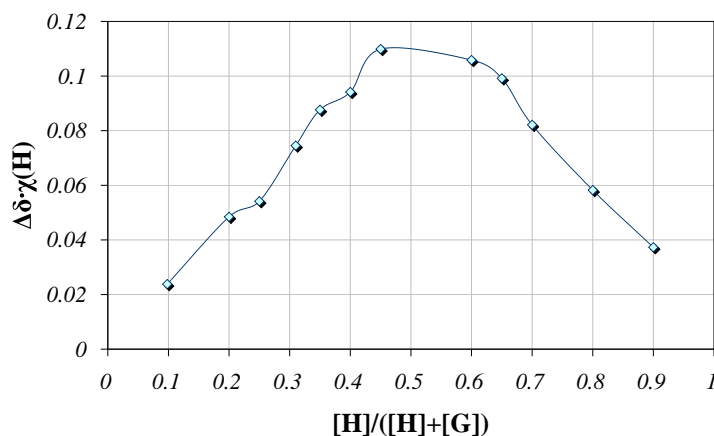


Figure 88 Job plot of receptor **107** with tetrabutylammonium acetate in CD_3CN

The Job plot confirmed that the stoichiometry was 1:1 host:guest.

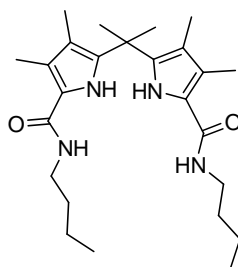
2.5 Binding properties of dipyrromethane tweezer receptors in DMSO- d_6

The binding properties of the dipyrromethane based tweezer receptors were investigated with a series of anions in DMSO-0.5% H_2O . DMSO is very hygroscopic, so it is very difficult to keep it dry, and, as the presence of water can affect the value of the binding constant, it was decided to add to every titration a known amount of water (0.5%) to standardise the conditions.

Anion (TBA salt)	Receptor $K_a (M^{-1})$					
	101	102	107	104	105	106
AcO^-	182	76	247	383	170	374
$H_2PO_4^-$	421	329	772	390	799	257
BzO^-	97	46	89	113	101	109
Cl^-	27	a	a	a	a	29

Table 7 Binding constants measured by NMR titration in DMSO- d_6 -0.5% H_2O . The curves were fitted according the 1:1 host:guest binding model. ^aNo significant shift was observed during the titration.

Tweezer 101



Upon addition of anions to a solution of tweezer **101** in DMSO- d_6 -0.5% H_2O the pyrrole protons and the amide protons moved downfield. This indicated that the host formed a hydrogen bond interaction with the guest. The shift of the amide and pyrrole protons was monitored and the binding constants (table 7) were determined using the average between the values obtained by fitting the two curves, which were in good agreement, in a 1:1

host:guest model. Upon addition of chloride to a solution of tweezer **101** the shift of the amide and pyrrole protons was very small and the constant calculated was low, close to the limit of reliability of NMR titrations. Tweezer **101** was selective ~ 2:1 for dihydrogen phosphate over acetate, ~ 2:1 for acetate over benzoate and ~ 4:1 for benzoate over chloride.

The shift of the pyrrole protons upon addition of the various guests was plotted (figure 89), showing the selectivity trend.

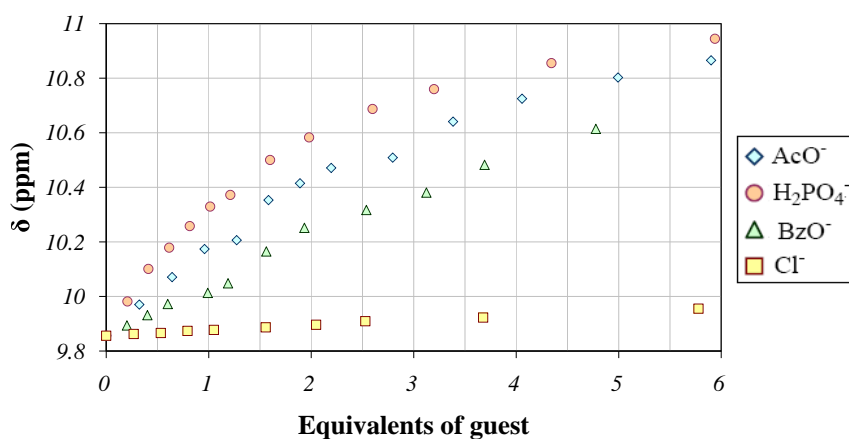
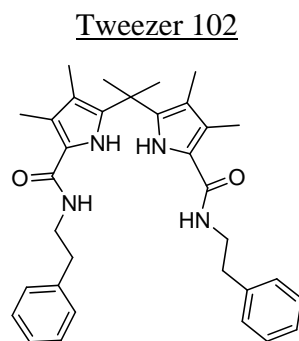


Figure 89 Curve obtained by plotting the chemical shift of the pyrrole (a) proton upon addition of anions to a solution of tweezer **101** in DMSO- d_6 -0.5% H_2O against the equivalents of guest.



Upon addition of anion guests to a solution of tweezer **102** in DMSO- d_6 -0.5% H_2O the pyrrole and amide protons shifted ($\Delta\delta \approx 0.8$ ppm) downfield. The binding constants were measured as the average of the values obtained by monitoring the shift of the two protons and fitting the curves in a 1:1 host:guest binding model. Tweezer **102** was selective ~ 4:1 for dihydrogen phosphate over acetate and ~ 2:1 for acetate over benzoate. Upon addition

of chloride to a solution of tweezer **102** no significant change in the chemical shift of the pyrrole and amide proton was observed, so it could be concluded that the host did not bind to the guest. The shift of the pyrrole protons upon addition of the various guests was plotted (figure 90), showing the selectivity trend.

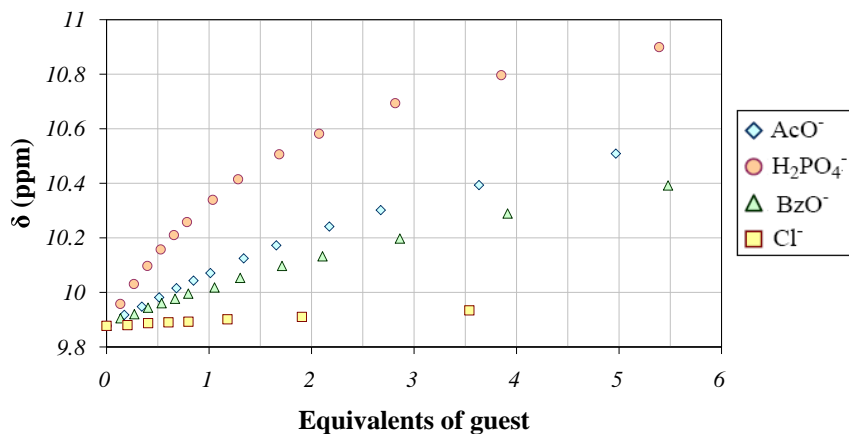
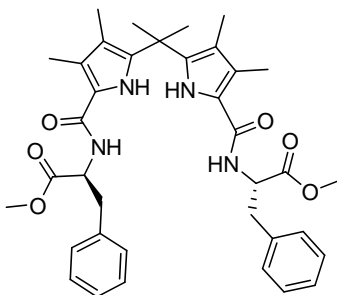


Figure 90 Curve obtained by plotting the chemical shift of the pyrrole (a) proton upon addition of anions to a solution of tweezer **102** in DMSO-*d*₆-0.5% H₂O against the equivalents of guest.

Tweezer 107



Upon addition of anion guests to a solution of tweezer **107** in DMSO-*d*₆-0.5% H₂O the pyrrole and amide protons shifted downfield. The shift of the amide and pyrrole protons was monitored and the binding constant (table 7) was the average between the values obtained by fitting the two curves, which were in good agreement, in a 1:1 host:guest model. Tweezer **107** was selective ~ 3:1 for dihydrogen phosphate over acetate and ~ 3:1 for acetate over benzoate. Upon addition of chloride to a solution of tweezer **102** no

significant change in the chemical shift of the pyrrole and amide proton was observed, so again it could be concluded that the host did not bind to the guest.

The shift of the pyrrole protons upon addition of the various guests was plotted (figure 91), showing the selectivity trend.

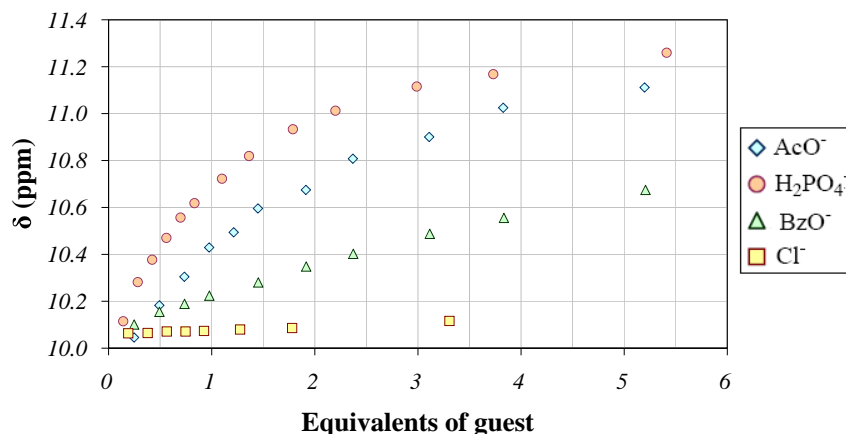
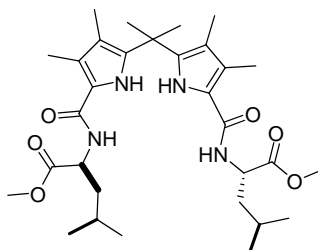


Figure 91 Curve obtained by plotting the chemical shift of the pyrrole (a) proton upon addition of anions to a solution of tweezer **107** in DMSO-*d*₆-0.5% H₂O against the equivalents of guest.

Tweezer 104



The amide and pyrrole protons shifted downfield as in the previous receptors analysed. The binding constants (table 7) were measured as the average of the value obtained by monitoring the shift of the two protons and fitting the curves in a 1:1 host:guest binding model. In this case there was no selectivity between acetate and phosphate. Tweezer **104** was selective ~ 4:1 for dihydrogen phosphate and acetate over benzoate. While no significant shift was observed upon addition of chloride to the solution of tweezer **104** in DMSO-*d*₆ -0.5% H₂O, therefore, it could be stated that no complex was formed. The shift

of the pyrrole protons upon addition of the various guests was plotted (figure 92), showing the selectivity trend.

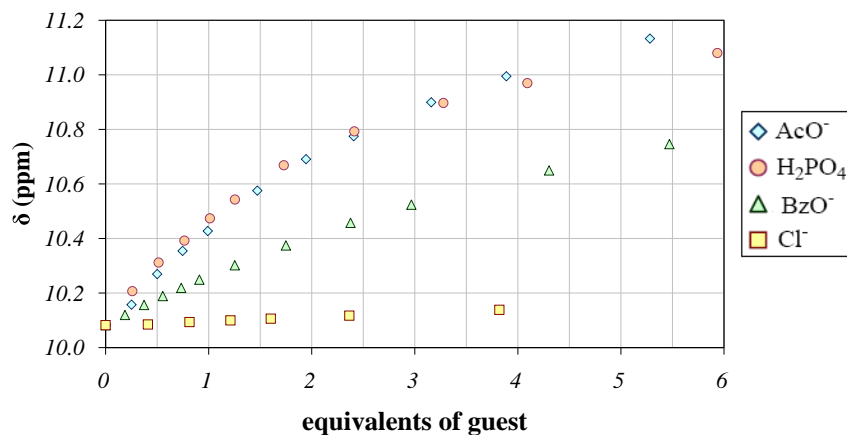
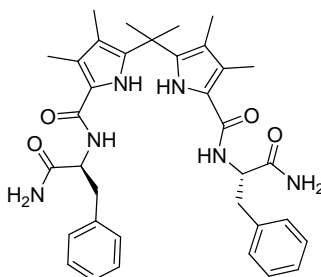


Figure 92 Curve obtained by plotting the chemical shift of the pyrrole (a) proton upon addition of anions to a solution of tweezer **104** in DMSO-*d*₆-0.5% H₂O against the equivalents of guest

Tweezer 105



Upon addition of anion guests to a solution of tweezer **105** in DMSO-*d*₆-0.5% H₂O the pyrrole and amide protons shifted downfield, apart from chloride, which did not provoke any significant change in the spectrum, and therefore it was assumed that no complex was formed. The binding constants (table 7) were calculated as the average of the values obtained from fitting the curves of the chemical shift of the pyrrole and amide protons in a 1:1 binding model. Tweezer **105** was selective ~ 5:1 for dihydrogen phosphate over acetate and ~ 1.7:1 for acetate over benzoate. The shift of the pyrrole protons upon addition of the various guests was plotted (figure 93), showing the selectivity trend.

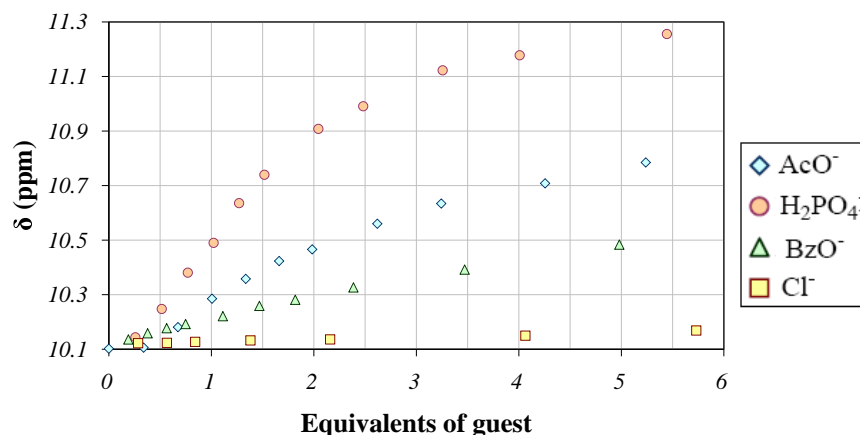
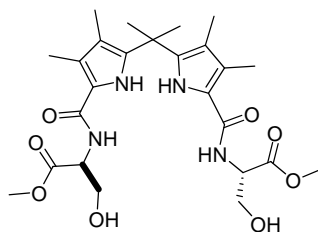


Figure 93 Curve obtained by plotting the chemical shift of the pyrrole (a) proton upon addition of anions to a solution of tweezer **105** in DMSO-*d*₆-0.5% H₂O against the equivalents of guest.

Tweezer 106



Upon addition of anions to a solution of tweezer **106** in DMSO-*d*₆-0.5% H₂O a downfield shift of the pyrrole and amide protons was observed for every guest apart from dihydrogen phosphate. When dihydrogen phosphate was added the pyrrolic and amidic protons broadened and were impossible to monitor. A small upfield movement ($\Delta\delta \approx 0.3$ ppm) was observed for the signal of the CH protons, and thus the binding constant was calculated following the signal of these protons. In all the other cases, the binding constants were calculated as the average of the values obtained by monitoring the shift of the three sets of protons (pyrrole, amide and CH), which were in good agreement, and by fitting the curves in a 1:1 host:guest binding model. In this tweezer there was little selectivity for acetate over phosphate (1.4:1). Tweezer **106**, however was selective for dihydrogen phosphate (2.5:1) over benzoate and for benzoate over chloride (5:1). The shift of the CH protons upon addition of the various guests was plotted (figure 94), showing the selectivity trend.

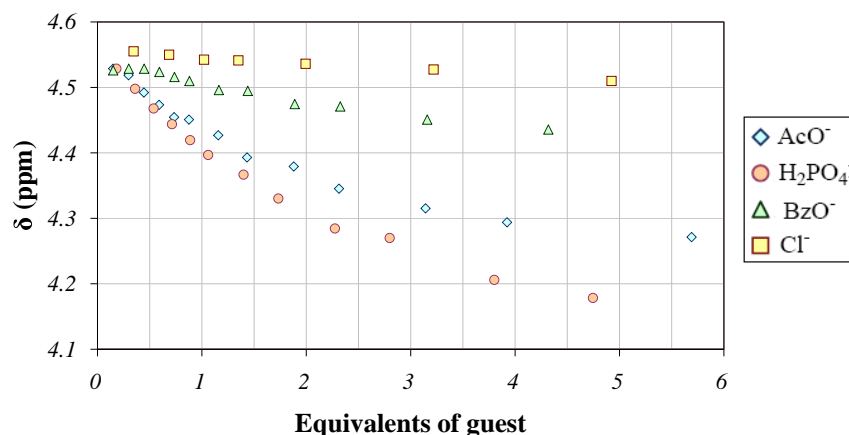


Figure 94 Curve obtained by plotting the chemical shift of the CH (c) proton, upon addition of anions to a solution of tweezer **106** in DMSO- d_6 -0.5% H₂O against the equivalents of guest.

2.5.1 Conclusions

Comparing the value of the binding constants obtained for these tweezer receptors (table 7, pg 72) it was observed that the lower stability constants were obtained with tweezer **102**.

The simple achiral tweezer receptors **101** and **102** were clearly selective for dihydrogen phosphate. The achiral tweezer with the phenyl ring (**102**) had less affinity with anionic guests than the tweezer with a simple alkyl chain (**101**).

Among the tweezer receptors with an amino acid moiety, the selectivity changed according to the nature of the side chain. When the amino acid was a phenylalanine, and the side chain consisted of a phenyl ring, there was a clear selectivity for dihydrogen phosphate. In the cases where the residue was an alkyl chain (leucine, **104**) or an alcohol (serine, **106**) there was no significant difference between acetate and dihydrogen phosphate. Little difference in the binding properties was observed between receptor **105** and **107** so it could be stated that the presence of additional hydrogen bonding donors did not increase the affinity of the host for simple anionic guests. In DMSO- d_6 -0.5% H₂O the tweezer receptor revealed selectivity for oxo-anions and the complexes formed with chloride had a very low stability constant (e.g. $K_a = 27 \text{ M}^{-1}$ with tweezer **101**) or no complex was formed.

2.5.2 Binding constants with dihydrogen phosphate in DMSO-5% H_2O

As the dipyrromethane unit was found to be a good binding unit for dihydrogen phosphate, it was decided to test the binding properties of receptors **105** and **106** in a more competitive environment, increasing the percentage of water in the solvent.¹ The results were compared to those previously obtained in the group (table 8).

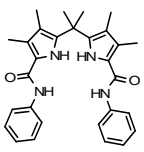
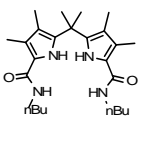
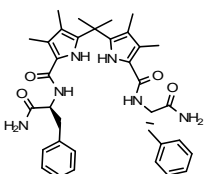
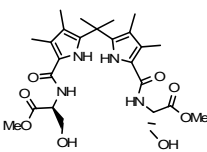
	Receptor			
	$K_a (M^{-1})$			
Anion (TBA salt)	79 	101 	105 	106 
$H_2PO_4^-$	1092 ¹	81 ¹	239	100

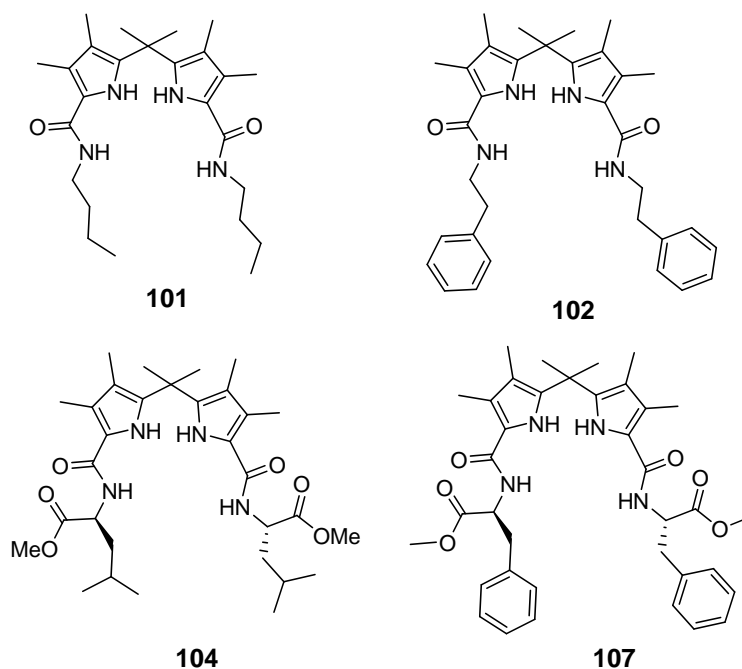
Table 8 Binding constants measured by NMR titration in DMSO- d_6 -5% H_2O . The curves were fitted according the 1:1 host:guest binding model.

The difference between receptor **79** and the other tweezer receptors was due to the nature of the amide: the aromatic amidic bond is more acidic than the alkyl one and this may explain the higher binding constant. The amino acid residue, however, played a role in increasing the binding constant, particularly when the residue was a phenylalanine the binding constant measured was threefold the binding constant measured with receptor **101**.

2.6 Binding properties in CD_3CN

2.6.1 Receptors **101**, **102**, **104** and **107**

In this section will be discussed the binding properties of dipyrromethane based receptors in CD_3CN . The goal of this comparison was to check whether the presence of the ester of the amino acid, and the presence of a phenyl ring could play a role in stabilising the complex with acetate.

**Figure 95**

As the binding constant of **107** with acetate is on the order of 10^4 , close to the limit of the reliability of NMR techniques,¹⁴⁰ it was decided add a certain percentage of H₂O in the solvent to decrease the strength of the interaction.

In order to decide the necessary amount of water a pilot experiment was done with 1% and 2% H₂O (table 9).

Receptor	Solvent		
	K_a (M ⁻¹)		
	CD ₃ CN	CD ₃ CN-1% H ₂ O	CD ₃ CN-2% H ₂ O
107	$>10^4$	$1.1 \cdot 10^3$	$1.4 \cdot 10^2$

Table 9 Binding constants measured by NMR titration of tetrabutylammonium acetate with tweezer **107** in different mixtures of CD₃CN- H₂O. The curves were fitted according the 1:1 host:guest binding model.

As the value the binding constant was greatly affected by adding a small amount of water, it was decided that any comparison between receptors should be done with the same batch of freshly prepared solvent mixture. A series of comparative studies were

carried out (table 10). Upon addition of acetate to a solution of tweezer receptor in CD_3CN -1% H_2O the pyrrole and amide protons shifted downfield. The binding constants (table 10) were calculated as the average of the values obtained by monitoring the shift of the two sets of protons and fitting the curves in a 1:1 host:guest binding model.

<i>Anion</i> (TBA salt)	Receptors					
	$K_a (M^{-1})$					
	104	107	101	107	101	102
AcO^-	2725 ^a	1538 ^a	490 ^a	1220 ^b	416 ^b	486 ^b

Table 10 Binding constants (M^{-1}) measured by NMR titration of different tweezer with acetate in CD_3CN - 1% H_2O . ^aSamples tested in the same solvent batch. ^bSamples analysed in the same solvent batch.

From these data (table 10) it can be stated that the binding ability of the receptors **101** and **102** was much lower than the one obtained with the receptors with ester functionalities. This could be ascribed to the difference of the acidity of the amide *NH*. The presence of the phenyl ring did not make a significant difference.

2.6.2 Receptors with polar functionalities

a) Hydroxyl vs phenyl ring

The properties of the receptors bearing polar functionalities were investigated in CD_3CN with acetate and compared to receptor **104**. Acetate a simple organic carboxylate and should not have secondary interaction with the host. NMR titrations were performed between tweezer receptors **106** and **107** and the resulting curve was analysed according the 1:1 host:guest binding model (Table 11).

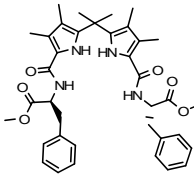
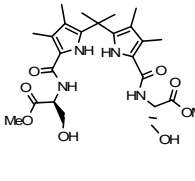
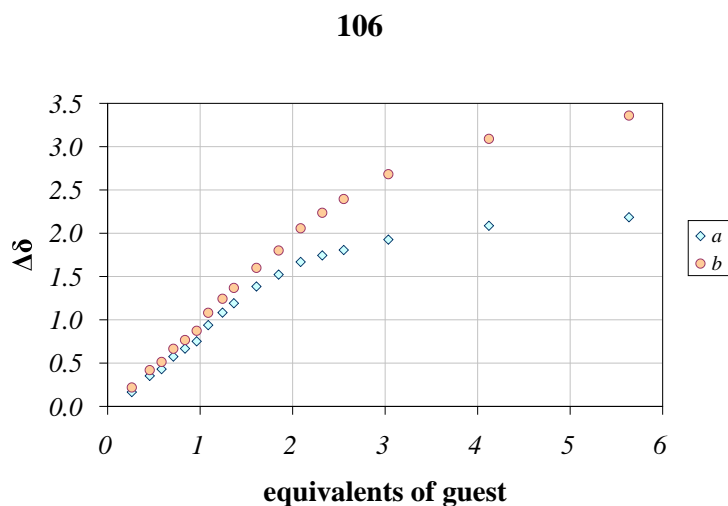
	Receptor	
	K_a (M^{-1})	
<i>NH proton monitored</i>	107 	106 
NH pyrrole	16357	1088
NH amide	13998	668

Table 11 Apparent binding constants measured in CD_3CN by titration of tweezer **107** and **106** with tetrabutylammonium acetate as a guest and calculated according the binding model 1:1 host:guest.

Theoretically, in presence of a binding process with a 1:1 stoichiometry, the binding constants calculated by the analysis of the shift of two different protons should give the same binding constant within the experimental error (§2.4.1). This behaviour was observed in the case of receptor **107** but not for receptor **106**. The discrepancy was also noted by plotting the difference of chemical shift measured for the two protons in the titration with acetate (figure 96).



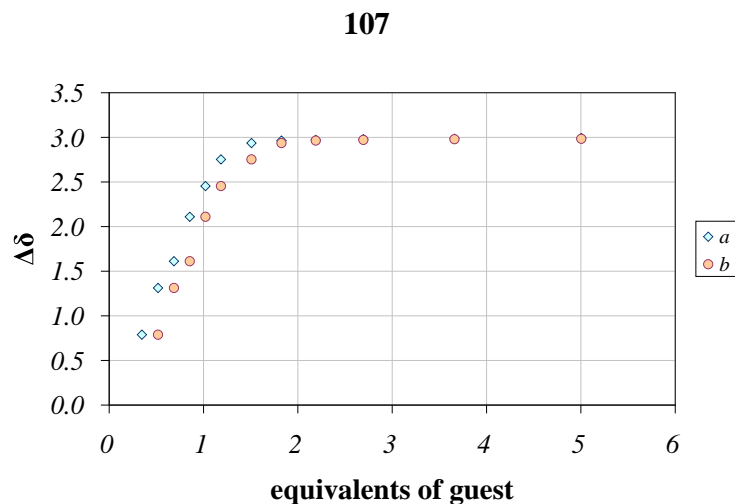
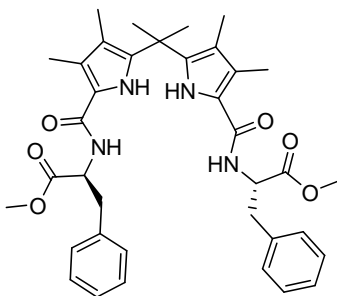


Figure 96 Compared difference of the chemical shift of the pyrrole NH (a) and of the amide proton (b) for receptors **106** and **107**.

This suggested that the process involved was not a simple 1:1 binding. Firstly the binding stoichiometry was investigated. It can be studied both with a Job Plot and by the analysis of the UV titration (§2.4.2 and 2.4.3).¹⁴¹

Tweezer 107



A Job Plot experiment was performed for receptor **107** (figure 97) and it confirmed that the complex formed has a 1:1 stoichiometry.

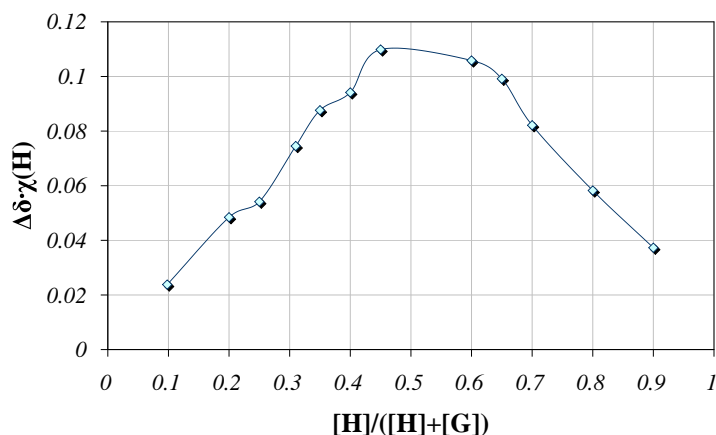


Figure 97 Job plot of receptor **107** with tetrabutylammonium acetate in CD_3CN .

The UV titration of receptor **107** showed one isosbestic point (figure 98), which confirmed the result obtained from the Job Plot, and the stoichiometry is assumed to be 1:1. The binding constant is 15300 M^{-1} , which is in very good agreement with the NMR experiment.

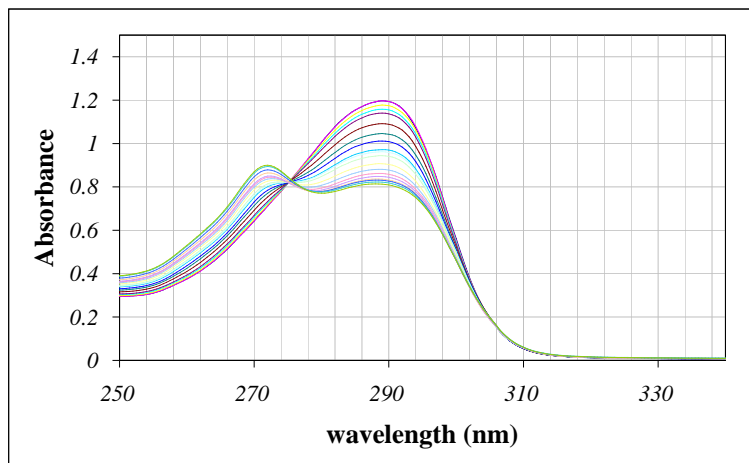
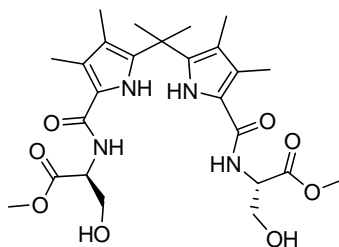


Figure 98 Superimposed absorption spectra obtained from the titration of **107** with tetrabutylammonium acetate in CH_3CN .

Tweezer 106

The analysis of receptor **106** gave a peculiar Job Plot. It seemed that the situation is a complex mixture of equilibria. The pyrrole set of protons had predominately 1:1 behaviour, while the amide protons indicated a 1:2 (host:guest) complex (figure 99).

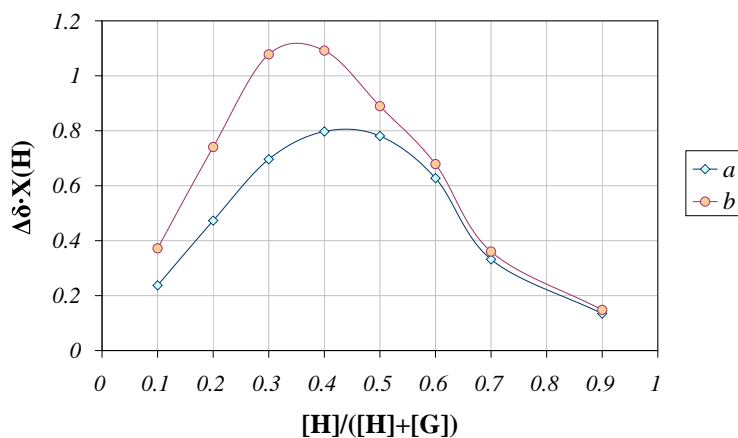


Figure 99 Job plot of receptor **106** with tetrabutylammonium acetate in CD_3CN . The pyrrole (a) and amide (b) protons were monitored.

This interpretation was confirmed by the UV titration, the superimposition of the spectra obtained from the titration did not give a clear isobestic point (figure 100).

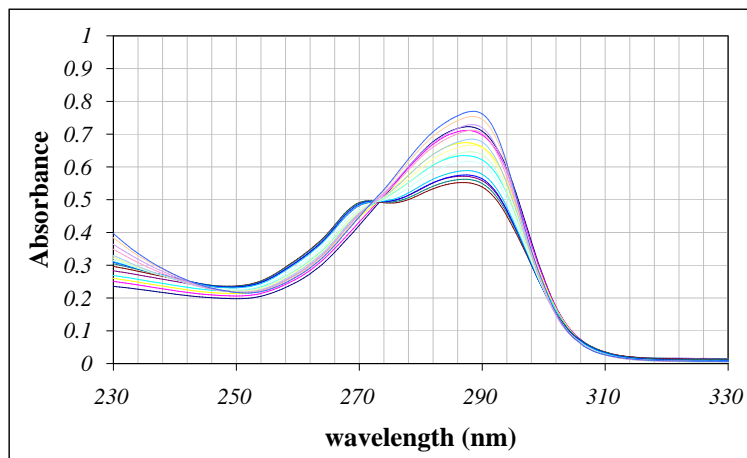


Figure 100 Superimposed absorption spectra obtained from the titration of **106** with tetrabutylammonium acetate in CH_3CN

The curve obtained from plotting the variation of the absorbance at 289 nm showed that the absorbance increased upon addition of up to two equivalents of guest, after that quantity of guest added the absorbance decreased again. As in the UV titration the presence or the disappearance of absorption bands represented the changes of the concentration of species in solution. It can be said that upon addition of tetrabutylammonium acetate a new species was formed, very likely this was the 1:1 host guest complex, and, after the addition of two equivalents of guest, the concentration of this species decreased, probably in favour of the 1:2 complex formation (figure 101).

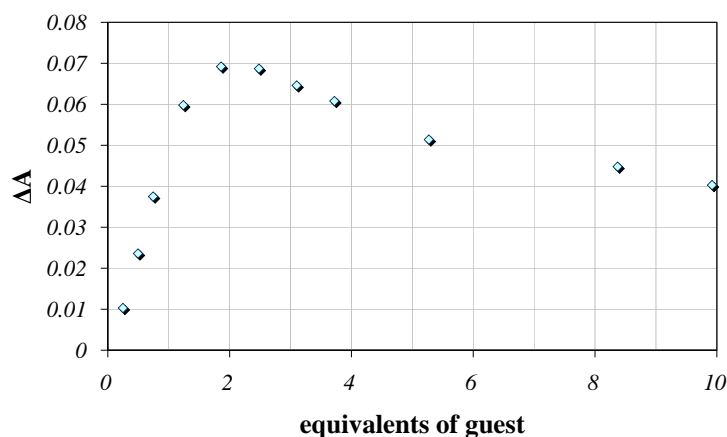
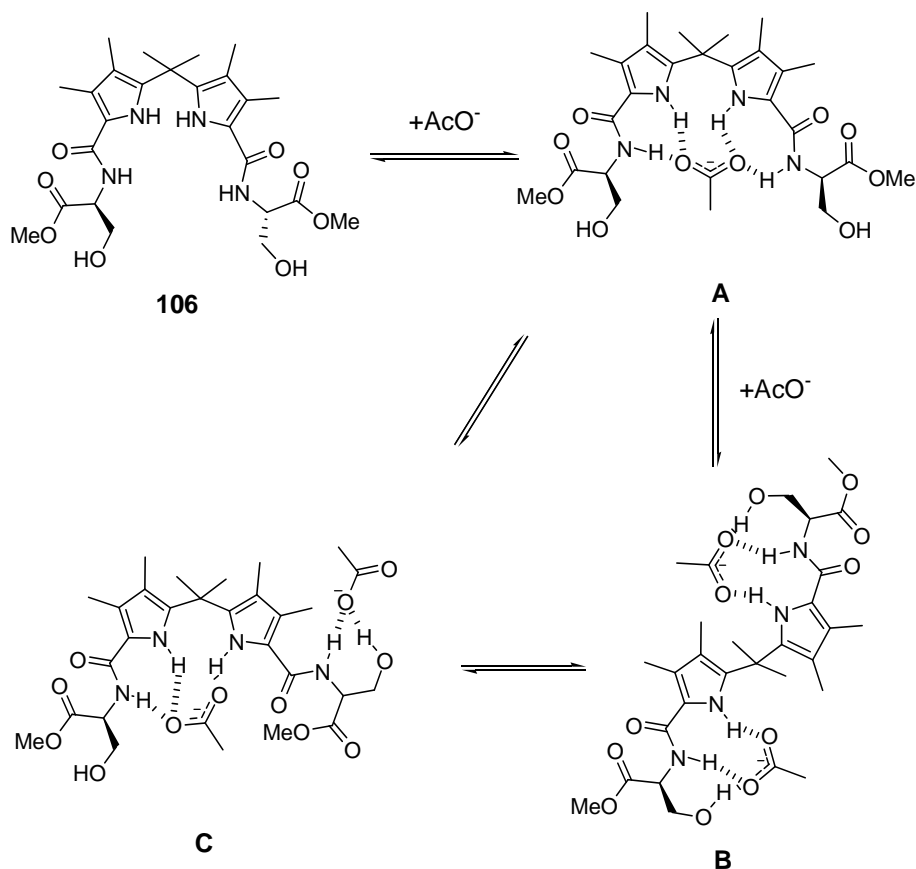


Figure 101 Curve obtained by plotting the difference of absorbance (ΔA) at 289 nm observed upon addition of tetrabutylammonium acetate to a solution of **106** in CH_3CN .

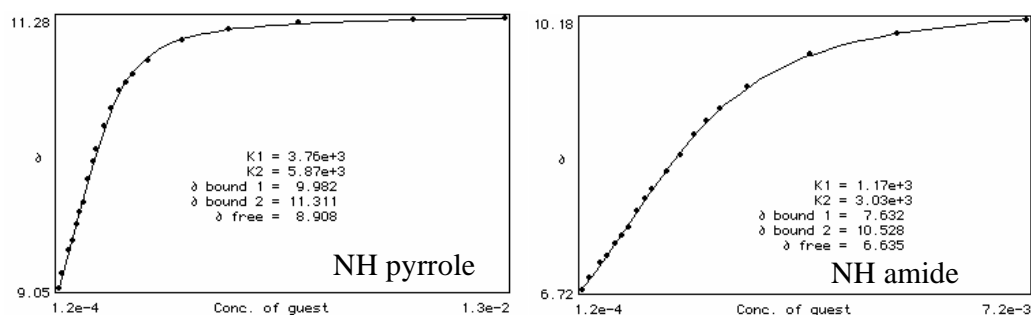
With these results in hand a possible binding model was envisaged. The first equivalent of guest bound to the pyrrole and amide protons as in **A** (scheme 22). The second equivalent of guest would mostly interact with one of the amides and the OH as in **B** and **C**. To allow the complexation with the second equivalent of guest it was supposed that a change of conformation occurred: via a rotation at the carbon that links the two pyrrole units as it was envisaged in **B** (scheme 21) or via a rotation of the bond between the C in position two of the pyrrole and the carbonyl to yield **C** (scheme 21). The two rotations envisaged for the formation of these two models were observed in similar systems in the literature. The rotation envisaged in **B** was observed by Gale¹ and co-workers in the crystal structure of tweezer **101**. The rotation in conformation **C** was observed in the crystal structure of the amido pyrrole.⁷⁷



Scheme 21 Proposed binding mode of receptor **106** with acetate

The analysis of the binding constant was performed with TitNMR. As the binding constant is a macroscopic value we would expect that the value obtained from monitoring

the shift of the two sets of protons is the same. By analysing the data with the 1:2 host:guest binding model it was not possible to obtain convergence in the data. The conclusion that can be taken from these data is that both the $K_{1:1}$ and the $K_{1:2}$ (host:guest) have a magnitude of around 10^3 and that the $K_{1:1}$ has a value that is around twice than $K_{1:2}$ (figure 101). So it could be stated that in these conditions the 1:1 complex is favoured but there was a significant presence of the 1:2 host: guest complex.



<i>NH proton monitored</i>	$K_{1:1}$ (M^{-1})	$K_{1:2}$ (M^{-1})
NH pyrrole	7500	2835
NH amide	2340	1515

Figure 102 NMRTit output (HGG model) for the titration of **106** with tetrabutylammonium acetate (in the output are shown the microscopic values which are corrected in the table).

To confirm the role played by the hydroxyl groups in the stabilisation of the 1:2 host:guest complex receptor **108** (figure 103) was synthesised and its properties were analysed by NMR titration. As tweezer **108** was not symmetric the two pyrrole (a and b) and the two amide (c and d) protons are not equivalent and their plot can be followed independently (figure 103).

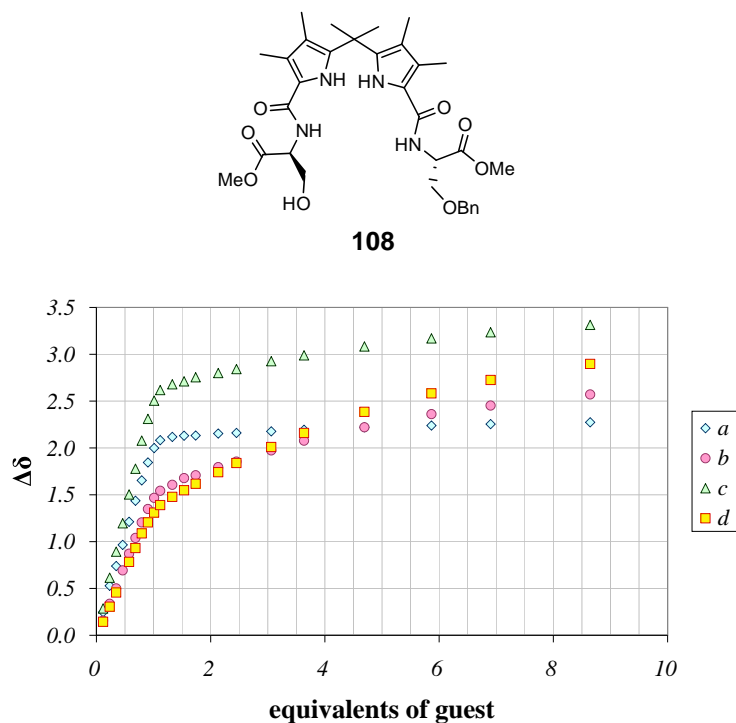


Figure 103 Curves obtained by plotting the chemical shift of the pyrrole (*a* and *b*) and amide (*b* and *c*) protons, upon addition of acetate to a solution of tweezer **108** in CD_3CN .

The shape of the curves suggested that the binding process is not a pure 1:1 (host:guest) stoichiometry. To check the stoichiometry a Job Plot was performed (figure 104).

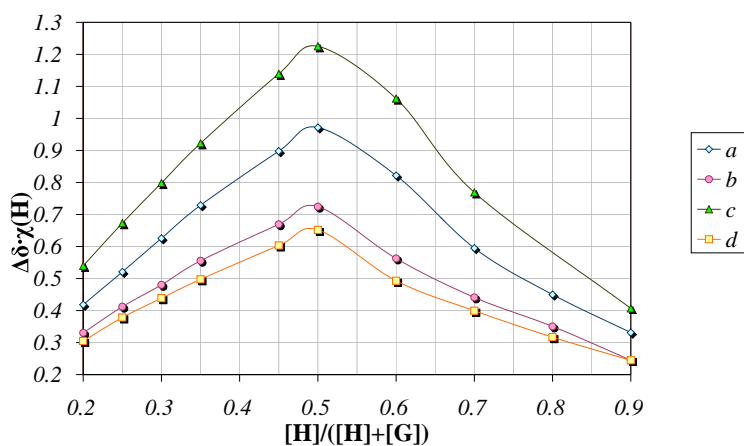
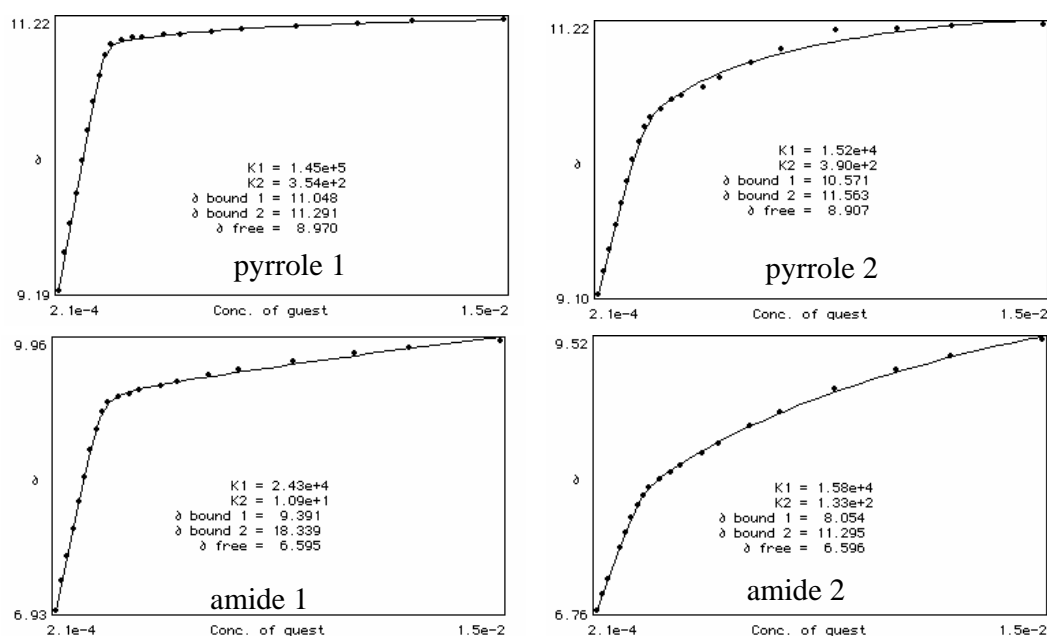


Figure 104 Job plot of receptor **108** with tetrabutylammonium acetate in CD_3CN

The Job Plot gave 1:1 (host:guest) as predominant binding stoichiometry, however the shape of the curves obtained by the titration suggests that the 1:2 (host: guest) complex was also present in solution, but its formation was much more disfavoured than in the case of tweezer **106**.

So bearing in mind that the predominant binding process was the 1:1, the curves were treated assuming the 1:1 and 1:2 binding stoichiometry (figure 105).



<i>NH</i> <i>monitored</i>	$K_{1:1}$ (M^{-1})	$K_{1:2}$ (M^{-1})
pyrrole 1	$2.8 \cdot 10^5$	177
pyrrole 2	$3 \cdot 10^4$	195
amide 1	$4.8 \cdot 10^4$	5
amide 2	$3.1 \cdot 10^4$	66

Figure 105 NMRTit output (HGG model) for the titration of **108** with tetrabutylammonium acetate

In both cases a precise convergence for the value of the association constants using all four protons was not found but it does provide a reasonable estimate of $K_{1:1} > 10^4$ and $K_{1:2} \approx 10^2$ e.g. $K_{1:2}$ is two order of magnitude lower than $K_{1:1}$, confirming the attenuated

character of 1:2 binding in comparison with **106**. As for **106** the non-convergent values obtained from different protons could be ascribed to the presence of multiple equilibria.

b) Amide vs Ester

Upon addition of acetate to a solution of tweezer **105** in CD₃CN-1% H₂O the pyrrole and the amide proton had a downfield shift. Both were monitored and the curves fitted according the 1:1 binding model (table 11). Two significantly different values were obtained.

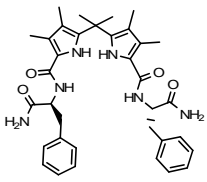
	Receptor K_a (M ⁻¹)
<i>NH proton monitored</i>	105 
NH pyrrole	1579
NH amide	541

Table 12 Apparent binding constants measured in CD₃CN-1% H₂O by titration of tweezer **105** with tetrabutylammonium acetate as guest and calculated according the binding model 1:1 host:guest.

Theoretically, in presence of a binding process with a 1:1 stoichiometry, the binding constants calculated by the analysis of the shift of two different protons should give the same binding constant within the experimental error (§2.4.1). The discrepancy was also noted by plotting the difference of chemical shift measured for the two protons in the titration with acetate (figure 106).

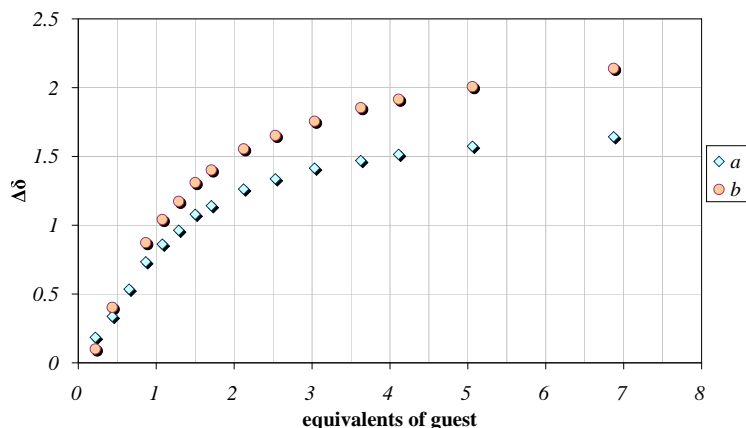


Figure 106 Compared difference of the chemical shift of the pyrrole (a) and of the amide protons (b) for receptor **105**.

In this case no agreement was found between the values obtained by fitting the two curves. It was then decided to perform a Job Plot in CD_3CN to investigate the stoichiometry of binding. In the Job Plot the pyrrole (a) and amide (b) protons were monitored (figure 107).

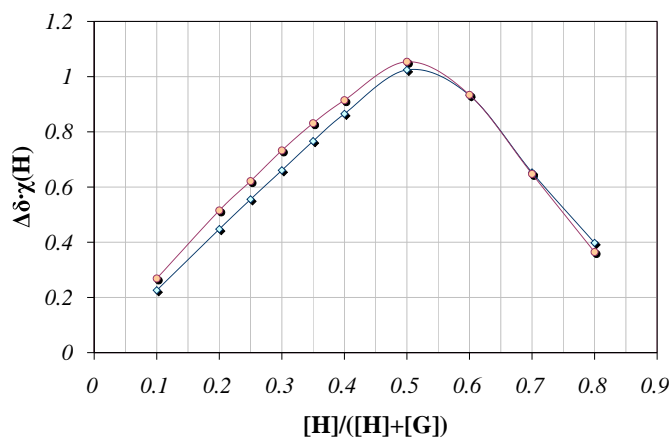


Figure 107 Job plot of receptor **105** with tetrabutylammonium acetate in CD_3CN . The pyrrole (a) and the amide (b) protons were monitored.

As the maximum of the curve was at 0.5 the principal process that took place in solution was, therefore, the formation of a 1:1 host:guest complex. The UV titration confirmed the

binding stoichiometry with the presence of an isosbetic point and with the shape of the curve of the difference of absorbance versus the equivalents of guests (figure 108).

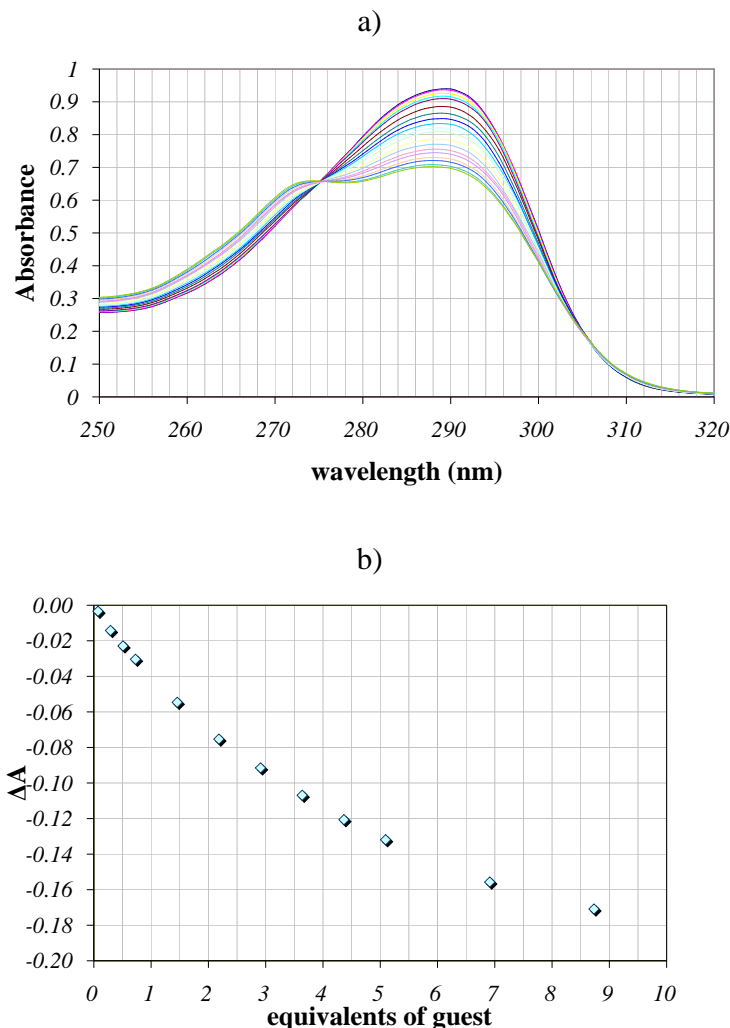


Figure 108 a) Superimposed absorption spectra obtained from the titration of **105** with tetrabutylammonium acetate in CH_3CN . b) Curve obtained by plotting the difference of absorbance (ΔA) at 289.5 nm observed upon addition of tetrabutylammonium acetate to a solution of **105** in CH_3CN .

The binding constant calculated by fitting the UV data with the 1:1 model is 9500 M^{-1} . So the anomalies in the NMR titration curves could not be ascribed to a multiple binding process. It was decided to analyse more carefully the NMR spectra as the movement of protons not directly involved in the binding process could explain the processes taking place in solution (figure 109).

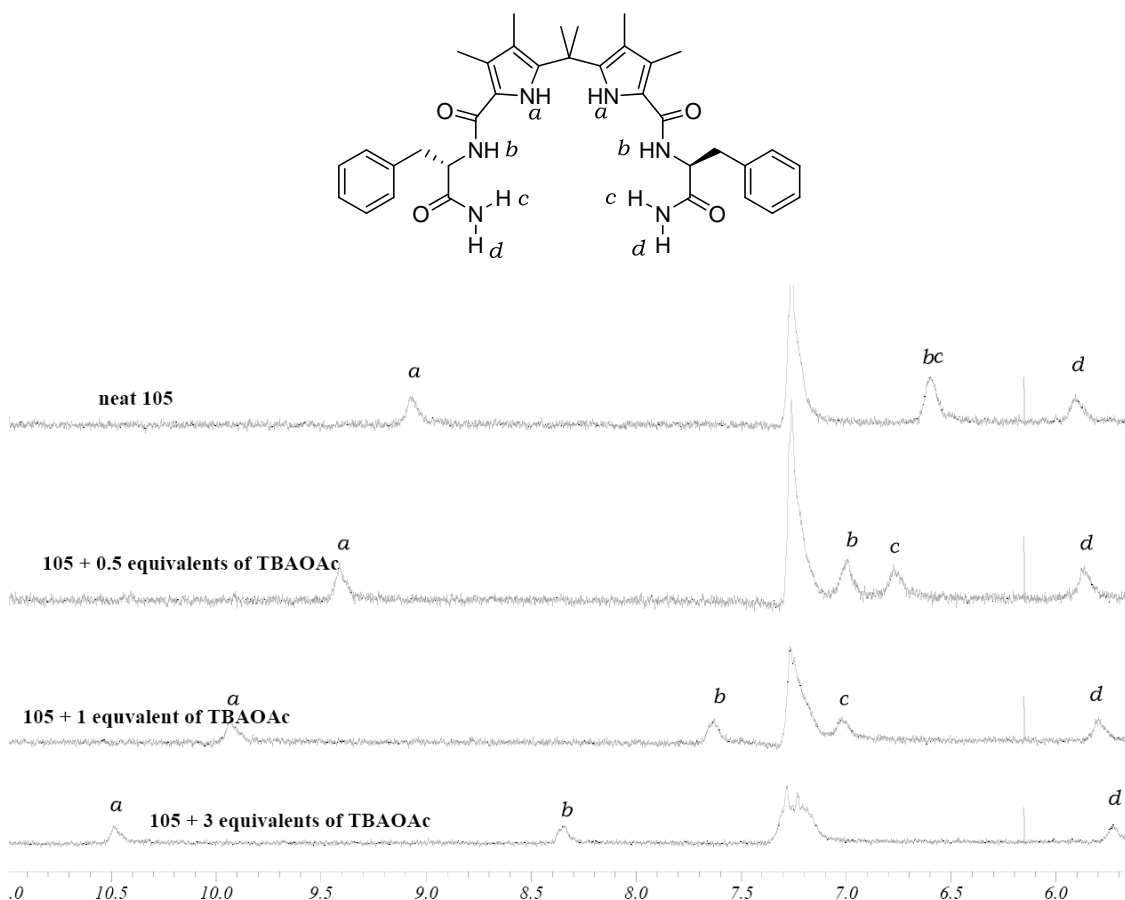


Figure 109 Changes observed in the chemical shift of the pyrrolic (a) amidic (b, c and d) protons upon addition of the tetrabutylammonium acetate to a solution of **105** in CD_3CN -1% H_2O .

The pyrrole (a) and amide protons (b) had a downfield shift of $\Delta\delta \approx 1.5\text{--}2$ ppm, but the two protons belonging to the primary amide moved in opposite directions: one (c) moved of $\Delta\delta \approx 1$ ppm downfield and the other (d) moved of $\Delta\delta \approx 0.2$ ppm upfield. If the first three movements are the indication of the formation of hydrogen bonds the latter is indicative of the breaking of a hydrogen bond. This movement could be plotted against the equivalents of guest added (figure 110).

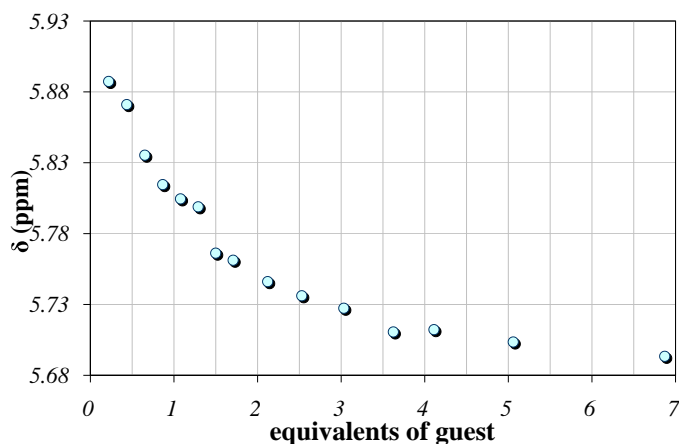
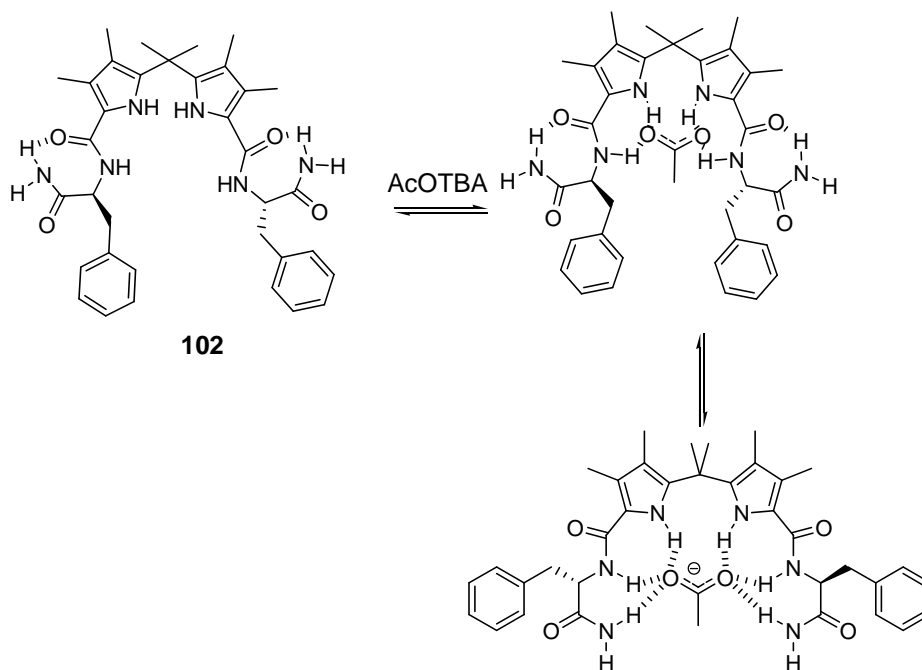


Figure 110 Curve obtained by plotting the chemical shift of the amide (d) proton, upon addition of anions to a solution of tweezer **105** in CD_3CN - 1% H_2O .

A change in the conformation of the host molecule could be envisaged at the beginning of the titration when the amides of the side chain can form intramolecular hydrogen bonding with the adjacent carbonyls (scheme 22) and by addition of the guest this hydrogen bond is broken to promote a stronger interaction with the guest. Then the complex of the host with the guest can adopt different 1:1 conformations, by virtue of the several hydrogen bond donor groups. In this manner, different 1:1 species can be in equilibrium, some of them with minor participation of the amide protons in the binding.

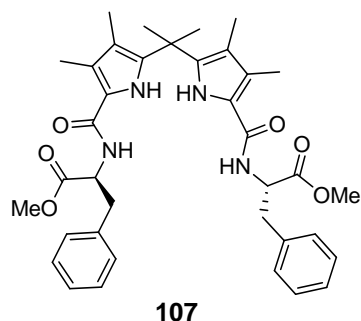


Scheme 22 Proposed binding modes of receptor **105** with acetate

c) Receptors with polar functionalities: acetate vs phosphate selectivity

As in $\text{DMSO-}d_6$ -0.5% H_2O it was observed that the selectivity between acetate and dihydrogen phosphate was correlated with the nature of the amino acid residue. The comparison was made in CD_3CN to check if any change occurred on changing the polarity of the solvent. In $\text{DMSO-}d_6$ -0.5% H_2O the tweezer presenting pendant phenyl rings showed marked selectivity for dihydrogen phosphate (**102**, **107** and **105**), whereas this selectivity was attenuated (**101** and **104**) or even reversed (**106**) in absence of this moiety.

The properties of tweezer **107** were analysed by NMR titration and the value of the binding constants was, for both anions, $K_a \approx 10^4 \text{ M}^{-1}$. As this value was very close to the limits of reliability of NMR titrations, UV titrations were performed to obtain a more accurate value. The binding constants were compared (figure 111).



Anion (TBA salt)	$K_a (M^{-1})$
AcO^-	15300
$H_2PO_4^-$	15400

Figure 111 Binding constants measured by UV titration in CH_3CN of receptor **107**. The curves were fitted according the 1:1 host:guest binding model.

No clear selectivity was observed for this system between acetate and dihydrogen phosphate. This was also confirmed by superimposing the curves obtained by plotting the difference of absorbance at 289 nm against the concentration of the guest. The two curves have a very similar shape (figure 112).

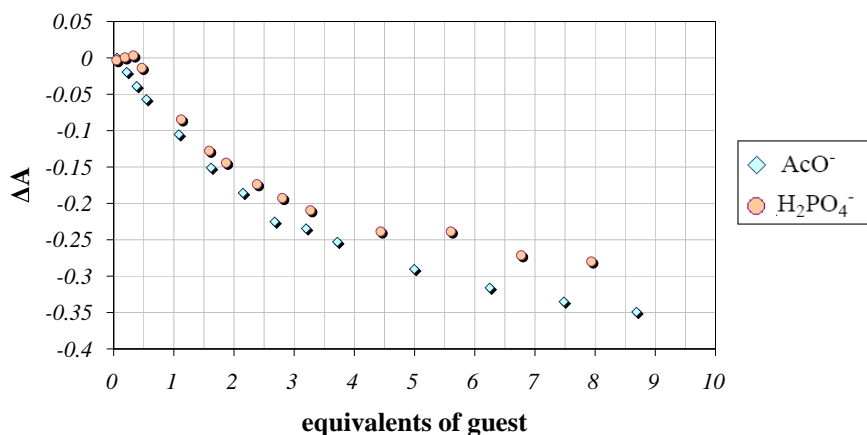
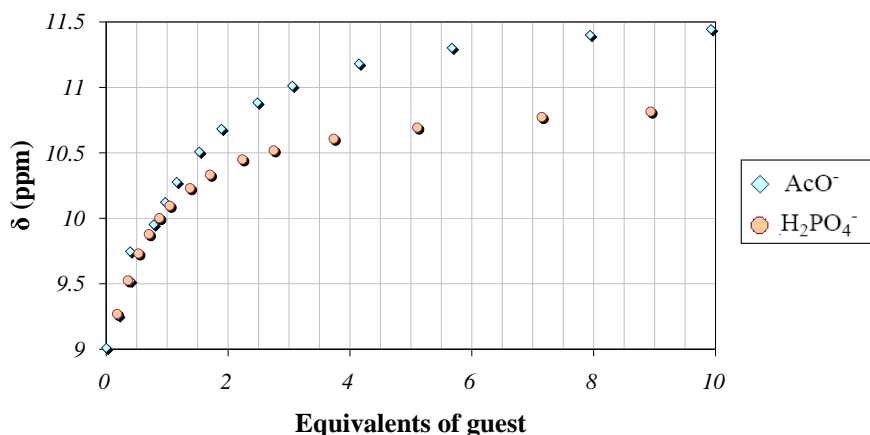


Figure 112 Curve obtained by plotting the difference of absorbance (ΔA) at 289 nm observed upon addition of tetrabutylammonium acetate and phosphate to a solution of **107** in CH_3CN .

By adding a small quantity of water to the solvent the measurement could be done by NMR titration. In this case, the selectivity for dihydrogen phosphate increased. As it can be seen in the value of the binding constants and by superimposing the curves obtained by monitoring the movement the pyrrole protons (figure 113), there was a moderate selectivity for dihydrogen phosphate.



Anion (TBA salt)	K_a (M^{-1})
AcO^-	1058
H_2PO_4^-	1737

Figure 113 Binding constants measured by NMR titration of receptor **107** in CD_3CN -1% H_2O . The curves were fitted according the 1:1 host:guest binding model.

Receptor **105** was analysed by UV titration in neat CH_3CN . Upon addition of acetate to the receptor solution in acetonitrile a decrease of the intensity of the band at 289.5 nm was observed. By plotting the change of the absorbance against the concentration of guest the binding constant was calculated ($K_a = 9500 \text{ M}^{-1}$). The same procedure was undertaken for the titration with dihydrogen phosphate, but in this case the curve could not be fitted (figure 114) in an appropriate manner and a reliable value for the binding constant could not be calculated. However by superimposing the curves a clear selectivity for the dihydrogen phosphate could be seen.

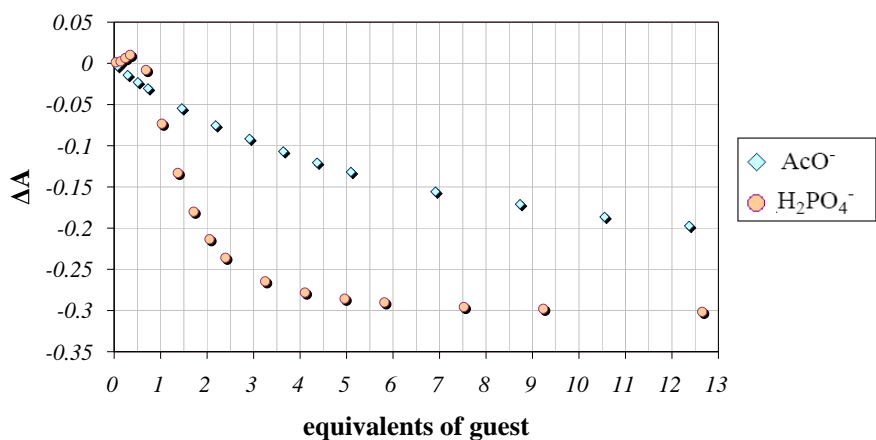


Figure 114 Compared difference of absorbance for host **105** at 289.5 nm with acetate and dihydrogen phosphate.

The difference was also observed by NMR titration in CD_3CN -1% H_2O . As it was not possible to have a reliable estimate of the macroscopic binding constant due to the difference in the value observed by monitoring the pyrrole and amide protons, it was decided to compare the binding constants calculated by monitoring the same protons (i.e. the pyrrole) with both guests.

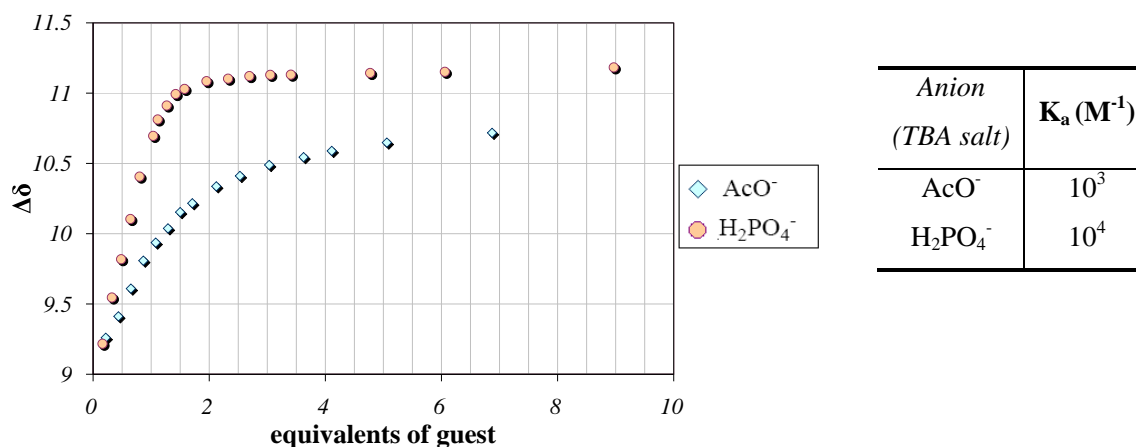
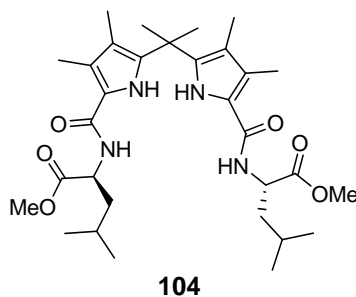


Figure 115 Compared difference of the chemical shift of the pyrrolic NH of host **105** with acetate and dihydrogen phosphate. Binding constants measured by NMR titration in CD_3CN -1% H_2O . The curves were fitted according the 1:1 host:guest binding model.

Binding studies on receptor **107** in CH_3CN and CD_3CN -1% H_2O , show opposite behaviour to that observed in DMSO, and demonstrated that, in these media, the phenyl

ring does not play an essential role in the selectivity for dihydrogen phosphate. The fact that the presence or the absence of the pendant phenyl rings is no longer essential in acetate/dihydrogen phosphate selectivity was confirmed by the NMR titrations of the receptor with the leucine residue in CD_3CN -1% H_2O . Tweezer **104** had a modest selectivity for phosphate over acetate (1.3:1), while in $\text{DMSO}-d_6$ -0.5% H_2O the ratio was in favour of acetate (1:1.5).



Anion (TBA salt)	$K_a (\text{M}^{-1})$
AcO^-	1554
H_2PO_4^-	2054

Figure 116 Binding constants measured by NMR titration of receptor **104** in CD_3CN -1% H_2O . The curves were fitted according the 1:1 host:guest binding model.

Tweezer receptor **105**, which had a phenyl ring on the amino acid residue and a polar functionality, was selective for dihydrogen phosphate in any solvent mixture analysed. **107** had a phenyl group in the amino acid side chain and it was selective for dihydrogen phosphate only in more polar solvents as $\text{DMSO}-d_6$ -0.5 H_2O ; in acetonitrile no clear selectivity was observed. Therefore, it can be concluded that the combination of appended phenyl rings and polar functionalities ensure a general selectivity for dihydrogen phosphate.

2.7 Tweezer receptors bearing substituents on the phenyl ring

By analysing the changes induced on the chemical shift by the addition of acetate to receptor **107**, a significant change was observed for the aromatic pattern (figure 117).

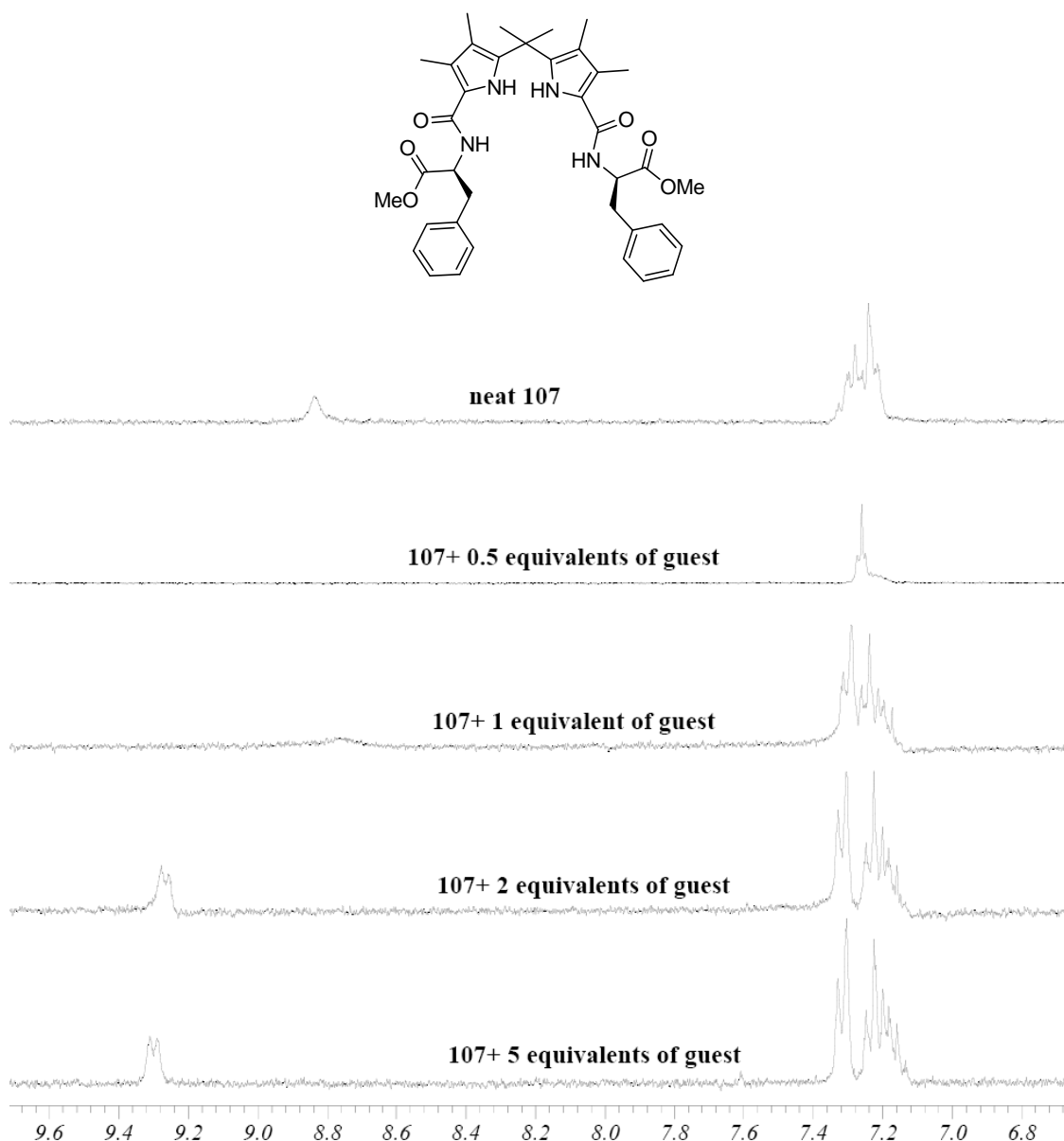


Figure 117 Changes observed in the chemical shift of the aromatic protons upon addition of the tetrabutylammonium acetate to a solution of **107** in CD_3CN .

These changes could be caused by conformational changes occurring during the binding process or by a direct involvement of the phenyl ring in the interaction with the guest.

By adding substituents on the phenyl ring it was possible to investigate which of these hypotheses was more appropriate. The substituents modulate the π system's electron density and therefore the properties of the whole ring are affected.

2.7.1 Anion- π interactions

Studies on the strength of interactions between a π system and an anionic guest have been pioneered by Dey¹⁴² who found that the interaction between an electron deficient aromatic ring and the anions can generate energies comparable to those achieved with hydrogen bonds. An anion- π interaction can be identified by crystallographic evidence, in a crystal structure of the complex. Some evidence can be also extracted from the NMR studies in solution.¹⁴³ One of the parameters is the influence on the binding constant played by the electronic properties of the phenyl ring.¹⁴⁴ The shift of the aromatic CHs during the titration may also give an idea of their involvement in the binding process.

Another interpretation of the interactions between an anion and an aromatic ring involves the formation of a hydrogen bond from the aromatic CH to the anion. This type of interaction was recently investigated and it can have energies comparable to those involved when the hydrogen bond donor group is X-H, where X is typically an oxygen or nitrogen atom.¹⁴⁵ However, the study of these interactions is at its early stages and a series of papers dealing with the nature of such interactions and the experimental methods able to identify them has been recently produced.^{146,147}

2.7.2 Analysis of receptors bearing substituents on the phenyl ring in CD_3CN

A receptor bearing an electron donating group (**110**, figure 118) and one with an electron withdrawing group (**109**, figure 118) were synthesised and their properties were analysed and compared to **107**. If the phenyl ring played a role, the complexes formed between acetate and **110** should be less stable than those formed between acetate and **109**. The π system of an electron rich ring (e.g. as in **110**) is not prone to anion- π interactions and the polarity of its CHs is reduced decreasing the strength of any putative CH-anion interactions.

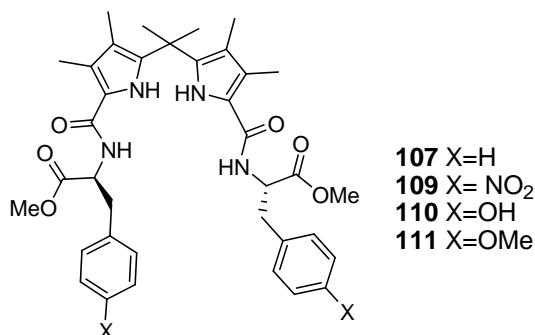


Figure 118 Tweezer receptors bearing substituents on the phenyl ring.

The properties of **107**, **109** and **110** have been compared in CD₃CN-1% H₂O (table 12) using the same batch of solvent as the binding constants in neat CD₃CN were too high to be analysed by NMR titration and the minimal presence of water had a dramatic effect on the value of the binding constant (§ 2.6.1).

Anion (TBA salt)	Receptor K _a (M ⁻¹)		
	109	107	110
AcO ⁻	3090	846	686

Table 13 Binding constants measured by NMR titration of different receptors with acetate in CD₃CN-1% H₂O. The curves were fitted according to the 1:1 host:guest binding model.

By adding an electron withdrawing group (**109**) on the phenyl ring the overall binding constant was significantly increased. Adding an electron donating group (**110**) on the same position, the binding constant decreased slightly compared to the reference compound **107**. A series of explanations can be given for such behaviour, including that the presence of the nitro group can increase the acidity of the amide NH, and as a consequence increase its ability to hydrogen bond to the anion. This would be more significant if there was a conjugated system between the two species, but this was not the case here. Therefore, the difference observed between compound **107** and **109** can be ascribed to an interaction between the anion and the aromatic ring, that is perturbed by the presence of a substituent that changes the electronic properties of the ring.

Upon addition of acetate to a solution of receptor **109** in CD_3CN - 1% H_2O the pyrrole and the amide protons shifted ($\Delta\delta \approx 2$ ppm) downfield, one of the aromatic protons shifted 0.1 ppm upfield, while the other aromatic protons shifted 0.1 ppm downfield. Although the value of the movement of the aromatic protons was small it was possible to monitor them (figure 119).

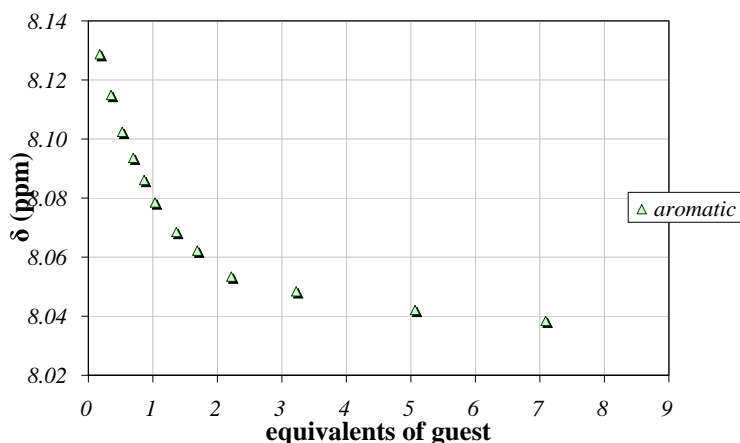


Figure 119 Shift of the aromatic protons of receptor **109** upon addition of tetrabutylammonium acetate in CD_3CN .

The shift is clear and the curve generated has a neat shape and the binding constant calculated from this shift was $K_a = 3400 \text{ M}^{-1}$, which agreed with the value obtained for the amide and pyrrole protons. With these data it is not possible to state exactly how the presence of the electron withdrawing group affects the binding, but it can be said that it increased the binding constant.

Tweezer receptor **110** bound acetate less strongly than tweezer receptor **107**. The result was not so evident in CD_3CN -1% H_2O , but the difference is accentuated in neat CD_3CN .

Anion (TBA salt)	Receptor $K_a (\text{M}^{-1})$	
	107	110
AcO^-	$1.1 \cdot 10^4$	$6.5 \cdot 10^3$

Table 14 Binding constants measured by NMR titration in CD_3CN . The curves were fitted according the 1:1 host:guest binding model.

As the phenol could interact with acetate in solution and interfere with the formation of the complex, a methylated version of tweezer **110** was analysed (**111**, figure 118). An NMR titration was carried to investigate the properties of tweezer receptor **111**.

It was not possible to calculate the binding constants of the interactions between tweezer **111** and acetate in acetonitrile because precipitation occurred during the experiment and the same happened with every other anion.

Tweezer **107**, **109** and **111** were tested also with other anions apart from acetate in mixtures of acetonitrile and water by means of NMR titration.

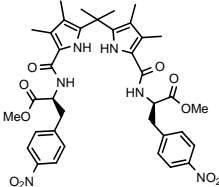
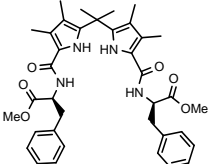
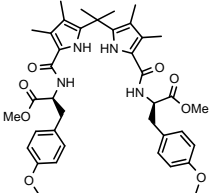
	Receptor		
	$K_a (M^{-1})$		
Anion (TBA)	109	107	111
			
AcO ⁻	3065	1058	a
H ₂ PO ₄ ⁻	3926	1737	a
BzO ⁻	4284	1016	a
Cl ⁻	324	135	a
HSO ₄ ⁻	b	b	b

Table 15 Binding constants measured by NMR titration in CD₃CN-1% H₂O. The curves were fitted according the 1:1 host:guest binding model. ^aFormation of a precipitate in the solution. ^bNo changes were observed in the spectrum upon addition of anion.

The results (Table 14) showed how receptor **109** binds more strongly than **107** with every anion tested. Receptor **109** was selective for oxo-anions and in particular for benzoate and phosphate, however the differences observed among the three oxo-anions were moderate.

2.7.3 Binding studies in DMSO-*d*₆ –0.5% H₂O

The stability constants of the complex formed between tweezer receptors **109**, **107** and **110** were also analysed in DMSO-*d*₆-0.5% H₂O. The results were summarised in the table 16 and they confirm the data obtained in acetonitrile.

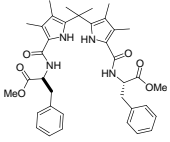
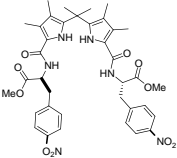
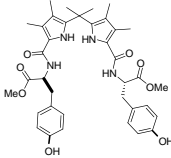
	Receptors		
	$K_a (M^{-1})$		
Anion (TBA salt)	107 	109 	110 
AcO ⁻	389	468	195
BzO ⁻	86	196	52
H ₂ PO ₄ ⁻	772	1670	299
Cl ⁻	a	a	a

Table 16 Binding constants measured by NMR titration in DMSO-*d*₆-0.5% H₂O. The curves were fitted according the 1:1 host:guest binding model. ^aNo changes were observed in the spectrum upon addition of the anion.

Every receptor showed a modest selectivity for dihydrogen phosphate. The highest binding constants were obtained with receptor **109**. This result confirms that the presence of the electron withdrawing substituents on the phenyl ring plays a determinant role in increasing the value of the binding constant.

2.8 Enantiomeric recognition

The enantioselectivity of the tweezers receptors was tested with a range of tetrabutylammonium salts of *N*-protected amino acids.

The first experiment was performed with tweezer receptor **103** and the tetrabutylammonium salts of the *N*Boc-protected phenylalanine in CDCl₃. It was expected that the pyrrole protons and the amide protons would form a hydrogen bond with the carboxylate group in the guest.

The experimental results were different: the chemical shift of pyrrole protons moved upfield during the NMR titrations with both enantiomers of the tetrabutylammonium salt of *N*Boc-phenylalanine (figure 120) and there were no appreciable differences between the two enantiomers.

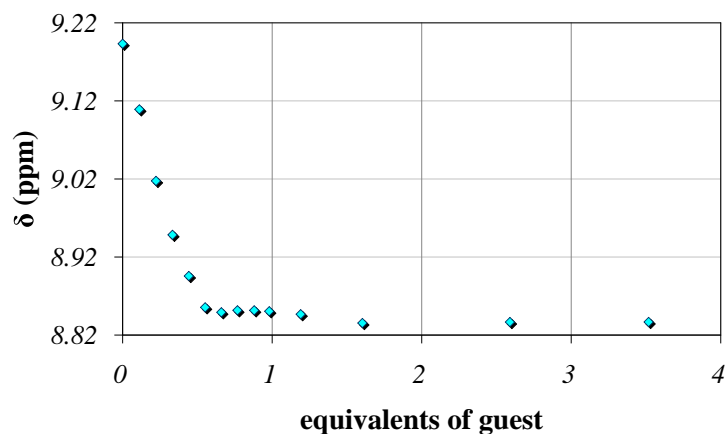


Figure 120 NMR titration of receptor **103** with *N*Boc-*L*-PheOTBA in $CDCl_3$.

As the shift was the opposite of the one expected, a dilution study was performed to investigate the possibility that a dimerisation process was occurring. The dimerisation constant was calculated with an NMR dilution study: a series of solutions was made and their spectra were recorded (figure 121).

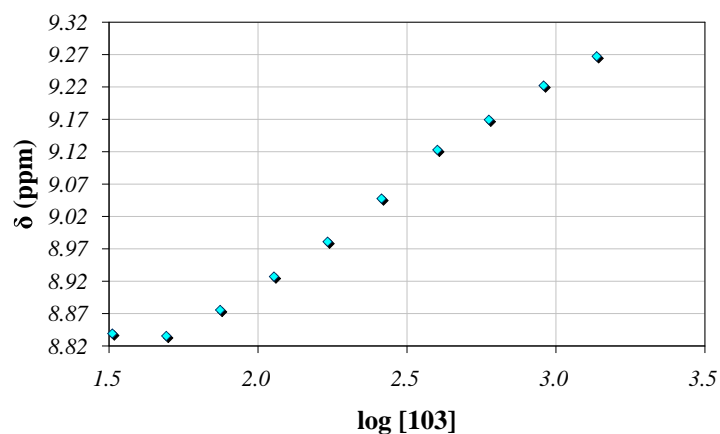
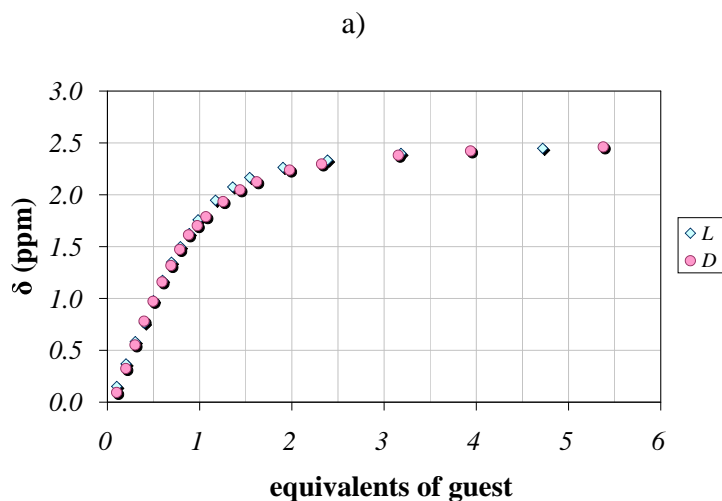


Figure 121 Chemical shift of the pyrrole protons vs the logarithm of the concentration of **103** in $CDCl_3$.

The chemical shift of the pyrrole protons moved from 8.84 ppm, at a concentration of 10^{-2} M, to 9.27 ppm, at a concentration of 10^{-4} M. The dimerisation constant was calculated with the program NMRTit_dil provided by Chris Hunter,¹³⁹ and gave a value of 270 M^{-1} .

A more competitive solvent was then chosen to disrupt the dimerisation process. A dilution study in CD_3CN confirmed that the dimerisation process was negligible; the dimerisation constant had a value of 10 M^{-1} .



b)

Receptor	Enantiomer	
	$K_a (\text{M}^{-1})$	
	L	D
103	5940	4790

Figure 122 a) Curves obtained by plotting the chemical shift of the pyrrole protons upon addition of both enantiomers of the tetrabutylammonium salt of NBoc-Phe- O^- . b) Binding constants measured by NMR titration in CD_3CN . The curves were fitted according the 1:1 host:guest binding model.

Upon addition of the guest for both the pyrrole and amide protons a difference in the chemical shift ($\Delta\delta$) of around 2 ppm downfield was observed. Saturation was observed and the curve was fitted with the 1:1 host:guest binding model and the constants calculated are $K_a \approx 5 \cdot 10^3 \text{ M}^{-1}$ for both enantiomers of the phenylalanine. The lack of

differences between the two curves was corroborated by the small difference between the calculated stabilisation constants.

The enantioselectivity can be enhanced by increasing the number of hydrogen bond donors which can create further interactions with the amino acid guest. The properties of receptor **105**, that bears two primary amides, and of receptor **106**, which has two hydroxyl groups, were investigated towards a series of *N*-protected amino acids. The screening was done in CD₃CN, by means of NMR titrations.

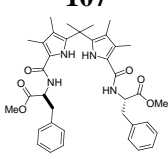
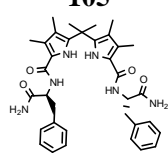
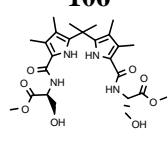
Amino acid	Receptors $K_a (M^{-1})$					
	107		105		106	
						
	K_a	$K_L:K_D$	K_a	$K_L:K_D^a$	K_a^b	$K_L:K_D$
NAc-PheOTBA	L 3840	1.4:1	L $K_{1:1}$ 1720	3:1	L 2330	1.5:1
	D 2570		$K_{1:2}$ 5 D $K_{1:1}$ 2780 $K_{1:2}$ 1		D 1540	
NBoc-PheOTBA	L 4380	1.5:1	L $K_{1:1}$ 2880	2:1	L 1920	1.2:1
	D 2860		$K_{1:2}$ 13 D $K_{1:1}$ 1710 $K_{1:2}$ 10		D 1620	
NAc-AlaOTBA	L 2810	1:1	L $K_{1:1}$ 4140	4:1	L 2120	1:1
	D: 2670		$K_{1:2}$ 18 D $K_{1:1}$ 3020 $K_{1:2}$ 6		D 1950	
NBoc-GlnOTBA	L 1550	1:1.2	L $K_{1:1}$ 1500	1:1.5	L 846	1.1:1
	D 1970		$K_{1:2}$ 6 D $K_{1:1}$ 1730 $K_{1:2}$ 8		D 736	

Table 17 Binding constant (M^{-1}) measured in CD₃CN. ^aCalculated from $K_{1:1} \cdot K_{1:2}$. ^bOnly pyrrole protons taken into account.

In the case of receptor **107** a good agreement was observed between the binding constants obtained from following the shift of the pyrrole and amide protons and the binding constant presented is the average of the values obtained by plotting the two sets of protons.

With receptor **105** a substantial agreement between the protons is achieved by treating the data with the 1:2 binding model. For receptor **106** it was not possible to achieve agreement between the binding constant of the two protons with either the 1:1 binding model or with the 1:2. This could mean that the processes taking place in solution were the result of multiple equilibria that are difficult to rationalise. Therefore, it was decided to take into consideration only the binding constants obtained by plotting the pyrrole protons with a 1: 1 binding model. From this screening a modest enantioselectivity was observed particularly with tweezers **107** and **106**. In most of the cases analysed the L enantiomer of the amino acid gives a slightly higher binding constant that in some cases is the double of the D isomer. The differences between the two enantiomers are not increased by functionalising the receptor or the guest with polar groups; by increasing the possibility of secondary interactions the binding process gets more complicated. It evolves from a 1:1 stoichiometry for receptor **107** to a 1:2 stoichiometry for receptor **105**, to become a mixture of equilibria not easy to rationalise for receptor **106**. In order to have accurate data, the titration of tweezer **107** the tetrabutylammonium salts of the *N*Boc-protected phenylalanine was repeated four times for the L enantiomer and three times for the D enantiomer. The results presented in the table are the average of the binding constant calculated from each titration. In the case of receptor **105** the selectivity was calculated on the overall binding process which is represented by the β_2 ($\beta_2 = K_{1:1} \cdot K_{1:2}$). The data obtained showed a pronounced selectivity for the L enantiomers of the amino acids tested apart from glutamine, which showed inversion of selectivity. In the case of **105**, the data have to be taken cautiously as the evaluation of the binding constants for multiple equilibria is not as accurate as the evaluation of the binding constant of a simple 1:1 binding process.

The other chiral receptors synthesised have also been tested for enantioselectivity with the tetrabutylammonium salts of both enantiomers of the *N*Boc-Phe (table 17).

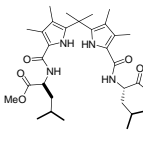
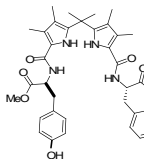
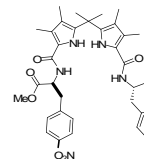
Amino acid	Receptors		
	K_a (M^{-1})		
	104	110	109
			
NBoc-L-PheOTBA	6794	3730	$>10^4$
NBoc-D-PheOTBA	6084	3030	$>10^4$
$K_L:K_D$	1.1:1	1.2:1	NA

Table 18 Binding constants measured by NMR titration in CD_3CN . The curves were fitted according the 1:1 host:guest binding model.

As the binding constant measured with receptor **109** is too high and cannot be determined by NMR titration it was decided to perform the measurements in mixtures of CD_3CN - 1% H_2O . These values were compared to those obtained with tweezer **107**. All the experiments were done in the same freshly prepared solvent batch.

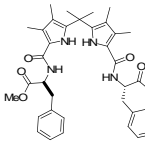
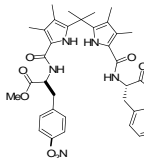
Amino acid	Receptors	
	K_a (M^{-1})	
	107	109
		
NBoc-L-PheOTBA	495	1592
NBoc-D-PheOTBA	645	1815
$K_L:K_D$	1.2:1	1:1.1

Table 19 Binding constants measured by NMR titration in CD_3CN -1% H_2O . The curves were fitted according the 1:1 host:guest binding model.

It was confirmed that the nitro-substituted receptor gives higher binding constants compared to the simple phenylalanine receptor. With these receptors minimal differences between the two enantiomers were recorded.

Analysing the data it can be stated that the tweezer receptors formed more stable complexes with the L enantiomer of the amino acids analysed. In some cases the binding constant measured with the L enantiomer is almost twice the value of the binding constant measured with the D enantiomer. It seems that the presence of water in the solvent mixture could affect the selectivity: tweezer **107** showed reduced selectivity in CD₃CN- 1% H₂O (table 16 and table 18), while tweezer **109** had a small selectivity for the D enantiomer (table 18).

The aim of the project was to synthesise molecules that could be used as active agents in the extraction of an amino acid, or that could be used as separating agent in HPLC chiral columns. For these applications a 1:2 selectivity for one of the enantiomers could be enough to achieve separation.

2.9 Conclusions

In this chapter the process of optimisation of the synthesis of diacid **82** was described.

The combination of the Zard-Barton method to obtain the pyrrole **92** and the transesterification reaction provided an efficient way to obtain a quantity of product (diacid **82**) sufficient to synthesise and study a variety of receptors. The coupling conditions were optimised and a series of dipyrromethane based receptors were synthesised and their binding properties were investigated with simple anions and amino acids in different solvents.

In DMSO-*d*₆-0.5% H₂O the simple achiral tweezer receptors **101** and **102** were clearly selective for dihydrogen phosphate. The achiral tweezer with the phenyl ring (**102**) had less affinity with anionic guests than the tweezer with a simple alkyl chain (**101**).

Among the tweezer receptors with an amino acid moiety, the selectivity changed according to the nature of the side chain. When the amino acid was a phenylalanine, and the side chain included a phenyl ring, there was a clear selectivity for dihydrogen phosphate. In the cases where the residue included an alkyl chain (leucine, **104**) or an

alcohol (serine, **106**) there was no significant difference between acetate and dihydrogen phosphate. A small difference in the binding properties was observed between receptor **105** and **107** so it could be stated that the presence of additional hydrogen bonding donors did not increase the affinity of the host for simple anionic guests. In DMSO-*d*₆-0.5% H₂O all tweezer receptors revealed selectivity for oxo-anions and the complexes formed with chloride had a very low stability constant (e.g. $K_a = 27 \text{ M}^{-1}$ with tweezer **101**) or no complex was formed.

Tweezers **105**, **106** and **101** also formed stable complexes with tetrabutylammonium dihydrogen phosphate in the more competitive solvent DMSO-*d*₆-5% H₂O.

In CD₃CN-1% H₂O the ability of the receptors **101** and **102** to bind acetate was much lower than receptors with ester functionalities. The presence of the phenyl ring did not have a significant influence in selectivity.

Polar functionalities did not increase the stability constants of the complex formed by the receptor and acetate, but complicated the binding process by stabilising the 1:2 host:guest complex as in **106**, or by forming internal hydrogen bonding in **105**. However the presence of a polar functionality combined with a phenyl ring determined the selectivity for dihydrogen phosphate over acetate in acetonitrile.

It was also demonstrated that substituents on the phenyl ring of the phenylalanine based receptors played an active role: the binding constant was increased four times by the presence of an electron withdrawing substituent, while the complex was destabilised by the presence of an electron donating substituent. This effect was prominent in acetonitrile, but it also played a role in DMSO.

Tweezer receptors formed more stable complexes with the L enantiomer of the amino acid analysed. In some case the binding constant measured with the L enantiomer is almost twice the value of the binding constant measured with the D enantiomer. The presence of water in the solvent mixture led to a depletion of the selectivity: tweezer **107** showed reduced selectivity in CD₃CN-1% H₂O, while tweezer **109** had a small selectivity for the D enantiomer.

Chapter III

Macrocyclic dipyrrromethane based receptors

3.1 Chiral macrocyclic dipyrrromethane based receptors

A macrocyclic structure is more preorganised than an acyclic structure: the higher preorganisation can lead to an increased affinity for the guest (macrocyclic effect)²⁵ and to an increased enantioselectivity.^{56,107}

A series of chiral macrocycles with general structure **126** was designed. The carboxylate binding site and the chiral residue is the same as it was in the acyclic receptors. The new elements introduced are two amides that can further interact with the guest and an alkyl chain that closes the southern end of the macrocycle (figure 123).

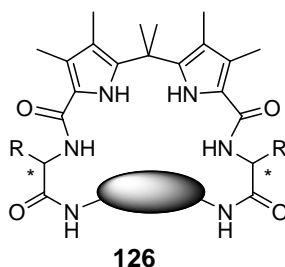
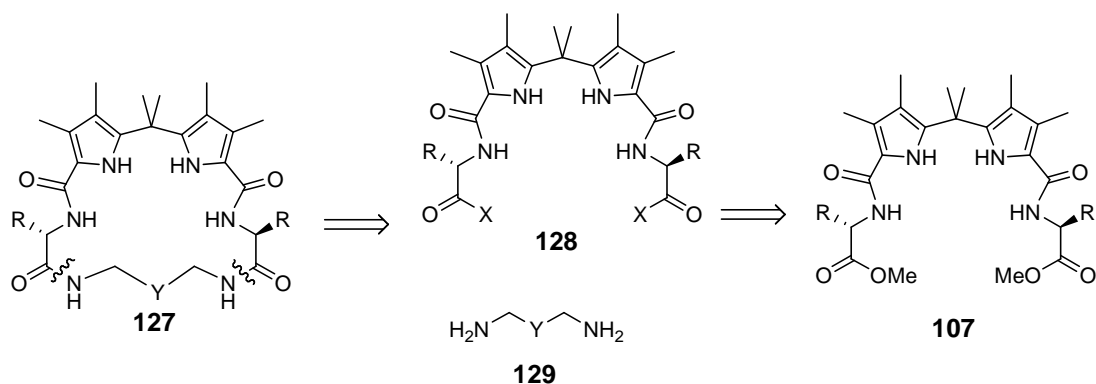


Figure 123

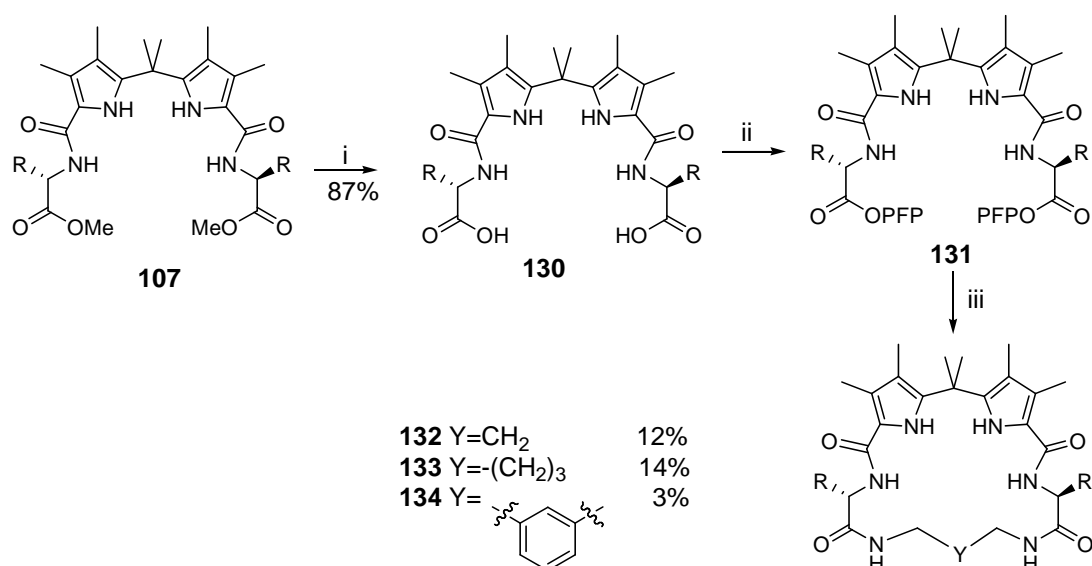
3.2 Synthesis

As a chiral unit the phenylalanine amino acid was chosen because tweezer **107** showed moderate enantioselectivity and its synthesis was already optimised. The retrosynthetic approach undertaken in the synthesis of the general structure **127** (scheme 23) consisted of simultaneous disconnection of the two amide bonds to give the diamine **129** and the activated ester **128**. In this way the size and the rigidity of the macrocycle can be easily modulated by varying the length of the alkyl chain. The activated ester can be formed by FGI (functional group interconversion) from tweezer receptor **107**.

**Scheme 23**

The length of diamine **129** might play a crucial role both in the synthesis and in the binding properties of the macrocycle. A chain which was too short would generate an extremely constrained system which would be energetically disfavoured and therefore difficult to synthesise. On the other hand a chain which was too long would give a less preorganised system and this could decrease the advantages of having a macrocyclic structure.

The choice of the alkyl chain length in amine **129** was made on the basis of previous studies done by Sessler, who used the equivalent of a three carbons chain to close a dipyrromethane based macrocycle¹¹¹ The synthetic protocol that was used has been previously optimised in the group (scheme 24).¹⁴⁸

**Scheme 24** i) LiOH, THF; ii) PFPOH, EDC, DCM; iii) **129**, TBACl, Et₃N, DCM.

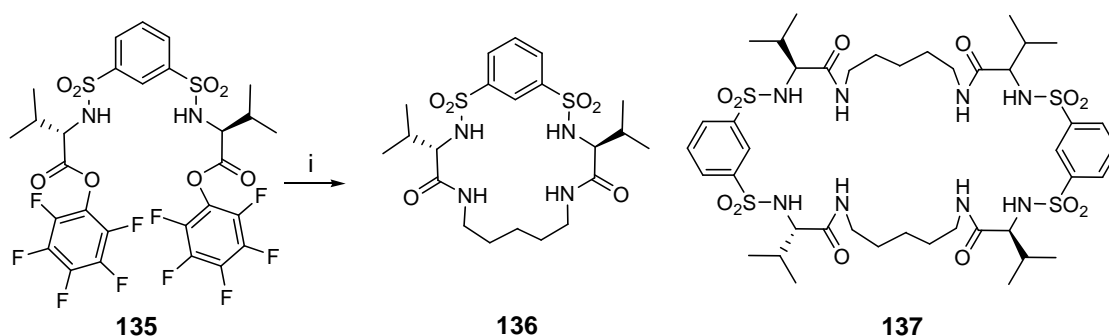
Ester **107** was hydrolysed to give diacid **130** in good yield. It was decided to perform the peptide coupling by activating the ester with pentafluorophenyl ester which was formed with EDC and pentafluorophenol. The excess of pentafluorophenol and the EDC side product were washed away in the basic work up. The pentafluorophenyl ester was chosen as activated ester, because it was efficiently used in the past in the group¹⁴⁹ and in the literature¹⁵⁰ for the synthesis of macrocycles. Furthermore the activated ester can be isolated and it does not require the use of additives and as a result the reaction mixture is relatively clean. The macrocyclisation step was performed under high dilution and by concomitant slow addition of the reagents and in the presence of tetrabutylammonium chloride as an anion template. Macrocycles **132** and **133** were isolated in low yields, but still reasonable for this type of reaction. Macrocycle **134**, however, was obtained in very low yield.

3.3 Anion template directed macrocyclisation

3.3.1 Sulphonamide based macrocycle

While the role of cations as templating agent was well established and widely used particularly for the synthesis of crown ethers,¹⁵¹ only a few examples exist where anions are used as a tool to increase the efficiency of macrocyclisation reactions..¹⁵²

A recent study on a macrocyclisation reaction (scheme 25) in our group investigated the role of chloride. It was noticed that by adding the TBACl to the reaction mixture the yield of **136** increased significantly and the byproduct [2+2] **137** was not detected.



Scheme 25 i) 1,5-diaminopentane, TBACl, Et₃N, DCM.

To ascertain that the differences noted could be ascribed to the presence of the chloride rather than to differences in coupling conditions a control experiment was carried out.

Four different reactions were performed under the same conditions (table 20) varying exclusively the equivalents of chloride.

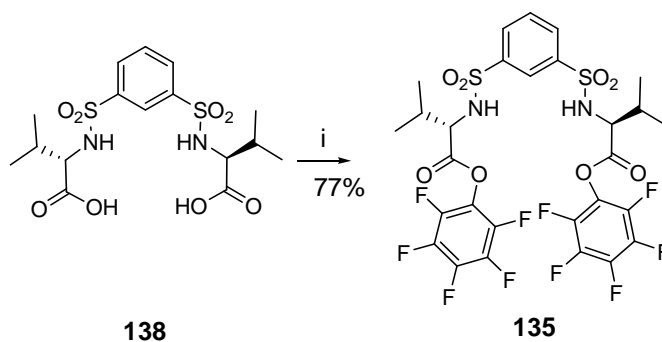
<i>TBACl</i> equivalents	Compound isolated	
	Yield (%)	
	136	137
0	28	26
1	65	a
2	79	a
4	79	a

Table 20 Yields of macrocycle obtained by varying the equivalents of *TBACl* present in solution.¹⁴⁸ ^aCompound not present in the reaction mixture

It was proved that the presence of the chloride had a tangible effect on the yields and on the selectivity for the [1+1] macrocycle. The highest yield was obtained when two equivalents of anion were present in solution.

Starting from these encouraging results it was decided to check whether changing the nature of the anion led any changes on the yields in the reaction.

So some fresh pentafluorophenyl ester **135** was synthesised from diacid **138**, which was still present in the laboratory (scheme 26).



Scheme 26 i) EDC, Pentafluorophenol, DCM.

Pentafluorophenyl ester **135** was obtained in good yield and used after purification by column chromatography. An experiment with four different macrocyclisation reactions was performed under the same conditions apart from the nature of the anion present

(table 21). Based on the results previously obtained (table 20), it was decided to add two equivalents of anion.

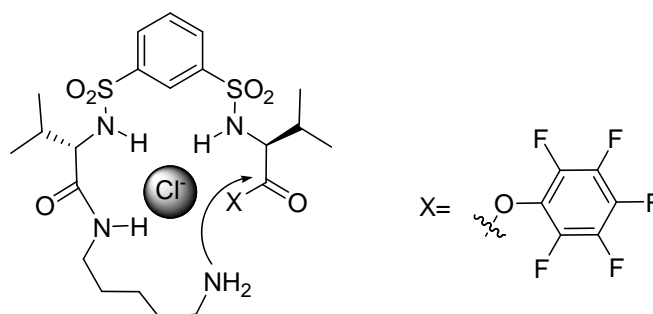
<i>Anion</i> (TBA salt)	Compound isolated
	Yield (%)
	136
Cl ⁻	68
Br ⁻	65
AcO ⁻	21
H ₂ PO ₄ ⁻	a

Table 21 Yields (%) of macrocycle **136** obtained. ^aCompound not present in the reaction mixture.

The highest yields were obtained when the anion present was chloride or bromide. In presence of acetate the quantity of macrocycle isolated is comparable to the reaction performed in absence of the anion, while in presence of dihydrogen phosphate no product was detected; [2+2] macrocycle **137** was never observed.

A preliminary conclusion was that while spherical anions such as chloride and bromide play a role in increasing the macrocyclisation yield, the acetate did not play any role, and phosphate inhibited the reaction.

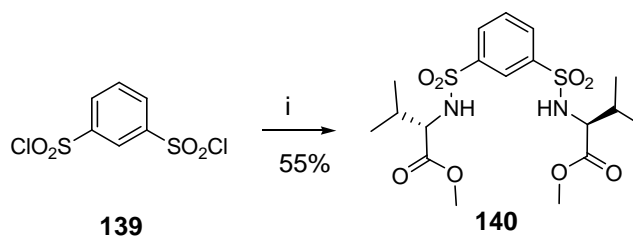
A plausible mechanism that could explain the role of the anion template was proposed.¹⁴⁸ The anion present in the reaction mixture could interact with the acyclic intermediate, favouring a syn-syn conformation. In this way the formation of the intramolecular amide bond is accelerated (scheme 27).



Scheme 27 Proposed mechanism for the mediated templated effect.¹⁴⁸

A comparison between the yields obtained in the macrocyclisation reaction and the binding properties of this type of substrate was carried out.

It was decided to analyse the binding properties of the starting material and the product of the macrocyclisation reaction. So tweezer **140** was synthesised as a model in order to evaluate the binding properties of the starting material (scheme 28).



Scheme 28 i) H_2N -L-Val-OMe·HCl, Et_3N , DCM.

The methyl ester of the valine was coupled with sulfonyl chloride **139** in presence of triethyl amine to give tweezer receptor **140** in reasonable yield. Its binding properties were tested in $CDCl_3$ which has a polarity comparable to dichloromethane, which was the solvent used for the macrocyclisation reaction. The anions tested were acetate and chloride.

Upon addition of TBACl to a solution of tweezer the sulfonamide (*a*, fig 124) protons moved 0.2 ppm downfields, the signal broadened during the titration but it was still visible, while the aromatic CH (*b*), which was assigned as the proton between the two sulfonamide moieties, had a very small shift (<0.1 ppm) upfield (fig. 124).

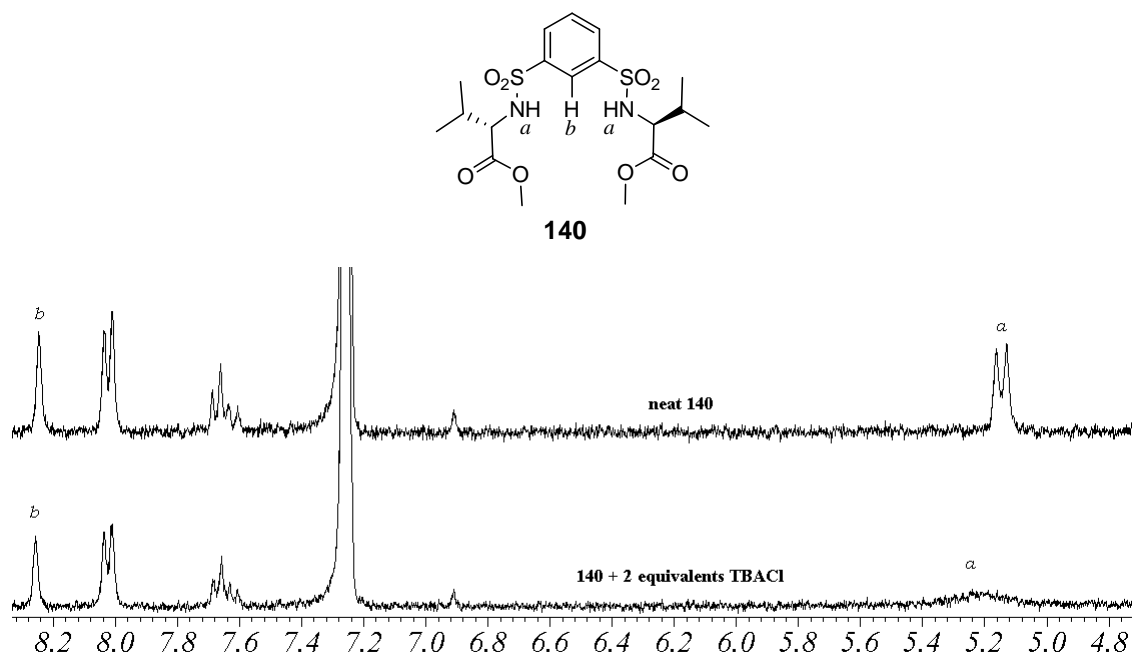


Figure 124 ^1H NMR in CDCl_3 of neat receptor **140** and of receptor **140** in presence of 2 equivalents of guests. The sulfonamide (a) and the aromatic (b) protons were monitored.

The shape of the curve obtained by plotting the chemical shift of the sulfonamide (a) protons did not fit into any curve fitting program (figure 125).

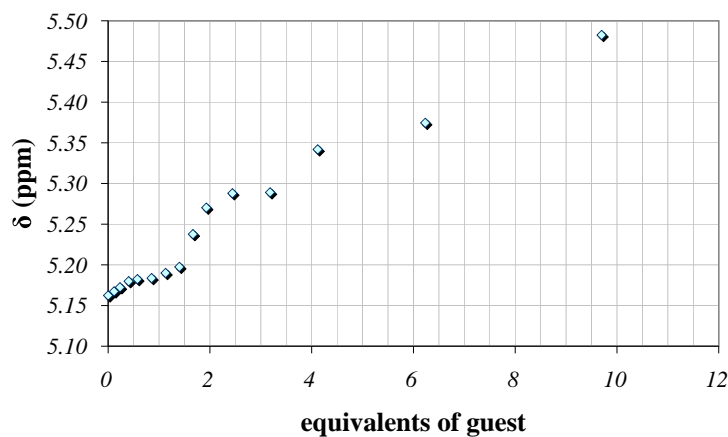


Figure 125 Chart obtained by monitoring the changes in the chemical shift of the sulfonamide (a) protons upon addition of TBACl to a solution of tweezer **140** in CDCl_3 .

When acetate was added to a solution of tweezer **140** in CDCl_3 the signal of the sulfonamide protons disappeared, while the CH aromatic (*b*) proton had a downfield shift of 0.2 ppm (fig 126).

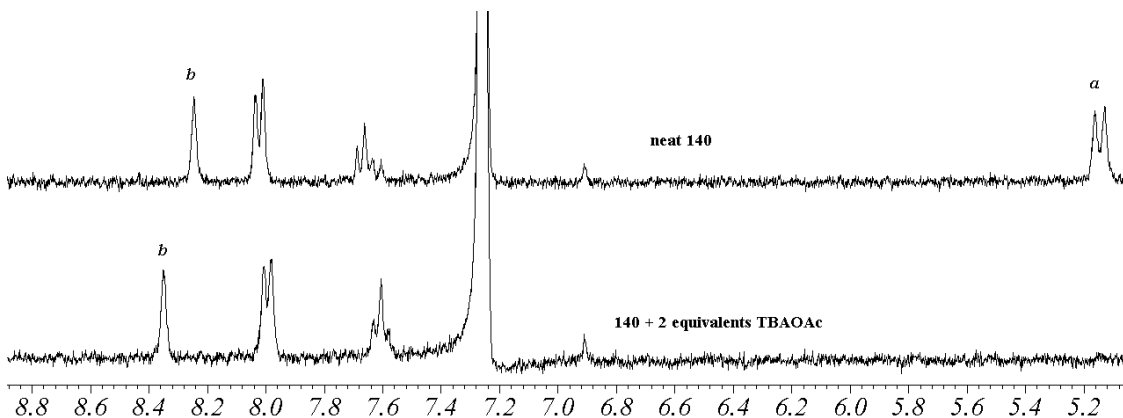


Figure 126 ^1H NMR of neat receptor **140** and of receptor **140** in presence of 2 equivalents of guests. The sulfonamide (*a*) and the aromatic (*b*) protons were monitored.

By plotting the shift of the aromatic proton the binding constant was calculated with the 1:1 binding model giving $K_{1:1} = 692 \text{ M}^{-1}$ (figure 127).

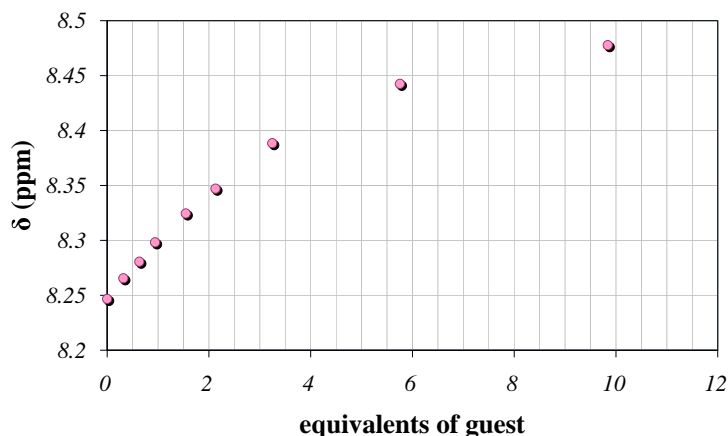
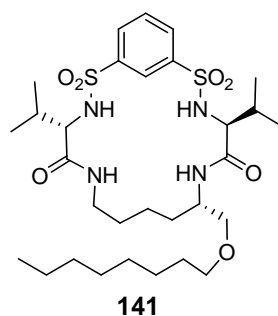


Figure 127 Chart obtained by monitoring the changes in the chemical shift of the aromatic (*a*) proton upon addition of TBA acetate to a solution of tweezer **140** in CDCl_3 .

It was not possible to compare the binding properties of receptor **140** with the two anions. Looking at the changes in the spectra, however, it was clear that some interaction occurred, but with the result obtained it could not be rationalised.

The following step consisted on evaluating the binding properties of the product towards a series of anions. As macrocycle **136** was not soluble in chloroform macrocycle **141** was analysed instead (figure 128).



Anion (TBA salt)	Receptor K_a (M^{-1}) 141
AcO^{-a}	$K_{1:1} 5 \cdot 10^4$
Cl^{-a}	$K_{1:2} 20$
Br^{-a}	$>10^4$
$H_2PO_4^-$	3590

Figure 128 Binding constants measured in $CDCl_3$. ^aData obtained previously in the group.¹⁴⁸

The stability constant for the complex formed between receptor **141** and dihydrogen phosphate was much lower than the one recorded with any other anion. Upon addition of dihydrogen phosphate the signals of the sulphonamidic protons and one amide proton disappeared while the remaining amide proton shifted 2.4 ppm downfield and it reached saturation. The curve was fitted with the 1:1 binding model (figure 129).

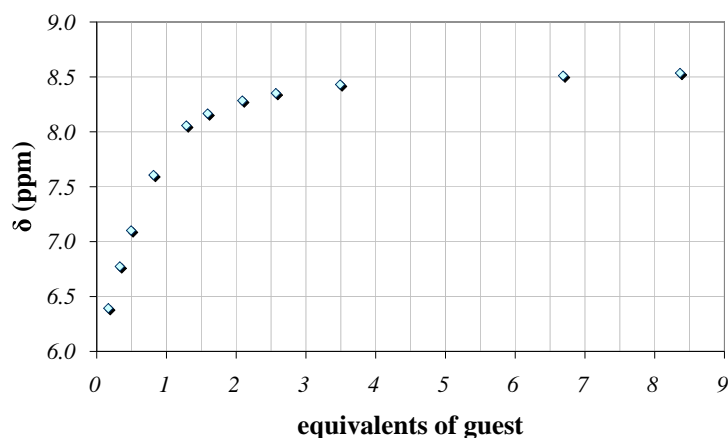


Figure 129 Chart obtained by monitoring the changes in the chemical shift of one amide proton upon addition of TBA acetate to a solution of macrocycle **141** in CDCl_3 .

An interesting correlation was found, the higher stability constants between macrocycle **137** and the anions corresponded to a higher yields in the macrocyclisation reaction.

3.2.2 Dipyrromethane based macrocycle

The same methodology was applied to the synthesis of dipyrromethane based macrocycles. The studies on this system were carried out on the synthesis of macrocycle **132**. An experiment with four different macrocyclisation reactions, carried out in the same conditions apart from the nature of the anion, was undertaken (table 22).

<i>Anion</i> (TBA salt)	Compound isolated
	Yield (%) 132
none	7
Cl^-	14
AcO^-	a
H_2PO_4^-	b

Table 22 Yields of macrocycle **132** obtained in presence of various anions. ^aThe product could not be isolated. ^bNo product was detected in the reaction mixture.

The yield in the presence of tetrabutylammonium chloride is doubled if compared to the reaction where no anion was added. However, although the result is encouraging the

difference is too small to be confidently ascribed to the template effect: it was calculated on the isolated compound and so other factors could have influenced the results. Further experiments would be needed to corroborate the data.

When acetate was used as templating agent the TLC showed the presence in the reaction mixture of new compounds, with an R_f very similar to the macrocycle that are not present in the other mixtures and this prevented also the isolation of the product and calculation of the yield. As in the case of macrocycle **136**, when the phosphate was added to the reaction mixture no product was detected.

The binding properties of the starting material and the product were also analysed in $CDCl_3$, solvent with a polarity comparable to DCM, which was the solvent used in the macrocyclisation reaction.

Tweezer **107** was chosen as a model compound of the starting material. As for receptor **103** (§ 2.8) there was no evidence of the formation of hydrogen bonds between the tweezer receptor and the acetate (figure 130).

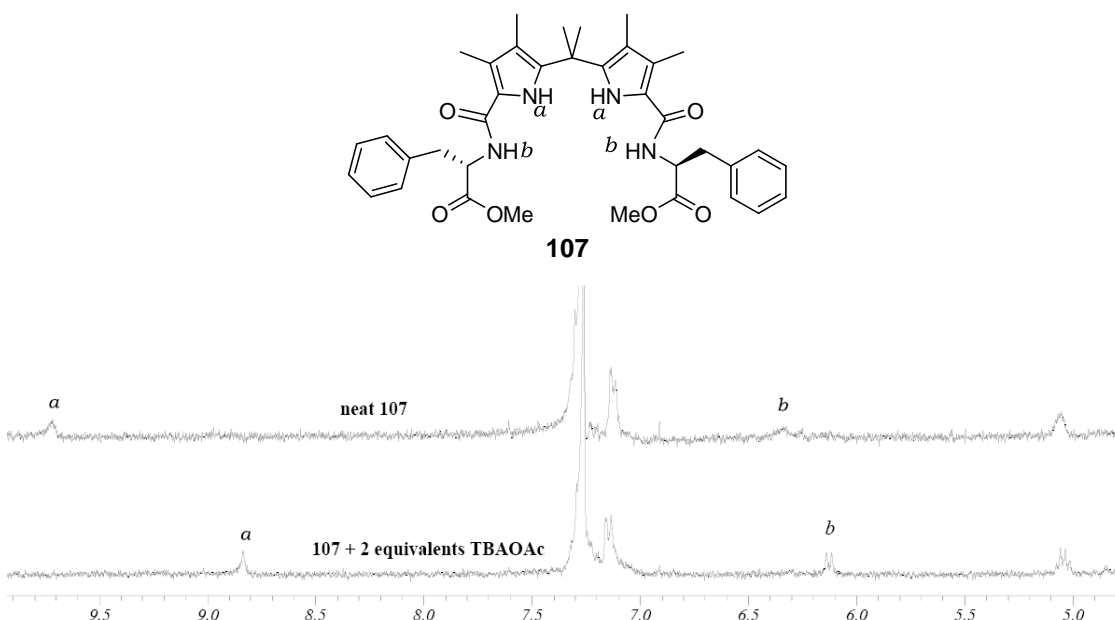


Figure 130 Shift observed in the pyrrole (a) and amide (b) protons upon addition of tetrabutylammonium acetate.

Upon addition of the guest the signal belonging to the pyrrole protons had an upfield shift ($\Delta\delta \approx 1\text{ppm}$), and it was also noted that the signals were more defined than in the

spectrum of the receptor only. So it was concluded that in chloroform the presence of the guest induced some changes on the NMR spectrum, but this cannot be clearly identified as the formation of a hydrogen bond between tweezer **107** and acetate. Therefore, it was thought that a dimerisation process was taking place in these conditions. The dimerisation constant was measured by means of NMR techniques (figure 131).

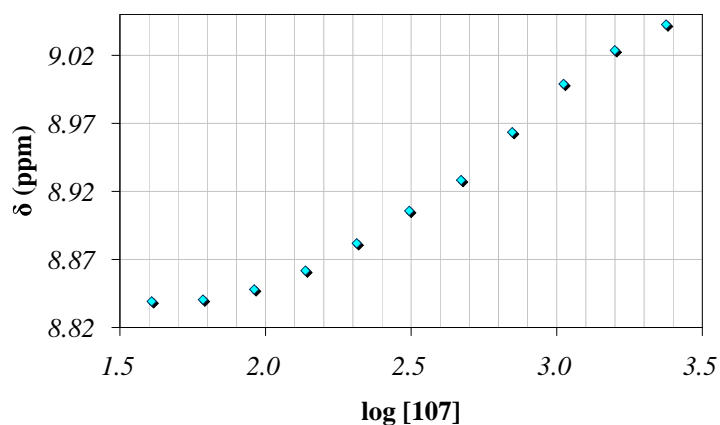


Figure 131 Dimerisation study of tweezer **107** in $CDCl_3$

The shift of the pyrrole protons (*a*) was analysed: it moved from 8.84 ppm when the concentration was 10^{-2} M to 9 ppm when the concentration was 10^{-4} M. The dimerisation constant calculated is $K_d = 1990 \text{ M}^{-1}$. The lack of binding ability in the starting material could explain the reason why the presence of the anion in the macrocyclisation did not play a dramatic role.

The binding properties of the product **132** were analysed in $CDCl_3$ by means of NMR titrations. Upon addition of acetate the signal of the pyrrole (*a*) and amide (*b* and *c*) protons shifted downfield and broadened, the pyrrole (*a*) and one of the amide (*c*) disappeared. The CH (*d*) signal moved upfield (figure 132).

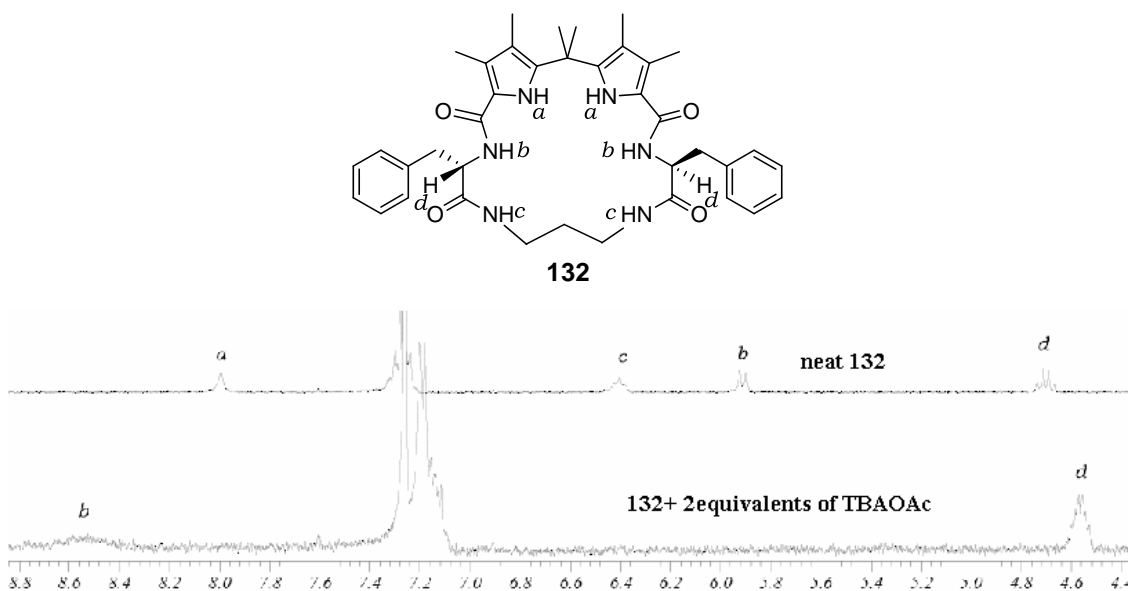


Figure 132 Shift observed in the amide (*b*) and CH (*d*) protons of receptor **132** upon addition of tetrabutylammonium acetate in CDCl₃.

The curves formed by the other amide signal and the CH were plotted and a similar binding constant was found ($K_a > 10^4$).

Upon addition of chloride the amide and pyrrole protons showed a downfield shift of about 1.5 ppm, and the CH (*d*) showed a moderate upfield shift.

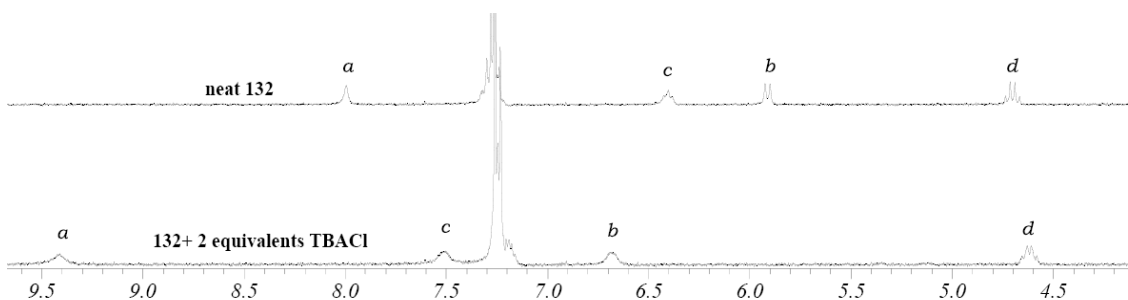


Figure 133 Shift observed in the pyrrole (*a*), amide (*b,c*) and CH (*d*) protons of receptor **132** upon addition of tetrabutylammonium chloride in CDCl₃.

The binding constants calculated on the basis of these shifts were in agreement. Therefore, the binding constant was calculated as the average of the values obtained ($K_a = 982 \text{ M}^{-1}$).

In the case of dihydrogen phosphate the signal of the pyrrole protons had a downfield shift that could be followed, although it showed some broadening at the later stages of the titration (figure 134).

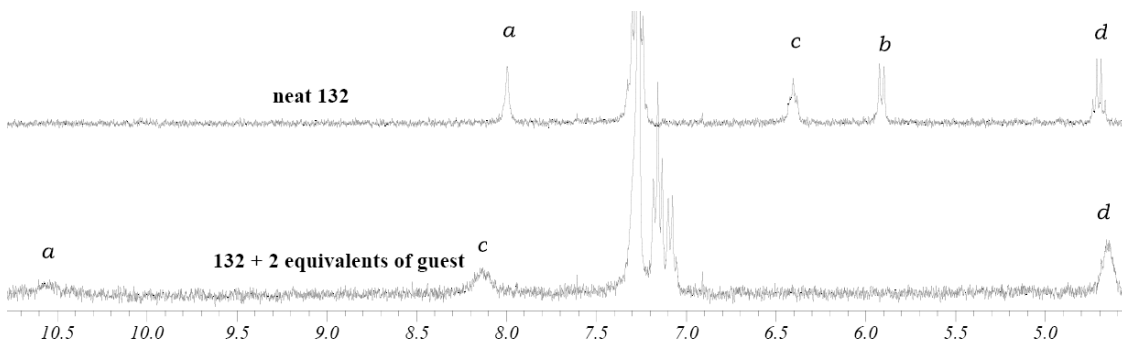


Figure 134 Shift observed in the pyrrole (a) and CH (d) protons of receptor **132** upon addition of tetrabutylammonium dihydrogen phosphate in $CDCl_3$.

The CH (d) proton had an upfield shift up to one equivalent of guest added and then it changed to a downfield movement (figure 135). The shape of the curve suggested that the macrocycle changed conformation during the titration, but was not suitable for the calculation of the constant. For this purpose the signal of the pyrrole protons was chosen, although it was not optimal because it showed significant broadening. The constant calculated had a large error, but at least it gave an idea of the order of magnitude of the association constant.

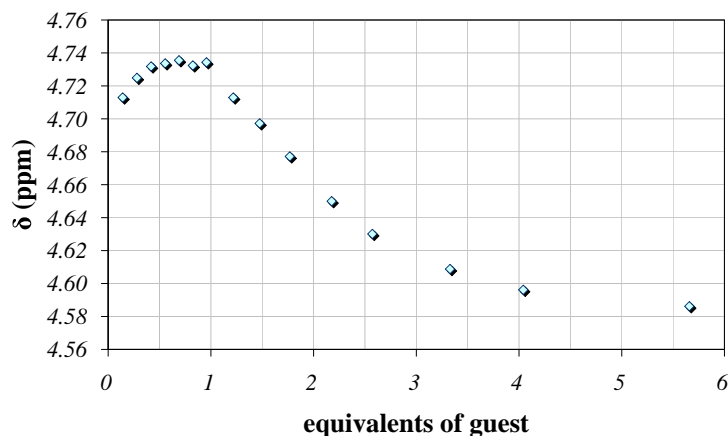


Figure 135 Chart obtained by monitoring the changes in the chemical shift of the CH (d) protons upon addition of TBA dihydrogen phosphate to a solution of macrocycle **132** in $CDCl_3$.

The results of the binding constants were summarised in figure (136). In $CDCl_3$ macrocycle **132** showed a marked selectivity for acetate.

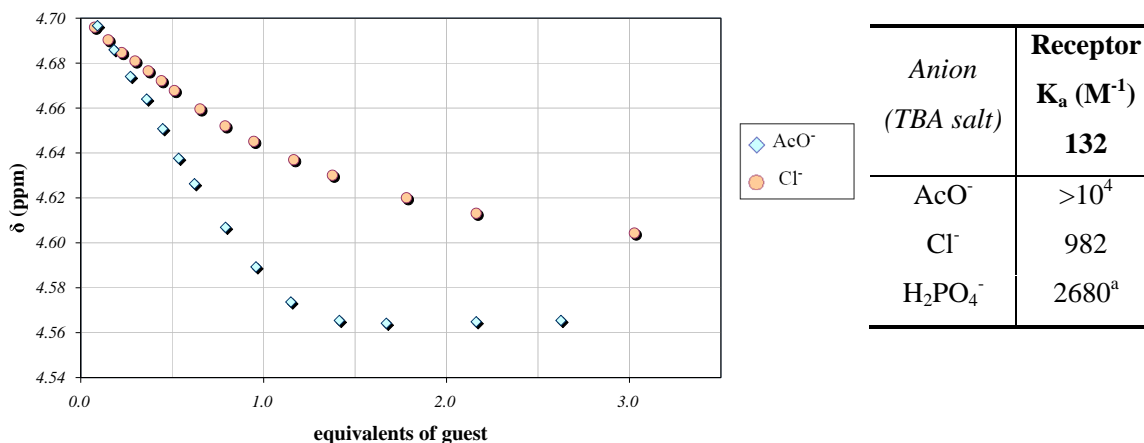


Figure 136 Binding constants measured in $CDCl_3$. ^aMeasured on the pyrrole protons.

A preliminary conclusion on the effect of anions as template agent in the macrocyclisation reaction can be made. The highest yields were obtained when both the starting material and the product were interacting with the anion in the solvent used in the reaction (e.g. **136**). From this standpoint, the low yield obtained with macrocycle **132**

could be explained by the tendency to dimerise of acyclic dipyrromethane intermediates such as **107**. Further studies are needed to investigate this matter better.

3.4 Dipyrromethane-based chiral macrocycles: binding properties

The properties of the dipyrromethane based macrocycles **132**, **133** and **134** were analysed by means of NMR titrations.

3.4.1 Binding properties in $CDCl_3$

The binding properties of receptor **132** in $CDCl_3$, partially explained in § 3.2.2, were also tested in presence of benzoate and hydrogen sulfate.

Upon addition of benzoate the pyrrole (a) and one amide (c) signal broadened, the remaining amide proton had a downfield shift of around 2 ppm, while the CH (d) had an upfield shift (figure 137).

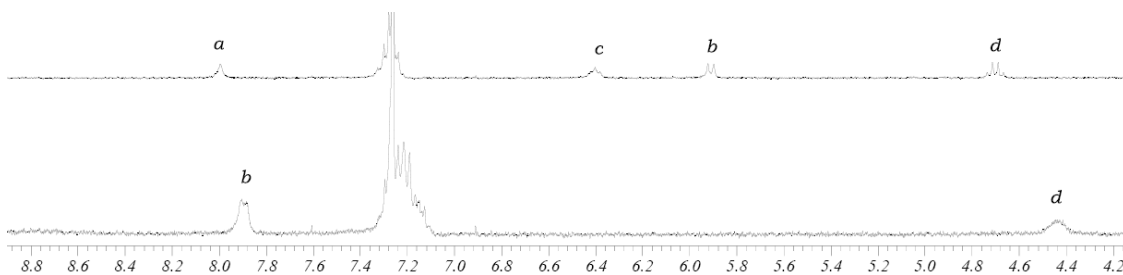


Figure 137 Shift observed in the amide (b) and CH (d) protons upon addition of TBA benzoate to a solution of macrocycle **132** in $CDCl_3$.

The binding constant was calculated on the CH (d) shift using the 1:1 host:guest model and was $K_a > 10^4 M^{-1}$.

Upon addition of hydrogen sulfate there was a general downfield movement for every analysed proton. The pyrrole protons had the largest shift ($\Delta\delta \approx 1$ ppm), the amide signals had a shift of 0.5 ppm and the CH (d) a shift of 0.2 ppm (fig. 138).

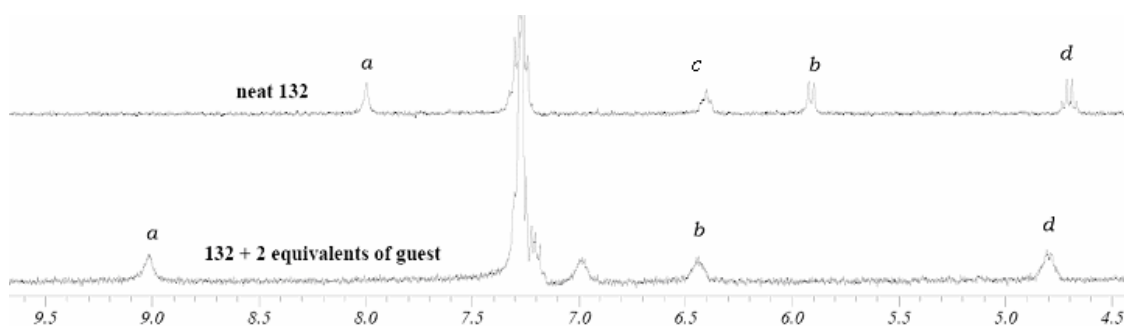
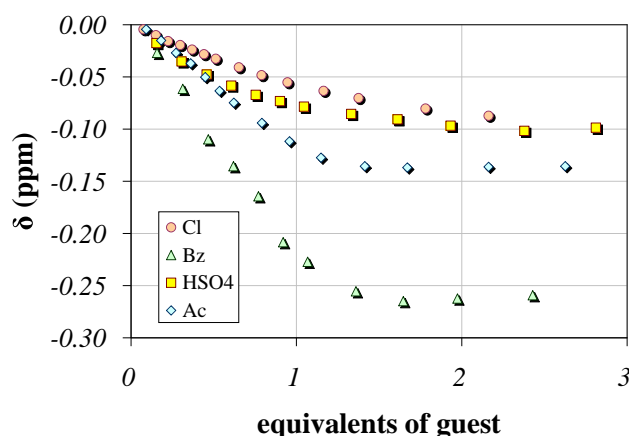


Figure 138 Shift observed in the pyrrole (a), amide (b, c) and CH (d) protons upon addition of tetrabutylammonium hydrogen sulfate to a solution of macrocycle **132** in $CDCl_3$.

The binding constant was calculated using the curves generated by the shift from all the protons and the average value was $K_a = 2400 \text{ M}^{-1}$.

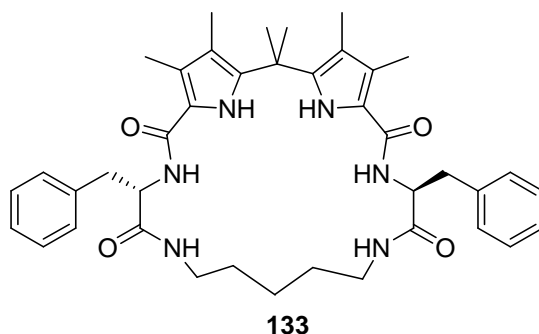
Summarising the data presented on the binding properties in $CDCl_3$, macrocycle **132** showed a clear selectivity for carboxylates (acetate and benzoate). The binding constants calculated for other oxo-anions as hydrogen sulfate and dihydrogen phosphate were similar and of an order of magnitude lower than those obtained with the carboxylates. The anion that gave the lowest stability constant was chloride (figure 139).



Anion (TBA salt)	Receptor K_a (M^{-1}) 132
AcO^-	$>10^4$
Cl^-	982
H_2PO_4^-	2680 ^a
BzO^-	$>10^4$
HSO_4^-	2400

Figure 139 Binding constants measured in $CDCl_3$. ^aMeasured on the pyrrole protons.

On changing the length of the alkyl chain as in macrocycle **133** (figure 140), the stability constant of the complex with hydrogen sulfate in $CDCl_3$ decreased.

**Figure 140**

Upon addition of hydrogen sulfate to a solution of **133** in CDCl_3 the signals moved in the same fashion as in the case of **132**; the constant, however, was more than three times lower ($K_a = 685 \text{ M}^{-1}$). There was not an appreciable difference between the binding constants calculated between the two macrocycles and chloride ($K_a = 600 \text{ M}^{-1}$).

3.4.2 Binding properties in $\text{DMSO}-d_6$

In $\text{DMSO}-d_6$ a general decrease of the binding constants was expected, as this solvent is more competitive and it had higher affinity for the macrocycle making the desolvation process less energetically favourable.

The binding properties of macrocycle **132** were tested with a series of anions.

Upon addition of bromide and hydrogen sulfate no substantial differences were observed in the spectra, indicating that no complex was formed.

Upon addition of acetate and benzoate a significant downfield shift was observed for the pyrrole and amide protons. Although the signal broadened, it was possible to monitor them and calculate the binding constants with reasonable accuracy. In the case of acetate the constant was calculated from the average of the curves obtained monitoring the amide and the CH (d) protons ($K_a = 6240 \text{ M}^{-1}$). So it was in the case of benzoate ($K_a = 1948 \text{ M}^{-1}$).

Upon addition of dihydrogen phosphate the signal of the pyrrole and amide protons underwent a severe broadening that impeded the precise measurement of their chemical shifts, causing an error in the constant. By monitoring the change in the chemical shift of the CH (d) protons the constant could be calculated with more precision ($K_a = 3660 \text{ M}^{-1}$).

When chloride was added to the macrocycle solution moderate shifts were observed in the spectra and no broadening occurred. The constant calculated was significantly lower than in the previous cases ($K_a = 154 \text{ M}^{-1}$).

Generally, upon addition of an anion to the solution the pyrrole and the amide protons shifted downfield, while the C_αH protons shifted upfield. The results obtained are summarised in figure 141.

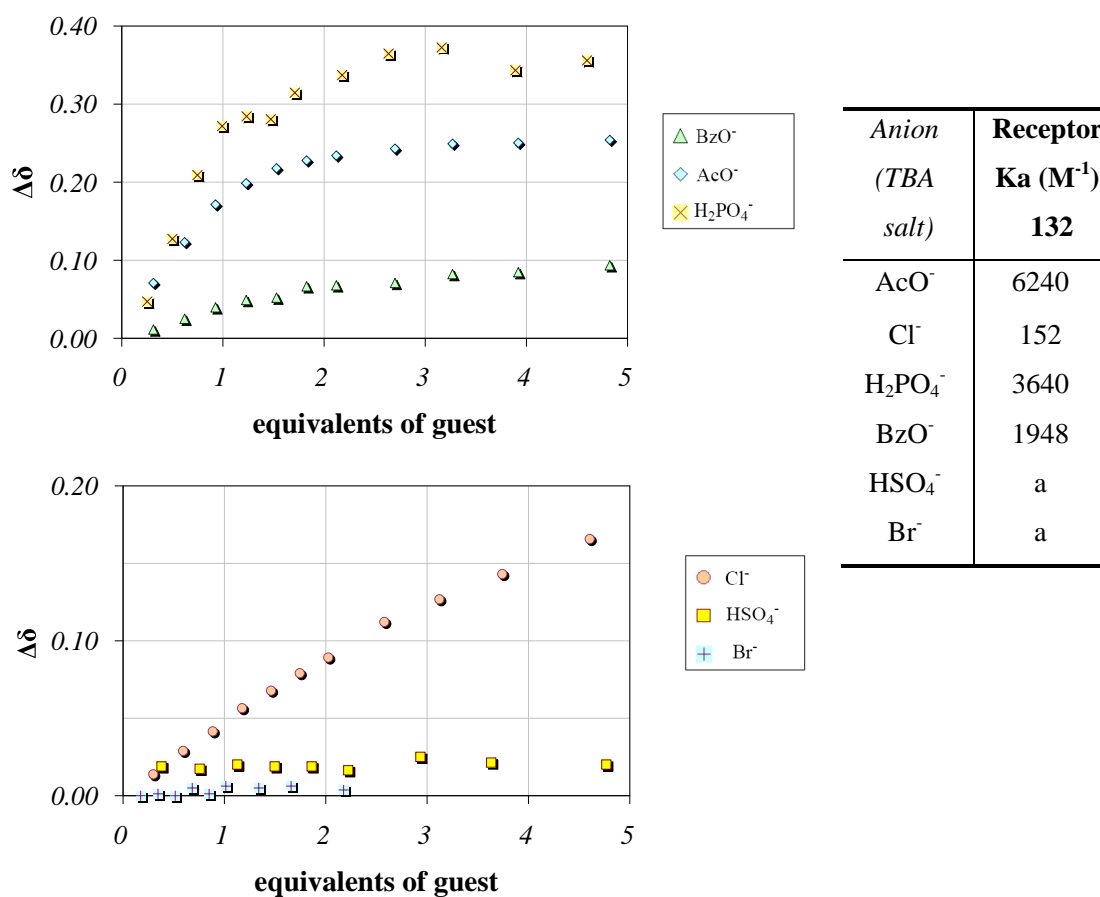


Figure 141 Binding properties of receptor **132** in $\text{DMSO}-d_6$ -0.5% water. ^aNo differences observed in the spectrum upon addition of guest

Macrocycle **132** in $\text{DMSO}-d_6$ showed a moderate selectivity for acetate over dihydrogen phosphate ($K_{\text{AcO}^-}:K_{\text{H}_2\text{PO}_4^-} \approx 2:1$). Although this result has to be taken cautiously due to the poor precision of the data obtained with the phosphate, this selectivity trend confirmed

the data obtained in CDCl_3 . It was also noticed that the selectivity changed with the rigidity of the system. Macrocycle **134**, for example was larger than macrocycle **132**. However, the phenyl ring in the southern chain gave a certain rigidity to the cycle: in this case there was almost no selectivity between the two species. In macrocycle **133**, which displayed a longer chain at the southern end, the selectivity was inverted ($K_{\text{AcO}^-} : K_{\text{H}_2\text{PO}_4^-} \approx 1:2$); the difference was further increased in tweezer **102** ($K_{\text{AcO}^-} : K_{\text{H}_2\text{PO}_4^-} \approx 1:5$) that was the less rigid and pre-organised system.

The values of the binding constants obtained with macrocycles **132** and **133** were substantially higher than these obtained for acyclic receptor **105**. Considering that the cyclic and acyclic systems have the same number of hydrogen bond donors, the difference could be ascribed to the macrocyclic effect (table 24).

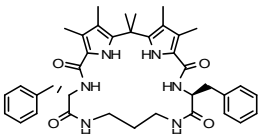
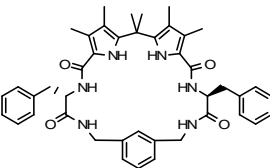
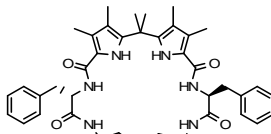
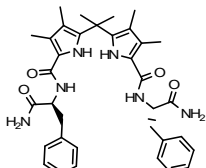
	Receptor			
	$K_a (\text{M}^{-1})$			
Anion (TBA salt)	132 	134 	133 	105 
AcO^-	6240	2089	3330	170
H_2PO_4^-	3600	1500	5630	799
$K_{\text{AcO}^-} / K_{\text{H}_2\text{PO}_4^-}$	1.7:1	1.4:1	1:1.7	1:4.7

Table 23 Binding constants measured in $\text{DMSO}-d_6$ -0.5% water.

Upon addition of anions to a solution of macrocycle **134** in $\text{DMSO}-d_6$ a downfield shift was observed for the pyrrole and the amide protons.

In this case the macrocycle formed stable complexes with oxo-anions; the complex formed with chloride showed a low binding constant.

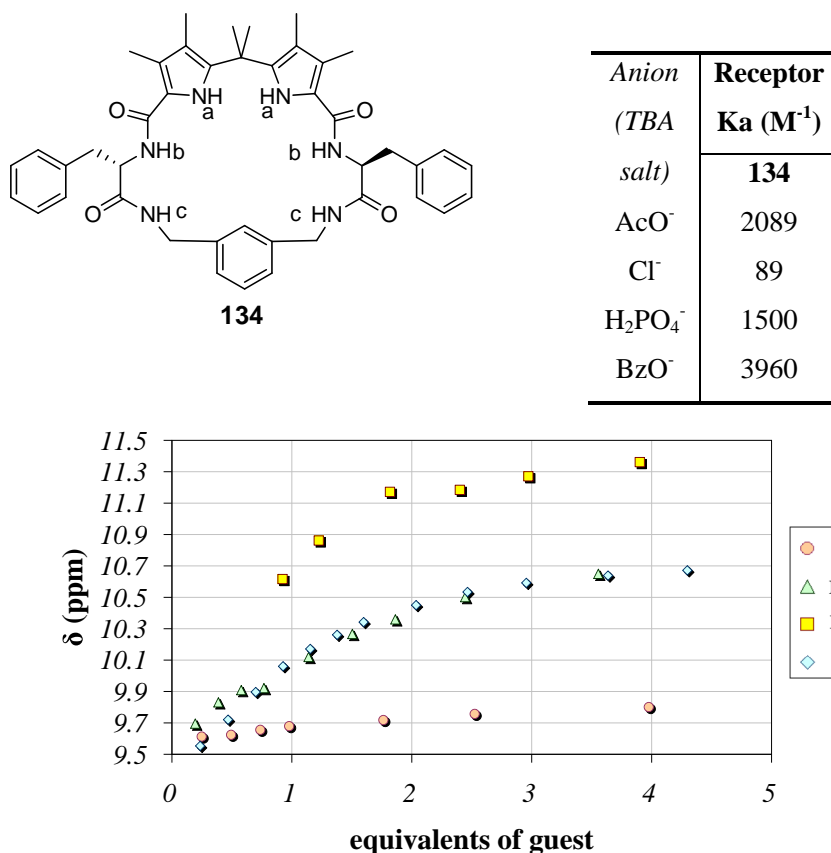


Figure 142 Binding properties of receptor **134** in DMSO-*d*₆-0.5% water. In the chart is represented the shift of the pyrrole protons (a).

In the titrations of macrocycle **134** in DMSO-*d*₆ no broadening was observed, so it was possible to monitor every proton that could make a hydrogen bond. The protons that had the largest shift are likely to be most involved in the hydrogen bonding process.⁵⁷ In this case the protons able to give hydrogen bonding were monitored: the pyrrole (a fig 142) and the amide (b and c fig 142) protons.

Upon addition of acetate to a solution of host the major shift was observed for the pyrrole (a) and the amide (b) protons. The shift of the second pair of amide protons was smaller and, therefore, it seemed to be less involved in the binding process. The same trend was observed when other anions were added to a solution of the host (figure 143).

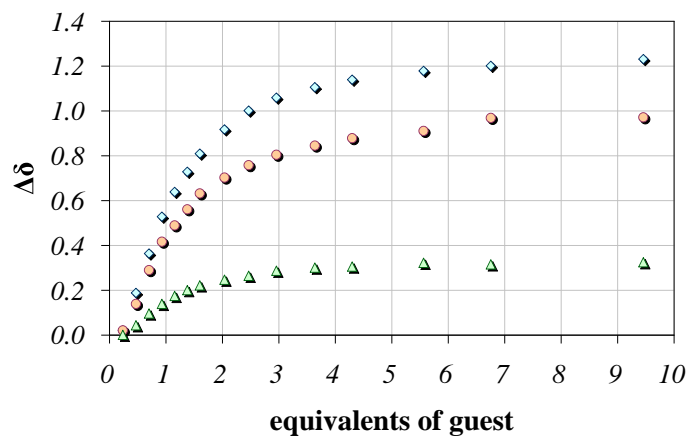
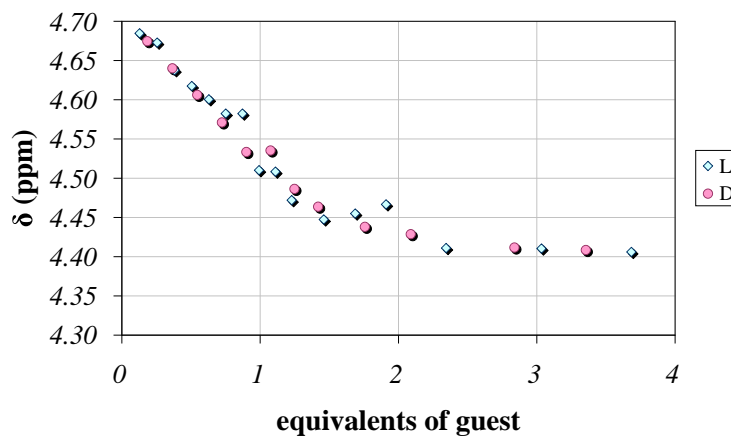


Figure 143 Differences in the chemical shifts ($\Delta\delta$) observed when tetrabutylammonium acetate was added to a solution of **134** in $\text{DMSO-}d_6$ - 0.5% water.

3.4 Enantiomeric recognition

The enantioselectivity of macrocycles **132**, **133** and **134** was tested by comparing the stability constants of the complexes formed by the receptors and the two enantiomers of the *N*Boc phenylalanine tetrabutylammonium salt.

The enantioselectivity of receptor **132** was tested in CDCl_3 and in $\text{DMSO-}d_6$ - 0.5% water. Upon addition of the amino acid to a solution of **132** in CDCl_3 the pyrrole and amide protons underwent severe broadening and so the stability constant was calculated on the basis of the shift of the CH (d) protons (figure 144).



Amino acid	Receptors
	K _a (M ⁻¹)
	132
NBoc-L-PheOTBA	3040
NBoc-D-Phe-OTBA	3570

Figure 144 Binding constants of macrocycle **132** with the two enantiomers of tetrabutylammonium NBoc-Phenylalanine in CDCl₃. In the chart are represented the curves obtained from the CH (d) protons.

The binding constants obtained for the two enantiomers were not substantially different as illustrated also by the two curves superimposed, so it could be stated that in these conditions there was no enantioselectivity.

In DMSO-*d*₆-0.5% H₂O, upon addition of the amino acid in the host solution the signal from the pyrrole protons broadened and it was not visible in most of the spectra recorded. However, when more than one equivalent of guest was added the protons involved in the binding (pyrrole, amide and CH protons) were splitted in two signals. A possible explanation was that two non equivalent complexes were formed and the equilibrium between them was slow on the NMR timescale. This phenomenon was observed with both enantiomers of the amino acid. To calculate the binding constant the average of the chemical shift of the two signals was considered. The binding constants obtained with the

two amino acids were of the order of 10^2 M^{-1} and were very similar, so neither in this solvent enantioselectivity was observed (figure 145).

<i>Anion</i>	Receptor K_a(M⁻¹) 132
NBoc-L-Phe-OTBA	667
NBoc-D-Phe-OTBA	655

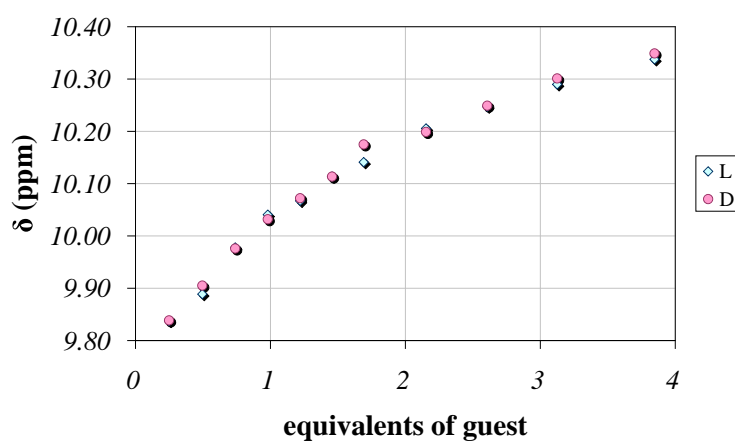
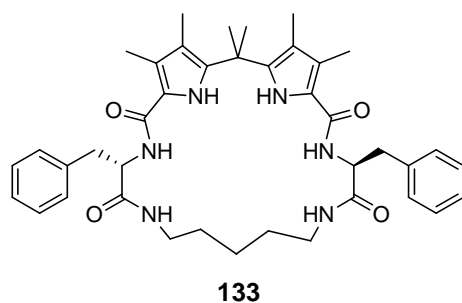


Figure 145 Binding constants of macrocycle **132** with the two enantiomers of tetrabutylammonium NBoc-Phenylalanine in DMSO-*d*₆ 0.5% H₂O. In the chart are represented the curves obtained from the pyrrole protons.

The binding properties of macrocycle **133** were analysed to check if a more flexible system could show some enantioselectivity. Upon addition of the two enantiomers of the amino acid to a solution of macrocycle **133** in DMSO-*d*₆-0.5% H₂O a behaviour similar to **132** in the same solvent was observed (figure 146).



<i>Anion</i>	Receptor K_a (M⁻¹)
	133
<i>N</i> Boc-L-Phe-OTBA	122
<i>N</i> Boc-D-Phe-OTBA	117

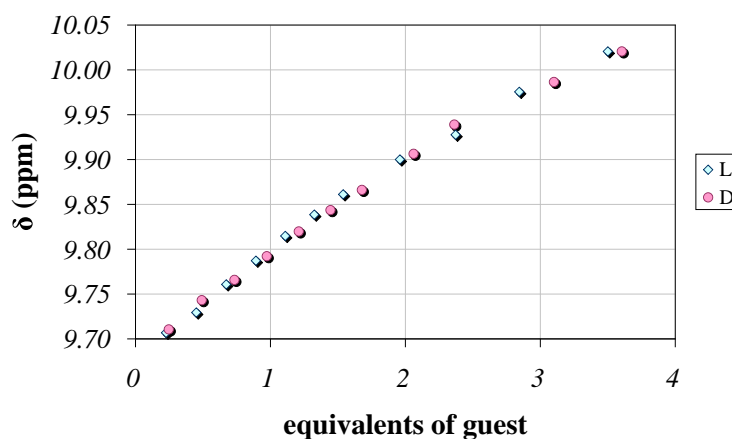
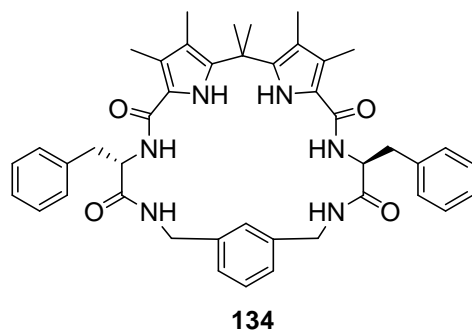


Figure 146 Binding constants of macrocycle **133** with the two enantiomers of tetrabutylammonium *N*Boc-Phenylalanine in DMSO-*d*₆-0.5% H₂O. In the chart are represented the curves obtained from the pyrrole protons.

The binding constants obtained for this receptor were six times lower than those obtained with the smaller macrocycle **132** and again no enantioselectivity was observed.

Receptor **134** was soluble in acetonitrile therefore the enantioselectivity was tested also in this solvent. Upon addition of the amino acids to a solution of macrocycle **134** in CD₃CN the pyrrole and amide protons showed a downfield movement and a broadening which did not prevent the possibility of monitoring the shift of the signals and calculating the binding constant (figure 147).



<i>Amino acid</i>	Receptor
	K_a (M⁻¹)
NBoc-L-PheOTBA	9120
NBoc-D-PheOTBA	10800
K _L /K _D	1:1.2

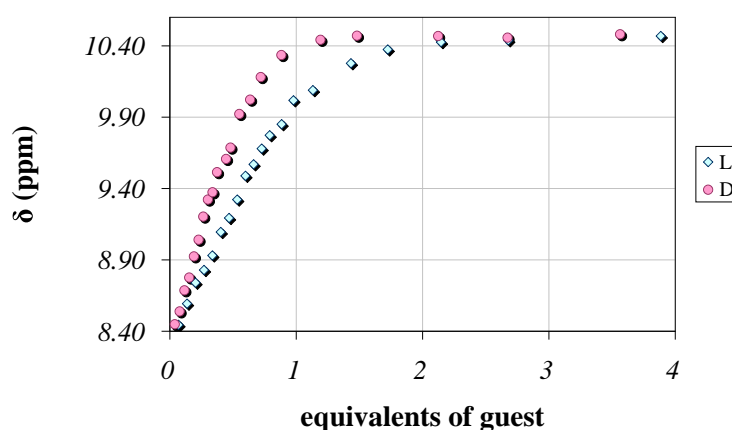


Figure 147 Binding constants of macrocycle **134** with the two enantiomers of tetrabutylammonium NBoc-Phenylalanine in CD₃CN. In the chart are represented the curves obtained from the pyrrole protons.

The complexes generated by the two enantiomers of the phenylalanine and macrocycle **134** had different binding constants in CD₃CN: the difference was observed both in the numerical values and by the superimposition of the curves. This result had to be considered cautiously because the value of the binding constants was close to the reliability limit of the NMR titration. However, it could be stated that in CD₃CN macrocycle **134** formed more stable complexes with the D enantiomer of the NBoc-protected phenylalanine.

The same study was repeated in DMSO-d₆ 0.5% H₂O; in this case the binding constants were expected to be lower. The signals of the protons shifted in a similar fashion to the titrations conducted in CD₃CN (figure 148).

<i>Amino acid</i>	Receptor K_a (M⁻¹)
	134
NBoc-L-PheOTBA	438
NBoc-D-PheOTBA	238
K _L /K _D	1.8:1

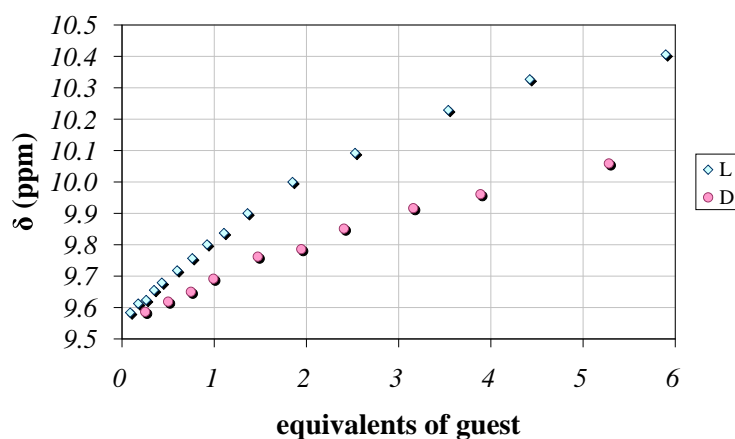


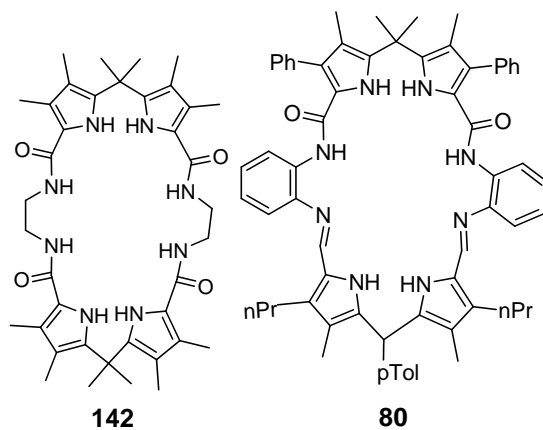
Figure 148 Binding constants of macrocycle **134** with the two enantiomers of tetrabutylammonium NBoc-Phenylalanine in DMSO-*d*₆ 0.5% H₂O. In the chart are represented the curves obtained from the pyrrole protons.

In this solvent the selectivity was inverted compared to the results obtained in acetonitrile: in this case the L enantiomer formed a more stable complex with the macrocycle. The difference between the two constants was also higher in DMSO-*d*₆.

It could be stated that the presence of the phenyl ring in the southern chain produced some enantioselectivity: the receptors that do not contain this moiety showed substantially equivalent results for the two enantiomers.

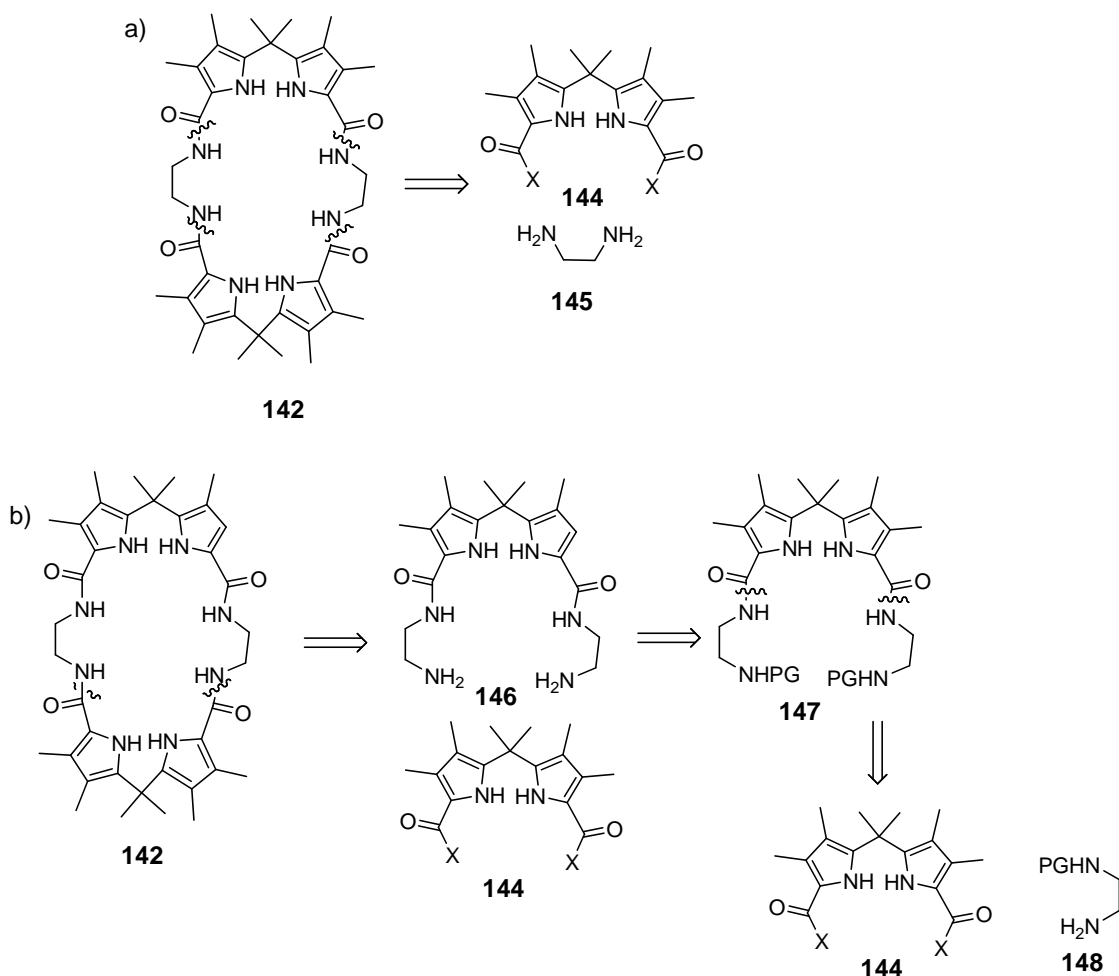
3.5 Achiral macrocyclic dipyrromethane based receptors

The dipyrromethane macrocycles were found to be good receptors for oxo-anions, so it was decided to synthesise a macrocycle bearing two dipyrromethane units, to increase the binding ability of the system (fig. 149).

**Figure 149**

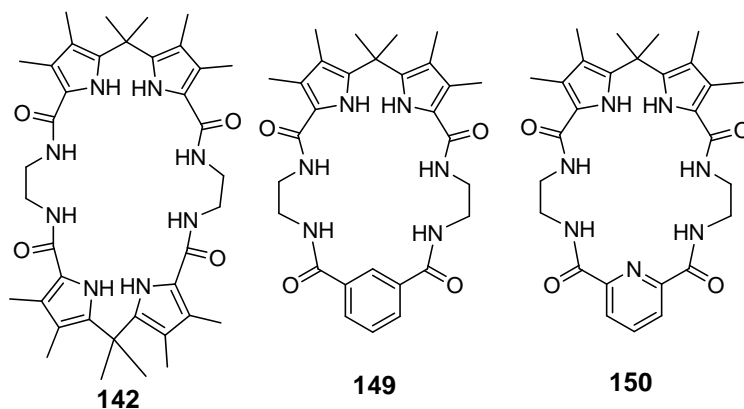
The efficacy of a similar structure in binding oxo-anions was proved by Sessler:¹⁵³ for example macrocycle **80** (§1.5) bound strongly acetate ($K_a = 4 \cdot 10^6 \text{ M}^{-1}$) in CH_3CN .

Two synthetic pathways could be envisaged for the synthesis of receptor macrocycle **142**: in one case the four amides could be formed simultaneously, in one step (a, scheme 29); in the other case they could be formed in separate steps (b, scheme 29).

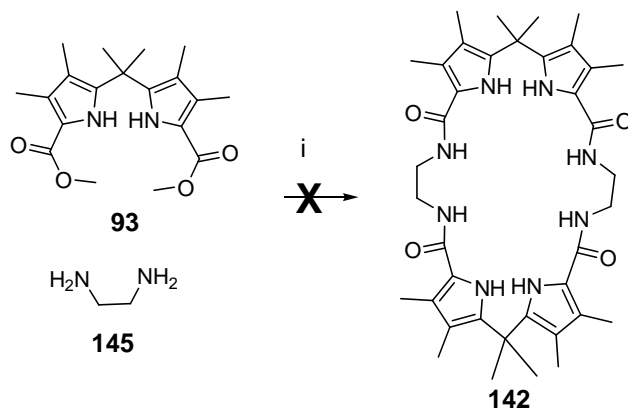


Scheme 29 Retrosynthetic analysis of macrocycle **142**.

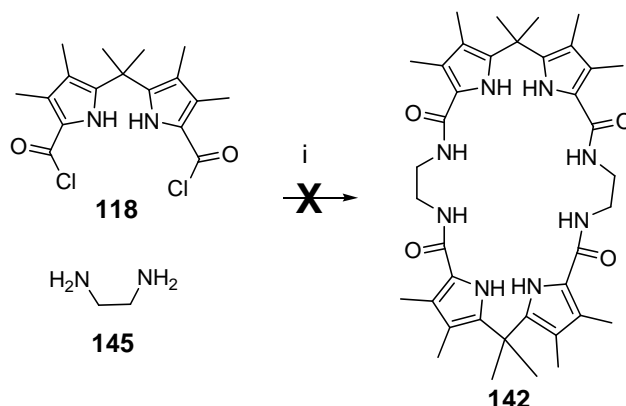
The first pathway seemed faster and desirable, but it was expected that the purification process would be more difficult due to the possible formation of oligomers and other side products. The second pathway was longer, but it could open the pathway to a series of new macrocycles, as tweezer **146** could be coupled to different units. The original idea consisted of inserting in the southern end of the molecule an aromatic moiety bearing a hydrogen bond donor (**142**), a unit without functionalities able to give hydrogen bond interactions (**149**) and a hydrogen bond acceptor (**150**) (figure 150).

**Figure 150**

In the first synthetic pathway presented in scheme 29 the amides were formed by coupling the amine with a carbonyl bearing a leaving group. Jurzack and co-workers have demonstrated that an amide can be formed in reasonable yields by coupling a methyl ester with an amine. This procedure was applied in the synthesis of tetralactams.⁵⁴ The same procedure was applied in the synthesis of **142** (scheme 30).

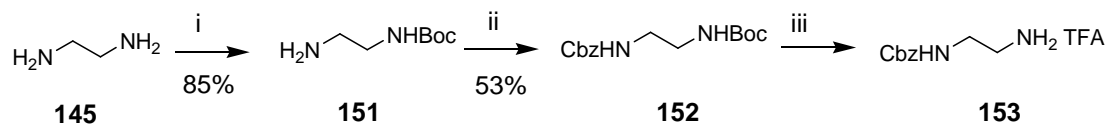
**Scheme 30 i) DCM**

Unfortunately, no reaction occurred between the starting materials. It was then decided to use a more reactive intermediate and the acyl chloride was chosen (scheme 31).

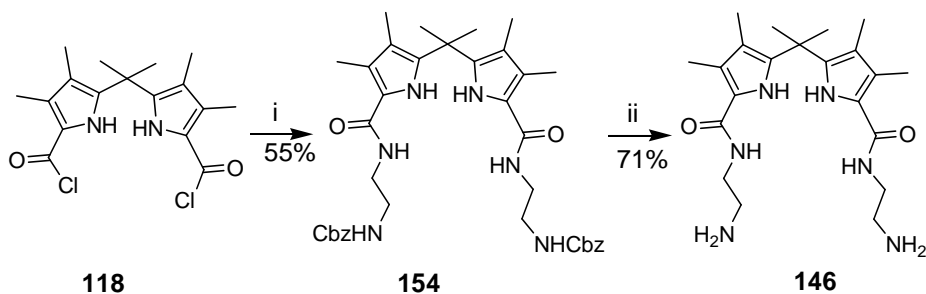
Scheme 31 *i) DCM*

In this case the starting materials reacted, but a complicated mixture was generated. Therefore, the second synthetic route was undertaken. As dipyrromethane based tweezers are generally acid sensitive (§ 2.3), a protective group that could be cleaved in neutral conditions was used. The choice fell on benzyl carbamate, as it can be removed by hydrogenolysis.

The direct synthesis of mono-Cbz-protected-ethylene-diamine failed, so a multistep procedure previously optimised in the group was followed.

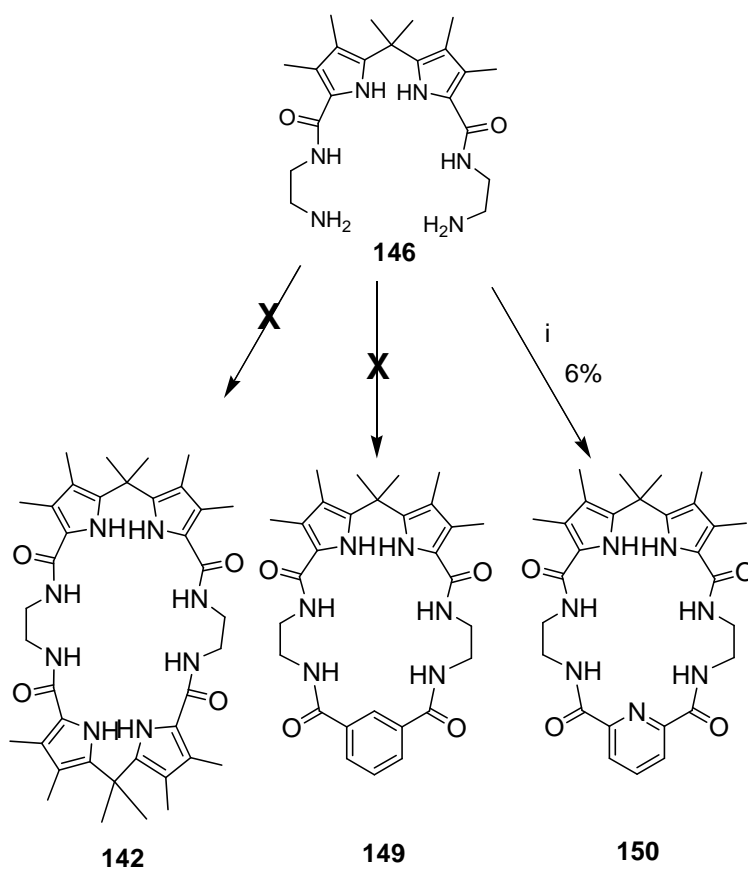
Scheme 32 *i) Boc₂O, DCM; ii) CbzCl, DCM/aqNaHCO₃; iii) TFA, DCM.*

Amine **152** was obtained after two protection steps in good yield and deprotected in presence of TFA to achieve salt **153** which was the precursor of tweezer **146** (scheme 33).

Scheme 33 *i) Et₃N, DCM; ii) H₂, Pd/C, MeOH.*

By reacting acyl chloride **118** with salt **151** in presence of triethylamine in DCM tweezer **152** was obtained in reasonable yield. The deprotection of tweezer **154** gave diamine **146** smoothly and in good yield.

So the route was opened to the macrocycles **142**, **149** and **150**. Amine **146** was insoluble in apolar organic solvents, so tetrabutylammonium chloride was added to the macrocyclisation reaction to obtain solubility in DCM and to act as template agent. The reactions between amine **146** and the suitable acyl chloride to obtain macrocycles **141**, **149** and **150** were undertaken in DCM in presence of tetrabutylammonium chloride and triethylamine (scheme 34).



Scheme 34 i) pyridine-2,6-dicarboyl dichloride, Et_3N , $TBACl$, DCM .

Unfortunately only one of the planned macrocyclisation reactions worked, and only macrocycle **150** was obtained in poor yields and in small quantity which was sufficient

only to carry out a couple of binding studies. Due to time constraints it was not possible to optimise the macrocyclisation reactions.

The binding properties of macrocycle **150** were tested with acetate and hydrogen sulfate in DMSO-0.5% H₂O.

Upon addition of acetate to a solution of macrocycle **150** in DMSO-*d*₆-0.5% H₂O the pyrrole (*a*) and the amide (*b*) protons showed a significant downfield shift ($\Delta\delta \approx 2$ ppm), while the second set of amide (*c*) protons showed a minor downfield shift ($\Delta\delta \approx 0.5$ ppm). The change in the shift of amide protons *c* (figure 151) was small compared to the pyrrole and the other amide; the reason for such behaviour could be that it was involved in an intramolecular hydrogen bond with the pyridine nitrogen. Further evidence was that the chemical shift of this proton in the neat host solution was higher than the one expected for an aliphatic amide. The intramolecular hydrogen bond pattern was exploited in the past to obtain preorganised systems (§1.4.1 and literature⁵⁵).

The binding constant was calculated as the average of the values obtained monitoring the shift of the three sets of protons, giving $K_a = 1.4 \cdot 10^4 \text{ M}^{-1}$.

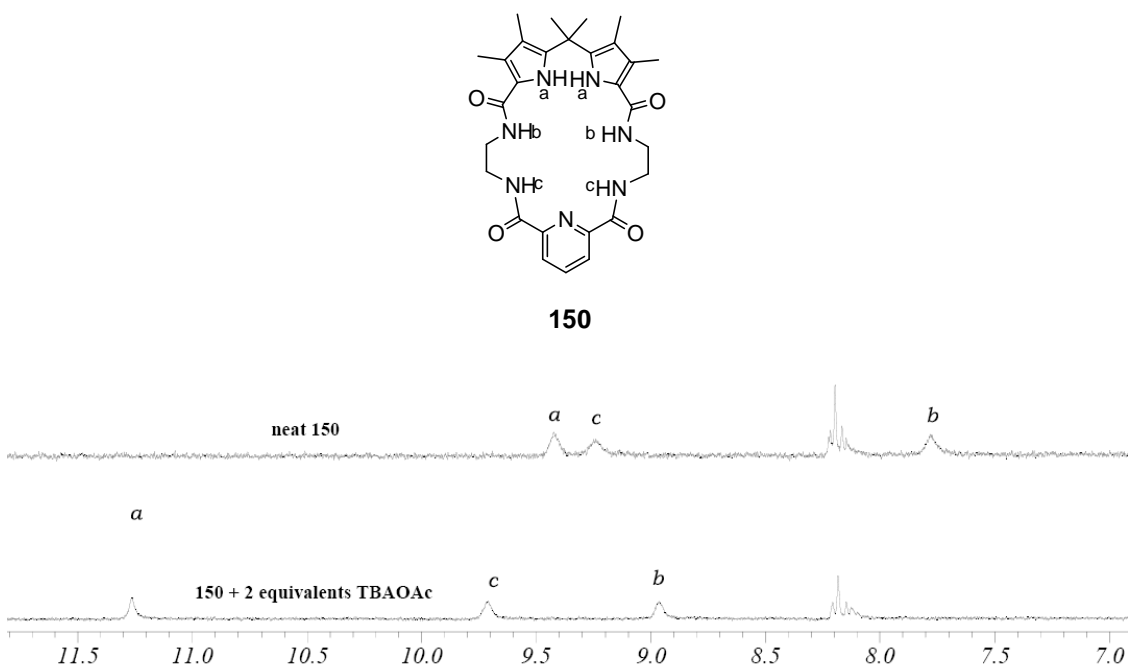


Figure 151 Shift observed in the pyrrole (*a*) and amide (*b,c*) protons of receptor **150** upon addition of tetrabutylammonium acetate in DMSO-*d*₆-0.5%.

Upon addition of hydrogen sulfate to a solution of **150** in DMSO- d_6 -0.5% water the pyrrole and amide protons moved downfield ($\Delta\delta \approx 0.2$ -0.4 ppm), but after few additions of the guest solution they broadened and were difficult to monitor (fig. 152). Only amide proton *c* could be reasonably followed and, therefore, the binding constant was calculated by monitoring this proton only. The constant calculated was $K_a = 1.4 \cdot 10^2 \text{ M}^{-1}$, but the error calculated was very high (50%). To confirm this data a titration with another technique (i.e. ITC: isothermal calorimetry) would be necessary.

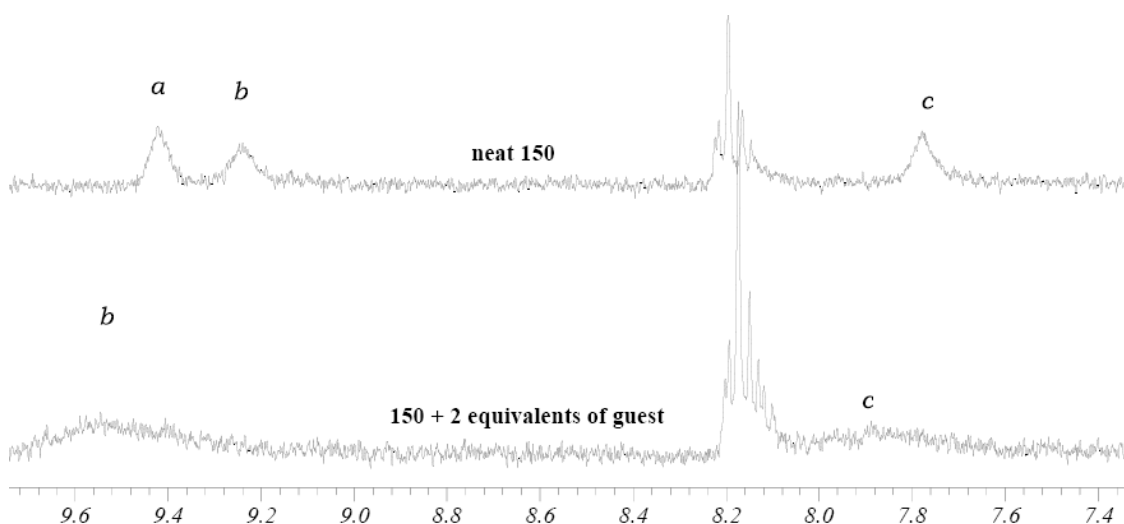


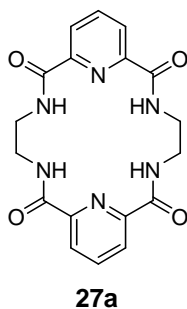
Figure 152 Shift observed in the pyrrole (*a*) and amide (*b*, *c*) protons upon addition of tetrabutylammonium hydrogen sulfate to a solution of receptor **150** in DMSO- d_6 -0.5% H_2O .

The binding properties of macrocycle **150** are summarised in table 25.

Anion (TBA salt)	Receptor $K_a \text{ (M}^{-1}\text{)}$ 150
AcO^-	$1.4 \cdot 10^4$
HSO_4^-	$1.4 \cdot 10^2$

Table 24 Stability constants measured in DMSO- d_6 -0.5% water.

Macrocycle **150** bound anions much more strongly than its analogue with a pyridine instead of the dipyrromethane unit, previously reported in the literature.⁵⁴ The binding constants of receptor **27a** with acetate ($K_a = 2640 \text{ M}^{-1}$) was more than five times smaller than the one measured with macrocycle **150**. While macrocycle **27a** could not bind hydrogen sulfate ($K_a < 5 \text{ M}^{-1}$), macrocycle **150** formed a complex with this anion with a stability constant of $K_a = 10^2 \text{ M}^{-1}$.



3.6 Conclusions

In this chapter the synthesis of a series of dipyrromethane based chiral macrocycles has been described. A preliminary study on the role of the anions as template agent in the macrocyclisation reaction was undertaken on bis-sulfonamide based structure as well as on the dipyrromethane based macrocycle. A correlation between the binding properties of the product and the yields obtained in the macrocyclisation was found. Chloride, in both cases, had the best results as template agent and did not generate side products unlike acetate. With dihydrogen phosphate no product was detected in the macrocyclisation reaction.

The binding properties of dipyrromethane based macrocycles were investigated with anions and amino acids in CDCl_3 and in $\text{DMSO}-d_6$ -0.5% water.

In $\text{DMSO}-d_6$ -0.5% water the binding constants measured for the macrocyclic system were ten times higher than those calculated for the tweezer receptors, due to the macrocyclic effect.

The selectivity between acetate and phosphate was a function of the host flexibility: the smallest and more rigid macrocycle was selective for acetate, while the larger and more flexible macrocycle and the tweezer were selective for dihydrogen phosphate.

Macrocycle **134** was the unique in the series that showed a 1:2 enantioselectivity for the L enantiomer of the tetrabutylammonium salt of the *N*Boc-PheO⁻ in DMSO-*d*₆-0.5% water.

An achiral macrocycle was synthesised, although the synthesis was not optimised due to time constraints. A preliminary study on the binding properties of macrocycle **150** showed a good affinity for acetate and it bound to hydrogen sulfate.

3.8 General conclusions

In chapter II the optimisation of a protocol was described which allowed the preparation in an efficient way of a quantity of diacid **82** sufficient to synthesise and study a variety of receptors.

A series of open chain receptors was synthesized to understand the role of each single component in the recognition of simple anions and amino acids.

It could be concluded that in DMSO-*d*₆ there was no much difference in the value obtained for the binding constants ($K_a \approx 10^2 \text{ M}^{-1}$ for oxo-anions) but there were significant differences in the selectivity. Among the tweezer receptors with an amino acid moiety, the selectivity changed according to the nature of the side chain. When the amino acid was a phenylalanine, and the side chain consisted of a phenyl ring, there was a clear selectivity for dihydrogen phosphate. In the cases where the residue included an alkyl chain (leucine, **104**) or an alcohol (serine, **106**) there was no significant difference between acetate and dihydrogen phosphate. Not much difference in the binding properties was observed between receptor **105** and **107** so it could be stated that the presence of additional hydrogen bonding donors did not increase the affinity of the host for simple anionic guests. In DMSO-*d*₆-0.5% H₂O the tweezer receptors revealed selectivity for oxo-anions and the complexes formed with chloride had a very low stability constant (i.e. $K_a = 27 \text{ M}^{-1}$ with tweezer **101**) or no complex was formed.

In CD₃CN the differences were accentuated. In CD₃CN-1% H₂O the ability of binding acetate of the receptors **101** and **102** was much lower than the one obtained with the receptors with ester functionalities. The presence of the phenyl ring did not play a significant role in selectivity. Polar functionalities did not increase the stability constants of the complex formed by the receptor and acetate, but complicated the binding process

by stabilising the 1:2 host:guest complex as in **106**, or by forming internal hydrogen bonding in **105**. However the presence of a polar functionality combined with a phenyl ring determined the selectivity for dihydrogen phosphate vs acetate in acetonitrile (**105**).

It was also demonstrated that substituents on the phenyl ring of the phenylalanine based receptors played a role: the binding constant was four times increased by the presence of an electron withdrawing substituent, while the complex was destabilised by the presence of an electron donating substituent. This effect was prominent in acetonitrile, but it played a role also in DMSO.

Tweezer receptors formed more stable complexes with the L enantiomer of the amino acids analysed. In some case the binding constant measured with the L enantiomer was almost twice the value of the binding constant measured with the D enantiomer.

The tweezer receptors with higher enantioselectivity were the ones with the phenylalanine side chain.

In the third chapter a series of chiral macrocycles was synthesized starting from tweezer receptor **107**. The macrocyclic structure was expected to bind anions more strongly and to enhance the enantioselective recognition.

The synthesis of the macrocycles was described and the role of the anions as template agent was investigated. The results showed that in presence of chloride the yield of macrocycle **132** was increased, but the result had to be taken cautiously as the differences of the yields were small.

The binding constants of the macrocyclic receptors were higher than the ones obtained for the acyclic systems due to the macrocyclic effect, but only receptor **136** showed some enantioselectivity.

The synthesis of a simple, achiral macrocycle was undertaken, but it still needs some optimization. Macrocycle **150** was synthesized in small quantity that allowed a couple of binding studies to be undertaken. Macrocycle **150** had very good binding properties as it binds acetate strongly ($K_a = 10^4 \text{ M}^{-1}$) in DMSO-*d*₆-0.5% H₂O, and it formed stable complexes with hydrogen sulfate. The binding constants measured were higher if compared to a similar structure present in the literature.⁵⁴

Chapter IV

Experimental

4.1 General Experimental

Experiments were carried out under room atmosphere unless otherwise specified. Experiments requiring dry conditions were carried out under nitrogen atmosphere and with dried glassware. Solvents and reagents were of commercial grade and they were used without further purification, and, where necessary, distilled prior to use. THF and ether were distilled under nitrogen from benzophenone and sodium; DCM and Et₃N were distilled from calcium hydride. For the petroleum ether (PE) the fractions boiling between 40 °C and 60 °C were used.

Flash column chromatography was performed on Sorbsil C60, 40-60 mesh silica.

4.2 Instrumentation

Proton NMR spectra were obtained at 300 MHz on a Bruker AC 300 and at 400 MHz on a Bruker DPX 400 spectrometer. Carbon NMR spectra were recorded at 75.5 MHz on a Bruker AC 300 spectrometer and at 100 MHz on a Bruker DPX 400 spectrometer. Spectra were referenced to the residual solvent peak for the deuterated solvents. Infra-red spectra were recorded on BIORAD Golden Gate FTS 135. Melting points were determined in open capillary tubes using a Gallenkamp Electrothermal melting point apparatus. Optical Rotations were measured on a PolAr2001 polarimeter using the solvent stated, the concentration given is in g/ 100mL. Mass spectra were obtained on a VG analytical 70-250 SE normal geometry double focusing mass spectrometer. All electron ionisation spectra were recorded on a ThermoQuest TraceMS single quadrupole GC-MS mass analyser with an electron ionisation ion source using DCM as solvent. All electrospray (ES) spectra were recorded on a Micromass Platform quadrupole mass analyser with an electrospray ion source using acetonitrile as solvent. High resolution accurate mass measurements were carried out at 10,000 resolution on a Bruker Apex III FT-ICR mass spectrometer. Microanalyses were performed by Medac Ltd., Surrey.

4.3 Experimental for NMR binding studies

Obtaining association constants by ^1H NMR titration experiments involves titration of a solution of host with a specific guest and recording a ^1H NMR spectrum after each addition. Upon complexation, protons in the host or guest may undergo a change in chemical shifts. In particular, protons involved in hydrogen bonding undergo a dramatic shift and therefore are used to determine association constants. After the data from the titration experiment have been acquired, curve fitting software is employed to determine the association constant. Free host and guest are in equilibrium with the host-guest complex. As association and dissociation is fast on the NMR time scale, only a time averaged spectrum of the host (or guest) and the host-guest complex is observed. Therefore, any observed chemical shift (δ_{obs}) is the mole fraction weighted average of the shifts observed in the free (δ_{free}) and complexed (δ_{bound}) molecule. During the curve fitting procedure, after an initial estimate for K_a and $\Delta\delta$, the theoretical δ_{obs} is obtained for each point. The theoretical values are then compared with the experimentally observed ones and the sum of the difference between each point is determined by the following equation:

$$\text{Sum of differences} = \sum (\delta_{\text{obs (experimental)}} - \delta_{\text{obs(theoretical)}})$$

If the sum of differences is positive (or negative), the K_a is increased (or decreased) and the value $\Delta\delta$ recalculated and the whole calculation repeated until the values converge. A detailed explanation of the theoretical basis to the above discussion has been published by Wilcox.¹⁵⁴ A more recent review on the determination of association constants from solution NMR data has been published by Fielding.¹⁵⁵

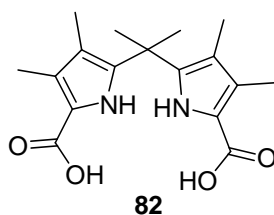
4.4 Method used for obtaining binding constants

All ^1H NMR titration experiments were conducted on a Brüker AM 300 spectrometer at 298 K. Deuterated solvents of commercial grade were used. Inorganic guests, such as TBA acetate, dihydrogen phosphate, fluoride, chloride and bromide were of commercial grade. TBA salts of the amino acids and mandelic acid were prepared by adding a solution of known concentration of TBA hydroxide in MeOH to a solution of the acid in MeOH and removing the solvent under reduced pressure and finally under high vacuum

for several days. The correct stoichiometry was verified performing NMR experiments with long inter-scan delays. A sample of host was dissolved in the deuterated solvent or solvent mixture. A portion of this solution was used as the host NMR sample and the remainder used to dissolve a sample of the guest, so that the concentration of the host remained constant throughout the titration. Successive aliquots of the guest solution were added to the host NMR sample and ^1H NMR sample recorded after each addition. The changes in chemical shifts of all the host signals as a function of guest concentration were analysed with purpose-written software, kindly provided by Hunter, where a 1:1 binding mode or a 1:2 mode was assumed (see Appendix A for details). These programs fit the data to the appropriate binding model to yield the association constant, the bound chemical shift and the free chemical shift. When more than one proton could be monitored during the same titration the binding constant expressed in the text is the average of the values obtained. When only one proton could be monitored and there was a good fit with the NMRTit program the error has been assumed to be $< 10\%$ according with calculations made with the program EQNMR.¹⁵⁶ In the case of poor fit the value of the binding constant has to be considered purely indicative.

4.5 Synthesis in Chapter II

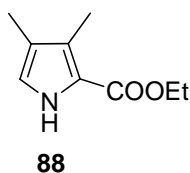
5,5'-(propane-2,2-diyl)bis(3,4-dimethyl-1H-pyrrole-2-carboxylic acid) (**82**)



Pd/C 10% w/w (250 mg, 0.24 mmol) was added to a solution of **97** (319 mg, 0.64 mmol) in dry THF previously degassed with nitrogen. After degassing again the mixture was stirred for 2 h under 1 atm of H_2 . The mixture was filtered through a celite pad and the solvent was evaporated *in vacuo* to give diacid **82** as a white solid (200 mg, 98%) that was used without further purification.

Rf: 0.15 (MeOH/DCM : 8/92) **Mp** = 160°C (decomposition) **IR** (neat) ν_{\max} = 2905 (w, br), 1625 (s), 1460 (m), 1265 (s), 1192 (m), 1140 (m), 936 (m), 747(w) **¹H-NMR** (400 MHz, DMSO-*d*₆) δ = 11.90 (2 H, br s, COOH), 10.01 (2 H, s, NH), 2.11 (6 H, s, CH₃), 1.62 (6 H, s, CH₃), 1.40 (6 H, s, CH₃) **¹³C NMR** (100 MHz, DMSO-*d*₆) δ = 162.41 (C), 138.49 (C), 126.67 (C), 116.02 (C), 115.33 (C), 35.84 (C), 27.16 (CH₃), 10.29(CH₃), 8.81 (CH₃) **LRMS** (ES⁻, acetonitrile + Et₃N) 317.4 (M-H)⁻.

Ethyl 3,4-dimethyl-1H-pyrrole-2-carboxylate (88)¹⁵⁷



Diethyl malonate **83** (40 mL, 0.370 mol), followed by a solution of sodium nitrite (35 g, 0.51 mol) in water (40 mL) was added dropwise to a solution of sodium hydroxide (7 g, 0.235 mol) in acetic acid (70 mL). After stirring overnight at room temperature, the reaction mixture was extracted with ether (2 x 60mL) and the combined organics were washed with water (2 x 120 mL) and with sat. aq. NaHCO₃ (2 x 200 mL) and dried over magnesium sulphate. The solvent was evaporated *in vacuo* to give **87** (32 g, 46%) as a pale yellow oil that was used without further purification.

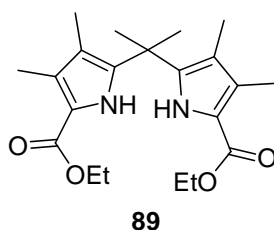
Sodium metal (5.5 g 0.25 mol) was added portionwise over a period of two hours to a solution of 2-butanone **85** (23.6 mL, 0.24 mol) and ethylformate **86** (18.7 mL, 0.23 mol) in dry ether (250 mL) at 0°C. After stirring overnight at room temperature, under nitrogen, the solvent was evaporated *in vacuo* and the solid **22** (25 g) obtained was used for the subsequent step.

Anhydrous sodium acetate (0.386 mol, 29.2 g) and the oximinomalonate **84** (33.7 g 0.178 mol) were added to a solution of **87** (25 g) in acetic acid (100 mL). The suspension was brought to 90°C (barely reflux) and zinc (36 g, 0.55 mol) was added portionwise such that the temperature of the reaction could be controlled between 95-100°C. The reaction mixture was heated at reflux for 3 hours. The solution was poured into ice and was left overnight in the fridge. The solution was then filtered and the solid was dissolved in DCM. The aqueous layer was extracted with DCM (3 x 100mL) and the combined

organic layers were washed with NaHCO_3 (4 x 200 mL, sat aq). The organic layer was dried over MgSO_4 and the solvent was evaporated *in vacuo*. The residue was purified by chromatography (PE/ Et_2O : 100/0 \rightarrow 80/20) to afford pyrrole **88** as a white solid (4.430 g, 15%).

Rf 0.62 (PE/EA : 80/20) **Mp** 75-80°C (lit.¹⁵⁸ 90-91°C) **IR** (neat) ν_{max} 3323 (w, br), 2909 (w), 1655 (m), 1268 (s), 1148 (s), 1098 (m), 1025 (m), 921 (w), 776(m), 596 (s) **¹H-NMR** (300 MHz, CDCl_3) δ = 8.75 (1 H, broad s, *NH*), 6.65 (1 H, s, *NHCH*), 4.31 (2 H, q, J = 7 Hz, OCH_2CH_3), 2.28 (3 H, s, CH_3), 2.01 (3 H, s, CH_3), 1.35 (3 H, t, J = 7 Hz OCH_2CH_3) (literature¹⁵⁸) **¹³C NMR** (75 MHz, CDCl_3) δ = 161.87 (C), 126.70 (C), 120.69 (C), 120.15 (CH), 119.41 (C), 59.92(CH_2), 14.66 (CH_3), 10.35 (CH_3), 10.03 (CH_3) (lit.¹⁵⁸) **LRMS** (EI, 70eV) 167.04 (100, M^+), 121.04 (68), 93.05 (48.31), 66.06 (30).

Diethyl 5,5'-(propane-2,2-diyl)bis(3,4-dimethyl-1H-pyrrole-2-carboxylate)¹¹⁶ (89**)**

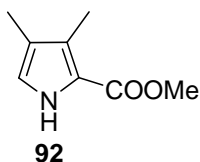


2,2-dimethoxypropane (2 mL, 16 mmol) and *p*-toluenesulfonic acid (0.11 g, 0.6 mmol) were added to a solution of carboethoxy pyrrole **88** (1 g, 6 mmol) in dry DCM (50 mL). After stirring for 24 hours at room temperature, the reaction mixture was quenched with NaHCO_3 (50 mL, 5% aq). The aqueous layer was extracted with DCM (2 x 50mL) and the combined organic layers were dried over MgSO_4 , filtered and the solvent evaporated *in vacuo*. Purification of the residue by column chromatography (MeOH/DCM : 0 \rightarrow 1%) afforded dipyrromethane **89** as a colourless solid (800 mg, 71%).

Rf: 0.37 (PE/EA : 80/20) **Mp** 110-115 °C (literature¹¹⁶ 122-124°C) **IR** (neat) ν_{max} 2360 (s), 2342 (m), 1663 (w), 1425 (w), 1263 (w), 1137 (w), 1088 (w) **¹H-NMR** (300 MHz, CDCl_3) δ = 8.60 (2 H, broad s, *NH*), 4.31 (4H, q, J = 7 Hz, OCH_2CH_3), 2.21 (6 H, s, CH_3), 1.66 (6 H, s, CH_3), 1.55 (6 H, s, CH_3), 1.36 (6 H, t, J = 7 Hz, OCH_2CH_3) (literature¹¹⁶) **¹³C NMR** (75 MHz, CDCl_3) δ = 163.11 (C), 137.29 (C), 128.53 (C), 117.04

(C), 116.22 (C), 59.93 (CH₂), 35.94 (C) 26.88 (CH₃), 14.73 (CH₃), 10.60 (CH₃), 9.28 (CH₃) (lit. ¹¹⁶) **LRMS** (ES⁺, acetonitrile) 375.3, (M+H)⁺, 397.3 (M + Na)⁺.

Methyl 3,4-dimethyl-1H-pyrrole-2-carboxylate (**92**)



*Method A: Paal Knorr pyrrole synthesis*¹⁵⁷

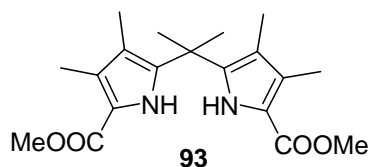
92 was synthesised following the same procedure as for **88** with the following quantities: dimethylmalonate **90** (40 mL, 0.370 mol), sodium nitrite (35 g, 0.51 mol), sodium hydroxide pellets (7 g, 0.235 mol), sodium metal (5.5 g, 0.25 mol), 2-butanone **85** (23.6 mL, 0.26 mol), ethylformate **86** (20 mL, 0.246 mol), sodium acetate (33.4 g, 0.408 mol) and zinc (40 g, 0.6 mol). The crude product from the reaction was recrystallised (DCM/PE) to afford pyrrole **92** (4.4 g, 15%) as a yellow crystalline solid.

*Method B: Zard- Barton*¹⁵⁷

DBU (15 mL, 0.1 mol) was added dropwise to a solution of methyl isocyanoacetate **100** (5g, 0.05 mol) and 3-nitrobutan-2-yl acetate **99** (8.13 g, 0.050 mol) in THF (50 mL) at 0°C. The reaction mixture was stirred at 60°C overnight. The solution was diluted in DCM (150 mL), washed with aq. HCl (150 mL, 5%) and the organic layer was dried over MgSO₄ and the solvent was evaporated *in vacuo*. The residue was purified by chromatography (PE/EA: 90/10) to afford pyrrole **92** as a white solid (4 g, 52%).

Rf: 0.25 (PE/EA: 80/20) **Mp** 78-84 °C (DCM: PE) **IR** (neat) ν_{\max} 3300 (w, br), 2929 (w, br), 1664 (s), 1440 (m), 1394 (m), 1269 (s), 1192(m), 1150(s) **¹H-NMR** (400 MHz, CDCl₃) δ = 8.75 (1 H, broad s, NH), 6.66 (1 H, d, J = 3 Hz, NHCH), 3.84 (3 H, s, OCH₃), 2.27 (3 H, s, CH₃), 2.01 (3 H, s, CH₃) **¹³C NMR** (100 MHz, CDCl₃) δ = 162.14 (C), 126.75 (C), 120.24 (C), 120.24 (CH), 119.02 (C), 116.90 (C), 50.98 (CH₃), 10.19 (CH₃), 9.87 (CH₃) **LRMS** (EI, 70eV) 153.13 (100 M⁺), 121.09 (63.34), 93.10 (47.84), 66.08 (39.8) **HRMS** calculated for C₈H₁₁NO₂ 153.07898 measured 153.07890.

Dimethyl 5,5'-(propane-2,2-diyl)bis(3,4-dimethyl-1H-pyrrole-2-carboxylate) (**93**)

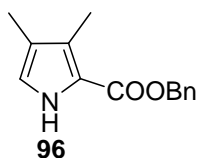


The synthesis of **93** followed the same procedure as for **89** with the following quantities: dimethoxypropane (4 mL, 32 mmol), *p*-toluene sulfonic acid (0.26 g, 1.3 mmol) and carbomethoxy pyrrole **92** (2 g, 13 mmol).

Purification of the residue by column chromatographic (PE/EA : 80/20) afforded dipyrromethane **93** as a colourless solid (1.2 g, 53%).

Rf: 0.55 (PE/EA : 80/20) **Mp** 132-138 °C **IR** (neat) ν_{\max} 3481 (w), 2949 (br,w), 1697 (s), 1496 (m), 1441 (m), 1250 (s), 1138 (m), 1076 (s), 767 (m) **¹H-NMR** (400 MHz, CDCl₃) δ = 8.55 (2 H, br s, NH), 3.81 (6 H, s, OCH₃), 2.18 (6 H, s, CH₃), 1.63 (6 H, s, CH₃), 1.51 (6 H, s, CH₃) **¹³C NMR** (100 MHz, CDCl₃) δ = 162.35 (C), 137.41 (C), 128.84 (C), 117.11 (C), 116.00 (C), 51.10 (CH₃), 35.95 (C), 26.86 (CH₃), 10.56 (CH₃), 9.25 (CH₃) **LRMS** (ES⁺, acetonitrile) 347.3, 100 (M+H)⁺, 369.3 (M+Na)⁺.

Benzyl 3,4-dimethyl-1H-pyrrole-2-carboxylate (**96**)



*Method A: Paal Knorr pyrrole synthesis*¹⁵⁷

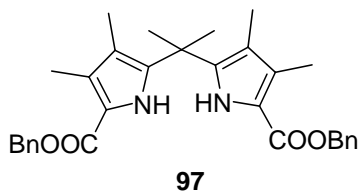
96 was synthesised following the same procedure as for **88** with the following quantities: dibenzylmalonate **90** (15 g, 0.05 mol), sodium nitrite (5.48 g, 0.08 mol), sodium hydroxide pellets (1.4 g, 0.07 mol), sodium metal (1.8 g 0.080 mol), 2-butanone **85** (8 mL, 0.082 mol), ethylformate **86** (6 mL, 0.077 mol), sodium acetate (6.4 g, 0.08 mol) and zinc (7.8 g, 0.120 mol). The crude product from the reaction was purified by column chromatography to afford pyrrole **92** (800 mg, 8.7%) as a yellow oil.

*Method B: via transesterification from 92*¹¹⁹

NaHMDS (60 mL, 1 M sol in THF) was added to a solution of **92** (4.5 g, 0.029 mol) in benzyl alcohol (300 mL) at 80°C. After stirring at reflux temperature for 3.5 hours the reaction mixture was poured onto ice and extracted with DCM (3 x 250 mL). The combined organic layers were washed with water, dried over MgSO₄ and concentrated *in vacuo*. The residue was purified by column chromatography (PE /EA/ toluene: 80/20/1) afforded pyrrole **96** (3.1 g, 45%) as a colourless solid.

Rf 0.67 DCM **Mp** 75-77 °C (lit.¹⁵⁹ 73-74°C) **IR** (neat) ν_{\max} 3313 (s), 1655 (s), 1463 (m), 1406 (s), 1365 (m), 1272 (s), 1217 (w), 1151 (s), 1099 (m), 994 (w), 921 (w), 769 (m), 729 (s), 689 (m), 599 (s) **¹H-NMR** (400 MHz, CDCl₃) δ = 8.65 (1 H, br s, NH), 7.1-7.4 (5 H, m, PhH), 6.58 (1 H, d, J = 1.5 Hz, NHCH), 5.23 (2 H, s, OCH₂Ph), 2.21 (3 H, s, CH₃), 1.93 (3 H, s, CH₃) (literature¹⁵⁹) **¹³C NMR** (100 MHz, CDCl₃) δ = 161.50 (C), 136.63 (C), 128.70 (CH), 128.22 (CH), 127.29 (C), 120.85 (C), 120.53 (CH), 119.04 (C), 65.73 (CH₂), 10.48 (CH₃), 10.04 (CH₃) (lit.¹⁵⁹) **LRMS** (EI, 70eV) 229.17 (19.56 M⁺), 91.07 (100), 207.08 (10.11), 138.08 (13.00), 122.08 (18.89), 77.02 (12.44), 65.05 (22.75) **HRMS** calculated for C₁₄H₁₅NO₂ 229.11028 measured 229.11065.

Dibenzyl 5,5'-(propane-2,2-diyl)bis(3,4-dimethyl-1H-pyrrole-2-carboxylate) (97)



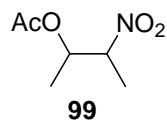
The synthesis of **97** followed the same procedure as for **89** with the following quantities: dimethoxypropane (1.02 mL, 9 mmol), *p*-toluenesulfonic acid (0.07 g, 0.4 mmol) and carbobenzyl pyrrole **96** (789 mg, 3.4 mmol).

Purification of the residue by column chromatographic (PE/EA: 80/20) afforded bispyrrole **97** as a colourless solid (400 mg, 46%).

Rf: 0.5 DCM **Mp**= 112-114°C (DCM:PE) **IR** (neat) ν_{\max} 3380(w), 1671 (m), 1650 (m), 1432 (w), 1418 (w), 1260 (s), 1132 (m), 1084 (w) **¹H-NMR** (400 MHz, CDCl₃) δ = 8.63 (2 H, br s, NH) 7.44-7.32 (10 H, m, Ph), 5.32 (4 H, s, OCH₂Ph), 2.22 (6 H, s, CH₃), 1.65 (6 H, s, CH₃), 1.56 (6 H, s, CH₃) **¹³C NMR** (100 MHz, CDCl₃) δ = 161.80 (C), 137.67

(C), 136.78 (C), 129.05 (C), 128.67 (CH), 128.15 (2 CH), 117.19 (C), 115.92 (C), 65.70 (CH₂), 36.06 (C), 26.81 (CH₃), 10.73(CH₃), 9.34 (CH₃) **LRMS** (ES⁺, acetonitrile) 521.1 (M+Na⁺) **HRMS**: (calculated for C₃₁H₃₄N₂O₄ 499.2591) measured 499.2602.

3-nitrobutan-2-yl acetate (**99**)

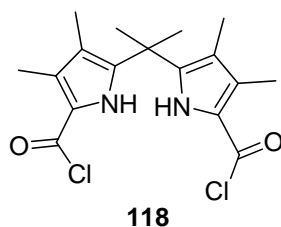


3-nitro-2-butanol (mixture of diastereoisomers) **98** (47 g, 0.4 mol) was added dropwise to a solution of acetic anhydride (60 mL, 0.6 mol) and DMAP (1.2 g, 0.01 mol) in DCM (90 mL). The resulting solution was stirred for 3 hours at room temperature, quenched with MeOH (100 mL) and stirred for 30 minutes. The resulting solution was poured into a suspension of NaHCO₃ (52 g) in water (260 mL) and extracted with DCM (3x150mL). The combined organic layers were dried over Na₂SO₄, filtered through a SiO₂ pad, concentrated *in vacuo* to give **99** (61.45 g, 95%, mixture of diastereoisomers) as a light green oil that was used without further purification.

Rf: 0.56 (PE/EA : 80/20) **IR** (neat) ν_{\max} = 2993 (w, br), 1741 (s), 1550 (m), 1449 (w), 1373 (m), 1227 (s), 1092 (m), 1025 (m) **¹H-NMR** (300 MHz, CDCl₃) δ = 5.30-5.16 (1 H, m, CH), 4.62-4.53 (1 H, m, CH), 1.97-1.94 (3 H, m, COCH₃), 1.49-1.45 (3 H, m, CH₃), 1.24-1.20 (3 H, m, CH₃) (it is a mixture of two isomers) (literature¹⁵⁷) **¹³C NMR** (75 MHz, CDCl₃) δ = 169.61-169.42 (C), 85.40-84.34 (CH), 70.47-69.75 (CH), 20.59-20.56 (CH₃), 15.85-15.55(CH₃), 15.37-15.33 (CH₃) (it is a mixture of two isomers) (literature¹⁵⁷) **LRMS** (ES⁺, acetonitrile) 184 (M+Na⁺).

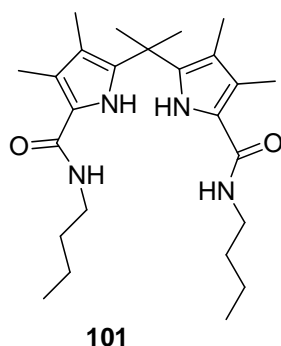
Synthesis of tweezers **101**, **102** and **109**

The synthesis of tweezer **101**, **102** and **109** was performed starting from the same batch of 5,5'-(propane-2,2-diyl)bis(3,4-dimethyl-1H-pyrrole-2-carbonyl chloride) **118**.



(1-Chloro-2-methyl-propenyl)-dimethyl-amine **117** (750 μL , 5.6 mmol) was added to a solution of diacid **82** (888 mg, 2.7 mmol) in THF (8 mL). After stirring the resulting solution at room temperature for 30 minutes, the solvent was evaporated *in vacuo* to yield chloride **118** which was and re-dissolved in 8.8 mL of DCM to yield a 0.3 M solution which was used immediately for the following step.

5,5'-(propane-2,2-diyl)bis(N-(butyl)-3,4-dimethyl-1H-pyrrole-2-carboxamide) (101)

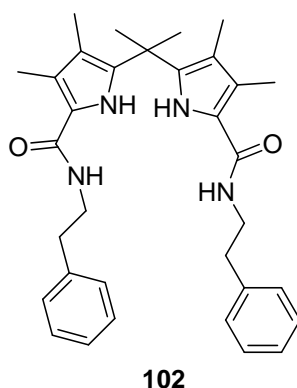


A solution of acyl chloride **118** (3 mL, 0.3 M in DCM) was added to a solution of *n*-butylamine (2 mL, 20 mmol) in DCM (15 mL). After stirring the resulting solution at room temperature for 1 hour, the solvent was evaporated *in vacuo* and the residue was purified by column chromatography (PE:EA 40:60) to afford **101** (346 mg, 90%) as a colourless solid.

Rf: 0.51 (PE/EA : 30/70) **M.p.**= 110- 115°C (litt 137°C) **IR** (neat) ν_{max} = 3311 (w), 2958 (w), 2929 (w), 2871 (w), 1587 (s), 1538 (m), 1495 (m), 1455 (w), 1295 (s), 1154 (m), 937 (w) **¹H-NMR** (400 MHz, DMSO-*d*₆) δ = 9.84 (2 H, s, PyrNH), 7.65 (2 H, t, J = 5.5 Hz, CONH), 3.20 (4 H, apparent q, J = 7Hz, CONHCH₂CH₂), 2.12 (6 H, s, CH₃), 1.60 (6 H, s, CH₃), 1.55-1.44 (4 H, m, CONHCH₂CH₂CH₂), 1.37 (6 H, s, CH₃), 1.40-1.26 (4 H, m, CH₂CH₂CH₃), 0.91 (6 H, t, J = 7 Hz, CH₂CH₃) **¹³C NMR** (100 MHz, DMSO-*d*₆) δ =

1.62.20 (C), 135.60 (C), 124.00 (C), 118.82 (C), 114.38 (C), 30.00 (CH₂), 35.59 (C), 31.70 (CH₂), 27.87 (CH₃) 19.72 (CH₂), 13.72 (CH₃), 10.35 (CH₃), 8.54 (CH₃) **MS** (ES⁺, acetonitrile) 451 (M+Na⁺) **HRMS** (calculated C₂₅H₄₁N₄O₂ 429.3224) measured 429.3213.

5,5'-(propane-2,2-diyl)bis(3,4-dimethyl-N-phenethyl-1H-pyrrole-2-carboxamide)
(102)

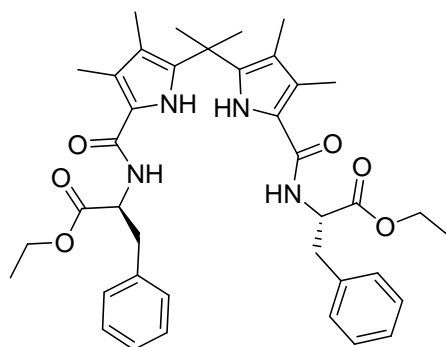


A solution of acyl chloride **118** (3 mL, 0.3 M in DCM) was added to a solution of *n*-butylamine (2 mL, 30 mmol) in DCM (15 mL). After stirring the resulting solution at room temperature for 1 hour, the solvent was evaporated *in vacuo* and the residue was purified by column chromatography (PE:EA 40:60) to afford **102** (440 mg, 80%) as a colourless solid.

Rf: 0.36 (PE/EA : 30/70) **M.p.**= 109-111°C **IR** (neat) ν_{max} = 3312 (w), 2922 (w), 1587 (s), 1538 (m), 1495 (m), 1454 (w), 1297 (s), 1193 (w), 1153 (w), 754 (w), 698 (m) **¹H-NMR** (400 MHz, DMSO-*d*₆) δ = 9.87 (2 H, s, PyrrNH), 7.79 (2 H, t, *J* = 5.5 Hz, CONH), 7.32-7.19 (10 H, m, PhH), 3.42 (4 H, apparent q, *J* = 7 Hz, CONHCH₂CH₂), 2.81 (4 H, apparent t, *J* = 8 Hz CONHCH₂CH₂Ph), 2.12 (6 H, s, CH₃), 1.60 (6 H, s, CH₃), 1.38 (6 H, s, CH₃) **¹³C NMR** (100 MHz, DMSO-*d*₆) δ = 161.25 (C), 139.70 (C), 135.74 (C), 128.62 (CH), 128.30 (CH), 126.02 (CH), 124.15 (C), 118.72 (C), 114.47 (C), 40.20 (CH₂), 35.66 (CH₂), 35.61 (C), 27.28 (CH₃), 10.34 (CH₃), 8.64 (CH₃) **MS** (ES⁺, acetonitrile) 547 (M+Na⁺) **HRMS** calculated C₃₃H₄₁N₄O₂ 525.3224 measured 525.3213 **Analytical (%)**

Calculated for $C_{33}H_{40}N_4O_2$ C, 75.54; H, 7.68; N, 10.67. Found C, 75.04; H, 7.67; N, 10.63.

(S)-2-[(5-{1-[5-((S)-1-Ethoxycarbonyl-2-phenyl-ethylcarbamoyl)-3,4-dimethyl-1H-pyrrol-2-yl]-1-methyl-ethyl}-3,4-dimethyl-1H-pyrrole-2-carbonyl)-amino]-3-phenyl-propionic acid ethyl ester (103)



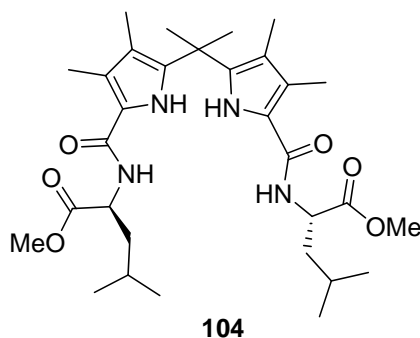
103

HOBt (342 mg, 2.54 mmol), EDC (621 mg, 3.24 mmol) and L-Phe-OEt·HCl (405 mg, 1.76 mmol) were added to a solution of **82** (220 mg, 0.7 mmol) and DIPEA (0.7 ml, 4.2 mmol) in freshly distilled DCM (10 mL). After stirring overnight at room temperature the solvent was evaporated *in vacuo*. Purification of the residue by column chromatography (DCM:MeOH 100:0 → 99:1) and recrystallisation (DCM:PE) afforded tweezer **33** as a pale yellow solid (277 mg, 60%).

Rf: 0.15 (MeOH:DCM 2:98) **M.p.** = 76-80 °C (DCM:PE) $[\alpha]_D^{24} = 112.1^\circ$ ($c = 1$, $CHCl_3$) **IR** (neat) $\nu_{max} = 3305$ (m, br), 2974 (w), 2925 (w), 2866 (w), 1733 (s), 1599 (s), 1580 (s), 1525 (m), 1491 (m), 1301 (m), 1276 (m), 1193 (s), 1148 (s), 1021 (m), 944 (w), 860 (w), 741 (m) **¹H-NMR** (400 MHz, $CDCl_3$) $\delta = 8.84$ (2 H, br s, PyrNH), 7.15-7.33 (10 H, m, PhH), 6.16 (2 H, d, $J = 7.5$ Hz, CONH), 5.03 (2 H, dt, $J = 7.5, 5.5$ Hz, CH), 4.20 (4 H, q, $J = 7$ Hz, OCH_2CH_3), 3.25 (2 H, dd, $J = 5.5, 16$ Hz, CHHPh), 3.20 (2 H, dd, $J = 5.5, 16$ Hz, CHHPh), 2.02 (6 H, s, CH_3), 1.63 (6 H, s, CH_3), 1.56 (6 H, s, CH_3), 1.27 (6 H, t, $J = 7$ Hz, OCH_2CH_3) **¹³C NMR** (100 MHz, $CDCl_3$) $\delta = 171.97$ (C), 161.52 (C), 136.31 (C), 136.17 (C), 129.59 (CH), 128.68 (CH), 127.27 (CH), 121.53 (C), 119.17 (C), 116.43 (C), 61.66 (CH_2), 53.45 (CH), 38.39 (CH_2), 35.85 (C), 27.03 (CH_3), 14.28 (CH_3), 10.72

(CH₃), 9.30 (CH₃) **MS** (ES⁺, acetonitrile) 691.3 (M+Na⁺) **HRMS** (calculated C₃₉H₄₈N₄O₆ 691.3466) measured 691.3450.

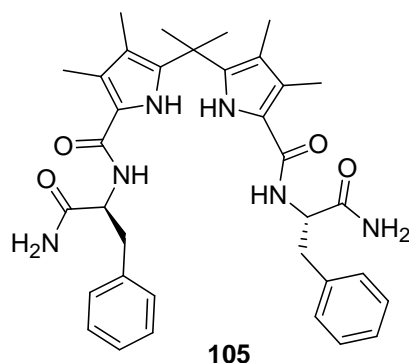
(S)-2-[(5-{1-[5-((S)-1-Methoxycarbonyl-3-methyl-butylcarbamoyl)-3,4-dimethyl-1H-pyrrol-2-yl]-1-methyl-ethyl}-3,4-dimethyl-1H-pyrrole-2-carbonyl)-amino]-4-methyl-pentanoic acid methyl ester (104)



PyBOP (527 mg, 0.1 mmol) was added to a solution of di acid **82** (123 mg, 0.38 mmol), Et₃N (0.5 mL, 2.5 mmol) and L-Leu-OMe·HCl in DCM (10 mL). After stirring overnight at room temperature the reaction mixture was diluted in DCM (50 mL) and washed with KHSO₄ (5 mL, 1M aq), K₂CO₃ (50 mL, 1M aq) and brine (50 mL). The organic layer was dried over MgSO₄ and the solvent evaporated *in vacuo*. Purification by column chromatography (EA:PE 40:60) afforded **104** as a colourless solid (45 mg, 20%).

Rf: 0.63 (EA:PE 70:30) **Mp** 109-111 °C [α]_D²⁹ = 22° (c = 0.1, CHCl₃) **IR** (neat) ν_{\max} = 3319 (m, br), 2955 (m), 1732 (s), 1605 (s), 1518 (s), 1296 (s), 1200 (s), 860 (w) **¹H-NMR** (400 MHz, DMSO-*d*₆) δ = 10.07 (2 H, s, PyrNH), 8.01 (2 H, d, *J* = 7.5 Hz CONH), 4.49 (2 H, m, CH), 3.65 (6 H, s, OCH₃), 2.16 (6 H, s, CH₃), 1.65-1.50 (6 H, m, CHCH₂CH(CH₃)₂ and CHCH₂CH(CH₃)₂), 1.64 (6 H, s, CH₃), 1.39 (6 H, s, CH₃), 0.94 (6 H, d, *J* = 6 Hz, CH(CH₃)CH₃), 0.89 (6 H, d, *J* = 6 Hz, CH(CH₃)CH₃) **¹³C NMR** (100 MHz, DMSO-*d*₆) δ = 173.75 (C), 161.04 (C), 136.31 (C), 125.59 (C), 118.01 (C), 114.82 (C), 51.71 (CH), 50.06 (CH₃), 40.03 (CH₂), 35.84 (C), 28.09 (CH), 24.36 (CH₃), 22.63 (CH₃), 21.47 (CH₃), 10.40 (CH₃), 8.67 (CH₃) **LRMS** (ES⁺, acetonitrile) 595 (M+Na)⁺ **HRMS** calculated for C₃₁H₄₈Na₁N₄O₆ 595.3466 measured 595.3462 **Analytical** (%) Calculated for C₃₁H₄₈N₄O₆·(1/3 H₂O) C, 64.33; H, 8.48; N, 9.68. Found C, 64.13; H, 8.39; N, 9.50.

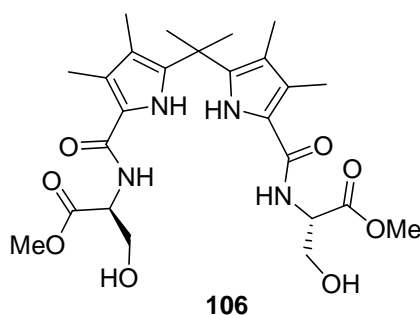
5,5'-(propane-2,2-diyl)bis(N-((S)-1-amino-1-oxo-3-phenylpropan-2-yl)-3,4-dimethyl-1H-pyrrole-2-carboxamide) (105)



HOBt (420 mg, 3.33 mmol), EDC (860 mg, 4.48 mmol) and L-Phenylalanine-NH₂ (480 mg, 2.39 mmol) were added to a solution of **82** (280 mg, 0.87 mmol) and DIPEA (2 mL, 11.8 mmol) in freshly distilled DCM (15 mL). After stirring overnight at room temperature the reaction mixture was diluted in DCM (100 mL) and washed with KHSO₄ (100 mL, 1M aq), K₂CO₃ (100 mL, 1M aq) and brine (100mL). The organic layer was dried over MgSO₄ and the solvent evaporated *in vacuo*. Purification by column chromatography (MeOH/DCM : 0→5%) afforded **105** as a pale yellow solid (110 mg, 20%).

Rf: 0.9 (MeOH/DCM : 8/92) **Mp**: 165-170 °C [α]_D²⁴ = -10.94° (c = 0.5, MeOH) **IR** (neat) ν_{\max} = 3305 (w, br), 2974 (w, br), 2360 (s), 2341 (m), 1743 (w), 1602 (w), 1507 (w), 1291 (w), 698 (w) **¹H-NMR** (400 MHz, DMSO) δ = 10.06 (2 H, s, PyrNH), 7.89 (2 H, d, *J* = 8 Hz, NH), 7.52 (2 H, s, CONHH), 7.30-7.15 (10 H, m, PhH), 7.03 (2 H, s, CONHH), 4.66 (2 H, apparent dt *J* = 5, 8.5 Hz, CH), 3.07 (2 H, dd, *J* = 5, 13.5 Hz, CHHPh), 2.89 (2 H, dd, *J* = 9, 13.5 Hz, CHHPh), 2.06 (6 H, s, CH₃), 1.63 (6 H, s, CH₃), 1.36 (6 H, s, CH₃) **¹³C NMR** (100 MHz, CDCl₃) δ = 173.63 (C), 160.78 (C), 138.31 (C), 136.08 (C), 129.15 (CH), 127.95 (CH), 126.15 (CH), 124.78 (C), 118.32 (C), 114.61 (C), 53.51 (CH), 37.83 (CH₂), 35.74 (C), 27.98 (CH₃), 10.36 (CH₃), 8.64 (CH₃) **LRMS** (ES⁺, acetonitrile) 611.3, 100(M+H)⁺, 633.2 (M+Na)⁺ **HRMS** calculated for C₃₅H₄₂N₆O₄ 611.3340 measured 611.3325.

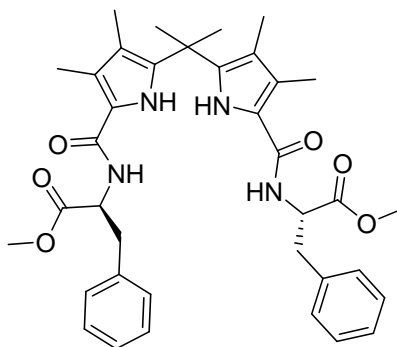
(S)-3-Hydroxy-2-[(5-{1-[5-((S)-2-hydroxy-1-methoxycarbonyl-ethylcarbamoyl)-3,4-dimethyl-1H-pyrrol-2-yl]-1-methyl-ethyl)-3,4-dimethyl-1H-pyrrole-2-carbonyl)-amino]-propionic acid methyl ester (106)



Pd/C 10% w/w (74 mg, 0.070 mmol) was added to a solution of **116** (123 mg, 0.17 mmol) in dry THF previously degassed with nitrogen. After degassing again the mixture was stirred for 3 days under 1 atm of H₂. The mixture was filtered through a celite pad and the solvent was evaporated *in vacuo*. Purification of the residue by column chromatography (MeOH/DCM 0 → 4%) afforded tweezer **106** as a colourless solid (62 mg, 70%)

Rf: 0.12 (DCM:MeOH 97:3) **Mp** 107-112 °C [α]_D²⁴ = 53.5° (c = 0.2, MeOH) **IR** (neat) ν_{\max} = 3319 (w,br), 2928 (w, br), 1734 (m), 1606 (m), 1519 (s), 1286 (m), 1211 (s), 1070 (m) **¹H-NMR** (400 MHz, CD₃CN) δ = 9.02 (2 H, s, PyrNH), 6.67 (2 H, d, *J* = 7.5 Hz, NH), 4.65 (2 H, m, CH), 3.95-3.90 (2 H, m, CHHO), 3.88-3.82 (2 H, m, CHHO), 3.73 (3 H, s, CH₃), 3.36 (2 H, apparent t, *J* = 6 Hz, OH), 2.20 (6 H, s, CH₃), 1.63 (6 H, s, CH₃), 1.51 (6 H, s, CH₃). **¹³C NMR** (100 MHz, CD₃CN) δ = 172.49 (C), 162.48 (C), 137.75 (C), 123.81 (C), 120.01 (C), 116.94 (C), 63.14 (CH₂), 55.76 (CH), 52.95 (CH₃), 36.80 (C), 27.53 (CH₃), 10.89 (CH₃), 9.32 (CH₃) **LRMS** (ES⁺, acetonitrile) 543.2 (M+Na)⁺ **HRMS** calculated for C₂₅H₃₆Na₁N₄O₈ 543.2425 measured 543.2432 **Analytical (%)** Calculated for C₂₅H₃₆N₄O₈·(1/2 H₂O) C, 56.70; H, 7.04; N, 10.58. Found C, 56.85; H, 6.91; N, 10.37.

(S)-2-[(5-{1-[5-((S)-1-Methoxycarbonyl-2-phenyl-ethylcarbamoyl)-3,4-dimethyl-1H-pyrrol-2-yl]-1-methyl-ethyl}-3,4-dimethyl-1H-pyrrole-2-carbonyl)-amino]-3-phenyl-propionic acid methyl ester (**107**)



107

Method A: EDC/HOBt mediated coupling

HOBt (715 mg, 5.6 mmol), EDC (1.39 g, 7.25 mmol) were added to a solution of di-acid **82** (489 mg, 1.54 mmol) and DIPEA (to allow the complete dissolution) in DCM (5 mL). After stirring one hour at room temperature the above solution was added slowly to a solution of L-PheOMe·HCl (859 mg, 3.99 mmol) and DIPEA (1.5 mL, 8.99 mmol) in DCM (10mL). After stirring overnight at room temperature the reaction mixture was diluted in DCM (100 mL) and washed with KHSO₄ (100 mL, 1M soln), K₂CO₃ (100 mL, 1M soln) and brine (100mL). The organic layer was dried over MgSO₄ and the solvent evaporated *in vacuo*. Purification of the residue by column chromatography (PE/EA 50:50) afforded tweezer **107** as a pale yellow solid (479 mg, 48%).

Method B: PyBOP mediated coupling

PyBOP (1.8 g, 3.4 mmol) was added to a solution of di acid **82** (500 mg, 1.5 mmol), DIPEA (1.6 mL, 10 mmol) and L-PheOMe·HCl (840 mg, 4.18 mmol) in DCM (20 mL). After stirring overnight at room temperature the reaction mixture was diluted in DCM (100 mL) and washed with KHSO₄ (100 mL, 1M aq), K₂CO₃ (100 mL, 1M aq) and brine (100mL). The organic layer was dried over MgSO₄ and the solvent evaporated *in vacuo*. Purification by column chromatography (EA:PE 50:50) afforded **107** as a pale yellow solid (604 mg, 63%).

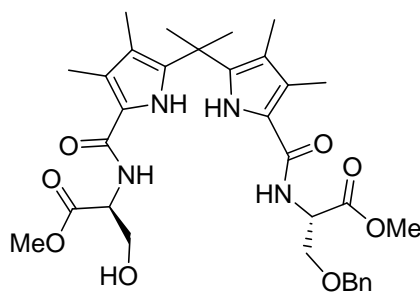
Method C: Acyl Chloride mediated Coupling

(1-Chloro-2-methyl-propenyl)-dimethyl-amine **117** (70 μ L, 0.53 mmol) was added to a solution of di-acid **82** (86 mg, 0.27 mmol) in THF (1.5mL). After stirring the resulting solution at room temperature for 15 minutes, the solvent was evaporated *in vacuo* to yield chloride **118** which was used without further purification.

A solution of di- chloride **118** in DCM was added to a solution of L-PheOMe·HCl (230 mg, 1 mmol) and Et₃N (0.5 mL, 3.4 mmol) in DCM (10mL). After stirring overnight at room temperature the reaction mixture was diluted in DCM (50 mL) and washed with KHSO₄ (50 mL, 1M aq), K₂CO₃ (50 mL, 1M aq) and brine (50 mL). The organic layer was dried over MgSO₄ and the solvent evaporated *in vacuo*. The TLC showed only one compound, but the NMR revealed the presence of the Ghosez reagent's side product. The yield was calculated on the ratio of the two compounds visible from the NMR spectrum. Yield= 56%

Rf: 0.35 (PE/EA 50:50) **M.p.**= 85-90 °C [α]_D²⁴ = 118.6 (C= 0.5, CHCl₃) **IR** (neat) ν_{\max} = 3290 (m, br), 2926(w, br), 1740 (s), 1582 (s), 1521 (s), 1491 (m), 1300 (s), 1209 (m), 1178 (s), 1150 (s), 869 (s), 575 (w) **¹H-NMR** (400 MHz, CDCl₃) δ = 8.77 (2 H, br s, PyrNH), 7.06-7.24 (10 H, m, PhH), 6.05 (2 H, d, *J* = 7 Hz, CONH), 4.97(2 H, dt, *J* = 7, 6 Hz, CH), 3.69 (6 H, s, OCH₃), 3.18 (2H, dd, *J* = 5.5, 14 Hz, CHHPh), 3.12 (2H, dd, *J* = 5.5, 14 Hz, CHHPh), 1.94 (6 H, s, CH₃), 1.55 (6 H, s, CH₃), 1.48 (6 H, s, CH₃) **¹³C NMR** (100 MHz, CDCl₃) δ = 171.47 (C), 161.56 (C), 136.36 (C), 136.08 (C), 129.50 (CH), 128.76 (CH), 127.34 (CH), 121.60 (C), 119.10 (C), 116.44 (C), 53.42 (CH₃), 53.48 (CH), 38.28 (CH₂), 35.84 (C), 27.02 (CH₃), 10.74 (CH₃), 9.30 (CH₃) **MS** (ES⁺, acetonitrile) 663.6 (M+Na⁺) **HRMS** calculated for C₃₇H₄₅N₄O₆ 641.3334 measured 641.3333 **Analytical (%)** Calculated for C₃₇H₄₄N₄O₆ C, 69.35; H, 6.92; N, 8.74. Found C, 69.00; H, 6.89; N, 8.76.

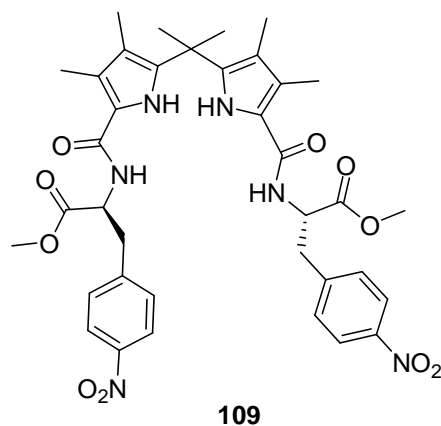
(S)-2-[(5-{1-[5-((S)-2-Benzoyloxy-1-methoxycarbonyl-ethylcarbamoyl)-3,4-dimethyl-1H-pyrrol-2-yl]-1-methyl-ethyl}-3,4-dimethyl-1H-pyrrole-2-carbonyl)-amino]-3-hydroxy-propionic acid methyl ester (108)

**108**

Pd/C 10% w/w (200 mg, 0.18 mmol) was added to a solution of **116** (190 mg, 0.27 mmol) in dry THF previously degassed with nitrogen. After degassing again the mixture was stirred overnight under 1 atm of H₂. The mixture was filtered through a celite pad and the solvent was evaporated *in vacuo*. Purification of the residue by column chromatography (MeOH/DCM 0 → 3%) afforded tweezer **106** as a colourless solid (43 mg, 38%)

Rf: 0.3 (DCM:MeOH 97:3) **Mp** 89-92 °C [α]_D²⁷ = 51° (c = 0.2, MeOH) **IR** (neat) ν_{\max} = 3324 (br w), 2949 (br,w), 1739 (m), 1607 (s), 1516 (s), 1417 (m), 1289 (s), 1208 (s), 1094 (m) **¹H-NMR** (400 MHz, DMSO-*d*₆) δ = 10.26 (2 H, s, PyrNH), 8.24 (1 H, d, *J* = 7.5 Hz, NH), 8.10 (1 H, d, *J* = 7.5 Hz, NH), 7.36 (5 H, m, PhH), 5.15 (1 H, apparent t, *J* = 5.5 Hz, OH), 4.79 (1 H, m, CH), 4.55 (3 H, m, CH + OCH₂Ph), 3.83-3.70 (4 H, m, CH₂), 3.67 (3 H, s, OCH₃), 3.66 (3 H, s, OCH₃), 2.13 (6 H, s, CH₃), 1.64 (6 H, s, CH₃), 1.39 (3 H, s, CH₃), 1.39 (3 H, s, CH₃) **¹³C NMR** (100 MHz, DMSO-*d*₆) δ = 171.14 (C), 171.32 (C), 161.04 (C), 161.89 (C), 137.89 (C), 136.63 (C), 136.43 (C), 128.25 (CH), 127.60 (CH x2), 125.91 (C), 118.04 (C), 117.83 (C), 114.88 (C), 114.79 (C), 72.07 (CH₂), 69.32 (CH₂), 61.39 (CH₂), 54.54 (CH₃), 51.94 (CH), 51.94 (CH), 51.77 (CH), 35.83 (C), 28.05 (CH₃), 10.50 (CH₃), 8.72 (CH₃), 8.68 (CH₃) **LRMS** (ES⁺, acetonitrile) 611 (M+H)⁺, 646 (M+Na)⁺ **HRMS** calculated for C₃₂H₄₃N₄O₈ 611.3075 measured 611.3068 **Analytical** (%) Calculated for C₃₂H₄₂N₄O₆·(1/3 H₂O) C, 62.32; H, 6.97; N, 9.08. Found C, 62.24; H, 6.81; N, 8.87.

(S)-2-[[5-(1-{5-[(S)-1-Methoxycarbonyl-2-(4-nitro-phenyl)-ethylcarbamoyl]-3,4-dimethyl-1H-pyrrol-2-yl}-1-methyl-ethyl)-3,4-dimethyl-1H-pyrrole-2-carbonyl]-amino]-3-(4-nitro-phenyl)-propionic acid methyl ester (109)



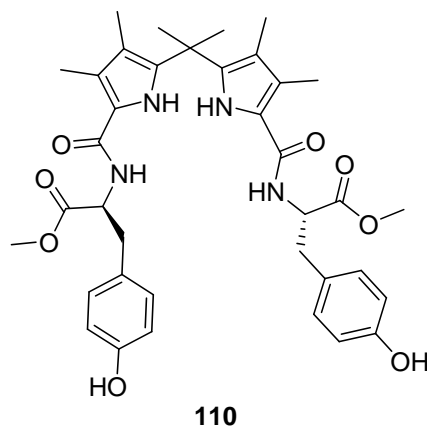
Phenylalanine **120** (700 mg, 2 mmol) was added to a solution of TFA (12 mL) and DCM (48 mL). After stirring at room temperature for 5 hours the excess TFA was removed *in vacuo* with toluene and the resulting TFA salt **121** was used without further purification.

A solution of acyl chloride **118** (2 mL, 0.3 M in DCM) was added dropwise to a solution of salt **121** and Et₃N (1 mL, 7 mmol) in DCM (30 mL). After stirring the resulting solution at room temperature for 1 hour, the solvent was evaporated *in vacuo* and the residue was purified by column chromatography (PE:EA 40:60) to afford **109** (156 mg, 30%) as a yellow solid.

Rf: 0.26 (EA:PE 70:30) **Mp** 107-109 °C [α]_D²⁹ = 128.5° (c = 0.1, MeOH) **IR** (neat) ν_{\max} = 3331 (w, br), 2952 (w), 1739 (m), 1605 (m), 1517 (s), 1436 (m), 1344 (s), 1275 (m), 1213 (m), 1016 (w), 857 (w) **¹H-NMR** (400 MHz, DMSO-*d*₆) δ = 10.00 (2 H, s, PyrrNH), 8.22-8.10 (2 H, m, partially obscured, CONH), 8.14 (4 H, d, *J* = 9 Hz, ArH), 7.55 (4H, d, *J* = 9 Hz, ArH), 4.74 (2 H, ddd, *J* = 6, 8, 9 Hz, CONHCH), 3.64 (6 H, s, OCH₃), 3.30 (2 H, m, CHHAr, partially obscured by H₂O), 3.18 (2 H, dd, *J* = 9, 13.5 Hz CHHAr), 2.05 (6 H, s, CH₃), 1.61 (6 H, s, CH₃), 1.34 (6 H, s, CH₃) **¹³C NMR** (100 MHz, DMSO-*d*₆) δ = 176.26 (C), 160.87 (C), 146.33 (C), 145.85 (C), 136.45 (C), 130.49 (CH), 125.40 (C), 123.24 (CH), 117.90 (C), 114.80 (C), 52.85 (CH₃), 51.92 (CH), 36.60 (CH₂), 35.75 (C), 27.87 (CH₃), 10.33 (CH₃), 8.55 (CH₃) **LRMS** (ES⁺, acetonitrile) 731 (M+H)⁺, 753 (M+Na)⁺ **HRMS** calculated for C₃₇H₄₃N₆O₁₀ 731.3035 measured 731.3024 **Analytical**

(%) Calculated for $C_{37}H_{42}N_6O_{10}$ C, 60.81; H, 5.79; N, 11.49. Found C, 60.44; H, 5.74; N, 11.33.

(S)-3-(4-Hydroxy-phenyl)-2-{[5-(1-{5-[(S)-2-(4-hydroxy-phenyl)-1-methoxycarbonyl-ethylcarbamoyl]-3,4-dimethyl-1H-pyrrol-2-yl]-1-methyl-ethyl)-3,4-dimethyl-1H-pyrrole-2-carbonyl]-amino}-propionic acid methyl ester (110)



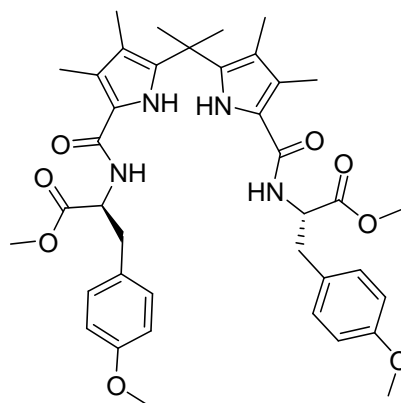
(1-Chloro-2-methyl-propenyl)-dimethyl-amine **117** (400 μ L, 3 mmol) was added to a solution of di-acid **82** (957 mg, 1.37 mmol) in THF (8 mL). After stirring the resulting solution at room temperature for 30 minutes, the solvent was evaporated *in vacuo* to yield chloride **118** which was used without further purification.

A solution of di-chloride **118** in DCM was added to a solution of L-TyrOMe·HCl (957 mg, 4 mmol) and Et_3N (2 mL, 28 mmol) in DCM (16mL). After stirring overnight at room temperature the solvent was evaporated *invacuo* and the residue purified by column chromatography (EA) afforded tweezer **109** as a pale yellow solid (600 mg, 67%).

Rf: 0.23 (EA:PE 70:30) **Mp** 120-125°C $[\alpha]_D^{27} = -4^\circ$ (c = 0.2, MeOH) **IR** (neat) $\nu_{max} = 3349$ (w,br), 2950 (w), 1732 (m), 1609 (s), 1513 (s), 1439 (m), 1363 (w), 1216 (s), 1016 (w), 947 (w) **1H -NMR** (300 MHz, DMSO- d_6) $\delta = 10.07$ (2 H, s, PyrNH), 9.23 (2 H, s, OH), 8.06 (2 H, d, $J = 9.5$ Hz, CONH), 7.03 (4 H, d, $J = 10$ Hz, ArH), 6.65 (4 H, d, $J = 10$ Hz, ArH), 4.53 (2 H, m, CH), 3.60 (6 H, s, OCH_3), 2.94 (4 H, m, CH_2Ar), 2.07 (6 H, s, CH_3), 1.63 (6 H, s, CH_3), 1.36 (6 H, s, CH_3) **^{13}C NMR** (100 MHz, DMSO- d_6) $\delta = 173.44$ (C), 162.23 (C), 156.9 (C), 137.65 (C), 131.45 (CH), 128.95 (C), 123.74 (C), 119.87 (C), 116.89 (C), 116.21 (CH), 54.75 (CH_3), 52.77 (CH), 37.43 (CH_2), 36.79 (C), 27.48 (CH_3), 10.81 (CH_3), 9.28 (CH_3) **LRMS** (ES^+ , acetonitrile) 695 ($M+Na$)⁺ **HRMS** calculated for

$C_{37}H_{45}N_4O_8$ 673.3232 measured 673.3225 **Analytical (%)** Calculated for $C_{37}H_{44}N_4O_8 \cdot (1/2 H_2O)$ C, 65.18; H, 6.65; N, 8.22. Found C, 65.23; H, 6.69; N, 8.10.

(S)-2-[[5-(1-{5-[(S)-1-Methoxycarbonyl-2-(4-methoxy-phenyl)-ethylcarbamoyl]-3,4-dimethyl-1H-pyrrol-2-yl}-1-methyl-ethyl)-3,4-dimethyl-1H-pyrrole-2-carbonyl]-amino]-3-(4-methoxy-phenyl)-propionic acid methyl ester (111)



111

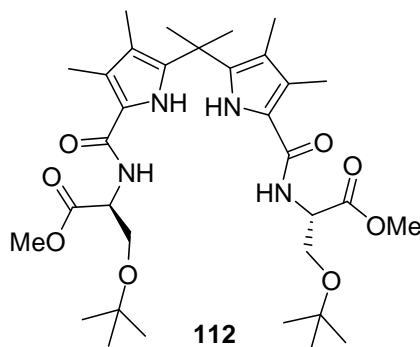
Tyrosine derivate **124** (314 mg, 1 mmol) was added to a solution of TFA (6 mL) and DCM (24 mL). After stirring at room temperature for 5 hours the excess TFA was removed *in vacuo* with toluene and the resulting TFA salt **125** was used without further purification.

PyBOP (457 mg, 0.88 mmol) was added to a solution of di acid **82** (127 mg, 0.4 mmol), DIPEA (0.4 mL, 4 mmol) and salt **125** in DCM (5 mL). After stirring overnight at room temperature the solvent evaporated *in vacuo*. Purification by column chromatography (EA:PE 60:40) afforded **110** as a colourless solid (61 mg, 21%).

Rf: 0.15 (PE/ EA : 40/60) **Mp** 120-129 °C $[\alpha]_D^{24} = 20^\circ$ (c = 0.2, MeOH) **IR** (neat) $\nu_{\max} = 3440$ (w), 2953 (w), 1732 (m), 1613 (m), 1511 (s), 1442 (m), 1247 (s), 1031 (m), 839 (s) **¹H-NMR** (400 MHz, CD₃CN) $\delta = 8.86$ (2 H, s, PyrNH), 7.13 (4 H, m, ArH), 8.45 (4 H, m, ArH), 6.29 (2 H, d, $J = 7.5$ Hz, CONH), 4.79 (2 H, m, CH), 3.75 (6 H, s, OCH₃), 3.69 (6 H, s, OCH₃), 3.16 (2 H, dd, $J = 6, 14$ Hz CHCHHAr), 3.05 (2 H, dd, $J = 7.5, 14$ Hz CHCHHAr), 2.04 (6 H, s, CH₃), 1.60 (6 H, s, CH₃), 1.46 (6 H, s, CH₃) **¹³C NMR** (100 MHz, CD₃CN) $\delta = 173.50$ (C), 162.16 (C), 159.73 (C), 137.61 (C), 131.38 (CH), 129.82 (C), 123.66 (C), 119.84 (C), 116.87 (C), 114.82 (CH), 55.85 (CH₃), 54.70 (CH₃), 52.48

(CH), 37.37 (CH₂), 36.73 (C), 27.44 (CH₃), 10.80 (CH₃), 9.24 (CH₃) **LRMS** (ES⁺, acetonitrile) 724 (M+Na)⁺ **HRMS** calculated for C₃₉H₄₈Na₁N₄O₈ 723.3364, found 723.3354.

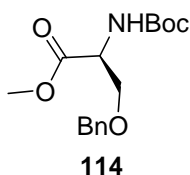
(S)-3-tert-Butoxy-2-[(5-{1-[5-(2-tert-butoxy-1-methoxycarbonyl-ethylcarbamoyl)-3,4-dimethyl-1H-pyrrol-2-yl]-1-methyl-ethyl}-3,4-dimethyl-1H-pyrrole-2-carbonyl)-amino]-propionic acid methyl ester (112)



PyBOP (1.22 g, 2.4 mmol) was added to a solution of di acid **82** (300 mg, 0.94 mmol), DIPEA (0.81 mL, 4.7 mmol) and L-Ser(*O**t*-but)OMe·HCl (596 mg, 2.8 mmol) in DCM (20 mL). After stirring overnight at room temperature the reaction mixture was diluted in DCM (100 mL) and washed with KHSO₄ (100 mL, 1M aq), K₂CO₃ (100 mL, 1M aq) and brine (100mL). The organic layer was dried over MgSO₄ and the solvent evaporated *in vacuo*. Purification by column chromatography (EA:PE 40:60) afforded **112** as a pale yellow solid (140 mg, 23%).

Rf: 0.40 (PE/EA : 60/40) **¹H-NMR** (300 MHz, CDCl₃) δ = 9.07 (2 H, s, PyrNH), 6.69 (2 H, br s, CONH), 4.88 (2 H, m, CONHCH), 3.90 (2 H, dd, *J* = 2.5, 8.5 Hz, CHCHHO), 3.78 (6 H, s, OCH₃), 3.67 (2 H, dd, *J* = 3, 8.5 Hz, CHCHHO), 2.24 (6 H, s, CH₃), 1.55 (6 H, s, CH₃), 1.16 (17 H, s, CH₃+ C(CH₃)₃) **LRMS** (ES⁺, acetonitrile) 634 (M+H)⁺, 655 (M+Na)⁺.

(S)-methyl 3-(benzyloxy)-2-(tert-butoxycarbonylamino)propanoate (114) ¹²³

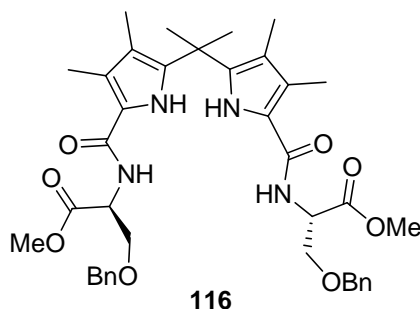


NaHCO₃ (1.71 g, 20.30 mmol) and CH₃I (0.4 mL, 7.45 mmol) were added sequentially to a solution of *N*Boc-L-Ser(OBn)-OH **113** (2.00 g, 6.77 mmol) in DMF (30 mL). After 8

days stirring at room temperature the mixture was filtered and concentrated *in vacuo*. The residue was partitioned between EA (100 mL) and water (100 mL), and the organic layer was washed with sodium thiosulphate (2 x 100 mL, 1M aq), NaHCO₃ (2 x 100 mL, 5% aq) and brine (2x100mL). The organic layer was dried and the solvent evaporated *in vacuo* to give **38** as a yellow solid (1.6 g, 76%) which was used without further purification.

Rf: 0.25 (PE/EA : 80/20) $[\alpha]_D^{22} = 33.1^\circ$ ($c = 1$, CHCl₃) **IR** (neat) $\nu_{\max} = 3031$ (br,w), 1675 (m), 1368 (w), 1202 (m), 1135 (m), 910 (w) **¹H-NMR** (400 MHz, CDCl₃) $\delta = 7.35$ -7.24 (5 H, m, PhH), 5.39 (1 H, d, $J = 8$ Hz, NH), 4.54 (1 H, d, $J = 12$ Hz, OCHHPh), 4.48 (1 H, d, $J = 12$ Hz, OCHHPh), 4.45-43 (1 H, m, partially obscured, CH), 3.86 (1 H, dd, $J = 2.5, 9.5$ Hz, CHCHHO), 3.74 (3 H, s, OCH₃), 3.68 (1 H, dd, $J = 3, 9$ Hz, CHCHHO), 1.45 (9 H, s, OC(CH₃)₃)(literature¹²³) **¹³C NMR** (75 MHz, CDCl₃) $\delta = 171.30$ (C), 155.62 (C), 137.74 (C), 128.56 (CH), 127.96 (CH), 127.74 (CH), 79.90 (C), 73.41 (CH₂), 70.14 (CH₂), 54.19 (CH), 52.53 (CH₃), 28.46 (CH₃) **LRMS** (ES⁺, acetonitrile) 332.3 (100) (M+Na)⁺, 310.3 (M+H)⁺

(S)-3-Benzyloxy-2-[(5-{1-[5-((S)-2-benzyloxy-1-methoxycarbonyl-ethylcarbamoyl)-3,4-dimethyl-1H-pyrrol-2-yl]-1-methyl-ethyl}-3,4-dimethyl-1H-pyrrole-2-carbonyl)-amino]-propionic acid methyl ester (116)



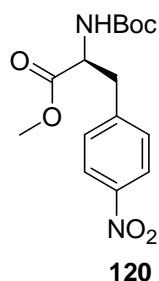
Serine derivate **114** (1.41 g, 4.7 mmol) was added to a solution of TFA (18 mL) and DCM (72 mL). After stirring at room temperature for 5 hours the excess TFA was removed *in vacuo* with toluene and the resulting TFA salt **115** was used without further purification.

PyBOP (2g, 3.8 mmol) was added to a solution of di-acid **82** (556 mg, 1.74 mmol), Et₃N (1 mL, 5 mmol) and salt **114** in DCM (20 mL). After stirring overnight at room temperature the reaction mixture was diluted in DCM (100 mL) and washed with KHSO₄

(100 mL, 1M aq), K₂CO₃ (100 mL, 1M aq) and brine (100mL). The organic layer was dried over MgSO₄ and the solvent evaporated *in vacuo*. Purification by column chromatography (EA:PE 60:40) afforded **116** as a pale yellow solid (1 g, 86%).

Rf: 0.15 (PE/ EA : 40/60) **Mp** 65-72 °C [α]_D²⁴ = 41.2° (c = 0.5, CHCl₃) **IR** (neat) ν_{\max} = 3301 (w, br), 2916 (w, br), 2896 (w, br), 2359 (w), 2341 (m), 1744 (w), 1605 (m), 1514 (m), 1295 (m), 1207 (m), 1156 (m), 1103 (m), 735(w) **¹H-NMR** (400 MHz, CDCl₃) δ = 8.80 (2 H, s, PyrNH), 7.24-7.32 (10 H, m, PhH), 6.57 (2 H, d, *J* = 8 Hz, NH), 4.90 (2 H, apparent td, *J* = 3, 8 Hz, CH), 4.55 (2 H, d, *J* = 12 Hz, OCHHPh), 4.50 (2 H, d, *J* = 12 Hz, OCHHPh), 3.96 (2 H, dd, *J* = 3, 9.5 Hz, CHHPh), 3.77 (2 H, dd, *J* = 3.5, 9.5 Hz, CHHPh partially obscured by OCH₃), 3.75 (3 H, s, OCH₃), 2.20 (6 H, s, CH₃), 1.61 (6 H, s, CH₃), 1.53 (6 H, s, CH₃) **¹³C NMR** (100 MHz, CDCl₃) δ = 171.23 (C), 161.72 (C), 137.66 (C), 136.22 (C), 128.46 (CH), 127.86 (CH), 127.63 (CH), 121.64 (C), 119.09 (C), 116.42 (C), 73.39 (CH₂), 70.03 (CH₂), 52.76 (CH₃), 52.62 (CH), 35.70 (C), 26.95 (CH₃), 10.83 (CH₃), 9.25 (CH₃) **LRMS** (ES⁺, acetonitrile) 723.4 (M+Na)⁺ **HRMS** calculated for C₃₉H₄₈Na₁N₄O₈ 723.3364, measured 723.3369

(S)-methyl 2-(tert-butoxycarbonylamino)-3-(4-nitrophenyl)propanoate (120)¹⁶⁰

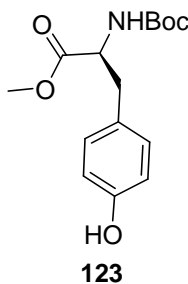


TMS-diazomethane (1 mL, aq 2M in Et₂O) was added to a solution of *N*Boc-L-*p*-nitroPheOH (442 mg, 1.42 mmol) in MeOH (16mL) and toluene (8 mL). The resulting solution was stirred at room temperature for 10 minutes and the solvent was evaporated *in vacuo* to yield **120** (460 mg, quantitative) as a yellow solid which was used without further purification.

Rf: 0.21 (PE/ EA : 80/20) **Mp**: 80-85 °C [α]_D²⁹ = 58.4° (c =1, CHCl₃) (literature¹⁶¹) **IR** (neat) ν_{\max} = 3356 (w), 1728 (m), 1686 (m), 1518 (s), 1252 (m), 1013 (w), 858 (w) **¹H-NMR** (400 MHz, CDCl₃) δ = 8.16 (2 H, d, *J* = 9 Hz ArH), 7.31 (2 H, d, *J* = 8.5 Hz, ArH) 5.04 (1 H, d, *J* = 4 Hz, NH), 4.62 (1 H, m, CH), 3.73 (3H, s, OCH₃), 3.27 (1 H, dd, *J* = 5.5,

13.5 Hz, CHCHHAr), 3.12 (1 H, dd, $J = 6.0, 13.5$ Hz, CHCHHAr), 1.41 (9 H, s, C(CH₃)₃) (literature¹⁶¹) **¹³C NMR** (100 MHz, CDCl₃) $\delta = 171.77$ (C), 155.06 (C), 147.33 (C), 144.38 (C), 130.38 (CH), 123.81 (CH), 80.51 (C), 54.28 (CH), 52.66 (CH₃), 38.57 (CH₂), 28.4 (CH₃) (lit¹⁶¹) **LRMS** (ES⁺, acetonitrile) 325 (M+H)⁺, 347 (M+Na)⁺ **HRMS** calculated for C₁₆H₂₃N₁Na₁O₅ 332.1468, found 332.1470.

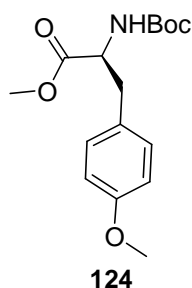
(S)-methyl 2-(tert-butoxycarbonylamino)-3-(4-hydroxyphenyl)propanoate (123)¹³⁷



A solution of Boc anhydride (2 g, 9.3 mmol) in THF (4mL) was added to a solution of L-Tyr-OMe·HCl **122** (2 g, 8.65 mmol) and NaHCO₃ (1.6 g, 19 mmol) in THF (20 mL) and MeOH (12 mL). After stirring overnight at room temperature, the resulted solution was concentrated *in vacuo*. The residue was dissolved in DCM (100mL), washed with water (2x 100mL), dried over MgSO₄ and concentrated *in vacuo*. The residue was recrystallised from DCM to afford tyrosine **124** (2.41 g, 95%) as a colourless solid.

Rf: 0.1 (PE/ EA : 80/20) **Mp**: 86-92 °C [α]_D²⁹ = 8.9° (c =1, CHCl₃) **IR** (neat) $\nu_{\max} = 3384$ (m), 2952 (br, w), 1713 (m), 1686 (s), 1516 (s), 1444 (m), 1367 (w), 1256 (m), 994 (m) **¹H-NMR** (400 MHz, CDCl₃) $\delta = 6.95$ (2 H, d, $J = 8$ Hz, ArH), 6.72 (2 H, d, $J = 8$ Hz, ArH), 6.12 (1 H, br s, OH), 5.03 (1 H, m, NH), 4.53-4.34 (1 H, m, CH), 3.70 (3 H, s, CH₃), 3.04-2.93 (2 H, m, CHCH₂Ar), 1.41 (9 H, s, OC(CH₃)₃) **¹³C NMR** (75 MHz, CDCl₃) $\delta = 172.80$ (C), 155.47 (C), 155.35 (C), 130.48 (CH), 127.53 (C), 115.66 (CH), 80.38 (C), 54.77 (CH), 52.41 (CH₃), 37.70 (CH₂), 28.43 (CH₃) **LRMS** (ES⁺, acetonitrile) 318 (M+Na)⁺ **HRMS** calculated for C₁₅H₂₁N₁Na₁O₅ 318.1312, found 318.1311.

(S)-methyl 2-(tert-butoxycarbonylamino)-3-(4-methoxyphenyl)propanoate (124)¹⁶²

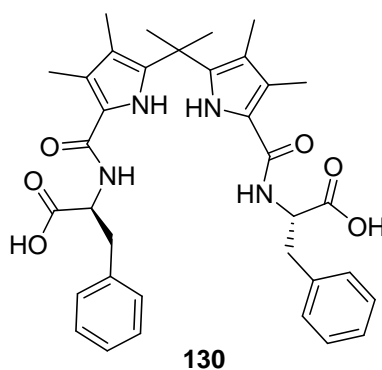


Methyl iodide (0.5 mL, 8.03 mmol) was added to a solution of **123** (1.44 g, 4.8 mmol) in DMF (20 mL) with K₂CO₃ (2g, 14 mmol). After stirring the resulting solution overnight at room temperature, the solvent was evaporated *in vacuo*. The residue was purified by column chromatography (SiO₂, DCM) to yield **124** (429 mg, 30%) as a colorless solid.

Rf: 0.35 (PE/ EA : 80/20) **Mp**: 80-85 °C [α]_D²⁹ = 4.1° (c =1, CHCl₃) **IR** (neat) ν_{\max} = 3394 (w), 3349 (w), 2958 (w, br), 1736 (s), 1699 (s), 1612 (w), 1444 (m), 1364 (m), 1245 (s), 1148 (s) **¹H-NMR** (400 MHz, CDCl₃) δ = 7.03 (2 H, d, *J* = 8.5 Hz, Ar*H*), 6.83 (2 H, d, *J* = 8.5 Hz, Ar*H*), 4.94 (1 H, br s, NH), 4.54 (1 H, m, CH), 3.78 (3 H, s, OCH₃), 3.71 (3 H, s, OCH₃), 3.06-2.95 (2 H, m, CH₂Ar), 1.42 (9 H, s, C(CH₃)₃) (literature¹⁶³) **¹³C NMR** (100 MHz, CDCl₃) δ = 172.57 (C), 158.85 (C), 130.43 (CH), 128.11 (C), 114.16 (CH), 80.03 (C), 55.39 (CH₃), 54.71 (CH) 52.31 (CH₃), 37.65 (CH₂), 28.46 (CH₃) (lit.¹⁶³) **LRMS** (ES⁺, acetonitrile) 332 (M+Na)⁺ **HRMS** calculated for C₁₆H₂₃N₁Na₁O₅ 332.1468, measured 332.1470.

4.6 Synthesis in Chapter III

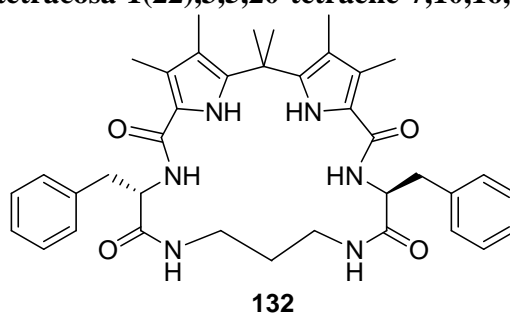
(S)-2-[(5-{1-[5-((S)-1-Carboxy-2-phenyl-ethylcarbamoyl)-3,4-dimethyl-1H-pyrrol-2-yl]-1-methyl-ethyl}-3,4-dimethyl-1H-pyrrole-2-carbonyl)-amino]-3-phenyl-propionic acid (**130**)



Tweezer **107** (1.33 g, 2.07 mmol) was added to a biphasic solution of THF (20 mL) and LiOH (1M, aq 20 mL). After stirring vigorously at room temperature for 24 hours the reaction mixture was extracted with Et₂O (2 x 30mL) and acidified (KHSO₄ 1M) and extracted with EA (3 x 50 mL), the organic solution was dried and the solvent evaporated *in vacuo* to achieve **130** as a white solid (1.16 g, 91%).

Rf: 0.48 (MeOH/DCM/AcOH : 2.5/95/2.5) $[\alpha]_D^{27} = 4.75^\circ$ (c =0.2, MeOH) **IR** (neat) $\nu_{\max} = 3303$ (w, br), 2924 (w, br), 2360 (s), 2343 (m), 1716 (w), 1590 (m), 1515 (s), 1418 (w), 1261 (m), 1192 (m) 1291 (w), 699 (m) **¹H-NMR** (400 MHz, DMSO) $\delta = 12.65$ (2 H, br s, COOH), 10.04 (2 H, s, PyrNH), 7.98 (2 H, d, J = 8 Hz, NH), 7.27-7.17 (10 H, m, PhH), 4.62 (2 H, ddd, J = 9, 8, 5 Hz, COCHCH₂Ph), 3.15 (2 H, dd, J = 5, 13.5 Hz COCHCHHPh), 3.00 (2 H, dd, J = 9, 13.5 Hz COCHCHHPh), 2.06 (6 H, s, CH₃), 1.63 (6 H, s, CH₃), 1.37 (6 H, s, CH₃) **¹³C-NMR** (100 MHz, DMSO) $\delta = 173.6$ (C), 160.9 (C), 137.9 (C), 136.2 (C), 129.1 (CH), 128.1 (CH), 126.3 (CH), 125.0 (C), 118.2 (C), 114.7 (C), 53.4 (CH), 37.0 (CH₂), 35.8 (CH), 28.0 (CH₃), 10.4 (CH₃), 8.6 (CH₃) **LRMS** (ES⁺, methanol) 613.4, (M+H)⁺, 635.4 (M+Na)⁺ **HRMS** calculated for C₃₅H₄₀N₄NaO₆ 635.2840, measured 635.2834.

(9S,17S)-9,17-Dibenzyl-2,2,4,5,21,22-hexamethyl-8,11,15,18,23,24-hexaaza-tricyclo[18.2.1.1*3,6*]tetracos-1(22),3,5,20-tetraene-7,10,16,19-tetraone (132)



Method A

A solution of EDC (287mg, 1.49 mmol) in DCM (15 mL) was added dropwise to a solution of tweezer **130** (306 mg, 0.5 mmol), pentafluorophenol (900 mg, 4.8 mmol) and DCM (15 mL) at 0°C. After stirring at room temperature overnight the reaction mixture was washed with (2 x 50mL) NaHCO₃ (5% aq), dried over MgSO₄ and the solvent evaporated *in vacuo* to achieve crude pentafluorophenyl ester **131** which was dissolved in

dry DCM (4mL). TBACl (360 mg, 1.29 mmol) was added in DCM (1mL). The mixture and a solution of 1,3-diaminopropane (41 μ L, 0.5 mmol) and dry Et₃N (0.5mL, 3.6 mmol) in DCM (5 mL) were added simultaneously, with a syringe pump into DCM (90 mL) at room temperature over a period of 2 hours. After stirring the resulting yellow solution overnight at room temperature the solvent was removed *in vacuo* and the residue purified with column chromatography (DCM \rightarrow DCM/MeOH : 98/2) to afford **132** as a colourless solid (40 mg, 12%).

Method B: anion template study

A solution of EDC (490 mg, 2.6 mmol) in DCM (40 mL) was added dropwise to a solution of tweezer **130** (747 mg, 1.2 mmol), pentafluorophenol (885 mg, 4.8 mmol) and DCM (20 mL) at 0°C. After stirring at room temperature overnight the reaction mixture was washed with (2x50mL) NaHCO₃ (5% aq), dried over MgSO₄ and the solvent evaporated *in vacuo* to achieve crude pentafluorophenyl ester **131** which was used without further purification. Pentafluorophenyl ester **131** was dissolved in DCM the resulting volume of the solution was 18 mL. 1, 3 diaminopropane (100 μ L, 1.2 mmol) and Et₃N (600 μ L, 4.3 mmol) were dissolved in DCM and the resulting volume of the solution was 18 mL.

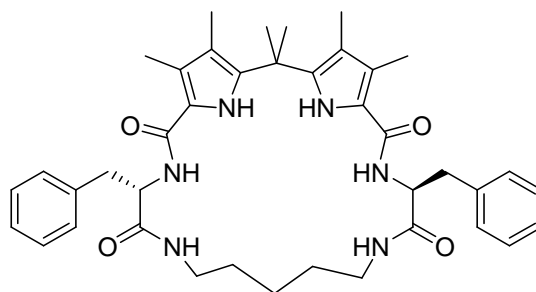
Sucessively 2 equivalents of TBACl (160 mg, 0.57 mmol), 2 equivalents of TBAOAc (174 mg, 0.58 mmol), 2 equivalents of TBA dihydrogen phosphate (193 mg, 0.57 mg) and O equivalents of anion were added to four different aliquots (4mL) of solution containing pentafluorophenol ester. Each mixture so obtained and an aliquot (4 mL) of solution containing the amines were added simultaneously, with a syringe pump, into 20 mL of DCM at room temperature. For each reaction the solvent was evaporated *in vacuo* and the residue was purified by column chromatography.

Macrocycle **132** was obtained with various yields: 0 equivalents of anion (12.2 mg, 7%), 2 equivalents TBACl (25 mg, 14%), 2 equivalents of TBA dihydrogen phosphate (0 mg, 0%), TBAOAc (it was not possible to isolate the product by column chromatography)

Rf: 0.48 (MeOH/DCM : 3/97) **Mp**: 147-151 °C [α]_D²⁹ = 7.0° (c =0.1, CHCl₃) **IR** (neat) ν_{\max} = 3294 (w), 2928 (w), 1739 (w), 1616 (s), 1495 (s), 1454 (m), 1276 (m), 698 (s) **¹H-NMR** (300 MHz, DMSO) δ = 9.77 (2H, s, PyrNH), 7.86 (2 H, d, *J* = 8.5 Hz, CONHCH),

7.70 (2 H, m, CONHCH₂), 7.27-7.17 (10 H, m, PhH), 4.62 (2 H, m, CH), 3.13-3.05 (4 H, m, CONHCHHPH and NHCHCHH superimposed), 2.80-2.74 (4 H, m, CONHCHHPH and NHCHCHH superimposed), 2.13 (6 H, s, CH₃), 2.05 (6 H, s, CH₃), 1.73 (6 H, s, CH₃), 1.43 (2 H, m, CH₂CH₂CH₂) ¹³C-NMR (75 MHz, DMSO) δ =171.1 (C), 161.0 (C), 138.3 (C), 135.8 (C), 128.9 (C), 128.1 (CH), 126.1 (CH), 124.3 (C), 119.3 (C), 114.0 (C), 53.7 (CH), 38.8 (C), 37.9 2x(CH₂), 35.7 (CH₂), 29.2 (CH₃), 10.6 (CH₃), 10.3 (CH₃) **LRMS** (ES⁺, acetonitrile) 651.3 (M+H)⁺, 673.4 (M+Na)⁺ **HRMS** calculated for C₃₈H₄₆N₆NaO₄ 673.3473, found 673.3486 .

(9S,19S)-9,19-Dibenzyl-2,2,4,5,23,24-hexamethyl-8,11,17,20,25,26-hexaaza-tricyclo[20.2.1.1*3,6*]hexacosa-1(24),3,5,22-tetraene-7,10,18,21-tetraone (133)



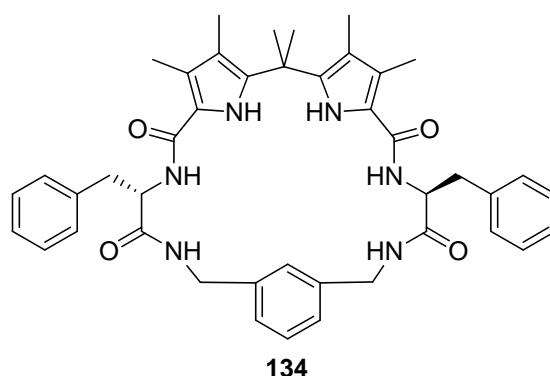
133

A solution of EDC (287mg, 1.49 mmol) in DCM (15 mL) was added dropwise to a solution of tweezer **130** (306 mg, 0.5 mmol), pentafluorophenol (900 mg, 4.8 mmol) in dry DCM (15 mL) at 0°C. After stirring at room temperature overnight the reaction mixture was washed with (2x50mL) NaHCO₃ (5% aq), dried over MgSO₄ and the solvent evaporated *in vacuo* to achieve crude pentafluorophenyl ester **131** which was dissolved in dry DCM (4mL). TBACl (360 mg, 1.29 mmol) was added in dry DCM (1mL). The mixture and a solution of 1,5-diaminopentane (60μL, 0.5 mmol) and dry Et₃N (0.5mL, 3.6 mmol) in dry DCM (5 mL) were added simultaneously, with a syringe pump into dry DCM (90 mL) at room temperature over a period of 2 hours. After stirring the resulting yellow solution overnight at room temperature the solvent was removed *in vacuo* and the residue purified with column chromatography (PE/EA : 50/50 →0/100) to afforded **133** as a colourless solid (50 mg, 14%).

Rf: 0.4 (MeOH/DCM : 3/97) **Mp:** decomposes at 180 °C [α]_D²⁹ = 5.5° (c=0.1, CHCl₃)

IR (neat) ν_{\max} = 3428 (w), 3291 (br w), 2932 (br w), 2360 (m), 2340 (m), 1651 (s), 1597 (w), 1581 (m), 1514 (s), 1455 (w), 1340 (w), 1292 (m), 1259 (m), 1184 (m), 1154 (w), 1107 (w), 737 (m), 696 (s), 631 (w), 467 (m) **¹H-NMR** (300 MHz, DMSO-*d*₆) δ = 9.69 (2 H, s, PyrNH), 7.74 (2 H, d, *J* = 8.5 Hz, CONHCH), 7.66 (2 H, dd, *J* = 6.5, 4.5 Hz, CONHCH₂), 7.27-7.14 (10 H, m, PhH), 4.61 (2 H, apparent q, *J* = 7.5 Hz, CH), 3.19 (2 H, m, CONHCHHCH₂), 3.03 (2 H, dd, *J* = 7.0, 13.5 Hz, NHCHCHHPh), 2.83 (2 H, dd, *J* = 8.0, 13.5 Hz, NHCHCHHPh), 2.73 (2 H, m, CONHCHHCH₂), 2.11 (6 H, s, CH₃), 2.00 (6 H, s, CH₃), 1.72 (6 H, s, CH₃), 1.33 (2 H, m, CONHCH₂CHH), 1.26 (2 H, m, CONHCH₂CHH), 1.14 (2 H, m, Q9NHCH₂CH₂CHH) **¹³C-NMR** (75 MHz, DMSO) δ = 170.93(C), 160.80 (C), 138.20 (C), 136.01 (C), 129.97 (CH), 128.09 (CH), 126.13 (CH), 123.98 (C), 119.34 (C), 113.99 (C), 53.98 (CH), 38.19 (CH), 37.83 (CH₂), 37.26 (CH₂), 28.95 (CH₃), 27.54 (CH₂), 22.06 (CH₂), 10.49(CH₃), 10.39 (CH₃) **LRMS** (ES⁺, acetonitrile) 679.3, (M+H)⁺, 701.4 (M+Na)⁺ **HRMS** calculated for C₄₀H₅₀N₆NaO₄ 701.3786, found 701.3775 **Analytical** Calculated for C₃₂H₄₂N₄O₄·(2/3 H₂O) C, 68.06; H, 7.57; N, 11.91. Found C, 67.94; H, 7.04; N, 11.61.

Macrocycle 134



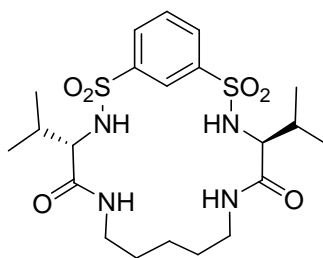
A solution of EDC (287mg, 1.49 mmol) in dry DCM (15 mL) was added dropwise to a solution of tweezer **130** (306 mg, 0.5 mmol), pentafluorophenol (900 mg, 4.8 mmol) and dry DCM (15 mL) at 0°C.

After stirring at room temperature overnight the reaction mixture was washed with (2x50mL) NaHCO₃ (5% aq), dried over MgSO₄ and the solvent evaporated *in vacuo* to achieve crude pentafluorophenyl ester **7** which was dissolved in dry DCM (4mL). TBACl (360 mg, 1.29 mmol) was added in dry DCM (1mL). The mixture and a solution of *m*-

xylenediamine (65 μ L, 0.5 mmol) and dry Et_3N (0.5 mL, 3.6 mmol) in dry DCM (5 mL) were added simultaneously, with a syringe pump into dry DCM (120 mL) at room temperature over a period of 2 hours. After stirring the resulting yellow solution overnight at room temperature the solvent was removed *in vacuo* and the residue purified with column chromatography (DCM \rightarrow DCM/MeOH : 98/2) to afford **134** as a colourless solid (12 mg, 3 %).

Rf: 0.51 (MeOH/DCM : 3/97) $[\alpha]_{\text{D}}^{29} = 4.0^\circ$ ($c = 0.1$, CHCl_3) **IR** (neat) $\nu_{\text{max}} = 3295$ (w,br), 2927 (w), 1615 (m), 1515 (s), 1495 (s), 1454 (m), 1266 (m), 1191 (w), 1152 (w) **$^1\text{H-NMR}$** (400 MHz, DMSO) $\delta = 9.54$ (2 H, s, PyrNH), 8.16 (2 H, apparent t, CONHCH₂), 7.53 (2 H, d, $J = 7$ Hz, CONHCH), 7.28-7.13 (10 H, m, PhH), 4.67 (2 H, ddd, $J = 6, 7, 9$ Hz, CH), 4.36 (2 H, dd, $J = 6, 14$ Hz, NHCHHAr), 3.95 (2 H, dd, $J = 4.5, 14$ Hz, NHCHHAr), 3.11 (2 H, dd, $J = 6, 13.5$ Hz, CHCHHPh), 2.90 (2 H, dd, $J = 9, 13.5$ Hz, CHCHHPh), 2.03 (6 H, s, CH₃), 1.92 (6 H, s, CH₃), 1.68 (6 H, s, CH₃) **$^{13}\text{C-NMR}$** (75 MHz, DMSO) $\delta = 171.02$ (C), 160.88 (C), 139.05 (C), 138.14 (C), 135.89 (C), 135.10 (C), 129.02 (CH), 128.48 (CH), 128.14 (CH), 128.0 (CH), 127.43 (CH), 126.23 (CH), 119.36 (C), 105.05 (C), 54.24 (CH), 41.60 (CH₂), 37.82 (C), 37.61 (CH₂), 28.51 (CH₃), 10.42 (CH₃), 10.33 (CH₃) **LRMS** (ES^+ , acetonitrile) 730.4 ($\text{M} + \text{NH}_4^+$), 735.5 ($\text{M} + \text{Na}^+$) **HRMS** calculated for $\text{C}_{43}\text{H}_{48}\text{N}_6\text{Na}_1\text{O}_4$ 735.3629 measured 735.3618

(S)-4,14-Diisopropyl-2,2,16,16-tetraoxo-2l6,16l6-dithia-3,6,12,15-tetraaza-bicyclo[15.3.1]henicosa-1(20),17(21),18-triene-5,13-dione (136)



136

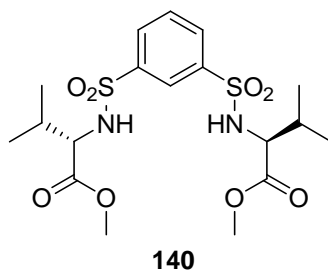
A solution of EDC (1.70 g, 8.8 mmol) in DCM (40 mL) was added dropwise to a suspension of tweezer **138** (1.89 g, 4.3 mmol), pentafluorophenol (2.18 g, 11 mmol) and DCM (20 mL) at 0°C. After stirring at room temperature overnight the reaction mixture was washed with (2x150 mL) NaHCO_3 (5% aq), dried over MgSO_4 and the solvent

evaporated *in vacuo*. The residue was filtered through a silica pad to yield pentafluorophenol ester **138** (2.58 g, 77%)

Pentafluorophenyl ester **138** (978 mg, 1.27 mmol) was dissolved in DCM the resulting volume of the solution was 18 mL. 1, 5 diaminopentane (148 μ L, 1.27 mmol) and Et₃N (600 μ L, 4.3 mmol) were dissolved in DCM and the resulting volume of the solution was 18 mL. Successively 2 equivalents of TBACl (160 mg, 0.57 mmol), 2 equivalents of TBAOAc (170 mg, 0.57 mmol), 2 equivalents of TBA dihydrogen phosphate (192 mg, 0.57 mg) and 2 equivalents of TBABr (181 mg, 0.56 mmol) were added to four different aliquots (4mL) of solution containing pentafluorophenol ester. Each mixture so obtained and an aliquot (4 mL) of solution containing the amines were added simultaneously, with a syringe pump, into 20 mL of DCM at room temperature. For each reaction the solvent was evaporated *in vacuo* and the residue was purified by column chromatography (EA/PE: 50:50 \rightarrow 75:25). Macrocycle **136** was obtained with various yields: 2 equivalents TBACl (98 mg, 68%), 2 equivalents of TBA dihydrogen phosphate (0 mg, 0%), 2 equivalents of TBAOAc (30 mg, 21 %), 2 equivalents of TBABr (180 mg, 65%)

Rf: 0.29 (EA:PE : 75/25) $[\alpha]_D^{24} = 134.4^\circ$ (c =0.5, CH₃CN) **IR** (neat) $\nu_{\max} = 3251$ (w), 2964 (w), 2873 (w), 1653 (s), 1557 (m), 1436 (m), 1328 (s), 1174 (s), 1133 (m), 1080 (m), 1054 (m), 935 (m) **¹H-NMR** (400 MHz, DMSO-*d*₆) $\delta = 8.15$ (1 H, t, $J = 2$ Hz, *ArH*), 8.08 (2 H, broad s, SO₂NH), 7.95 (2 H, dd, $J = 2, 8$ Hz, *ArH*), 7.80 (2 H, dd, $J = 7.0, 4.5$ Hz CONH), 7.67 (1 H, t, $J = 8$ Hz, *ArH*), 3.54 (2 H, br s, *CH*), 3.17-3.11 (2 H, m, NHCHH), 2.66-2.58 (2 H, m, NHCHH), 1.89 (2 H, m, CHCHC(CH₃)₂), 1.20-1.22 (2H, m, NHCH₂CHH), 1.07-1.02 (2 H, m, NHCH₂CHH), 0.91 (6 H, d, $J = 6.5$ Hz CHC(CH₃)CH₃), 0.97 (6 H, d, $J = 7$ Hz CHC(CH₃)CH₃), 0.68 (2 H, apparent quint $J=7.5$ Hz NHCH₂CH₂CH₂) **¹³C-NMR** (75 MHz, DMSO) $\delta = 169.55$ (C), 142.71 (C), 129.71 (CH), 129.24 (CH), 124.36 (CH), 61.79 (CH), 38.17 (CH₂), 31.10 (CH), 28.12 (CH₂), 23.36 (CH₂), 19.11 (CH₃), 18.22 (CH₃) **LRMS** (ES⁺, acetonitrile) 524.3 (M+Na)⁺ **Analytical** (%) Calculated for C₄₃H₄₈N₆O₄·(H₂O) C, 48.44; H, 6.97; N, 10.76. Found C, 48.8; H, 6.82; N, 10.79.

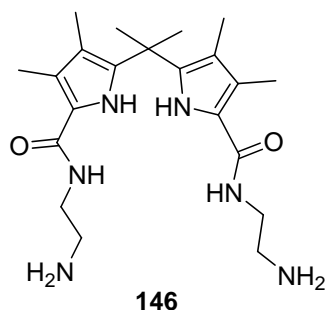
(S)-2-[3-((S)-1-Methoxycarbonyl-2-methyl-propylsulfamoyl)-benzenesulfonyl amino]-3-methyl-butyric acid methyl ester (140)



Benzenedisulfonyl chloride **139** (320 mg, 1.1 mmol) was added to a suspension of L-Val-OMe·HCl (539 mg, 3.21 mmol), Et₃N (2 mL, 13.8 mmol) in DCM (10 mL). After stirring overnight at room temperature, the reaction mixture was diluted in DCM (100 mL) and washed with KHSO₄ (100 mL, 1M aq), K₂CO₃ (100 mL, 1M aq) and brine (100 mL). The organic layer was dried over MgSO₄ and the solvent evaporated *in vacuo*. Purification by column chromatography (EA:PE 20:80) afforded **140** as a colourless oil (283 mg, 55%).

Rf: 0.7 (PE/ EA : 30/70) $[\alpha]_D^{24} = 10.7^\circ$ ($c = 0.5$, CH₃CN) **IR** (neat) $\nu_{\max} = 3275$ (w), 2965 (w), 1735 (s), 1586 (m), 1434 (m), 1335 (s), 1302 (m), 1264 (m), 1157 (s), 1138 (s), 920 (m), 579 (s) **¹H-NMR** (400 MHz, CDCl₃) $\delta = 8.26$ (1 H, t, $J = 1.5$ Hz, ArH), 8.02 (2 H, dd, $J = 1.5, 7.5$ Hz, ArH), 7.66 (2 H, apparent t, $J = 8.0$ Hz, ArH), 5.23 (2 H, d, $J = 9.0$ Hz SO₂NH), 3.82 (2 H, apparent q, $J = 5.0$ Hz NHCH), 3.50 (6 H, s, OCH₃), 2.08 (2 H, m, CH), 0.97 (6 H, d, $J = 6.5$ Hz, C(CH₃CH₃)), 0.88 (6 H, d, $J = 7$ Hz, C(CH₃CH₃)) **¹³C NMR** (100 MHz, CD₃CN) $\delta = 171.57$ (C), 141.46 (C), 131.21 (CH), 130.27 (CH), 126.08 (CH), 61.40 (CH₃), 52.63 (CH), 31.72 (CH), 19.11 (CH₃), 17.50 (CH₃) **LRMS** (ES⁺, acetonitrile) 487 (M+Na)⁺ **HRMS** calculated for C₁₈H₂₈Na₁N₂O₈S₂ 487.1179, measured 487.1175.

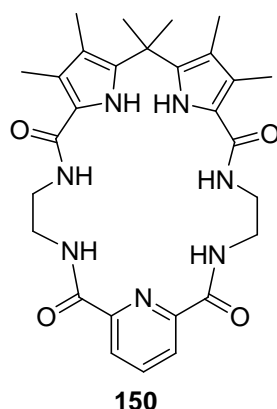
5,5'-(propane-2,2-diyl)bis(N-(2-aminoethyl)-3,4-dimethyl-1H-pyrrole-2-carboxamide) (146)



Pd/C 10% w/w (11 mg, 0.1 mmol) was added to a solution of **153** (250 mg, 0.37 mmol) in MeOH previously degassed with nitrogen. After degassing again the mixture was stirred overnight under 1 atm of H₂. The mixture was filtered through a celite pad and the solvent was evaporated *in vacuo* to yield amine **146** (106 mg, 71%) as a colourless solid.

Mp: 129-134°C **IR** (neat) ν_{\max} = 3290 (m, br), 2918 (m), 1587 (s), 1538 (s), 1494 (s), 1455 (m), 1290 (s) **¹H-NMR** (300 MHz, DMSO-*d*₆) δ = 9.93 (2 H, s, PyrNH), 7.73 (2 H, t, *J* = 7 Hz, CONH), 3.28 (8 H (4 H, br s, NH₂) (4 H, q, *J* = 8 Hz, CONHCH₂CH₂)), 2.66 (4 H, t, *J* = 8 Hz), 2.12 (6 H, s, CH₃), 1.60 (6 H, s, CH₃), 1.36 (6 H, s, CH₃) **¹³C NMR** (75 MHz, DMSO-*d*₆) δ = 161-45 (C), 135.75 (C), 124.13 (C), 118.81 (C), 114.45 (C), 42.03 (CH₂), 41.66 (CH₂), 35.61 (C), 27.87 (CH₃), 10.42 (CH₃), 8.74 (CH₃)

Macrocycle 150

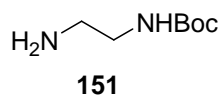


A solution of pyridinium di-chloride in DCM (5 mL) and a solution of tweezer **145** (42 mg, 0.1 mmol), TBACl (70 mg, 0.25 mmol) and dry Et₃N (0.1mL, 0.72 mmol) in dry DCM (5 mL) were added simultaneously, with a syringe pump into dry DCM (50 mL) at room temperature over a period of 2 hours. After stirring the resulting yellow solution overnight at room temperature the solvent was removed *in vacuo* and the residue purified with column chromatography (DCM/MeOH : 100/0 → 98.5/1.5) to afford **150** as a colourless solid (4 mg, 6.3%).

¹H-NMR (400 MHz, DMSO-*d*₆) δ = 9.42 (2 H, s, PyrNH), 9.14 (2 H, br s, CONH), 8.21-8.1 (3 H, m, ArH), 7.76 (2 H, br s, CONH), 3.55 (4 H, m, CONHCH₂CH₂), 3.41 (4 H, m,

CONHCH₂CH₂), 2.15 (6 H, s, CH₃), 2.02 (6 H, s, CH₃), 1.71 (6 H, s, CH₃) **LRMS** (ES⁺, acetonitrile) 532 (M+H)⁺, 568 (M+Na)⁺

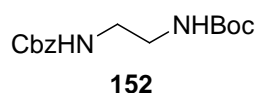
(2-Amino-ethyl)-carbamic acid tert-butyl ester (151)



A solution of Boc₂O (9.15 g, 41 mmol) in DCM (750 mL) was added dropwise to a solution of ethylenediamine **145** (16.8 mL, 0.25 mol) in DCM (50 mL) over a period of 36 hours. After stirring for 24 hours at room temperature the reaction mixture was washed with NaHCO₃ (sat aq, 2 x 500 mL), and water (2 x 500 mL). The organic layer was dried over MgSO₄ and the solvent evaporated *in vacuo* to afford **151** as a pale yellow oil (5.73 g, 85 %) which was used without further purification.

IR (neat) ν_{\max} = 3350 (w, br), 2977(w, br), 1687 (s), 1514 (m), 1455 (w), 1365 (s), 1250 (s), 1165 (s), 1041(w), 956 (w), 868 (w), 733 (s) **¹H-NMR** (300 MHz, CDCl₃) δ = 5.12 (1 H, br s, NHBoc), 3.20 (2H, apparent q, CH₂NHBoc), 2.83 (2 H, t, *J* = 6 Hz, CH₂NH₂), 2.62 (2 H, br s, CH₂NH₂), 1.42 (9 H, s, OC(CH₃)₃)(literature¹⁶⁴) **¹³C NMR** (75 MHz, CDCl₃) δ = 156.42 (C), 53.53 (C), 42.82 (CH₂), 41.70 (CH₂), 28.53 (CH₃) (lit¹⁶⁵)

(2-tert-Butoxycarbonylamino-ethyl)-carbamic acid benzyl ester (152)

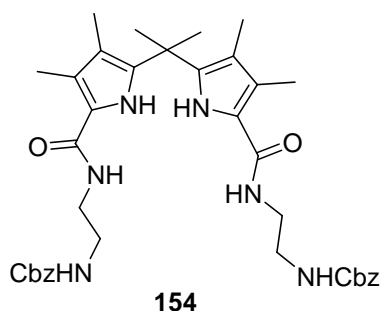


CbzCl (4.9mL, 34 mmol) was added to mixture of amine **151** (4.62 g, 28 mmol) in DCM (80 mL) and NaHCO₃ (sat) (90 mL). After stirring the resulting mixture vigorously for 48 hours, the phases were separated and the aqueous layer was extracted with DCM (2 x 150 mL), the combined organic layers were washed with water (2 x 100 mL), dried over MgSO₄, filtered and the solvent evaporated *in vacuo*. Purification of the residue by column chromatography (PE/EA: 70/30) afforded amine **152** as a colourless solid (4.5 g, 53%).

Rf: 0.48 (EA/PE : 50/50) **Mp**: 117-124 °C **IR** (neat) ν_{\max} = 2360 (s), 1684 (m), 1541 (m), 1265 (w), 1151 (w), 1132 (w), 699 (m) **¹H-NMR** (300 MHz, CDCl₃) δ = 7.36-7.30 (5 H, m, PhH), 5.16 (1 H, s br, NHBoc), 5.10 (2 H, s, CH₂Ph), 4.83 (1 H, s br, NHCbz), 3.28

(4H, apparent q, CbzHNCH₂CH₂NHBoc), 1.43 (9 H, s, OC(CH₃)₃) (literature¹⁶⁶) ¹³C NMR (75 MHz, CDCl₃) δ = 156.42 (C), 53.53 (C), 42.82 (CH₂), 41.70 (CH₂), 28.53 (CH₃)

2-[(5-{1-[5-(2-Benzyloxycarbonylamino-ethylcarbamoyl)-3,4-dimethyl-1H-pyrrol-2-yl]-1-methyl-ethyl}-3,4-dimethyl-1H-pyrrole-2-carbonyl)-amino]-ethyl}-carbamic acid benzyl ester (154)



Amine **152** (1.77 g, 6 mmol) was added to a solution of TFA (8 mL) and DCM (30 mL). After stirring at room temperature for 5 hours the excess TFA was removed *in vacuo* with toluene and the resulting TFA salt **153** was used without further purification.

(1-Chloro-2-methyl-propenyl)-dimethyl-amine **117** (750 μL, 5.6 mmol) was added to a solution of di-acid **82** (858 mg, 2.7 mmol) in THF (15 mL). After stirring the resulting solution at room temperature for 30 minutes, the solvent was evaporated *in vacuo* to yield chloride **118** which was used without further purification.

A solution of di-chloride **118** in DCM was added to a solution of **153** and Et₃N (3 mL, 42 mmol) in DCM (25 mL). After stirring overnight at room temperature the solvent was evaporated *in vacuo* and the residue purified by column chromatography (EA:PE 70:30) afforded tweezer **153** as a pale yellow solid (864 mg, 47%).

IR (neat) ν_{\max} = 3323 (m), 2938 (w), 1728 (m), 1685 (m), 1674 (m), 1579 (m), 1518 (s), 1241 (s), 952 (w) **¹H-NMR** (400 MHz, CDCl₃) δ = 8.83 (2 H, s, PyrNH), 7.33-7.29 (1 H, m, Ph), 6.11 (2 H, br s, CONH), 5.35 (2 H, br s, CONH), 5.10 (4 H, s, CH₂Ph), 3.55 (4 H, dd, *J* = 11, 5.5 Hz, CONHCH₂CH₂), 3.42 (4 H, dd, *J* = 11, 5.5 Hz, CONHCH₂CH₂), 2.14 (6 H, s, CH₃), 1.62 (6 H, s, CH₃), 1.62 (6 H, s, CH₃) **¹³C NMR** (100 MHz, CDCl₃) δ = 162.94 (C), 157.24 (C), 136.61 (C), 136.10 (C), 128.66 (CH), 128.27 (CH), 128.18 (CH),

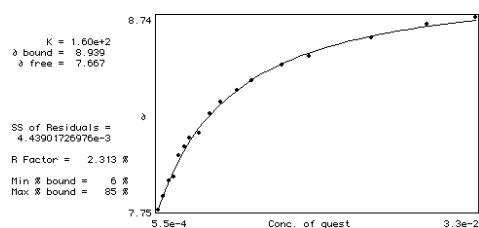
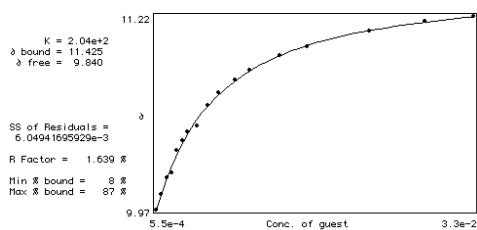
121.28 (C), 119.28 (C), 116.37 (C), 66.99 (CH₂), 41.57 (CH₂), 40.30 (CH₂), 35.82 (C), 27.09 (CH₃), 10.98 (CH₃), 9.37 (CH₃) **LRMS** (ES⁺, acetonitrile) 693 (M+Na)⁺ **HRMS** calculated for C₃₇H₄₆Na₁N₆O₆ 693.3371, measured 693.3356.

4.7 NMR titrations

Tweezer 101

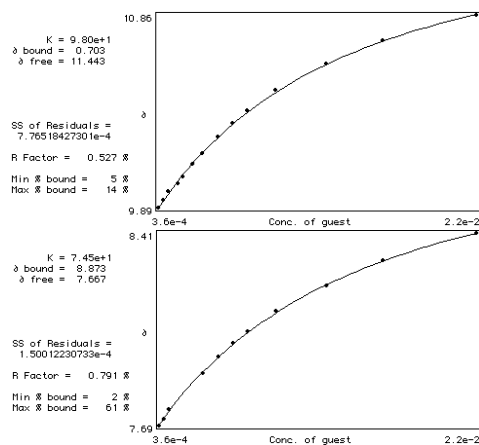
101 + TBAOAc in DMSO-*d*₆-0.5% water

Host Conc (M)	1.71E-03	Initial volume (μL)	600
Guest conc (M)	1.11E-01		
Volume of guest (μL)	δ NH pyrrole (ppm)	δ CONH (ppm)	
0	8.8562	7.6631	
3	9.9704	7.7485	
6	10.0709	7.8188	
9	10.1738	7.8966	
12	10.2064	7.9180	
15	10.3533	8.0272	
18	10.4148	8.0736	
21	10.4713	8.1163	
27	10.509	8.1439	
33	10.6408	8.2431	
40	10.7249	8.3046	
50	10.8027	8.3661	
60	10.8655	8.4163	
80	10.9609	8.4929	
100	11.0161	8.5394	
150	11.1153	8.6348	
200	11.1781	8.7038	
250	11.2157	8.7440	



101 + TBA OBz in DMSO-*d*₆-0.5% water

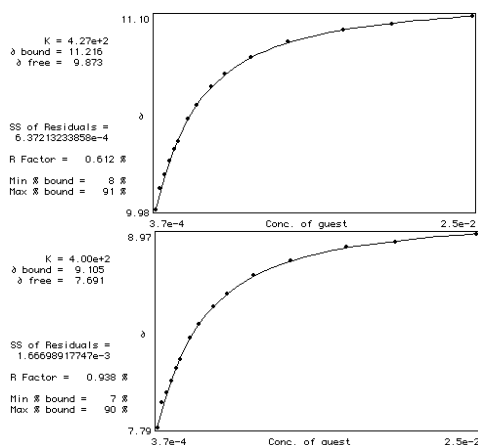
Host Conc (M)	1.78E-03	Initial volume (μL)	600
Guest Conc (M)	7.23E-02		
Volume of guest (μL)	δ NH pyrrole (ppm)	δ CONH (ppm)	
0	9.8512	7.6619	
3	9.8939	7.6945	
6	9.9315	7.7196	
9	9.9725	7.7523	
15	10.0131	-	
18	10.0483	-	
24	10.1098	-	
30	10.165	7.8866	
40	10.2516	7.9481	
50	10.3169	7.9996	
60	10.3809	8.041	
80	10.4826	8.1188	
120	10.6144	8.213	
170	10.7324	8.3034	
270	10.8642	8.4076	



101 + TBA dihydrogen phosphate in DMSO-*d*₆-0.5% water

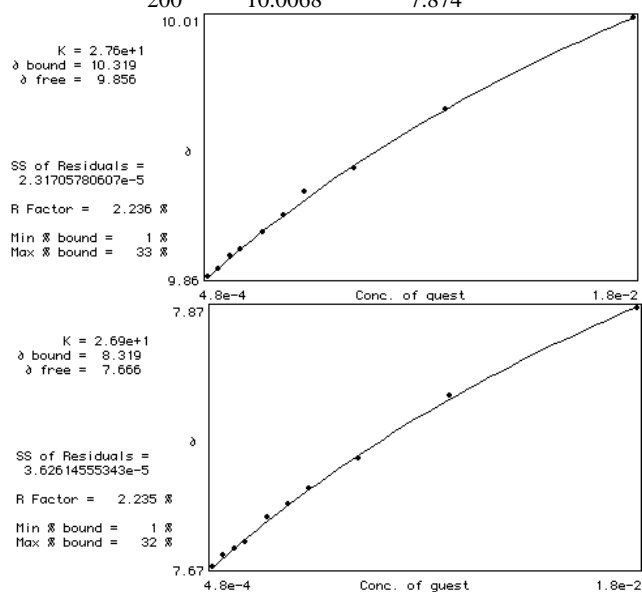
Host Conc (M)	1.78E-03	Initial volume (μL)	600
Guest conc (M)	7.40E-02		

Volume of guest (μL)	δ NH pyrrole (ppm)	δ CONH (ppm)
0	9.5812	7.6619
3	9.9817	7.7924
6	10.1010	7.9423
9	10.1788	8.0008
12	10.2579	8.0724
15	10.3295	8.1502
18	10.3721	8.2067
24	10.5002	8.3322
30	10.5830	8.4176
40	10.6872	8.5268
50	10.7600	8.6034
70	10.8554	8.7126
100	10.9446	8.8042
150	11.0136	8.8858
200	11.0500	8.9172
300	11.0952	8.9662

**101 + TBACl in DMSO-*d*₆-0.5% water**

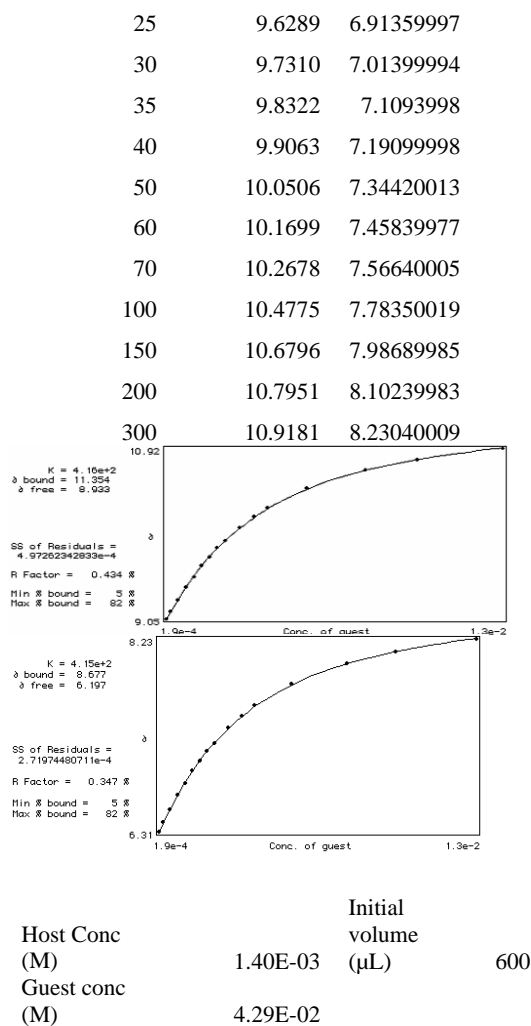
		Initial volume (μL)	600
Host Conc (M)	1.78E-03		
Hos Conc (M)	7.28E-02		

Volume of guest (μL)	δ NH pyrrole (ppm)	δ CONH (ppm)
4	9.8625	7.6744
8	9.8662	7.6832
12	9.8738	7.6883
16	9.8775	7.6933
24	9.8867	7.7121
32	9.8964	7.7221
40	9.9093	7.7347
60	9.9227	7.7573
100	9.9554	7.8063
200	10.0068	7.874

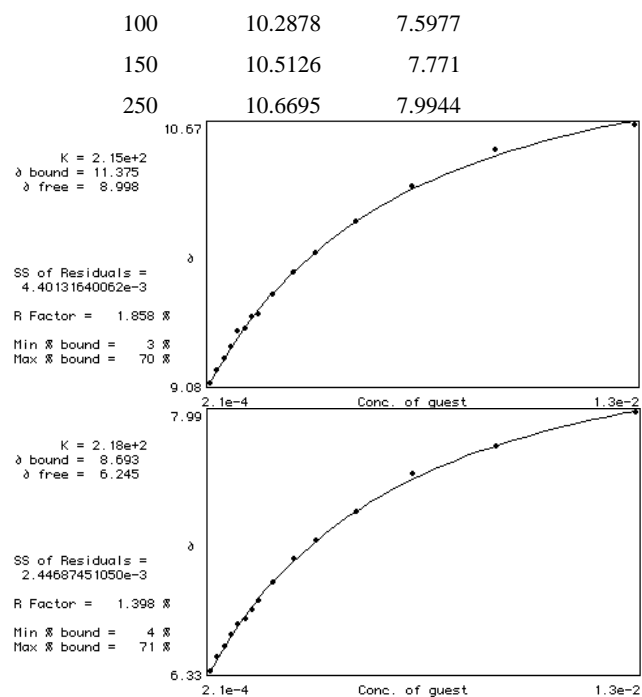
**101 + TBAOAc in CD₃CN -1% water**

		Starting volume (μL)	600
Host Conc (M)	1.82E-03		
Guest conc (M)	3.77E-02		

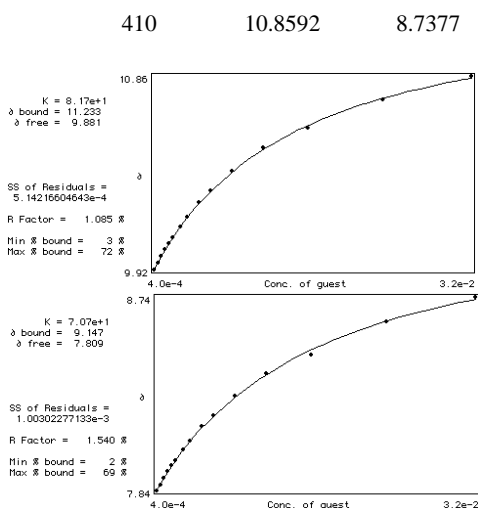
Volume of guest (μL)	δ NH pyrrole (ppm)	δ CONH (ppm)
3	9.0538	6.31230021
6	9.1317	6.4064002
10	9.2535	6.52570009
15	9.3929	6.67129993
20	9.5146	6.79559994



Volume of guest (μL)	δ NH pyrrole (ppm)	δ CONH (ppm)
0	9.0213	6.2533
3	9.0778	6.3324
6	9.1543	6.4165
9	9.2259	6.488
12	9.3025	6.5646
15	9.3916	6.6337
18	9.4104	6.6675
21	9.482	6.7203
24	9.497	6.7818
30	9.6201	6.9023
40	9.7607	7.0492
50	9.8774	7.1709
70	10.067	7.3555



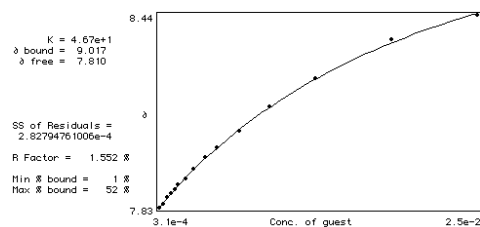
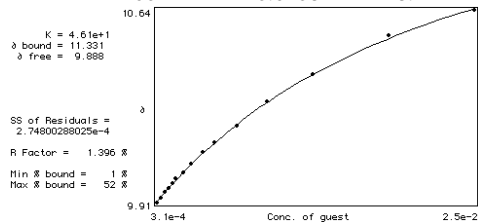
Volume of guest (μL)	δ NH pyrrole (ppm)	δ CONH (ppm)
0	9.8775	7.8012
3	9.9177	7.8389
6	9.9478	7.8627
9	9.9817	7.8966
12	10.0156	7.9293
15	10.0432	7.9531
18	10.0709	7.9782
24	10.1248	8.0284
30	10.1725	8.0699
40	10.2416	8.1364
50	10.3018	8.1879
70	10.3935	8.277
100	10.509	8.3824
150	10.6044	8.4678
250	10.7437	8.6235



102 + TBA OBz in DMSO- d_6 -0.5% water

Host Conc (M)	2.30E-03	Initial volume (μL)	600
Guest conc (M)	6.30E-02		

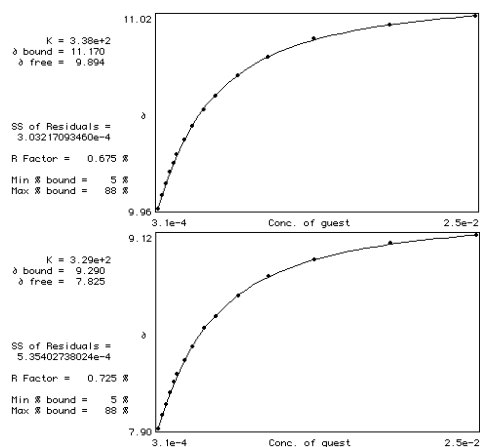
Volume of guest (μL)	δ NH pyrrole (ppm)	δ CONH (ppm)
0	9.8775	7.8012
3	9.9052	7.8263
6	9.9202	7.8364
9	9.9441	7.859
12	9.9604	7.8715
15	9.9767	7.8841
18	9.9955	7.9004
24	10.0181	7.9192
30	10.0533	7.9494
40	10.0972	7.987
50	10.1324	8.0171
70	10.1976	8.0699
100	10.2893	8.1464
150	10.3922	8.2381
250	10.5429	8.3636
400	10.6408	8.4414



102 + TBA dihydrogen phosphate in DMSO- d_6 -0.5% water

Host Conc (M)	2.30E-03	Initial volume (μL)	600
Guest conc (M)	6.20E-02		

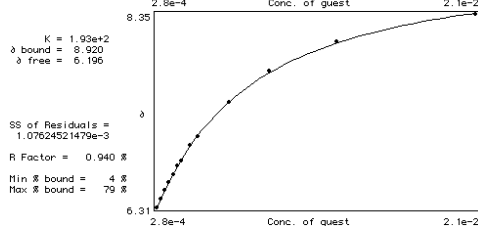
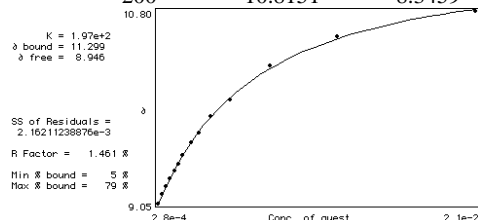
Volume of guest (μL)	δ NH pyrrole (ppm)	δ CONH (ppm)
0	9.8775	7.8012
3	9.9579	7.8979
6	10.0307	7.9782
9	10.0972	8.051
12	10.1575	8.1238
15	10.2102	8.1891
18	10.2579	8.2406
24	10.3395	8.326
30	10.4148	8.4113
40	10.5065	8.5281
50	10.5818	8.6046
70	10.6937	8.7314
100	10.7964	8.857
150	10.8994	8.9637
250	10.9734	9.0628
400	11.0236	9.1181



102 + TBAOAc in CD₃CN -1% water

Host Conc (M)	1.79E-03	Initial volume (μ L)	600
Guest conc (M)	8.46E-02		

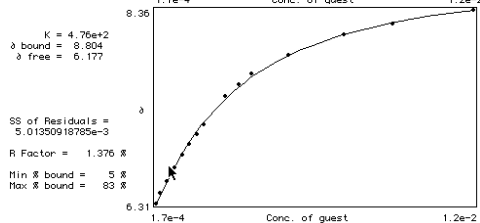
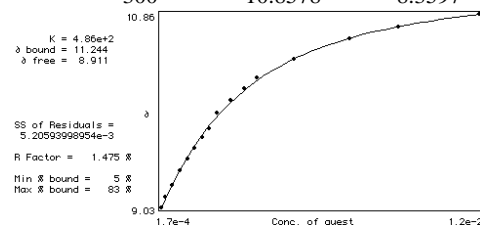
Volume of guest (μ L)	δ NH pyrrole (ppm)	δ CONH (ppm)
0	8.9937	6.2545
2	9.0527	6.3135
4	9.133	6.4027
6	9.2083	6.4981
8	9.2736	6.5747
10	9.3489	6.6588
12	9.4129	6.7454
14	9.4933	6.8044
18	9.6037	6.9651
22	9.6904	7.055
28	9.8448	-
38	9.9967	7.4145
60	10.3017	7.7408
100	10.5678	8.0509
200	10.8151	8.3459



Host Conc (M)	1.75E-03	Initial volume (μ L)	600
Guest conc (M)	3.52E-02		

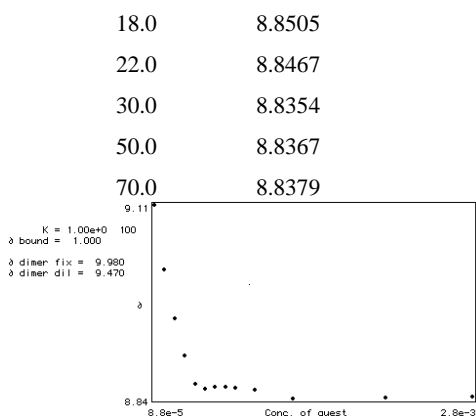
Volume of guest (μ L)	δ NH pyrrole (ppm)	δ CONH (ppm)
3	9.0276	6.3073
6	9.1267	6.4152

10	9.2359	6.5433
15	9.3728	6.6901
20	9.4832	6.8182
25	9.5899	6.9374
30	9.6853	7.0416
35	9.7682	7.1395
40	9.9201	-
50	10.0419	7.4471
60	10.1473	7.5638
70	10.2514	7.6830
100	10.4323	7.8827
150	10.6231	8.0911
200	10.7285	8.2141
300	10.8578	8.3597

**Tweezer 103****103 + NBoc-L-PheOTBA in CDCl₃**

Conc of Host (M)	1.58E-03	Initial volume (μ L)	600
Conc of Guest (M)	5.32E-02		

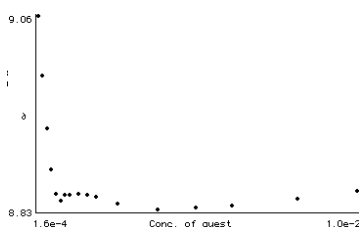
Volume of guest (μ L)	δ NH pyrrole (ppm)
2.0	9.1019
4.0	9.0175
6.0	8.9484
8.0	8.8957
10.0	8.8555
12.0	8.8492
14.0	8.8517
16.0	8.8517

**103+NBoc-D-PheOTBA in CDCl₃**

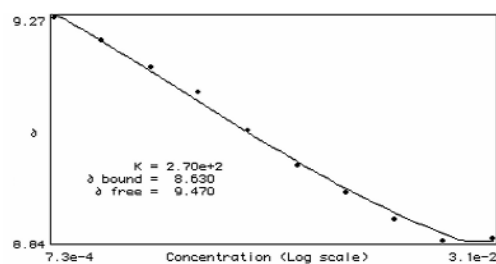
Conc of Host (M)	1.21E-03	Initial volume (μL)	600
Conc of Guest (M)	4.55E-02		

Volume of guest (μL) δ NH pyrrole (ppm)

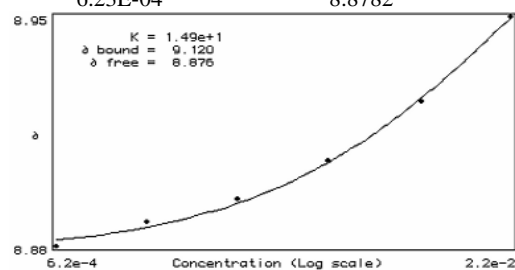
2.0	9.0614
4.0	8.9110
6.0	8.9283
8.0	8.8517
10.0	8.8442
12.0	8.8505
14.0	8.8505
16.0	8.8517
20.0	8.8505
24.0	8.8480
38.0	8.8405
58.0	8.8342
78.0	8.8354
98.0	8.8379
138.0	8.8467
178.0	8.8555

**103 dilution study in CDCl₃**

concentration	δ NH pyrrole (ppm)
3.08E-02	8.8392
2.03E-02	8.8354
1.34E-02	8.8756
8.84E-03	8.9271
5.84E-03	8.9810
3.85E-03	9.0476
2.50E-03	9.1229
1.68E-03	9.1693
1.10E-03	9.2221
7.30E-04	9.2673

**103 dilution study in CD₃CN**

concentration	δ NH pyrrole (ppm)
2.20E-02	8.5522
1.10E-02	8.9246
5.30E-03	8.9058
2.60E-03	8.8932
1.27E-03	8.8857
6.23E-04	8.8782

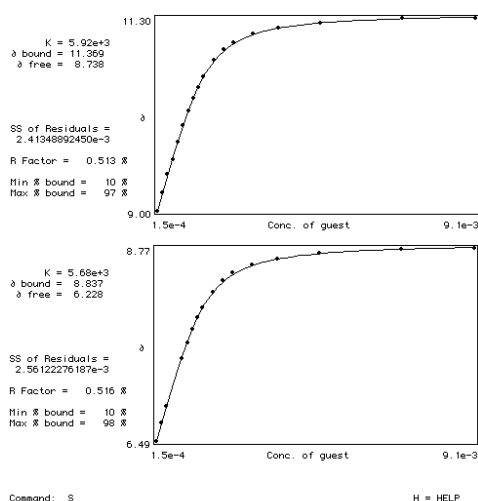
**103+ NBoc-L-PheOTBA in CD₃CN**

Conc of Host (M)	1.50E-03	Initial volume (μL)	600
Conc of Guest (M)	4.57E-02		

Volume of guest (μL) δ NH pyrrole (ppm)

2.0	9.1074
4.0	9.3246
6.0	9.5393
8.0	9.7188
10.0	9.9334

12.0	10.1305
14.0	10.3050
16.0	10.4544
18.0	10.5812
20.0	10.7142
24.0	10.9025
28.0	11.0306
32.0	11.1222
40.0	11.2189
51.0	11.2904
70.0	11.3545
110.00	11.4034
150.00	11.4135



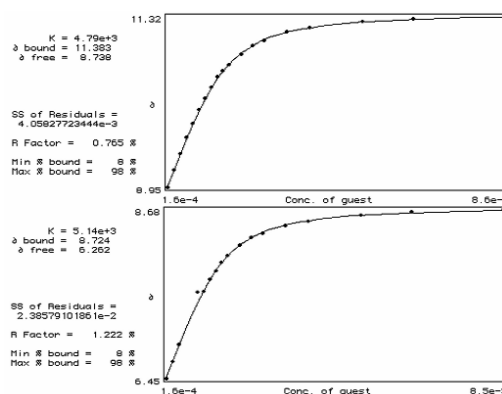
Command: S

H = HELP

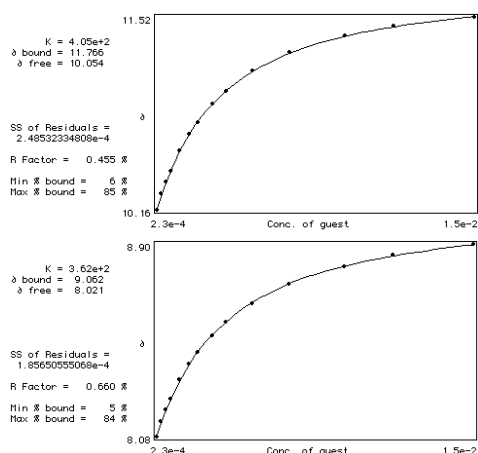
103+ NBoc-D-PheOTBA in CD₃CN

Conc of Host (M)	Conc of Guest (M)	Volume of guest (μL)	Initial volume (μL)	600
1.59E-03	4.80E-02			
Volume of guest (μL)	δ NH pyrrole (ppm)			
2	8.9497	6.4473		
4	9.1807	6.6675		
6	9.4079	6.8872		
8	9.6367	-		
10	9.8285	-		
12	10.0155	7.5839		
14	10.1737	7.5864		
16	10.3281	7.7440		
18	10.4687	7.8626		
20	10.5578	7.9712		

22	10.6444	8.0584
26	10.7900	8.1940
30	10.9030	8.2957
34	10.9808	8.3553
42	11.0938	8.4576
50	11.1528	8.5167
70	11.2369	8.5963
90	11.2784	8.6340
130	11.3173	8.6761

**Tweezer 104****104 + TBAOAc in DMSO-*d*₆-0.5% water**

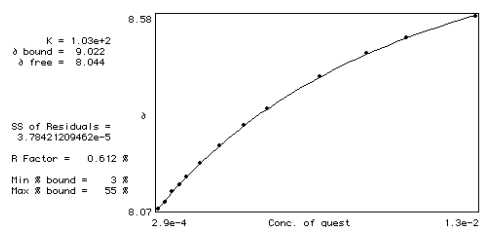
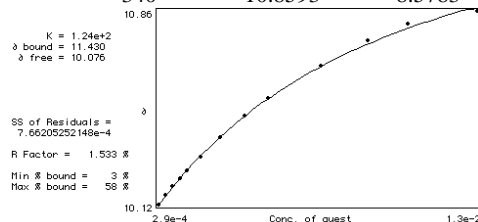
Host Conc (M)	Guest conc (M)	Volume of guest (μL)	Initial volume (μL)	600
9.10E-04	4.60E-02			
δ NH pyrrole (ppm)	δ CONH (ppm)			
3	10.1575	8.0768		
6	10.2697	8.1396		
9	10.3546	8.1903		
12	10.4274	8.2355		
18	10.5755	8.3190		
24	10.6910	8.3856		
30	10.7751	8.4370		
40	10.8994	8.5092		
50	10.9948	8.5645		
70	11.1329	8.6461		
100	11.2634	8.7296		
150	11.3827	8.8029		
200	11.4492	8.8513		
300	11.5170	8.9003		



104 + TBAOBz in DMSO-*d*₆-0.5% water

Host Conc (M)	1.53E-03	Initial volume (μL)	600
Guest conc (M)	3.48E-02		

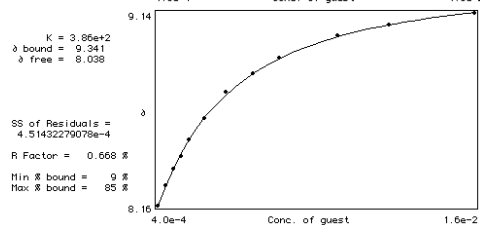
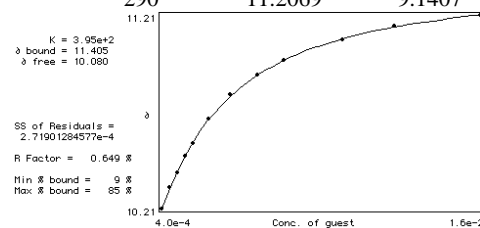
Volume of guest (μL)	δ NH pyrrole (ppm)	δ CONH (ppm)
5	10.1198	8.0711
10	10.1562	8.0887
15	10.1889	8.1151
20	10.2491	8.1351
25	10.2190	8.1540
35	10.3018	8.1891
50	10.3746	8.2356
70	10.4575	8.2908
90	10.5240	8.3335
140	10.6496	8.4176
190	10.7462	8.4804
240	10.8090	8.5218
340	10.8593	8.5783



104 + TBAdihydrogen phosphate in DMSO-*d*₆-0.5% water

Host Conc (M)	1.53E-03	Initial volume (μL)	600
Guest conc (M)	4.80E-02		

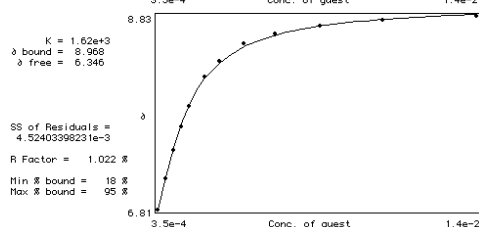
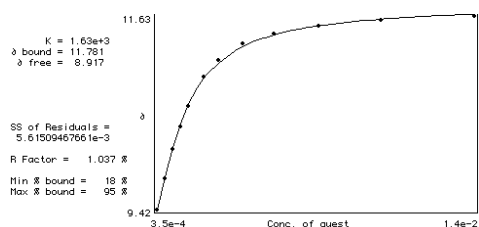
Volume of guest (μL)	δ NH pyrrole (ppm)	δ CONH (ppm)
5	10.2052	8.1615
10	10.3119	8.2632
15	10.3922	8.3460
20	10.4738	8.4088
25	10.5429	8.4929
35	10.6684	8.6046
50	10.7927	8.7352
70	10.8969	8.8331
90	10.9697	8.9122
140	11.0801	9.0227
190	11.1467	9.0766
290	11.2069	9.1407



104 + TBAOAc in CD₃CN -1% water

Host Conc (M)	1.38E-03	Initial volume (μL)	600
Guest conc (M)	7.00E-02		

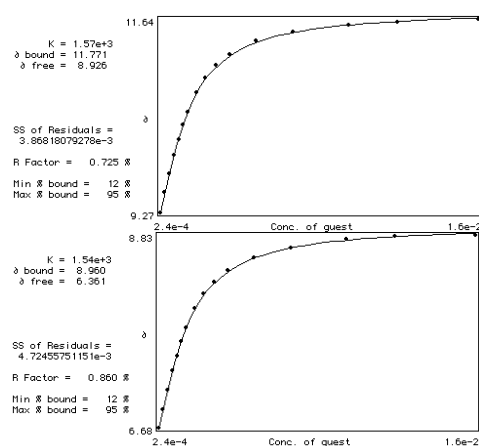
Volume of guest (μL)	δ NH pyrrole (ppm)	δ CONH (ppm)
3	9.4242	6.8088
6	9.7770	7.1333
9	10.1059	7.4308
12	10.3695	7.6743
15	10.5992	7.8850
21	10.9331	8.1915
27	11.1227	8.3585
37	11.3122	8.5379
50	11.4265	8.6416
70	11.5169	8.7219
100	11.5809	8.7834
150	11.6298	8.8311



Host Conc (M)	Guest conc (M)	Initial volume (μL)
1.51E-03	4.80E-02	600

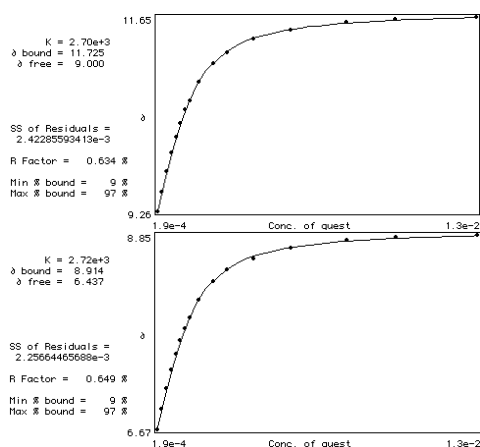
Volume of guest (μL)	δ NH pyrrole (ppm)	δ CONH (ppm)
0	9.0326	6.4341
3	9.2673	6.6801
6	9.5109	6.8822
9	9.7456	7.0944
12	9.9628	7.3128
15	10.1636	7.4772
18	10.3419	7.6354
21	10.4925	7.7973
27	10.7411	8.0107

33	10.9143	8.1739
40	11.0712	8.3070
50	11.2018	8.4288
70	11.3675	8.5781
100	11.4779	8.6836
150	11.5683	8.7765
200	11.5959	8.8116
300	11.6411	8.8292



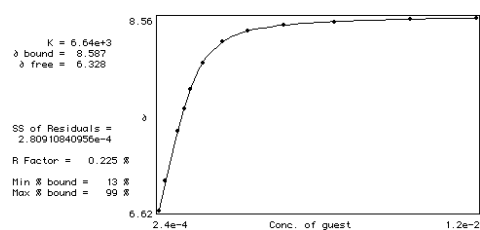
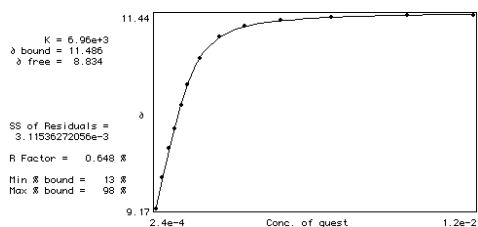
Conc of Host (M)	Starting volume (μL)
1.12E-03	600
Conc of Guest (M)	2.35E-02

Volume of guest (μL)	δ NH pyrrole (ppm)	δ CONH (ppm)
3	9.2585	6.6662
6	9.4920	6.8885
9	9.7469	7.1195
12	9.9791	7.3266
15	10.1737	7.5048
18	10.3431	7.6593
21	10.5051	7.7973
24	10.6093	7.9178
30	10.8428	8.1137
40	11.0762	8.3233
50	11.2106	8.4564
70	11.3800	8.5794
100	11.4855	8.7012
150	11.5784	8.7815
200	11.6110	8.8142
300	11.6462	8.8455

**104+ NBoc-L-PheOTBA in CD₃CN**

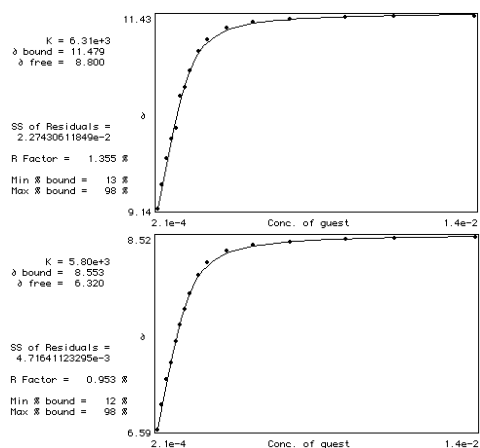
Conc of Host (M)	1.63E-03	Initial volume (μL)	600
Conc of Guest (M)	4.77E-02		

Volume of guest (μL)	δ NH pyrrole (ppm)	δ CONH (ppm)
3.0	9.1682	6.6249
6.0	9.5309	6.9186
9.0	9.8787	-
12.0	10.1071	7.4170
15.0	10.3820	7.6429
18.0	10.6243	7.8425
24.0	10.9256	8.1061
34.0	11.1880	8.3221
47.0	11.3148	8.4247
67.0	11.3800	8.4859
97.0	11.4102	8.5173
147.0	11.4340	8.5442
197.0	11.4415	8.5569

**104+ NBoc-D-PheOTBA in CD₃CN**

Conc of Host (M)	1.63E-03	Initial volume (μL)	600
Conc of Guest (M)	4.27E-02		

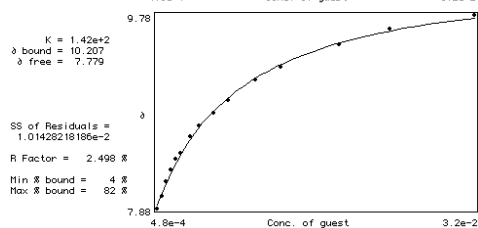
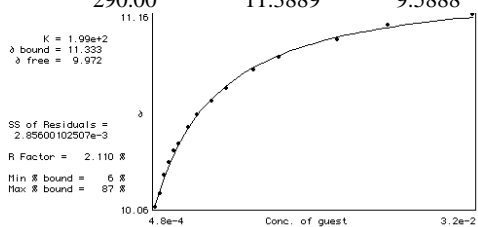
Volume of guest (μL)	δ NH pyrrole (ppm)	δ CONH (ppm)
3.0	9.1393	6.5885
6.0	9.4255	6.8383
9.0	9.7305	7.0868
12.0	9.9665	7.2613
15.0	10.0938	7.4747
18.0	10.4737	7.6354
21.0	10.5816	7.7886
24.0	10.7762	7.9530
30.0	11.0110	8.1338
36.0	11.1478	8.2593
50.0	11.2871	8.3766
70.0	11.3512	8.4338
100.0	11.3910	8.4671
150.0	11.4102	8.4909
200.0	11.424	8.5041
300.0	11.4302	8.5198

**Tweezer 105**

105 + TBAOAc in DMSO-*d*₆-0.5% water

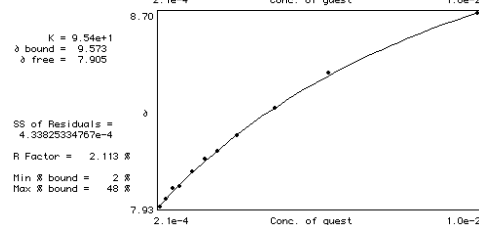
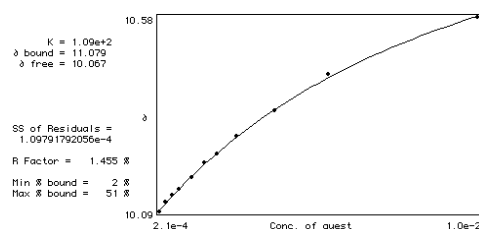
Conc of Host (M)	1.42E-03	Initial volume (μL)	600
Conc of Guest (M)	7.40E-02		

Volume of guest (μL)	δ NH pyrrole (ppm)	δ CONH (ppm)
3.00	10.0935	7.9293
6.00	10.1976	8.0636
9.00	10.3307	8.2268
12.00	10.4399	8.3900
15.00	10.5855	8.5758
18.00	10.6897	8.7113
24.00	10.8579	8.9034
30.00	10.9408	9.0252
40.00	11.0726	9.2298
50.00	11.1278	9.2612
70.00	11.2057	9.3629
90.00	11.2521	9.4219
140.00	11.3036	9.4746
190.00	11.3463	9.4922
290.00	11.3889	9.5888

**105 + TBAOBz in DMSO-*d*₆-0.5% water**

Conc of Host (M)	1.10E-03	Initial volume (μL)	600
Conc of Guest (M)	4.20E-02		

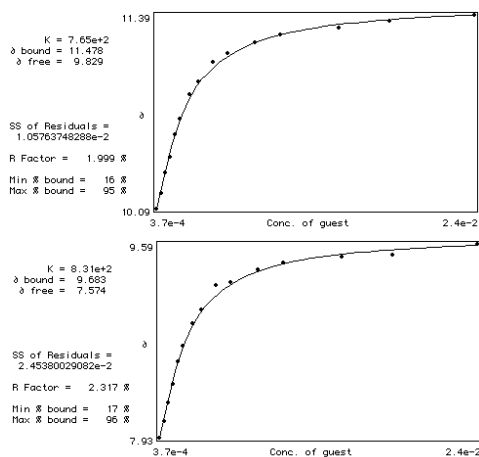
Volume of guest (μL)	δ NH pyrrole (ppm)	δ CONH (ppm)
3.00	10.0859	7.9280
6.00	10.1085	7.9600
9.00	10.1273	7.9996
12.00	10.1424	8.0080
18.00	10.1713	8.0674
24.00	10.2089	8.1180
30.00	10.2315	8.1540
40.00	10.2767	8.2054
60.00	10.3420	8.3197
90.00	10.4336	8.4590
190.00	10.5805	8.7000

**105 + TBAdihydrogen phosphate in DMSO-*d*₆-0.5% water**

Conc of Host (M)	1.42E-03	Initial volume (μL)	600
Conc of Guest (M)	7.40E-02		

Volume of guest (μL)	δ NH pyrrole (ppm)	δ CONH (ppm)
3.00	10.0935	7.9293
6.00	10.1976	8.0636
9.00	10.3307	8.2268
12.00	10.4399	8.3900
15.00	10.5855	8.5758
18.00	10.6897	8.7113
24.00	10.8579	8.9034
30.00	10.9408	9.0252
40.00	11.0726	9.2298

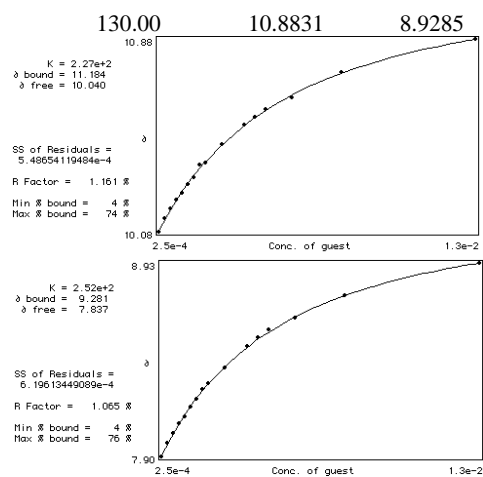
50.00	11.1278	9.2612
70.00	11.2057	9.3629
90.00	11.2521	9.4219
140.00	11.3036	9.4746
190.00	11.3463	9.4922
290.00	11.3889	9.5888



105 + TBAdihydrogen phosphate in DMSO-*d*₆-5% water

Conc of Host (M)	1.22E-03	Initial volume (μL)	600
Conc of Guest (M)	7.40E-02		

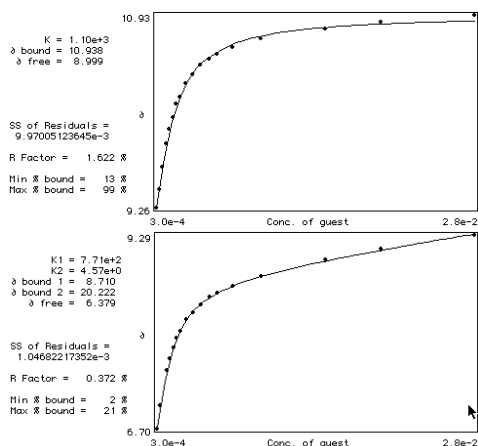
Volume of guest (μL)	δ NH pyrrole (ppm)	δ CONH (ppm)
2.00	10.0847	7.9016
4.00	10.1374	7.9732
6.00	10.1776	8.0234
8.00	10.2152	8.0730
10.00	10.2428	8.1100
12.00	10.2805	8.1615
14.00	10.3069	8.2029
16.00	10.3596	8.2569
18.00	10.3709	8.2875
24.00	10.4475	8.3718
32.00	10.5253	8.4835
36.00	10.5579	8.5318
40.00	10.5906	8.5720
50.00	10.6395	8.6373
70.00	10.7450	8.7528



105 + TBAOAc in CD₃CN -1% water

Conc of Host (M)	1.37E-03	Initial volume (μL)	600
Conc of Guest (M)	9.01E-02		

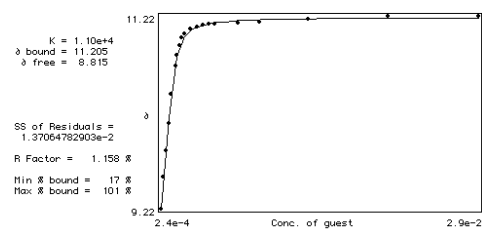
Volume of guest (μL)	δ NH pyrrole (ppm)	δ CONH (ppm)
2.00	9.2598	6.6989
4.00	9.4117	7.0015
6.00	9.6094	-
8.00	9.8084	7.4722
10.00	9.9364	7.6404
12.00	10.0381	7.7722
14.00	10.1536	7.9084
16.00	10.2163	7.9997
20.00	10.3369	8.1539
24.00	10.4109	8.2517
29.00	10.4888	8.3540
35.00	10.5446	8.4527
40.00	10.5892	8.5147
50.00	10.6482	8.6058
70.00	10.7172	8.7388
120.00	10.8038	8.9516
170.00	10.8616	9.0979
270.00	10.9265	9.2900



105 + TBA di hydrogen phosphate in CD_3CN -1% water

Conc of Host (M)	1.59E-03	Initial volume (μ L)	600
Conc of Guest (M)	5.57E-02		

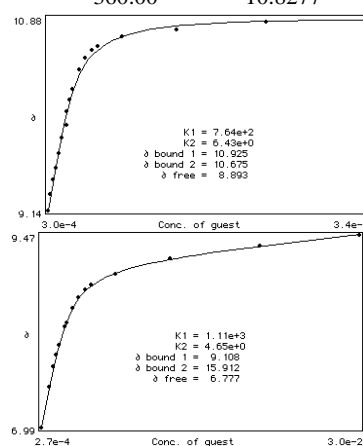
Volume of guest (μ L)	δ NH pyrrole (ppm)	δ CONH (ppm)
2.00	9.2171	6.63E+00
4.00	9.5460	-
6.00	9.8184	7.6850
8.00	10.1046	8.1036
10.00	10.4059	8.5141
13.00	10.6959	8.9347
14.00	10.8126	9.0991
16.00	10.9118	9.2391
18.00	10.9934	9.3520
20.00	11.0298	9.4017
25.00	11.0850	9.4625
30.00	11.1026	9.4769
35.00	11.1214	9.4813
40.00	11.1302	9.4807
45.00	11.1315	9.4801
65.00	11.1435	9.4663
85.00	11.1516	9.4593
135.00	11.1829	9.4410
235	11.2156	9.4607
385	11.2182	9.4819



105+ NAc-L-Phe-OTBA in CD_3CN

Conc of Host (M)	2.62E-03	Initial volume (μ L)	600
Conc of Guest (M)	8.06E-02		

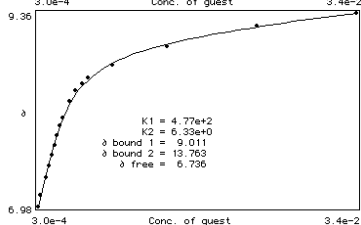
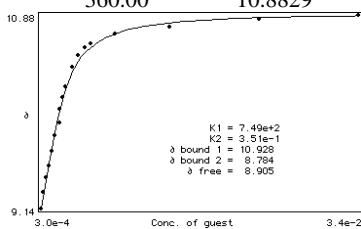
Volume of guest (μ L)	δ NH pyrrole (ppm)
2.00	9.1154
4.00	9.2410
6.00	9.3677
8.00	9.5309
11.00	9.7356
13.00	9.8435
15.00	9.9490
19.00	10.1348
21.00	10.1825
25.00	10.3180
30.00	10.4235
35.00	10.4975
40.00	10.5377
60.00	10.6218
110.00	10.7260
210.00	10.7725
360.00	10.8277



105+ NAc-D-Phe-OTBA in CD₃CN

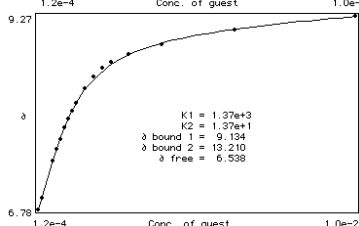
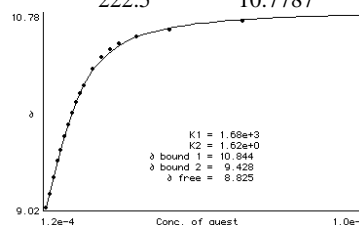
Conc of Host (M)	2.62E-03	Initial volume (μL)	600
Conc of Guest (M)	9.01E-02		

Volume of guest (μL)	δ NH pyrrole (ppm)	δ CONH (ppm)
2.00	9.1443	6.9838
4.00	9.2899	7.1182
6.00	9.4205	-
8.00	9.5272	7.3398
10.00	9.6602	7.4785
12.00	9.8021	7.6140
14.00	9.9126	7.7289
16.00	10.0381	7.8563
18.00	10.1435	7.9687
20.00	10.2352	8.0653
25.00	10.4147	8.2694
30.00	10.5226	8.4061
35.00	10.5854	8.4928
40.00	10.6268	8.5562
60.00	10.7074	8.7193
110.00	10.7775	8.9503
210.00	10.8415	9.1939
360.00	10.8829	9.3590

**105+ NBoc-L-Phe-OTBA in CD₃CN**

Conc of Host (M)	1.20E-03	Initial volume (μL)	600
Conc of Guest (M)	3.70E-02		

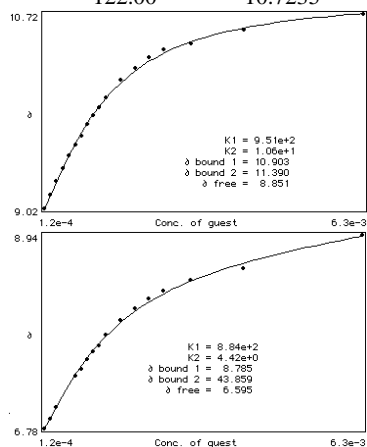
Volume of guest (μL)	δ NH pyrrole (ppm)	δ CONH (ppm)
2.00	9.0163	6.7793
4.00	9.1405	6.9293
6.00	9.2887	-
8.00	9.4355	-
10.00	9.5397	7.4069
12.00	9.6653	7.5557
14.00	9.7657	7.6825
16.00	9.8724	7.8256
18.00	9.9716	7.9436
20.00	10.0494	8.0459
22.00	10.1285	8.1375
27.00	10.2766	8.3359
32.00	10.3808	8.4834
37.00	10.4574	8.5894
42.00	10.5051	8.6672
52.00	10.5691	8.7658
72.50	10.6344	8.9014
122.5	10.7135	9.0815
222.5	10.7787	9.2671

**105+ NBoc-D-Phe-OTBA in CD₃CN**

Conc of Host (M)	1.20E-03	Initial volume (μL)	600
Conc of Guest (M)	3.70E-02		

Volume of guest (μL)	δ NH pyrrole (ppm)	δ CONH (ppm)
2.00	9.0200	6.7780
4.00	9.1393	6.8872
6.00	9.2548	7.0121

8.00	9.3677	-
10.00	9.4795	-
12.00	9.5786	7.3621
14.00	9.6502	7.4358
16.00	9.7531	7.5475
18.00	9.8310	7.6342
20.00	9.9000	7.7063
22.00	9.9916	7.8174
27.00	10.1410	7.9837
32.00	10.2502	8.1162
37.00	10.3406	8.2248
42.00	10.4084	8.3102
52.00	10.4650	8.4332
72.00	10.5854	8.5694
122.00	10.7235	8.9422

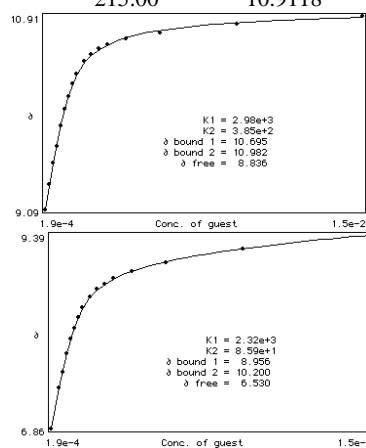


105+ NAc-L-Ala-OTBA in CD₃CN

Conc of Host (M)	1.28E-03	Initial volume (μL)	600
Conc of Guest (M)	5.80E-02		

Volume of guest (μL)	δ NH pyrrole (ppm)	δ CONH (ppm)
2.00	9.0916	6.8634
4.00	9.3238	-
6.00	9.5272	7.3931
8.00	9.6891	7.5927
10.00	9.8750	7.8387
12.00	10.0356	8.0258
14.00	10.1548	8.1702
16.00	10.2691	8.3164

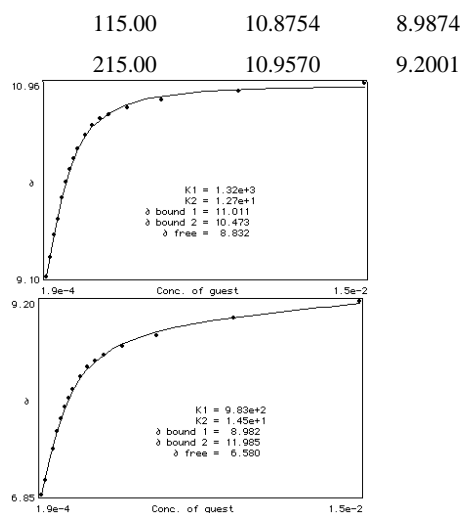
18.00	10.3620	8.4351
22.00	10.4800	8.5876
26.00	10.5490	8.6830
30.00	10.6005	8.7526
35.00	10.6406	8.8204
45.00	10.6971	8.9089
65.00	10.7549	9.0251
115.00	10.8365	9.2065
215.00	10.9118	9.3923



105+ NAc-D-Ala-OTBA in CD₃CN

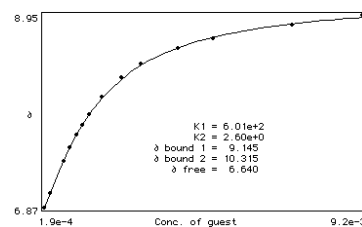
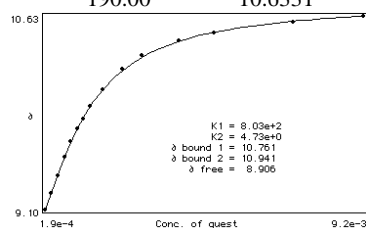
Conc of Host (M)	1.28E-03	Initial volume (μL)	600
Conc of Guest (M)	5.70E-02		

Volume of guest (μL)	δ NH pyrrole (ppm)	δ CONH (ppm)
2.00	9.0979	6.8484
4.00	9.2784	7.0241
6.00	9.4945	-
8.00	9.6489	7.4026
10.00	9.8536	7.6185
12.00	10.0055	7.7725
14.00	10.1297	7.9141
16.00	10.2327	8.0214
18.00	10.3256	8.1250
22.00	10.4549	8.2775
26.00	10.5452	8.3942
30.00	10.6105	8.4708
35.00	10.6557	8.5379
45.00	10.7210	8.6421
65.00	10.7888	8.7778

**105+ NBoc-L-Gln-OTBA in CD₃CN**

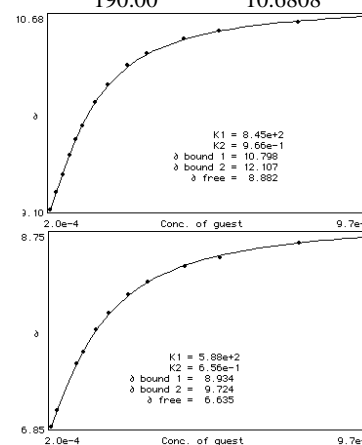
Conc of Host (M)	1.37E-03	Initial volume (μL)	600
Conc of Guest (M)	3.84E-02		

Volume of guest (μL)	δ NH pyrrole (ppm)	δ CONH (ppm)
3.00	9.1004	6.8722
6.00	9.2309	7.0228
9.00	9.3652	-
12.00	9.5109	7.3762
15.00	9.6351	7.5187
18.00	9.7368	7.6567
21.00	9.8146	7.7584
24.00	9.9138	7.8758
30.00	10.0481	8.0597
40.00	10.2113	8.2757
50.00	10.3180	8.4130
70.00	10.4360	8.5847
90.00	10.5001	8.6887
140.00	10.5854	8.8380
190.00	10.6331	8.9472

**105+ NBoc-D-Gln-OTBA in CD₃CN**

Conc of Host (M)	1.37E-03	Initial volume (μL)	600
Conc of Guest (M)	3.84E-02		

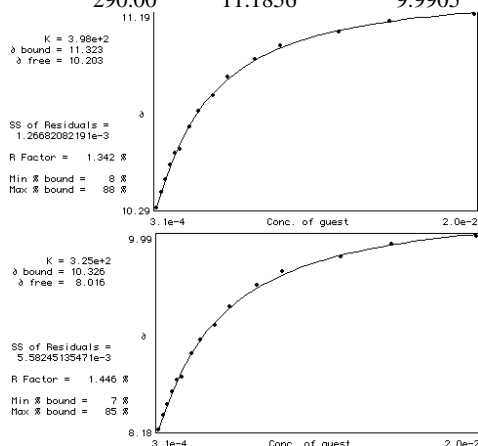
Volume of guest (μL)	δ NH pyrrole (ppm)	δ CONH (ppm)
3.00	9.0979	6.8452
6.00	9.2397	7.0046
9.00	9.3857	-
12.00	9.5397	-
15.00	9.6678	7.4672
18.00	9.7782	7.5807
24.00	9.9703	7.8030
30.00	10.1147	7.9668
40.00	10.2779	8.1513
50.00	10.3720	8.2744
70.00	10.4900	8.4275
90.00	10.5540	8.5185
140.00	10.6306	8.6585
190.00	10.6808	8.7541

**Tweezer 106****106 + TBAOAc in DMSO-*d*₆-0.5% water**

Conc of Host (M)	1.59E-03	Initial volume (μL)	600
Conc of Guest	6.29E-02		

(M)

Volume of guest (μL)	δ NH pyrrole (ppm)	δ CONH (ppm)	δ CH (ppm)
3.00	10.2893	8.1766	4.5286
6.00	10.3608	8.3071	4.5186
9.00	10.4186	8.4126	4.4922
12.00	10.4876	8.5318	4.4734
15.00	10.5416	8.6417	4.4545
18.00	10.5567	8.6699	4.4508
24.00	10.6621	8.8821	4.4269
30.00	10.7362	9.0139	4.3930
40.00	10.8090	9.1532	4.3792
50.00	10.8931	9.3258	4.3453
70.00	10.9772	9.5273	4.3152
90.00	11.0375	9.6516	4.2939
140.00	11.1027	9.7947	4.2713
190.00	11.1529	9.9102	4.2512
290.00	11.1856	9.9905	4.2448

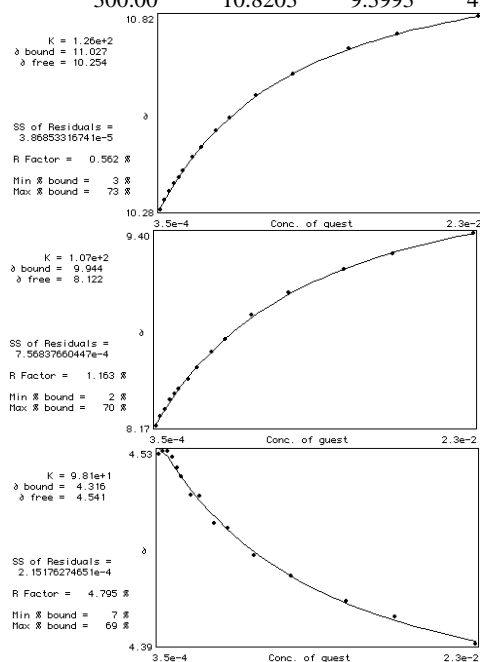


106 + TBAOBz in DMSO-*d*₆-0.5% water

Conc of Host (M1)	Conc of Guest (M1)	Initial volume (μL)	
2.32E-03	7.01E-02	600	

Volume of guest (μL)	δ NH pyrrole (ppm)	δ CONH (ppm)	δ CH (ppm)
3.00	10.2767	8.1676	4.5261
6.00	10.3031	8.2268	4.5286
9.00	10.3282	8.2695	4.5286
12.00	10.3495	8.3297	4.5236

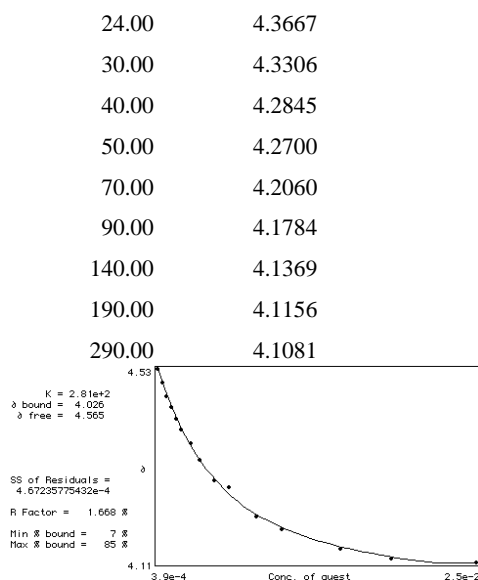
15.00	10.3671	8.3699	4.5160
18.00	10.3847	8.4038	4.5098
24.00	10.4236	8.4640	4.4960
30.00	10.4512	8.5406	4.4947
40.00	10.4977	8.6360	4.4746
50.00	10.5328	8.7151	4.4709
70.00	10.5968	8.8708	4.4508
100.00	10.6583	9.0151	4.4357
150.00	10.7274	9.1670	4.4169
200.00	10.7688	9.2662	4.4056
300.00	10.8203	9.3993	4.3855



106 + TBAdihydrogen phosphate in DMSO-*d*₆-0.5% water

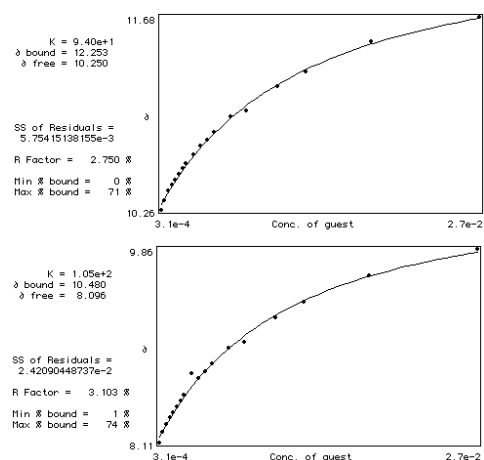
Conc of Host (M)	Conc of Guest (M)	Initial volume (μL)	
2.13E-03	7.75E-02	600	

Volume of guest (μL)	δ CH (ppm)
3.00	4.5286
6.00	4.4978
9.00	4.4678
12.00	4.4439
15.00	4.4194
18.00	4.3968



106 + TBAdihydrogen phosphate in DMSO- d_6 -5% water

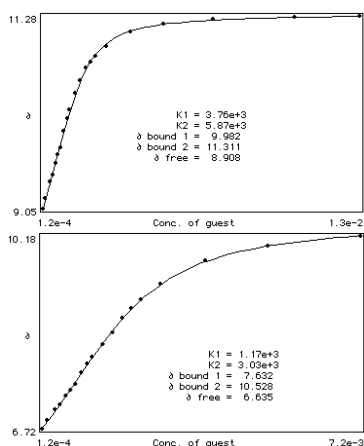
Conc of Host (M)	2.13E-03	Initial volume (μL)	600
Conc of Guest (M)	9.44E-02		
Volume of guest (μL)	δ NH pyrrole (ppm)	δ CONH (ppm)	
0	10.2227	8.0624	
2	10.2592	8.1126	
4	10.3295	8.2029	
6	10.4023	8.2745	
8	10.444	8.3385	
10	10.4801	8.3862	
12	10.5177	8.4327	
14	10.5642	8.4917	
16	10.6006	8.5413	
20	10.66085	8.6166	
24	10.7261	8.6963	
28	10.77195	8.7578	
32	10.8316	8.8268	
42	10.9408	8.9637	
52	10.9885	9.0164	
72	11.1668	9.2398	
92	11.2735	9.3842	
142	11.4931	9.6202	
242	11.6777	9.865	
231	10.5791	10.5791	
331	10.6143	10.6143	



106 + TBAOAc in CD₃CN

Conc of Host (M)	9.10E-04	Initial volume (μL)	600
Conc of Guest (M)	3.59E-02		

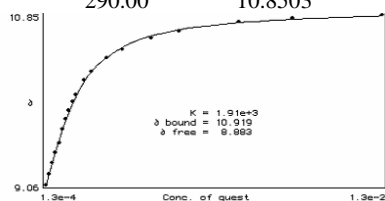
Volume of guest (μL)	δ NH pyrrole (ppm)	δ CONH (ppm)	δ CH (ppm)
2.00	9.0476	6.7159	4.6377
4.00	9.1669	6.8578	4.6239
7.00	9.3539	7.0586	4.6038
9.00	9.4318	7.1534	4.5950
11.00	9.5767	7.3053	4.5789
13.00	9.6690	7.4057	4.5699
15.00	9.7531	7.5124	4.5611
17.00	9.9396	7.7208	4.5398
19.50	10.0845	7.8824	4.5222
21.50	10.1925	8.0076	4.5122
25.50	10.3858	8.2392	4.4883
29.50	10.5239	8.4401	4.4695
33.50	10.6701	8.6962	4.4506
37.50	10.7448	8.8757	4.4368
41.50	10.8076	9.0345	4.4155
50.00	10.9281	9.3213	4.3904
70.00	11.0875	9.7293	4.3665
100.00	11.1855	9.9979	4.3427
150.00	11.2357	10.1835	4.3251
250.00	11.2671	10.2101	4.3163
350.00	11.2784	10.2276	4.3126

**106+ NBoc-L-Phe-OTBA in CD₃CN**

Conc of Host (M)	1.25E-03	Initial volume (μL)	600
Conc of Guest (M)	4.00E-02		

Volume of guest (μL) δ NH pyrrole (ppm)

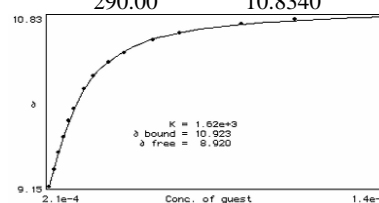
2.00	9.0627
4.00	9.1719
6.00	9.2887
8.00	9.4029
10.00	9.5033
12.00	9.6414
14.00	9.7506
16.00	9.8423
18.00	9.9352
20.00	10.0080
25.00	10.1573
30.00	10.2540
40.00	10.3921
50.00	10.4812
70.00	10.6030
91.00	10.6783
140.00	10.7699
190.00	10.8126
290.00	10.8503

**106+ NBoc-D-Phe-OTBA in CD₃CN**

Conc of Host (M)	1.25E-03	Initial volume (μL)	600
Conc of Guest (M)	4.20E-02		

Volume of guest (μL) δ NH pyrrole (ppm)

3.00	9.1531
6.00	9.3188
9.00	9.4857
12.00	9.6427
15.00	9.8046
18.00	9.9251
24.00	10.1134
30.00	10.2452
40.00	10.3820
50.00	10.4749
70.00	10.5967
90.00	10.6695
140.00	10.7599
190.00	10.8001
290.00	10.8340

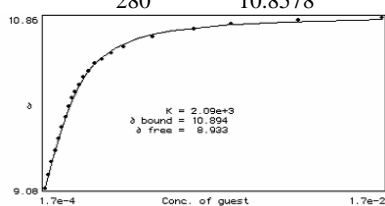
**106+ NAc-L-Phe-OTBA in CD₃CN**

Conc of Host (M)	1.78E-03	Initial volume (μL)	600
Conc of Guest (M)	5.23E-02		

Volume of guest (μL) δ NH pyrrole (ppm)

0	8.9648
2	9.0790
4	9.2184
6	9.3514
8	9.4719
10	9.5950
12	9.7155
14	9.8209
16	9.2939
18	10.0180

20	10.0845
22	10.1536
25	10.2377
28	10.3005
32	10.3733
36	10.4235
42	10.4850
50	10.5478
70	10.6532
100	10.7386
130	10.7863
190	10.8302
280	10.8578

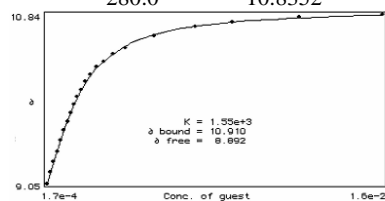
**106+ NAc-D-Phe-OTBA in CD₃CN**

Conc of Host (M)	0.00178000	Initial volume (μL)	600
Conc of Guest (M)	5.15E-02		

Volume of guest (μL) δ NH pyrrole (ppm)

2.0	9.0527
4.0	9.1719
6.0	9.2811
8.0	9.3891
10.0	9.5083
12.0	9.6113
14.0	9.7054
16.0	9.7946
18.0	9.8875
20.0	9.9653
22.0	10.0356
25.0	10.1260
28.0	10.2050
32.0	10.2804
36.0	10.3381
42.0	10.4122
50.0	10.4837
70.0	10.6030
100.0	10.7009

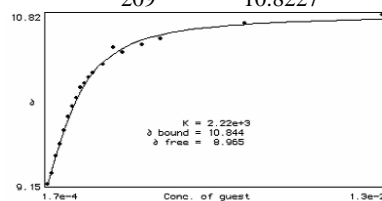
130.0	10.7524
190.0	10.8026
280.0	10.8352

**106+ NAc-L-AlaOTBA in CD₃CN**

Conc of Host (M)	1.50E-03	Initial volume (μL)	600
Conc of Guest (M)	5.20E-02		

Volume of guest (μL) δ NH pyrrole (ppm)

2	9.1455
4	9.2523
6	9.4167
8	9.5435
10	9.6778
12	9.8109
14	9.9163
16	9.9979
18	10.1008
20	10.1373
22	10.2038
24	10.2402
29	10.3281
34	10.3959
39	10.4436
49	10.5214
59	10.5804
109	10.7335
209	10.8227

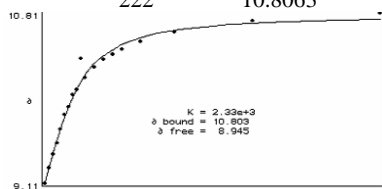
**106+ NAc-D-AlaOTBA in CD₃CN**

Conc of Host (M)	1.50E-03	Initial volume (μL)	600
Conc of Guest (M)	5.20E-02		

Volume of guest (μL) δ NH pyrrole (ppm)

2	9.1079
---	--------

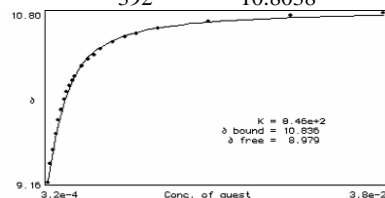
4	9.2598
6	9.3966
8	9.5109
10	9.6464
12	9.7870
14	9.8711
16	9.9841
18	10.0381
20	10.1347
22	10.1611
27	10.2615
32	10.3369
37	10.3883
42	10.4423
52	10.5151
72	10.6143
122	10.7285
222	10.8063

**106+ NBoc-L-GlnOTBA in CD₃CN**

Conc of Host (M)	1.79E-03	Initial volume (μL)	600
Conc of Guest (M)	9.53E-02		

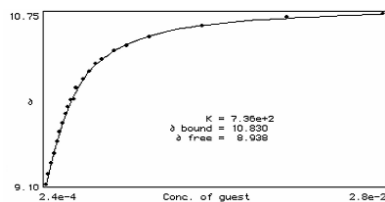
Volume of guest (μL)	δ NH pyrrole (ppm)
2	9.1569
4	9.3351
6	9.4682
8	9.6276
10	9.7619
12	9.8611
14	9.9590
16	10.0331
18	10.0921
20	10.1460
22	10.1850
27	10.2829
32	10.3482
37	10.3959
42	10.4486
52	10.5139
62	10.5641
72	10.6030
92	10.6519

142	10.7197
242	10.7750
392	10.8038

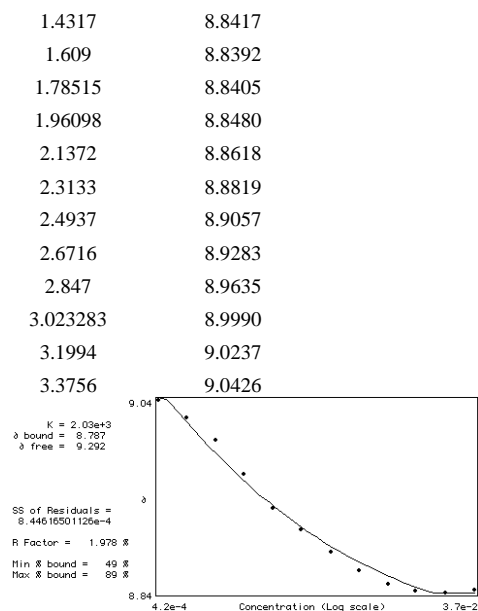
**106+ NBoc-D-GlnOTBA in CD₃CN**

Conc of Host (M)	1.79E-03	Initial volume (μL)	600
Conc of Guest (M)	7.10E-02		

Volume of guest (μL)	δ NH pyrrole (ppm)
0	9.1029
2	9.1029
4	9.2008
6	9.3050
8	9.4004
10	9.5121
12	9.6075
14	9.6841
16	9.7795
18	9.8460
20	9.9113
22	9.9226
24	10.0268
29	10.1109
34	10.1887
39	10.2588
44	10.3042
54	10.3833
64	10.4348
84	10.5176
134	10.6243
234	10.7059
384	10.7461

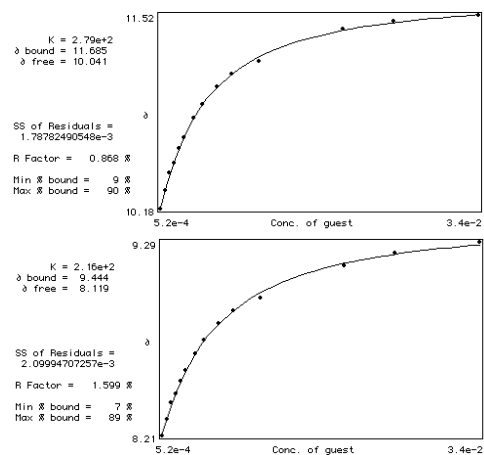
**Tweezer 107****Dilution study of 107 in CDCl₃**

log [107]	δ NH pyrrole
-----------	--------------



107 + TBAOAc in DMSO- d_6 -0.5% water

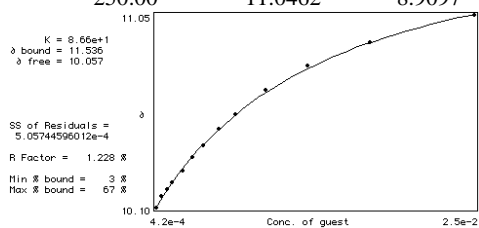
Conc of Host (M)	2.09E-03	Initial volume (μL)	600
Conc of Guest (M)	1.04E-01		
Volume of guest (μL)	δ NH pyrrole (ppm)	δ CONH (ppm)	
3.00	10.1826	8.2055	
6.00	10.3043	8.2983	
9.00	10.4292	8.3887	
12.00	10.4939	8.4370	
15.00	10.5956	8.5129	
18.00	10.6747	8.5726	
24.00	10.8071	8.6636	
30.00	10.9006	8.7416	
40.00	11.0249	8.8331	
50.00	11.1115	8.9053	
70.00	11.1994	8.9768	
140.00	11.4191	9.1595	
190.00	11.4731	9.2297	
290.00	11.5182	9.2931	

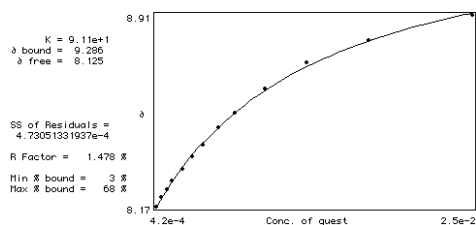


107 + TBAOBz in DMSO- d_6 -0.5% water

Conc of Host (M)	1.69E-03	Initial volume (μL)	600
Conc of Guest (M)	8.40E-02		

Volume of guest (μL)	δ NH pyrrole (ppm)	δ CONH (ppm)
3.00	10.1010	8.1653
6.00	10.1550	8.2017
9.00	10.1889	8.2318
12.00	10.2240	8.2644
18.00	10.2805	8.3096
24.00	10.3483	8.3598
30.00	10.4023	8.4050
40.00	10.4876	8.4703
50.00	10.5554	8.5293
70.00	10.6747	8.6222
100.00	10.7939	8.7239
150.00	10.9082	8.8105
250.00	11.0462	8.9097

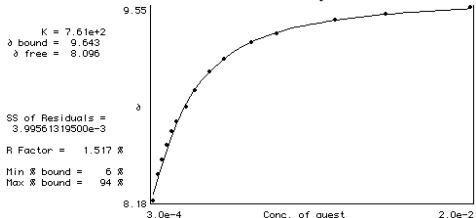
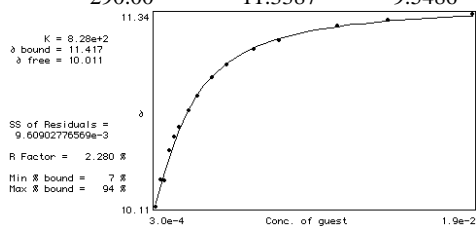




107 + TBAdihydrogenphosphate in DMSO-*d*₆-0.5% water

Conc of Host (M)	2.09E-03	Initial volume (μL)	600
Conc of Guest (M)	5.98E-02		

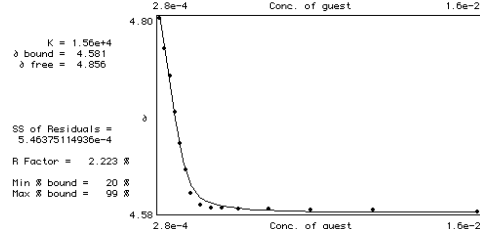
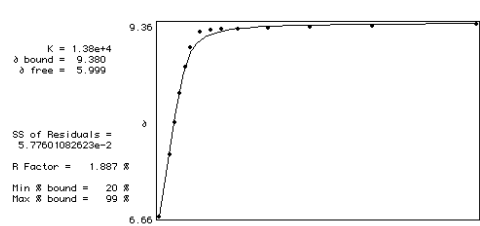
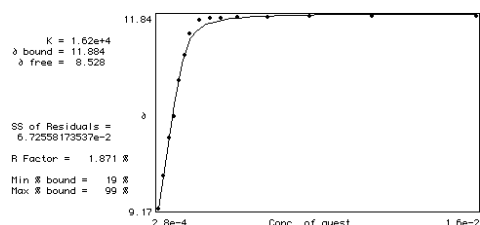
Volume of guest (μL)	δ NH pyrrole (ppm)	δ CONH (ppm)
3.00	10.1148	8.1828
6.00	10.2818	8.3649
9.00	10.3772	8.4666
12.00	10.4700	8.5707
15.00	10.5567	8.6661
18.00	10.6182	8.7377
24.00	10.7224	8.8429
30.00	10.8190	8.9569
40.00	10.9333	9.0879
50.00	11.0123	9.1783
70.00	11.1153	9.2963
90.00	11.1680	9.3591
140.00	11.2596	9.4583
190.00	11.2973	9.4941
290.00	11.3387	9.5486



107 + TBAOAc in CD₃CN

Conc of Host (M)	1.59E-03	Initial volume (μL)	600
Conc of Guest (M)	5.57E-02		

Volume of guest (μL)	δ NH pyrrole (ppm)	δ CONH (ppm)	δ CH (ppm)
3.00	9.1682	6.6550	4.7997
6.00	9.6251	-	4.7651
9.00	10.1486	7.5279	4.7344
12.00	10.4486	7.9832	4.6942
15.00	10.9469	8.3836	4.6590
18.00	11.2909	8.7464	4.6301
21.00	11.5897	9.0338	4.6044
27.00	11.7729	9.2397	4.5906
33.00	11.8006	9.2661	4.5881
40.00	11.8081	9.2774	4.5875
50.00	11.8156	9.2874	4.5862
70.00	11.8207	9.2975	4.5869
100.00	11.8282	9.3100	4.5849
150.00	11.8294	9.3326	4.5856
250.00	11.8382	9.3602	4.5837

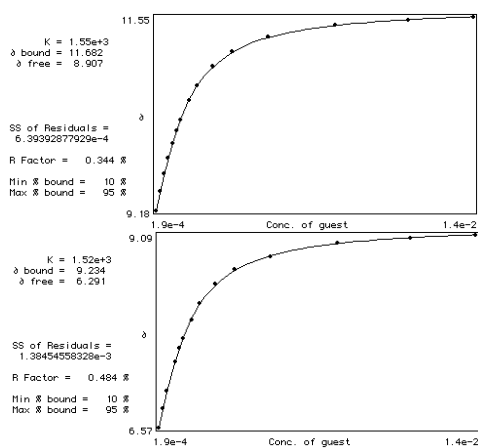
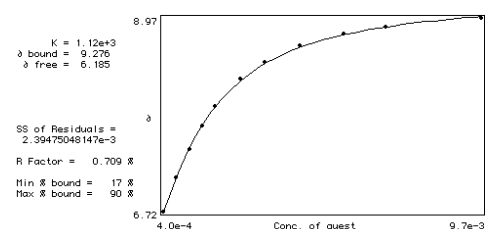
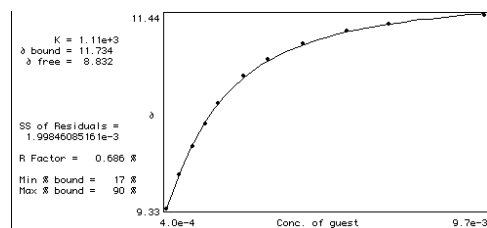


107 + TBAOAc in CD₃CN-1% water

Conc of Host (M)	1.26E-03	Initial volume (μL)	600
------------------	----------	---------------------	-----

Conc of Guest (M)	(μL)	
	5.60E-02	
Volume of guest (μL)	δ NH pyrrole (ppm)	δ CONH (ppm)
2	9.1782	6.5734
4	9.4155	6.8257
6	9.6263	7.0479
8	9.8159	-
10	9.9967	7.4308
12	10.1561	7.6116
14	10.2904	7.7408
18	10.5189	7.9794
22	10.7097	8.1890
30	10.9394	8.4450
40	11.1177	8.6346
60	11.2984	8.8054
100	11.4453	8.9773
150	11.5068	9.0502
200	11.5482	9.0891

25	10.4749	7.9423
35	10.7725	8.2580
45	10.9532	8.4514
60	11.1302	8.6403
80	11.2633	8.7783
100	11.3348	8.8545
150	11.4403	8.9661

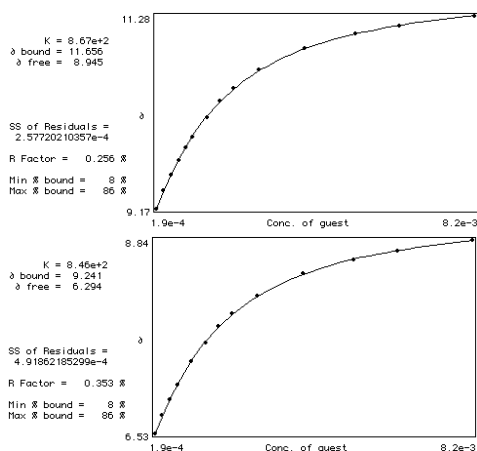


Conc of Host (M)	1.35E-03	Initial volume (μL)	600
Conc of Guest (M)	4.84E-02		

Volume of guest (μL)	δ NH pyrrole (ppm)	δ CONH (ppm)
5	9.3301	6.7184
10	9.6979	7.1088
15	10.0042	7.4408
20	10.2565	7.7070

Conc of Host (M)	1.12E-03	Initial volume (μL)	600
Conc of Guest (M)	2.35E-02		

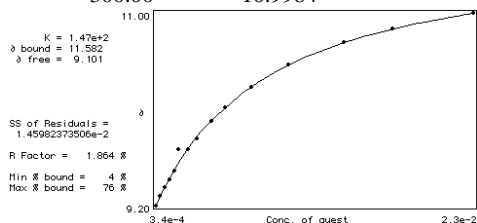
Volume of guest (μL)	δ NH pyrrole (ppm)	δ CONH (ppm)
5	9.1707	6.53E+00
10	9.3677	6.75E+00
15	9.5422	6.93E+00
20	9.6979	7.11E+00
25	9.8410	-
30	9.9578	7.39E+00
40	10.1724	7.61E+00
50	10.3444	7.80E+00
60	10.4862	7.95E+00
80	10.6871	8.17E+00
120	10.9218	8.43E+00
170	11.0875	8.60E+00
220	11.1742	8.70E+00
320	11.2809	8.84E+00

**107 + TBAAcO in CD₃CN-2% water**

Conc of Host (M)	Initial volume (μL)	
1.36E-03	600	
Conc of Guest (M)		
6.83E-02		

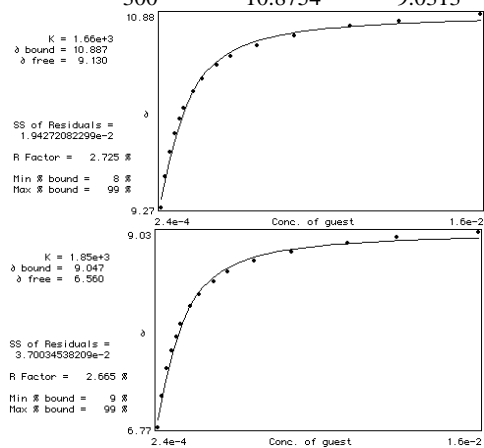
Volume of guest (μL) δ NH pyrrole (ppm)

3.00	9.1958
6.00	9.2824
9.00	9.3665
12.00	9.4380
15.00	9.5171
18.00	9.7155
24.00	9.7155
30.00	9.8184
40.00	9.9791
50.00	10.1084
70.00	10.3055
10.00	10.5126
150.00	10.7197
20.00	10.8490
300.00	10.9984

**107 + TBA dihydrogen phosphate in CD₃CN-1% water**

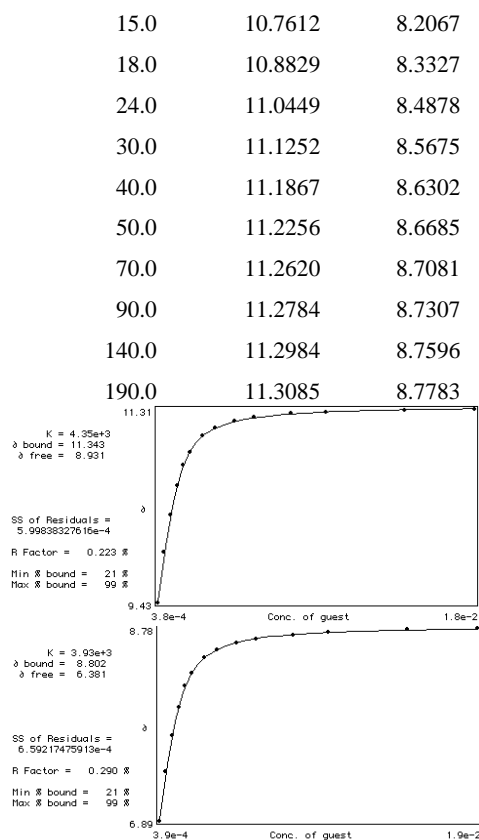
Conc of Host (M)	Initial volume	
1.36E-03	600	

Conc of Guest (M)	Volume of guest (μL)	δ NH pyrrole (ppm)	δ CONH (ppm)
4.86E-02	3	9.2698	6.773
	6	9.5259	7.132
	9	9.7318	7.4471
	12	9.8787	7.6618
	15	10.0017	7.8162
	18	10.0958	7.9693
	24	10.2302	8.1727
	30	10.3331	8.3031
	40	10.4498	8.4539
	50	10.5189	8.5656
	70	10.6080	8.6899
	100	10.6934	8.7991
	150	10.7737	8.9020
	200	10.8151	8.9635
	300	10.8754	9.0313

**107 + NAc-D-Phe-OTBA in CD₃CN**

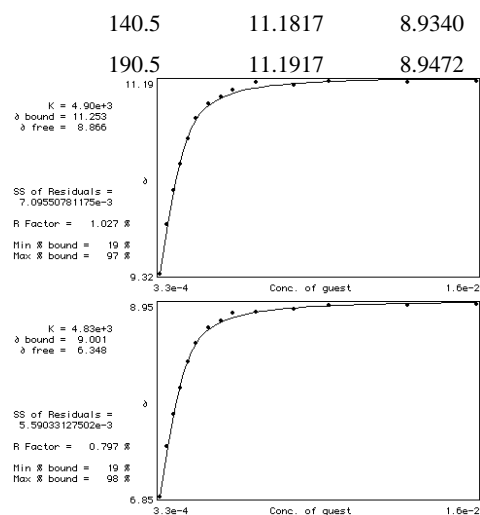
Conc of Host (M)	Initial volume (μL)	
1.49E-03	600	
Conc of Guest (M)		
7.60E-02		

Volume of guest (μL)	δ NH pyrrole (ppm)	δ CONH (ppm)
3.0	9.4318	6.8872
6.0	9.9176	7.3688
9.0	10.2791	7.7233
12.0	10.5603	8.0032

**107+ NAc-L-Phe-OTBA in CD₃CN**

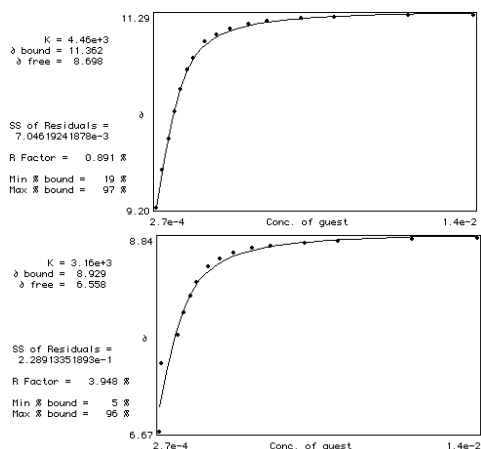
Conc of Host (M)	1.49E-03	Initial volume (μL)	600
Conc of Guest (M)	6.60E-02		

Volume of guest (μL)	δ NH pyrrole (ppm)	δ CONH (ppm)
3.0	9.3238	6.8471
6.5	9.8033	7.3981
9.5	10.1272	7.7477
12.5	10.3871	8.0271
16.0	10.6319	8.3132
20.0	10.8264	8.5223
26.0	10.9683	8.6848
32.0	11.0373	8.7608
38.0	11.1045	8.8436
50.0	11.1177	8.8525
70.5	11.1478	8.8913
90.5	11.1929	8.9353

**107+ NBoc-L-Phe-OTBA in CD₃CN**

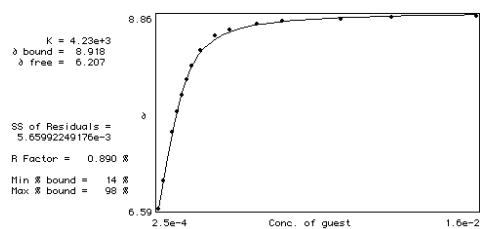
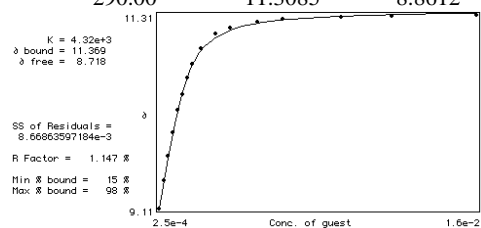
Conc of Host (M)	1.32E-03	Initial volume (μL)	600
Conc of Guest (M)	8.00E-02		

Volume of guest (μL)	δ NH pyrrole (ppm)	δ CONH (ppm)
3.00	9.1995	6.6732
6.00	9.6063	-
9.00	9.9465	7.4346
12.00	10.2415	7.7484
15.00	10.4825	7.9994
18.00	10.6933	8.1928
21.00	10.8189	8.3415
27.00	10.9997	8.5211
33.00	11.0750	8.6064
40.00	11.1378	8.6705
50.00	11.1892	8.7269
60.00	11.2194	8.7545
80.00	11.2495	8.7872
100.00	11.2658	8.8060
150.00	11.2821	8.8286
200.00	11.2909	8.8431



Conc of Host (M)	1.57E-03	Initial volume (μL)	600
Conc of Guest (M)	4.97E-02		

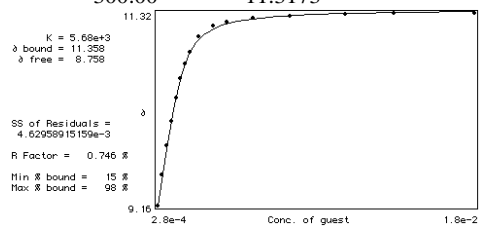
Volume of guest (μL)	δ NH pyrrole (ppm)	δ CONH (ppm)
3.00	9.1054	6.5897
6.00	9.4255	6.9211
9.00	9.6992	-
12.00	9.9653	7.4885
15.00	10.2201	7.7315
18.00	10.4059	7.9317
21.00	10.5854	8.1087
24.00	10.7411	8.2656
30.00	10.9256	8.4564
40.00	11.0913	8.6226
50.00	11.1629	8.7000
70.00	11.2294	8.7652
90.00	11.2545	8.7935
140.00	11.2771	8.8261
190.00	11.2909	8.8431
290.00	11.3085	8.8612



Conc of Host (M)	1.69E-03	Initial volume (μL)	600
Conc of Guest (M)	5.55E-02		

Volume of guest (μL) δ NH pyrrole (ppm)

3.0	9.1556
6.0	9.4983
9.0	9.8272
12.0	10.0996
15.0	10.3607
18.0	10.5754
21.0	10.7448
24.0	10.8766
30.0	11.0489
40.0	11.1654
50.0	11.2181
70.0	11.2595
100.0	11.2821
150.0	11.3022
200.00	11.3072
300.00	11.3173

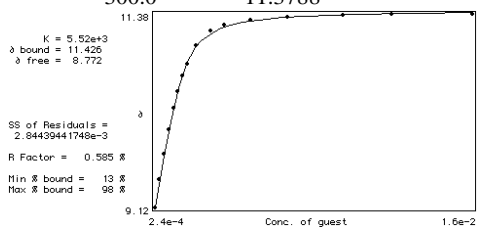


107+ NBoc-D-Phe-OTBA in CD₃CN

Conc of Host (M)	1.69E-03	Initial volume (μL)	600
Conc of Guest (M)	4.91E-02		

Volume of guest (μL) δ NH pyrrole (ppm)

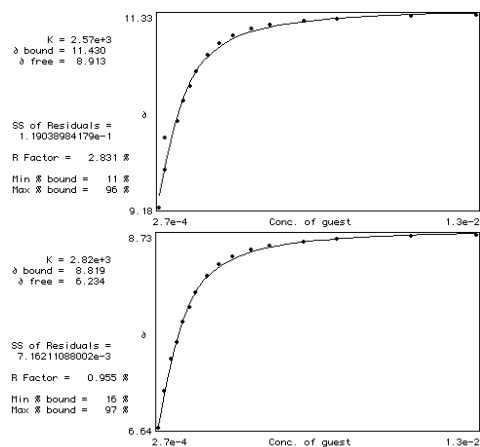
3.0	9.1205
6.0	9.4481
9.0	9.7381
12.0	10.0243
15.0	10.2728
18.0	10.4674
21.0	10.6570
24.0	10.7938
30.0	11.0034
40.0	11.1767
50.0	11.2445
70.0	11.3060
100.0	11.3386
150.0	11.3625
200.0	11.3675
300.0	11.3788



Conc of Host (M)	1.24E-03	Initial volume (μL)	600
Conc of Guest (M)	5.37E-02		

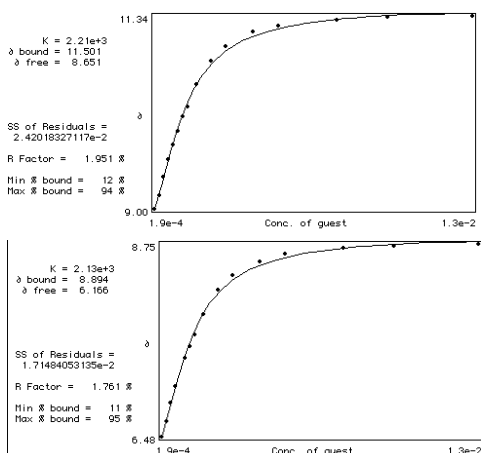
Volume of guest (μL)	δ NH pyrrole (ppm)	δ CONH (ppm)
3.00	9.1782	6.6362
6.00	9.5975	7.0328
9.00	9.9527	7.3843
12.00	10.1385	7.5664
15.00	10.3682	7.7798
18.00	10.5289	7.9455
21.00	10.6934	8.1036
27.00	10.8804	8.2850
33.00	11.0022	8.4049
40.00	11.0938	8.4941
50.00	11.1704	8.5637
60.00	11.2106	8.6052
80.00	11.2558	8.6491

100.00	11.2821	8.6785
150.00	11.3110	8.7131
200.00	11.3261	8.7294



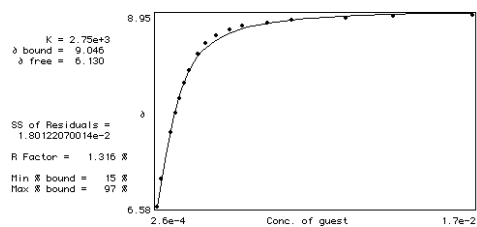
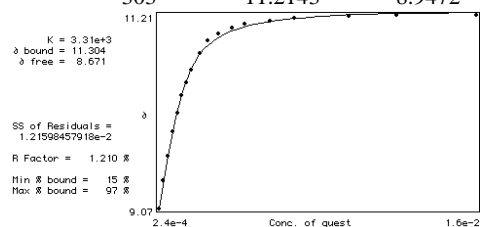
Conc of Host (M)	1.57E-03	Initial volume (μL)	600
Conc of Guest (M)	3.90E-02		

Volume of guest (μL)	δ NH pyrrole (ppm)	δ CONH (ppm)
3.0	9.0024	6.4774
6.0	9.1650	6.6500
9.0	9.3828	6.8697
12.0	9.5950	7.0680
15.0	9.7720	-
18.0	9.9477	7.4044
21.0	10.1172	7.5350
24.0	10.2425	7.6693
30.0	10.5126	7.9153
40.0	10.7900	8.2009
50.0	10.9721	8.3716
70.0	11.1465	8.5367
90.0	11.2231	8.6195
140.0	11.2947	8.6892
190.0	11.3223	8.7177
290.0	11.3436	8.7451

**107+ NAc-L-Ala-OTBA in CD₃CN**

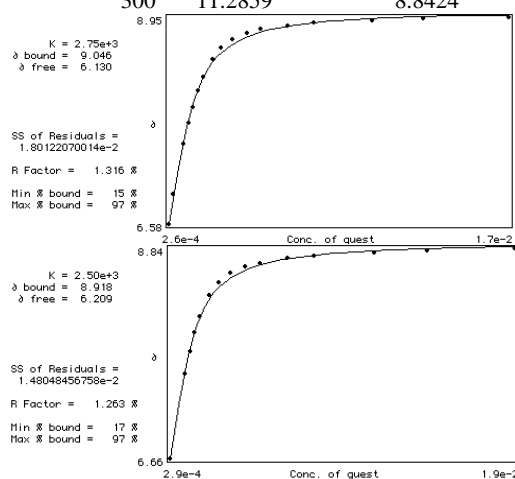
Conc of Host (M)	Initial volume (μL)	
1.41E-03	600	
Conc of Guest (M)		
5.20E-02		

Volume of guest (μL)	δ NH pyrrole (ppm)	δ CONH (ppm)
3	9.0691	6.5809
6	9.3778	6.9174
9	9.6464	-
12	9.9151	7.4985
15	10.1272	7.7384
18	10.3168	7.9216
21	10.4662	8.1137
24	10.6017	8.2568
30	10.7888	8.4608
36	10.9218	8.6039
43	11.0034	8.6936
53	11.0712	8.7677
63	11.1114	8.8079
83	11.1453	8.8505
103	11.1767	8.8782
153	11.1968	8.9089
203	11.2093	8.9259
303	11.2143	8.9472

**107+ NAc-D-Ala-OTBA in CD₃CN**

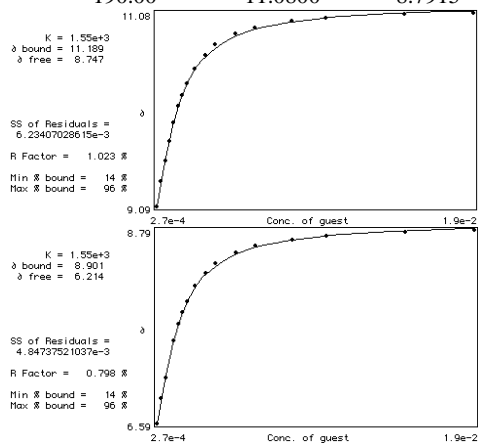
Conc of Host (M)	Initial volume (μL)	
1.41E-03	600	
Conc of Guest (M)		
5.83E-02		

Volume of guest (μL)	δ NH pyrrole (ppm)	δ CONH (ppm)
3	9.1443	6.5809
9	9.7544	-
12	10.0356	7.5400
15	10.2615	7.7672
18	10.4498	7.9718
21	10.6193	8.1288
27	10.8327	8.3522
33	10.9670	8.4859
40	11.0547	8.5795
50	11.1252	8.6466
60	11.1578	8.6849
80	11.2068	8.7345
100	11.2306	8.7596
150	11.2545	8.7947
200	11.2683	8.8155
300	11.2859	8.8424

**107+ NBoc-L-Gln-OTBA in CD₃CN**

Conc of Host (M)	Initial volume	
1.32E-03	600	

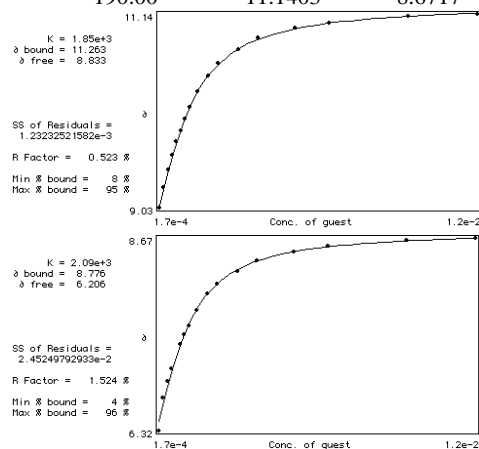
Conc of Guest (M)	(μL)	
	8.00E-02	
Volume of guest (μL)	δ NH pyrrole (ppm)	δ CONH (ppm)
2.00	9.0941	6.5885
4.00	9.3533	6.8734
6.00	9.5560	7.1031
8.00	9.7657	-
10.00	9.9515	7.5287
12.00	10.1172	7.7170
14.00	10.2314	7.8482
16.00	10.3544	7.9787
20.00	10.5076	8.1476
25.00	10.6444	8.2976
30.00	10.7499	8.4099
40.00	10.8603	8.5330
50.00	10.9256	8.6064
70.00	10.9909	8.6792
90.00	11.0260	8.7183
140.00	11.0624	8.7677
190.00	11.0800	8.7915



107+ NBoc-D-Gln-OTBA in CD₃CN

Conc of Host (M)	Starting volume (μL)	
	1.32E-03	600
Conc of Guest (M)	8.00E-02	
Volume of guest (μL)	δ NH pyrrole (ppm)	δ CONH (ppm)
2.00	9.0313	6.3191
4.00	9.2510	6.7190

6.00	9.4368	6.9149
8.00	9.5975	7.0705
10.00	9.7469	-
12.00	9.8724	7.3680
14.00	9.9916	7.4873
16.00	10.1190	7.6015
20.00	10.2942	7.7898
25.00	10.4662	7.9894
30.00	10.6030	8.1061
40.00	10.7538	8.2588
50.00	10.8792	8.3974
70.00	10.9833	8.5054
90.00	11.0423	8.5681
140.00	11.1089	8.6378
190.00	11.1403	8.6717

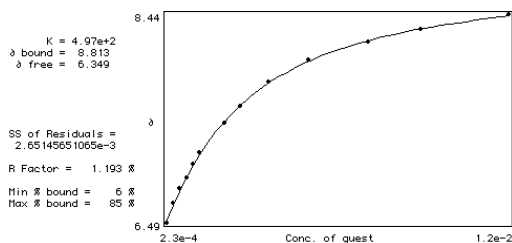


107+ NBoc-L-Phe-OTBA in CD₃CN-1%water

Conc of Host (M)	Initial volume (μL)	
	1.40E-03	600
Conc of Guest (M)	3.54E-02	

Volume of guest (μL)	δ NH pyrrole (ppm)	δ CONH (ppm)
4	9.1117	6.4868
8	9.2610	6.6675
12	9.3790	6.8069
16	9.4945	6.9086
20	9.5937	7.0328
24	9.6753	7.1421
30	9.7958	-
40	9.9578	7.4220

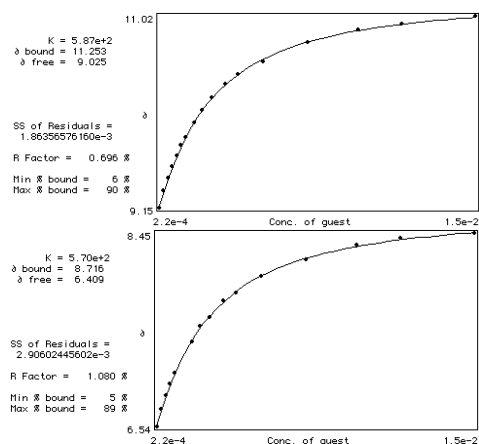
50	10.0896	7.5726
70	10.2766	7.8074
100	10.4586	8.0082
150	10.6406	8.1790
200	10.7398	8.2932
300	10.8503	8.4401



107 + NBoc-D-Phe-OTBA in CD₃CN-1% water

Conc of Host (M)	1.40E-03	Initial volume (μL)	600
Conc of Guest (M)	4.36E-02		

Volume of guest (μL)	δ NH pyrrole (ppm)	δ CONH (ppm)
3	9.1531	6.5357
6	9.3138	6.7027
9	9.4418	6.8408
12	9.5560	6.9588
15	9.6590	7.0605
18	9.7607	-
21	9.8372	-
27	9.9829	7.3768
33	10.1059	7.5300
40	10.2214	7.6191
50	10.3557	7.7785
60	10.4511	7.8626
80	10.5766	8.0183
120	10.7612	8.1877
170	10.8829	8.3334
220	10.9457	8.3999
320	11.0235	8.4539

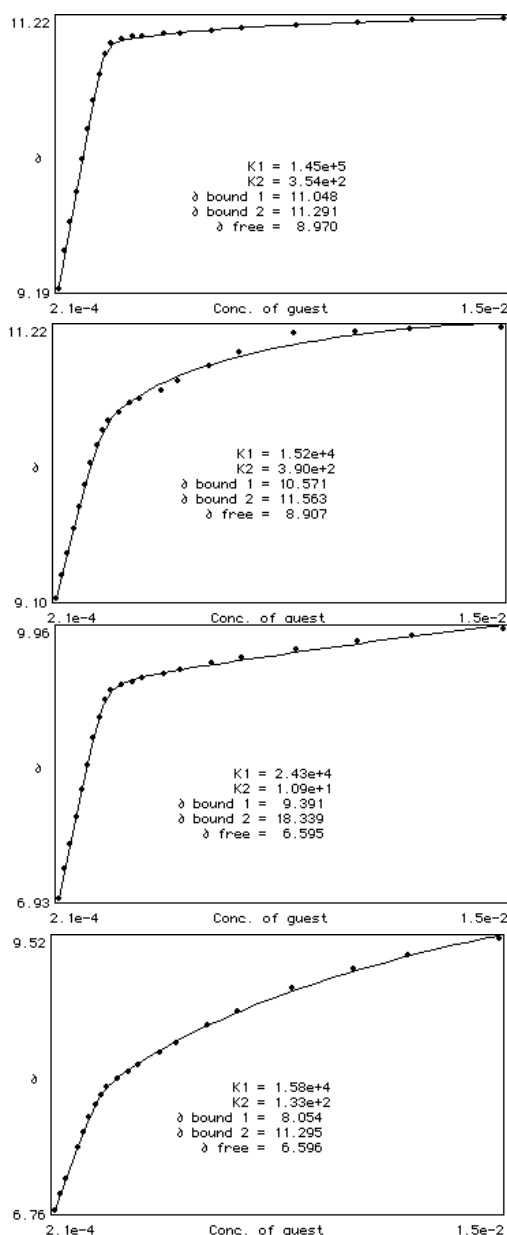


Tweezer 108

108 + TBAOAc in CD₃CN

Conc of Host (M)	1.79E-03	Initial volume (μL)	600
Conc of Guest (M)	4.20E-02		

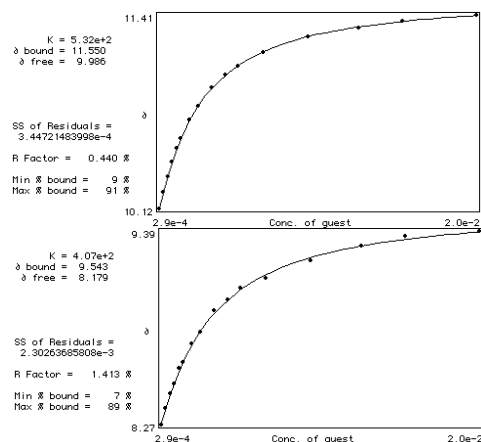
Volume of guest (μL)	δ NH pyrrole (ppm)	δ NH pyrrole (ppm)	δ CONH (ppm)	δ CONH (ppm)
3.0	9.1945	9.1029	6.9281	6.7636
6.0	9.4757	9.2836	7.2568	6.9243
9.0	9.6866	9.4481	7.5350	7.0755
12.0	9.9126	9.6402	7.8375	-
15.0	10.1586	9.8184	8.1451	7.4032
18.0	10.3833	9.9866	8.4200	7.5507
21.0	10.6005	10.1523	8.7200	7.7070
24.0	10.7925	10.2954	8.9522	7.8243
27.0	10.9457	10.4147	9.1468	7.9291
30.0	11.0298	10.4900	9.2598	8.0089
36.0	11.0649	10.5540	9.3213	8.0974
42.0	11.0775	10.6256	9.3527	8.1677
48.0	11.0800	10.6557	9.3966	8.2367
60.0	11.1013	10.7423	9.4418	8.3603
70.0	11.1076	10.8013	9.4838	8.4583
90.0	11.1239	10.9206	9.5680	8.6290
110.0	11.1415	11.0248	9.6301	8.7790
150.0	11.1679	11.1679	9.7249	9.0050
200.0	11.1867	11.3085	9.8115	9.2016
250.0	11.2018	11.4001	9.8767	9.3445
350.0	11.2206	11.5181	9.9559	9.5165



109 + TBAOAc in DMSO- d_6 -0.5% water

Conc of Host (M)	1.38E-03	Initial volume (μL)	600
Conc of Guest (M)	5.82E-02		
Volume of guest (μL)	δ NH pyrrole (ppm)	δ CONH (ppm)	
3.0	10.1198	8.2707	
6.0	10.2290	8.3624	
9.0	10.3332	8.4465	

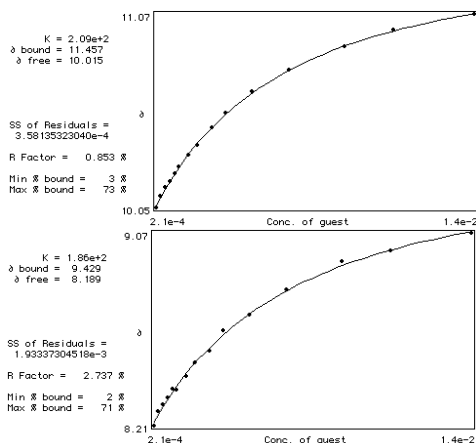
12.0	10.4324	8.5067
15.0	10.5215	8.5971
18.0	10.5855	8.6285
24.0	10.7086	8.7364
30.0	10.8040	8.8055
40.0	10.9245	8.9335
50.0	11.0111	8.9925
60.0	11.0701	9.0628
80.0	11.1605	9.1156
120.0	11.2659	9.2210
170.0	11.3262	9.3026
220.0	11.3726	9.3616
320.0	11.4128	9.3930
320.0	11.4128	9.3930



109+TBAOBz in DMSO- d_6 0.5% water

Conc of Host (M)	1.38E-03	Initial volume (μL)	600
Conc of Guest (M)	4.29E-02		
Volume of guest (μL)	δ NH pyrrole (ppm)	δ CONH (ppm)	
3	10.0545	8.2117	
6	10.1160	8.2745	
9	10.1575	8.3059	
12	10.1901	8.3360	
15	10.2340	8.3724	
18	10.2667	8.3711	
24	10.3307	8.4301	
30	10.3822	8.4917	

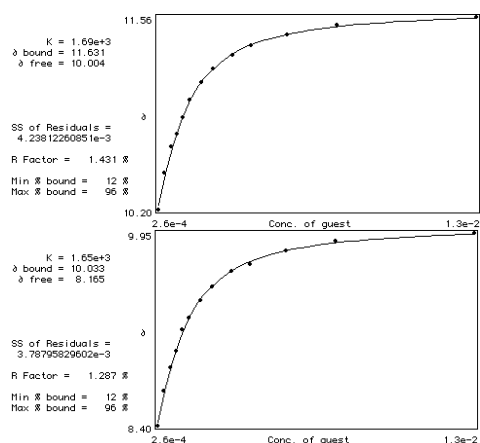
40	10.4751	8.5419
50	10.5504	8.6310
70	10.6621	8.7000
100	10.7789	8.8143
150	10.8994	8.9373
200	10.9910	8.9873
300	11.0739	9.0666



109 TBAdihydrogen phosphate in DMSO-*d*₆ 0.5% water

Conc of Host (M)	1.19E-03	Initial volume (μL)	600
Conc of Guest (M)	5.30E-02		

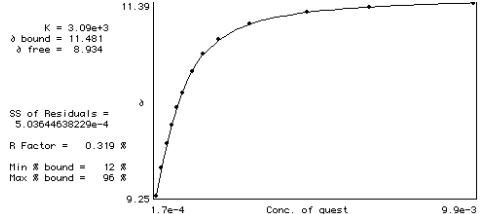
Volume of guest (μL)	δ NH pyrrole (ppm)	δ CONH (ppm)
3	10.2002	8.3963
6	10.4550	8.6737
9	10.6433	8.8620
12	10.7312	9.0013
15	10.8504	9.1733
18	10.9772	9.2637
24	11.0972	9.4055
30	11.1969	9.5198
40	11.2948	9.6440
50	11.3588	9.7005
70	11.4379	9.8123
100	11.5019	9.8863
200	11.5634	9.9541

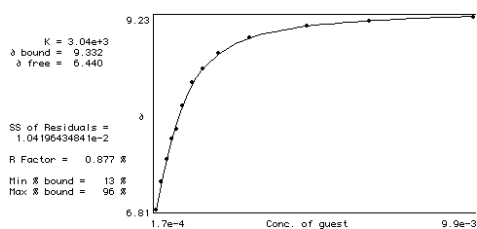


109+ TBAOAc in CD₃CN-1% water

Conc of Host (M)	9.48E-04	Initial volume (μL)	600
Conc of Guest (M)	3.36E-02		

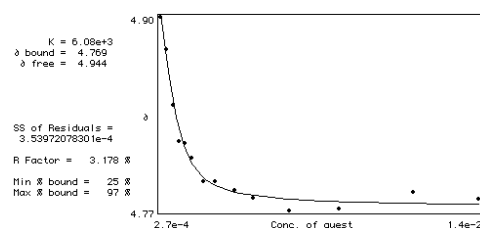
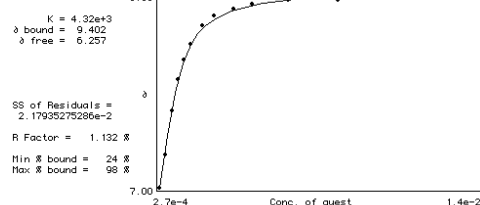
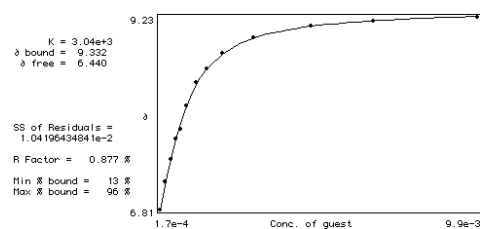
Volume of guest (μL)	δ NH pyrrole (ppm)	δ CONH (ppm)	δ COH (ppm)
3	9.2497	6.8057	8.1287
6	9.5560	7.1515	8.1149
9	9.8234	7.4408	8.1024
12	10.0356	7.6975	8.0936
15	10.2251	7.8141	8.0861
18	10.3908	8.1099	8.0785
24	10.6319	8.3961	8.0685
30	10.8189	8.5763	8.0622
40	10.9871	8.7702	8.0534
60	11.1566	8.9598	8.0484
100	11.2884	9.1054	8.0421
150	11.3436	9.1750	8.0384
250	11.3913	9.2265	8.0346



**109+TBAOBz in CD₃CN-1% water**

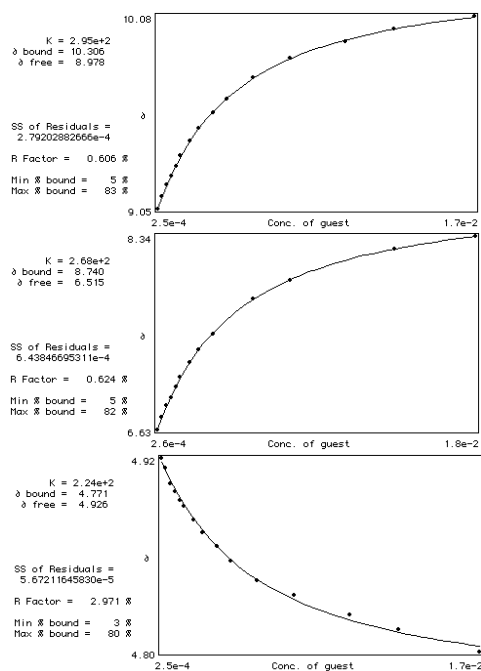
Conc of Host (M)	1.01E-03	Initial volume (μL)	600
Conc of Guest (M)	5.52E-02		

Volume of guest (μL)	δ NH pyrrole (ppm)	δ CONH (ppm)	δ CH (ppm)
3	9.4303	7.00E+00	4.9013
6	9.8987	7.39E+00	4.8787
9	10.2929	7.92E+00	4.8398
12	10.6369	8.30E+00	4.8147
15	10.8515	8.54E+00	4.8134
18	11.0248	8.72E+00	4.8134
24	11.2344	8.95E+00	4.7871
30	11.3361	9.06E+00	4.7871
40	11.4240	9.16E+00	4.7808
50	11.4679	9.21E+00	4.7758
70	11.5144	9.26E+00	4.767
100	11.5470	9.26E+00	4.7682
150	11.5708	9.32E+00	4.7795
200	11.5846	9.33E+00	4.7745

**109+TBACl in CD₃CN – 1% water**

Conc of Host (M)	1.01E-03	Initial volume (μL)	600
Conc of Guest (M)	5.03E-02		

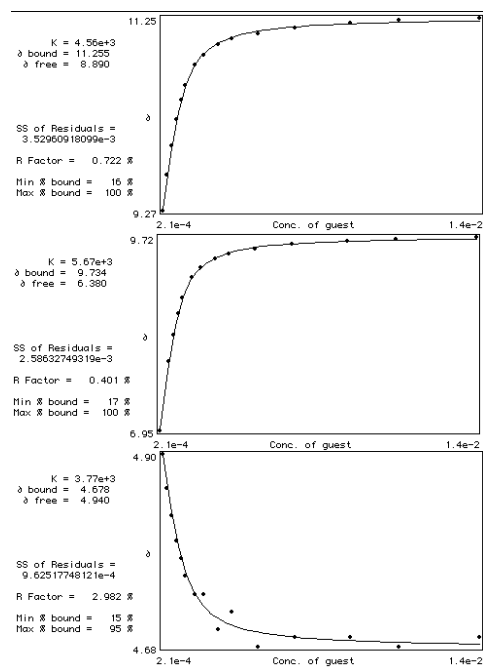
Volume of guest (μL)	δ NH pyrrole (ppm)	δ CONH (ppm)	δ CH (ppm)
3	9.0502	6.63E+00	4.9214
6	9.1167	6.74E+00	4.9151
9	9.1769	6.84E+00	4.9051
12	9.2234	6.91E+00	4.9001
15	9.2761	7.01E+00	4.8950
18	9.3326	7.09E+00	4.8913
24	9.4092	7.22E+00	4.8825
30	9.4795	7.34E+00	4.8749
40	9.5648	7.48E+00	4.8662
50	9.6367	-	4.8574
70	9.7469	7.79E+00	4.8448
100	9.8512	7.94E+00	4.8360
150	9.9439	-	4.8235
200	10.008	8.23E+00	4.8147
300	10.0795	8.34E+00	4.8009



109+TBA dihydrogenphosphate in CD_3CN – 1% water

Conc of Host (M)	1.01E-03	Initial volume (μL)	600
Conc of Guest (M)	4.20E-02		

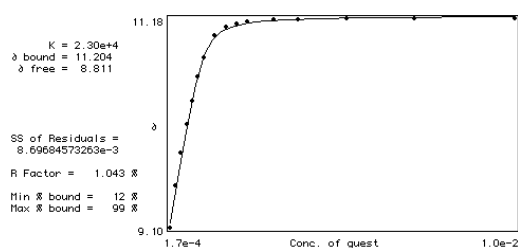
Volume of guest (μL)	δ NH pyrrole (ppm)	δ CONH (ppm)	δ CH (ppm)
3	9.2673	6.9525	4.8975
6	9.6326	-	4.8586
9	9.9352	7.9404	4.8298
12	10.2050	8.3133	4.8046
15	10.4072	8.6183	4.7795
18	10.5553	8.8380	4.7632
24	10.7586	9.1380	4.7431
30	10.8666	9.2836	4.7356
40	10.9733	9.4029	4.6954
50	11.0285	9.4770	4.7205
70	11.0875	9.5460	4.6829
100	11.1450	9.6075	4.6854
150	11.1892	9.6590	4.6917
200	11.2194	9.6816	4.6753
300	11.2482	9.7243	4.6854



109+NBoc-L-PheOTBA in CD_3CN

Conc of Host (M)	1.17E-03	Initial volume (μL)	600
Conc of Guest (M)	5.20E-02		

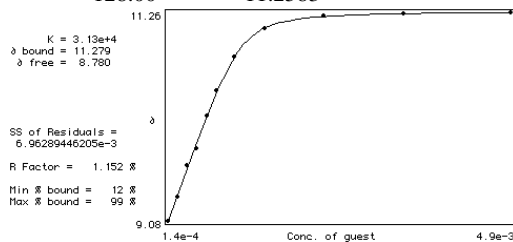
Volume of guest (μL)	δ CH (ppm)
2.00	9.0991
4.00	9.5171
6.00	9.8435
8.00	10.1235
10.00	10.3557
12.00	10.5967
14.00	10.7888
18.00	11.0047
22.00	11.0888
26.00	11.1227
30.00	11.1390
40.00	11.1603
50.00	11.1629
70.00	11.1704
100.00	11.1779
150.00	11.1792

**109+NBoc-D-PheOTBA in CD₃CN**

Conc of Host (M)	1.17E-03	Initial volume (μL)	600
Conc of Guest (M)	2.80E-02		

Volume of guest (μL)	δ pyr NH (ppm)
----------------------	----------------

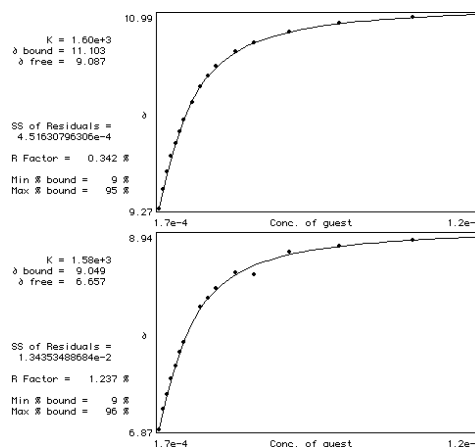
3.00	9.0815
6.00	9.3326
9.00	9.8372
12.00	9.6552
15.00	10.1762
18.00	10.4348
24.00	10.7863
34.00	11.0901
54.00	11.2168
84.00	11.2445
128.00	11.2583

**109+NBoc-L-PheOTBA in CD₃CN-1% water**

Conc of Host (M)	1.15E-03	Initial volume (μL)	600
Conc of Guest (M)	4.98E-02		

Volume of guest (μL)	δ NH pyrrole (ppm)	δ CONH (ppm)
2	9.2661	6.8684
4	9.4380	7.0843
6	9.5975	7.2400
8	9.7293	7.4082

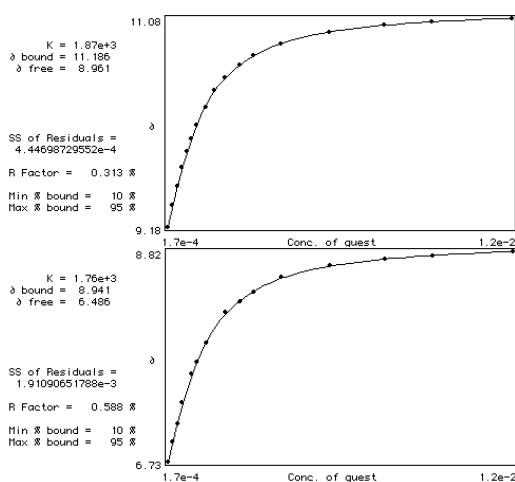
10	9.8485	7.5463
12	9.9527	7.6944
14	10.0532	-
18	10.2113	7.8011
22	10.3494	8.1739
26	10.4523	8.2719
30	10.5327	8.3685
40	10.6645	8.5443
50	10.7448	8.5183
70	10.8440	8.7614
100	10.9156	8.8229
150	10.9708	8.8870
200	10.9934	8.9447

**109+NBoc-D-PheOTBA in CD₃CN-1% water**

Conc of Host (M)	1.15E-03	Initial volume (μL)	600
Conc of Guest (M)	3.37E-02		

Volume of guest (μL)	δ NH pyrrole (ppm)	δ CONH (ppm)
3	9.1769	6.7278
6	9.3703	6.9211
9	9.5422	7.1044
12	9.7155	7.3153
15	9.8598	-
18	9.9841	7.5940
21	10.1034	7.7107
27	10.2678	7.9078

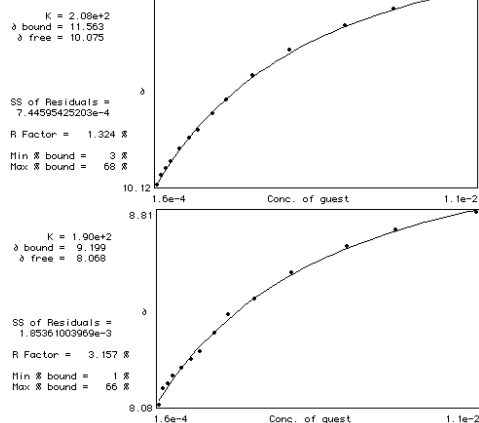
33	10.4185	-
40	10.5415	8.2166
50	10.6507	8.3196
60	10.7361	8.4099
80	10.8465	8.5568
120	10.9532	8.6748
170	11.0160	8.7388
220	11.0511	8.7756
320	11.0800	8.8192

**Tweezer 110****110+ TBAOBz in DMSO-*d*₆-0.5% water**

Conc of Host (M)	1.04E-03	Initial volume (μL)	600
Conc of Guest (M)	3.30E-02		

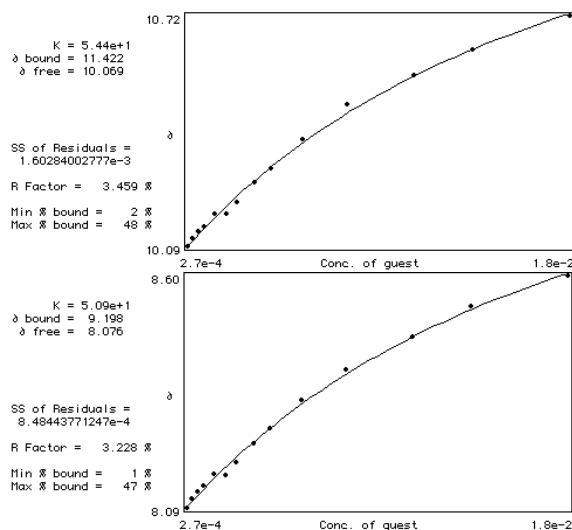
Volume of guest (μL)	δ NH pyrrole (ppm)	δ CONH (ppm)
3	10.116	8.08E+00
6	10.1600	8.14E+00
9	10.1951	8.16E+00
12	10.2290	8.19E+00
18	10.2918	8.22E+00
24	10.3470	8.25E+00
30	10.3859	8.28E+00
40	10.4700	8.35E+00
50	10.5378	8.42E+00
70	10.6571	8.48E+00
100	10.7864	8.58E+00

150	10.9094	8.68E+00
200	10.9898	8.74E+00
300	11.0801	8.81E+00

**110 + TBAOBz in DMSO-*d*₆-0.5% water**

Conc of Host (M)	1.04E-03	Initial volume (μL)	600
Conc of Guest (M)	5.40E-02		

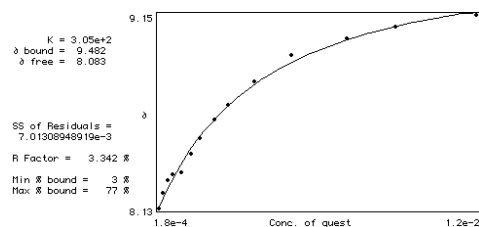
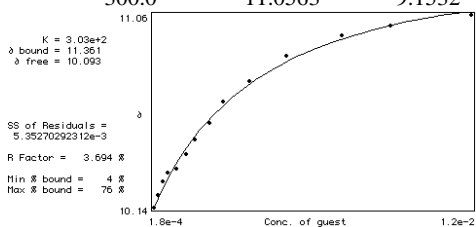
Volume of guest (μL)	δ NH pyrrole (ppm)	δ CONH (ppm)
3	10.0909	8.09
6	10.1123	8.1088
9	10.1299	8.1238
12	10.1449	8.1364
18	10.1788	8.164
24	10.1776	8.1603
30	10.2115	8.1879
40	10.2642	8.2306
50	10.3043	8.2644
70	10.3847	8.3247
100	10.4788	8.3912
150	10.5604	8.464
200	10.6306	8.5304
300	10.7236	8.5984



110+TBA dihydrogen phosphate in DMSO- d_6 0.5% water

Conc of Host (M)	1.04E-03	Initial volume (μL)	600
Conc of Guest (M)	3.70E-02		

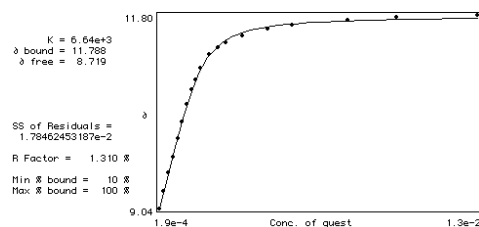
Volume of guest (μL)	δ NH pyrrole (ppm)	δ CONH (ppm)
3.0	10.1412	8.1314
6.0	10.1989	8.2105
9.0	10.2617	8.277
12.0	10.3043	8.3096
18.0	10.3244	8.3222
24.0	10.3935	8.4176
30.0	10.4625	8.5004
40.0	10.5403	8.6009
50.0	10.6445	8.6774
70.0	10.7412	8.8005
100.0	10.8617	8.9373
150.0	10.9571	9.0289
200.0	11.0048	9.0892
300.0	11.0563	9.1532

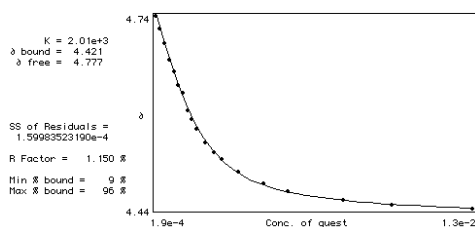


110+TBAOAc in CD_3CN

Conc of Host (M)	1.86E-03	Initial volume (μL)	600
Conc of Guest (M)	3.80E-02		

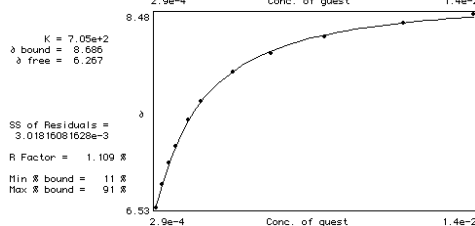
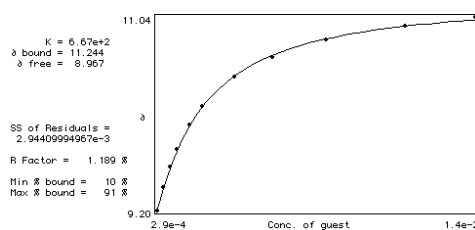
Volume of guest (μL)	δ NH pyrrole (ppm)	δ CH (ppm)
3.0	9.0389	4.74434996
6.0	9.2811	4.72305012
9.0	9.5473	4.69980001
12.0	9.7646	4.67344999
15.0	10.0331	4.65399981
18.0	10.2766	4.63329983
21.0	10.5201	4.61969995
24.0	10.7298	4.59250021
27.0	10.8766	4.57805014
30.0	11.0298	4.5630002
36.0	11.2294	4.54090023
42.0	11.3348	4.52535009
48.0	11.4001	4.51469994
60.0	11.4943	4.49459982
80	11.588	4.47580004
100	11.6449	4.46320009
150	11.7202	4.44934988
200	11.7579	4.44064999
300	11.7955	4.43555021



**110+TBAOAc in CD₃CN -1% water**

Conc of Host (M)	1.04E-03	Initial volume (μL)	600
Conc of Guest (M)	3.70E-02		

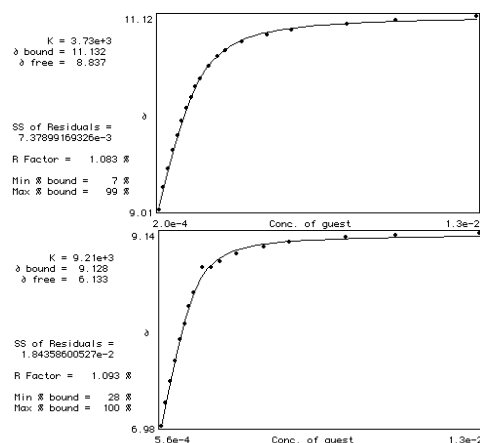
Volume of guest (μL)	δ NH pyrrole (ppm)	δ CONH (ppm)
3.0	9.2023	6.5289
6.0	9.4180	6.7611
9.0	9.6188	6.9798
12.0	9.7795	7.1490
18.0	10.0142	7.4126
24.0	10.1925	7.5946
30.0	10.4636	7.8902
40.0	10.6532	8.0855
50.0	10.8176	8.2474
70.0	10.9507	8.3905
100.0	11.0373	8.4796

**110+NBoc-L-PheOTBA in CD₃CN**

Conc of Host (M)	1.86E-03	Initial volume (μL)	600
Conc of Guest (M)	3.96E-02		

Volume of guest (μL)	δ NH pyrrole (ppm)
3	9.0050

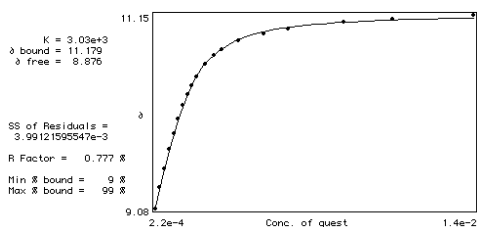
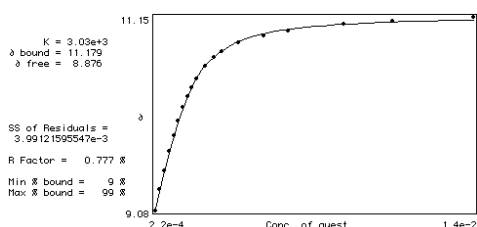
6	9.2447
9	9.4531
12	9.6477
15	9.8071
18	9.9703
21	10.1059
24	10.2264
27	10.3419
30	10.4298
36	10.5729
42	10.6771
48	10.7386
60	10.8365
80	10.9131
100	10.9608
150	11.0323
200	11.0725
300	11.1189

**110+NBoc-D-PheOTBA in CD₃CN**

Conc of Host (M)	1.86E-03	Initial volume (μL)	600
Conc of Guest (M)	4.32E-02		

Volume of guest (μL)	δ NH pyrrole (ppm)
3	9.0803
6	9.3087
9	9.5046
12	9.7172

15	9.8837
18	10.0331
21	10.1862
24	10.2967
27	10.3971
30	10.4888
36	10.6231
42	10.7172
48	10.7850
60	10.8729
80	10.9495
100	11.0009
150	11.0725
200	11.1089
300	11.1528

**Tweezer 139 + TBACl in CDCl₃**

Conc of Host (M)	2.20E-03	Initial volume (μL)	600
Conc of Guest (M)	7.70E-02		

Volume of guest (μL)	δ SNH (ppm)
0	5.1624
2	5.1674
4	5.1724
7	5.1799
10	5.1824
15	5.1837
20	5.1900
25	5.1975

30	5.2377
35	5.2703
45	5.2879
60	5.2891
80	5.3419
130	5.3745
230	5.4825

Tweezer 139 + TBAOAc in CDCl₃

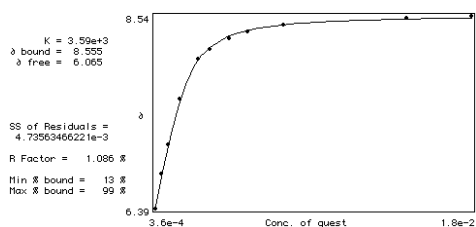
Conc of Host (M)	2.20E-03	Initial volume (μL)	600
Conc of Guest (M)	8.50E-02		

Volume of guest (μL)	δ SNH (ppm)
0	8.2467
5	8.2655
10	8.2806
15	8.2982
25	8.3245
35	8.3471
55	8.3885
105	8.4425
205	8.4777

Macrocycle 141 + TBA dihydrogenphosphate in CDCl₃

Conc of Host (M)	2.18E-03	Initial volume (μL)	600
Conc of Guest (M)	7.35E-02		

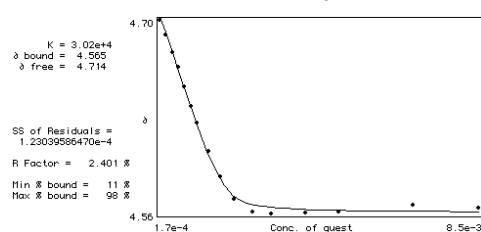
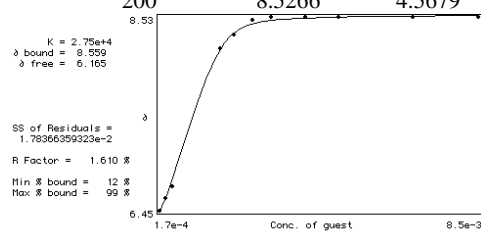
Volume of guest (μL)	δ SNH (ppm)
3	6.3938
6	6.7742
9	7.1018
15	7.6065
24	8.0571
30	8.1663
40	8.2843
50	8.3521
70	8.4312
150	8.5116
200	8.5354



Macrocycle 132 + TBAOAc in CDCl₃

Conc of Host (M)	1.85E-03	Initial volume (μL)	600
Conc of Guest (M)	3.40E-02		

Volume of guest (μL)	δ CONH (ppm)	δ CH (ppm)
3	6.4529	4.6967
6	6.5884	4.6859
9	6.7090	4.6740
12	-	4.6640
15	-	4.6508
18	-	4.6377
21	-	4.6263
27	-	4.6069
33	8.1965	4.5893
40	8.3367	4.5736
50	8.5003	4.5655
60	8.5279	4.5642
80	8.5291	4.5648
100	8.5254	4.5655
150	8.5329	4.5698
200	8.5266	4.5679

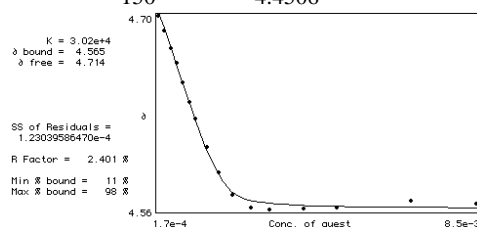


132+ TBAOBz in CDCl₃

Conc of Host (M)	1.85E-03	Initial volume (μL)	600
Conc of Guest (M)	3.40E-02		

Volume of guest (μL) δ CH (ppm)

3	4.6734
6	4.6389
9	4.5905
12	4.5648
15	4.5360
18	4.4920
21	4.4732
27	4.4450
33	4.4355
40	4.4380
50	4.4412
80	4.4431
100	4.4431
150	4.4506



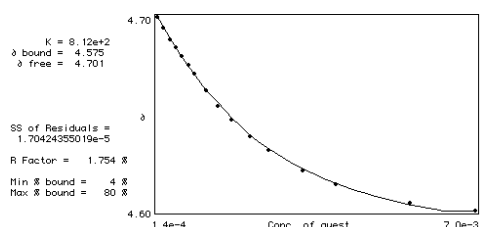
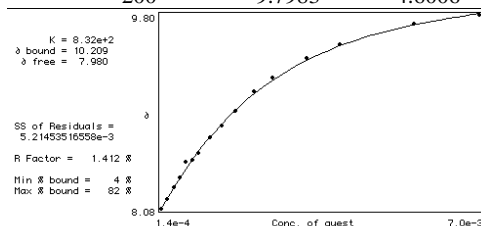
132+ TBACl in CDCl₃

Conc of Host (M)	1.85E-03	Initial volume (μL)	600
Conc of Guest (M)	2.80E-02		

Volume of guest (μL) δ pyrrole NH (ppm) δ CH (ppm)

3	8.0785	4.6960
6	8.1638	4.6904
9	8.2680	4.6847
12	8.3484	4.6810
15	8.4902	4.6765
18	8.5065	4.6722
21	8.5668	4.6678
27	8.7124	4.6596
33	8.8103	4.6521

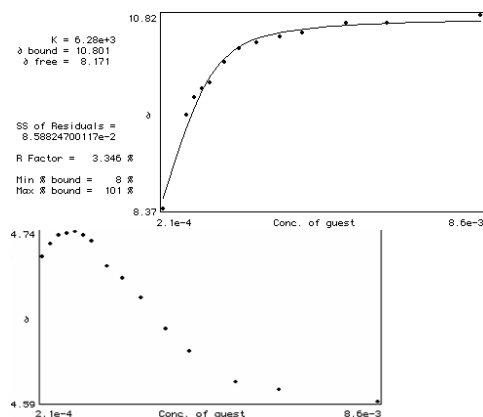
40	8.9384	4.6452
50	9.1141	4.6370
60	9.2340	4.6301
80	9.4104	4.6200
100	9.5321	4.6132
150	9.7142	4.6044
200	9.7983	4.6006



132+ TBA dihydrogenphosphate in CDCl₃

Conc of Host (M)	1.52E-03	Initial volume (μL)	600
Conc of Guest (M)	4.30E-02		

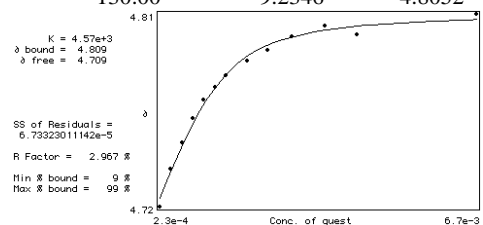
Volume of guest (μL)	δ NH pyrrole (ppm)	δ CH (ppm)
3.00	8.3697	4.7130
6.00	9.5497	4.7249
9.00	9.7794	4.7318
12.00	9.8849	4.7337
15.00	9.9602	4.7356
18.00	10.2213	4.7324
21.00	10.3983	4.7343
27.00	10.4736	4.7130
33.00	10.5402	4.6973
40.00	10.5920	4.6772
50.00	10.7109	4.6500
60.00	10.7134	4.6301
80.00	10.8214	4.6088
100.00	8.3697	4.5962
150.00	9.5497	4.5862



132+ TBA hydrogensulphate in CDCl₃

Conc of Host (M)	1.52E-03	Initial volume (μL)	600
Conc of Guest (M)	4.70E-02		

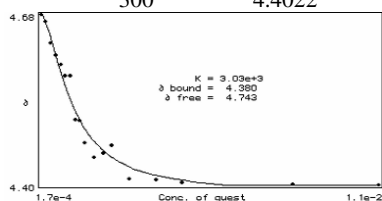
Volume of guest (μL)	δ NH pyrrole (ppm)	δ CH (ppm)
3.00	8.1789	4.7180
6.00	8.3534	4.7356
9.00	8.4952	4.7481
12.00	8.5994	4.7587
15.00	8.6948	4.7676
18.00	8.7551	4.7735
21.00	8.8126	4.7789
27.00	8.9007	0.7858
33.00	8.9670	4.7910
40.00	9.0087	4.7971
50.00	9.0677	4.8021
60.00	9.1016	4.7990
80.00	9.1580	4.7795
130.00	9.2346	4.8052



132+ NBoc-L-PheOTBA in CDCl₃

Conc of Host (M)	1.31E-03	Initial volume (μL)	600
Conc of Guest (M)	3.38E-02		

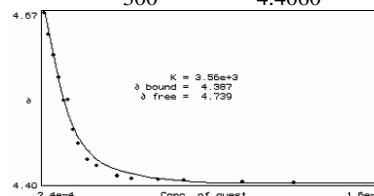
Volume of guest (μL)	δ NH pyrrole (ppm)
3	4.6847
6	4.6728
9	4.6376
12	4.6175
15	4.6006
18	4.5824
21	4.5824
24	4.5102
27	4.5083
30	4.4720
36	4.4475
42	4.4550
48	4.4667
60	4.4110
80	4.4104
100	4.4061
200	4.4035
300	4.4022

**132+ NBoc-D-PheOTBA in CDCl₃**

Conc of Host (M)	Initial volume (μL)	600
1.31E-03		
Conc of Guest (M)	4.83E-02	

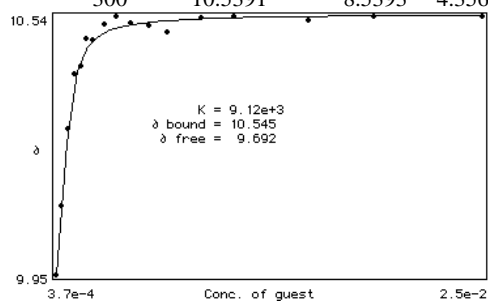
Volume of guest (μL)	δ NH pyrrole (ppm)
3	4.6747
6	4.6401
9	4.6062
12	4.5711
15	4.5335
18	4.5353
21	4.4864
24	4.4637
30	4.4380
36	4.4286
50	4.4117

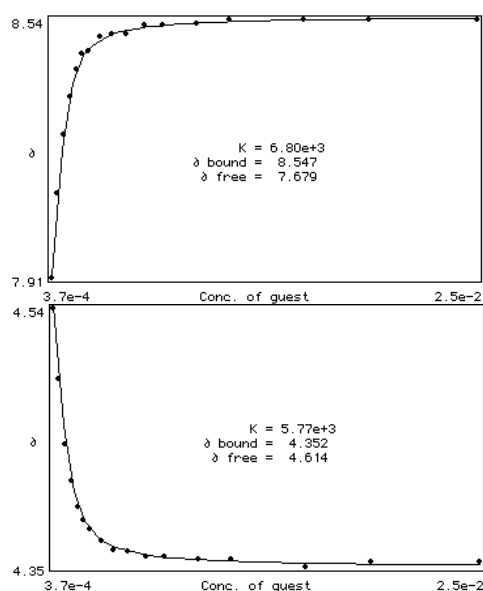
60	4.4085
80	4.4065
100	4.4054
150	4.4023
200	4.4016
300	4.4060

**132+TBAOAc in DMSO-*d*₆ -0.5% water**

Conc of Host (M)	Initial volume (μL)	600
1.18E-03		
Conc of Guest (M)	7.40E-02	

Volume of guest (μL)	δ pyrrole NH (ppm)	δ CONH (ppm)	δ CH (ppm)
3	9.9478	7.9099	4.5437
6	10.106	8.1151	4.4915
9	10.2805	8.2569	4.4432
12	10.4048	8.3511	4.4159
15	10.4236	8.4163	4.3968
18	10.4876	8.4540	4.3868
21	10.4839	8.4628	4.3805
27	10.5203	8.4962	4.3717
33	10.5378	8.5030	4.3654
40	10.5228	8.5030	4.3642
50	10.5178	8.5243	4.3604
60	10.5027	8.5243	4.3604
80	10.5353	8.5268	4.3579
100	10.5366	8.5362	4.3579
150	10.529	8.5387	4.3529
200	10.5391	8.5374	4.356
300	10.5391	8.5393	4.3566

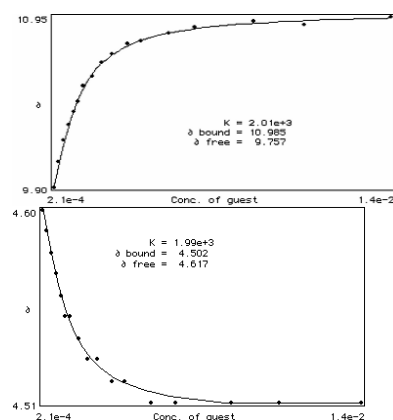




132+TBAOBz in DMSO-*d*₆-0.5% water

Conc of Host (M)	1.07E-03	Initial volume (μL)	600
Conc of Guest (M)	4.30E-02		

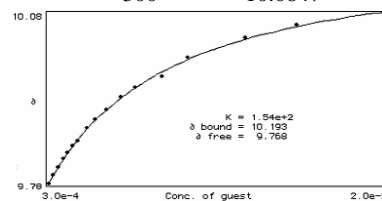
Volume of guest (μL)	δ pyrrole NH (ppm)	δ CH (ppm)
3	9.9039	4.6033
6	10.0583	4.5895
9	10.1926	4.5750
12	10.2855	4.5656
15	10.3684	4.5625
18	10.4311	4.5480
21	10.5254	4.5468
27	10.5805	4.5437
33	10.6672	4.5324
40	10.7186	4.5299
50	10.7826	4.5211
60	10.8015	4.5190
80	10.8441	4.5110
100	10.8831	4.5085
150	10.9207	4.5070
200	10.9019	4.5079
300	10.9496	4.5073



132+TBACl in DMSO-*d*₆-0.5% water

Conc of Host (M)	1.07E-03	Initial volume (μL)	600
Conc of Guest (M)	6.40E-02		

Volume of guest (μL)	δ pyrrole NH (ppm)
3	9.7846
6	9.7997
9	9.8123
12	9.8273
15	9.8386
18	9.8499
21	9.8600
27	9.8830
33	9.8976
40	9.9139
50	9.9365
60	9.9541
80	9.9729
100	10.0068
150	10.0420
200	10.0646
300	10.0847

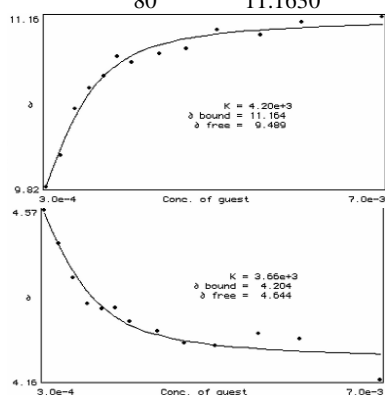


132+TBAdihydrogenphosphate in DMSO-*d*₆-0.5% water

Conc of Host (M)	1.18E-03	Initial volume (μL)	600
Conc of Guest	5.97E-02		

(M)

Volume of guest (μL)	δ pyrrole NH (ppm)	δ CH (ppm)
3	9.8217	4.5675
6	10.0671	4.4872
9	10.4349	4.4056
12	10.5993	4.3428
15	10.6922	4.3303
18	10.8454	4.3340
21	10.8027	4.3000
27	10.8655	4.2775
33	10.9119	4.2499
40	11.0575	4.2421
50	11.0174	4.2713
60	11.1165	4.2587
80	11.1630	4.1620

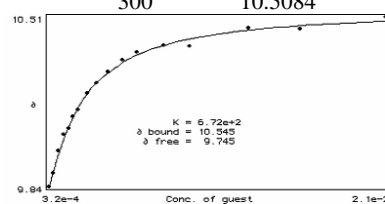


132+ NBoc-L-PheOTBA in DMSO-*d*₆-0.5% water

Conc of Host (M)	1.28E-03	Initial volume (μL)	600
Conc of Guest (M)	6.40E-02		

Volume of guest (μL)	δ NH pyrrole (ppm)
3	9.8374
6	9.8888
9	9.9780
12	10.0407
15	10.0671
18	10.1136
21	10.1411

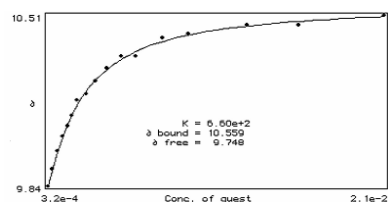
27	10.2056
33	10.2472
40	10.2899
50	10.3376
60	10.3684
80	10.3934
100	10.3922
150	10.4619
200	10.4581
300	10.5084



132+ NBoc-D-PheOTBA in DMSO-*d*₆-0.5% water

Conc of Host (M)	1.28E-03	Initial volume (μL)	600
Conc of Guest (M)	6.40E-02		

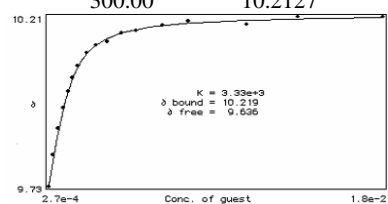
Volume of guest (μL)	δ NH pyrrole (ppm)
3	9.8386
6	9.9052
9	9.9761
12	10.0319
15	10.0722
18	10.1136
21	10.1750
27	10.1989
33	10.2491
40	10.3012
50	10.3490
60	10.3483
80	10.4179
100	10.4342
150	10.4694
200	10.4689
300	10.5083

**Macrocycle 133****133+TBAOAc in DMSO-*d*₆-0.5% water**

Conc of Host (M)	1.30E-03	Initial volume (μL)	600
Conc of Guest (M)	5.38E-02		

Volume of guest (μL) δ NH pyrrole (ppm)

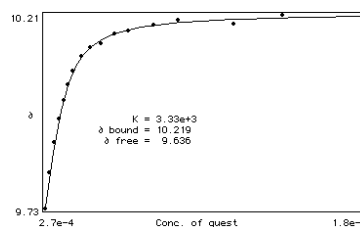
3.00	9.7269
6.00	9.8160
9.00	9.8926
12.00	9.9516
15.00	9.9980
18.00	10.0382
21.00	10.0721
27.00	10.1085
33.00	10.1311
40.00	10.1412
50.00	10.1650
60.00	10.1725
80.00	10.1863
100.00	10.1989
150.00	10.1901
200.00	10.2127
300.00	10.2127

**133+TBA dihydrogenphosphate in DMSO-*d*₆-0.5% water**

Conc of Host (M)	1.30E-03	Initial volume (μL)	600
Conc of Guest (M)	5.80E-02		

Volume of guest (μL) δ NH pyrrole (ppm)

3.00	9.7269
6.00	9.8160
9.00	9.8926
12.00	9.9516
15.00	9.9980
18.00	10.0382
21.00	10.0721
27.00	10.1085
33.00	10.1311
40.00	10.1412
50.00	10.1650
60.00	10.1725
80.00	10.1863
100.00	10.1989
150.00	10.1901
200.00	10.2127
300.00	10.2127

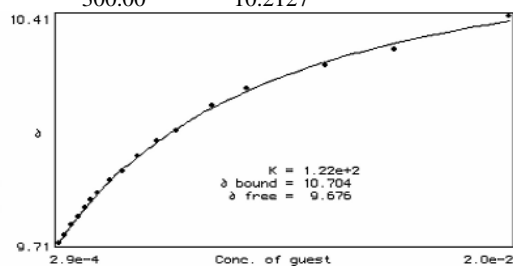
**133+NBoc-L-PheOTBA in DMSO-*d*₆-0.5% water**

Conc of Host (M)	1.30E-03	Initial volume (μL)	600
Conc of Guest (M)	5.38E-02		

Volume of guest (μL) δ NH pyrrole (ppm)

3.00	9.7269
6.00	9.8160
9.00	9.8926
12.00	9.9516
15.00	9.9980
18.00	10.0382
21.00	10.0721
27.00	10.1085

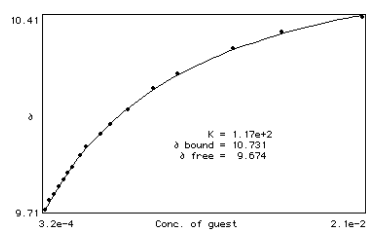
33.00	10.1311
40.00	10.1412
50.00	10.1650
60.00	10.1725
80.00	10.1863
100.00	10.1989
150.00	10.1901
200.00	10.2127
300.00	10.2127



133+ NBoc-D-PheOTBA in DMSO-*d*₆-0.5% water

Conc of Host (M)	1.29E-03	Initial volume (μL)	600
Conc of Guest (M)	6.40E-02		

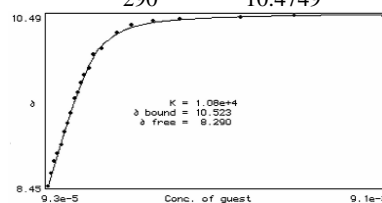
Volume of guest (μL)	δ NH pyrrole (ppm)
3.00	9.7106
6.00	9.7432
9.00	9.7658
12.00	9.7922
15.00	9.8198
18.00	9.8436
21.00	9.8661
26.00	9.9064
30.00	9.9390
40.00	9.9865
47.00	10.0206
60.00	10.0721
80.00	10.1525
100.00	10.2064
150.00	10.2981
200.00	10.3557
300.00	10.4123



Macrocycle 134 134+ NBoc-L-PheOTBA in CD₃CN

Conc of Host (M)	1.36E-03	Starting volume (μL)	600
Conc of Guest (M)	2.79E-02		

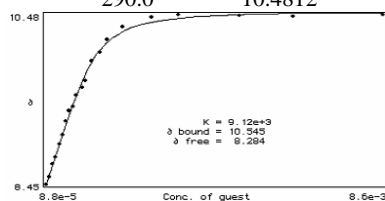
Volume of guest (μL)	δ NH pyrrole (ppm)
2	8.4451
4	8.5932
6	8.7401
8	8.8292
10	8.9309
12	9.0953
14	9.1938
16	9.3226
18	9.4895
20	9.5699
22	9.6797
24	9.7732
27	9.8510
30	10.0180
35	10.0896
45	10.2779
55	10.3745
70	10.4260
90	10.4385
140	10.4687
190	10.4900
290	10.4749



134+ NBoc-D-PheOTBA in CD₃CN

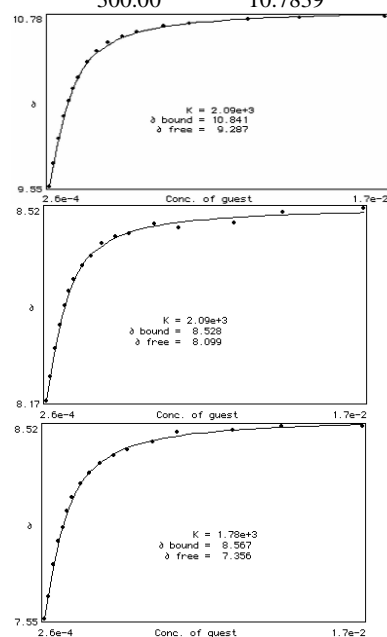
Conc of Host (M)	0.00136000	Starting volume	600
------------------	------------	-----------------	-----

		(μL)				
Conc of Guest (M)	0.02640000		12.00	10.0608	8.3109	7.9418
			15.00	10.1713	8.3467	8.0146
			18.00	10.2611	8.3724	8.0862
Volume of guest (μL)	δ NH pyrrole (ppm)		21.00	10.3420	8.3937	8.1571
2.0	8.4489		27.00	10.4500	8.4189	8.2280
4.0	8.5392		33.00	10.5341	8.4364	8.2833
6.0	8.6866		40.00	10.5918	8.4590	8.3297
8.0	8.7765		50.00	10.6383	8.4728	8.3705
10.0	8.9246		60.00	10.6720	8.4777	8.4038
12.0	9.0414		80.00	10.7111	8.4942	8.4358
14.0	9.2033		100.00	10.7337	8.4873	8.4941
16.0	9.3226		150.00	10.7638	8.4967	8.4967
18.0	9.3740		200.00	10.7738	8.5168	8.5168
20.0	9.5146		300.00	10.7839	8.5243	8.5243
24.0	9.6075					
26.0	9.6869					
30.0	9.9226					
35.0	10.0230					
40.0	10.1812					
50.0	10.3356					
70.0	10.4423					
90.0	10.4712					
140.0	10.4687					
190.0	10.4574					
290.0	10.4812					



134+ TBAOAc in DMSO- d_6 -0.5% water

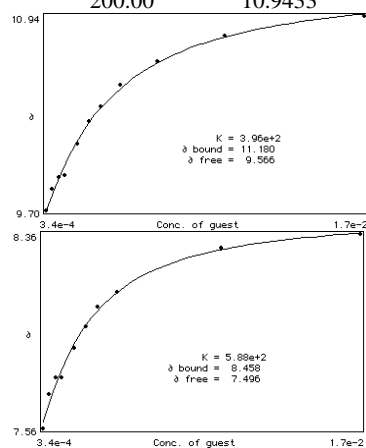
Conc of Host (M)	1.10E-03	Initial volume (μL)	600
Conc of Guest (M)	5.20E-02		
Volume of guest (μL)	δ NH pyrrole (ppm)	δ CONH (ppm)	δ CONH (ppm)
3.00	9.5534	8.1728	7.5464
6.00	9.7206	8.2155	7.6644
9.00	9.8964	8.2682	7.8150



134+ TBAOBz in DMSO- d_6 -0.5% water

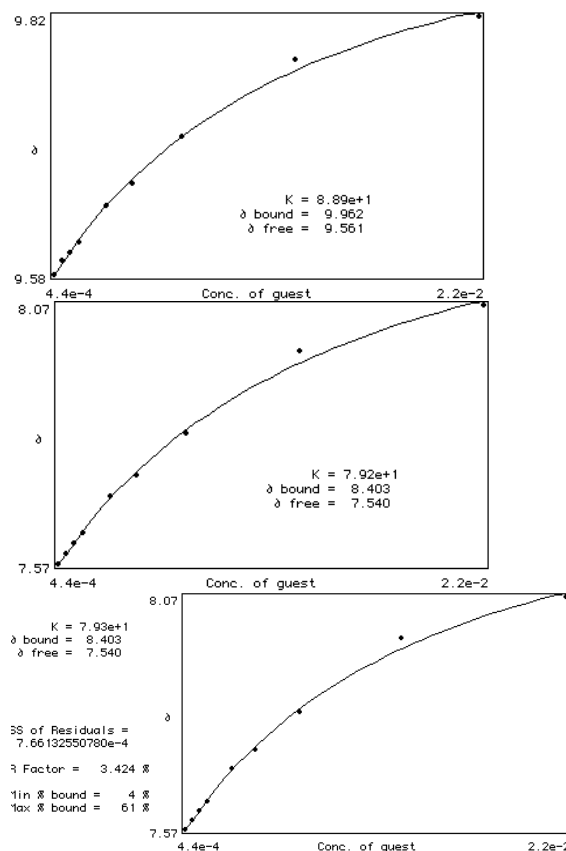
Conc of Host (M)	1.76E-03	Initial volume (μL)	600
Conc of Guest (M)	6.88E-02		
Volume of guest (μL)	δ NH pyrrole (ppm)	δ CONH (ppm)	
3.00	9.6955	7.5564	
6.00	9.8311	7.7033	
9.00	9.9089	7.7711	

12.00	9.9215	7.7749
18.00	10.1198	7.8904
24.00	10.2667	7.9757
30.00	10.3596	8.0596
40.00	10.5014	8.1238
60.00	10.6496	-
100.00	10.8165	8.3034
200.00	10.9433	8.3647

**134+ TBACl in DMSO-*d*₆-0.5% water**

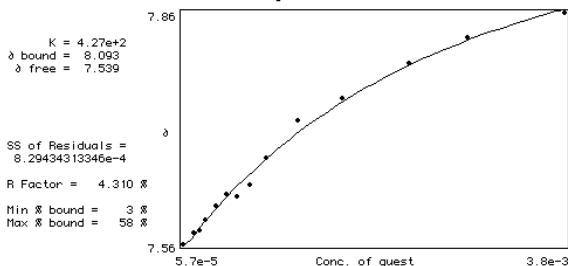
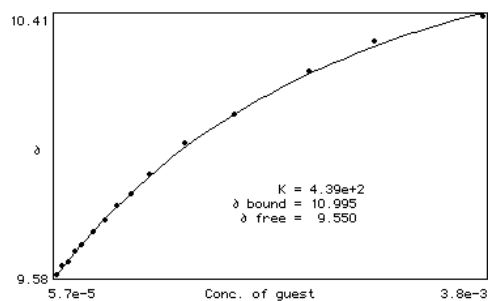
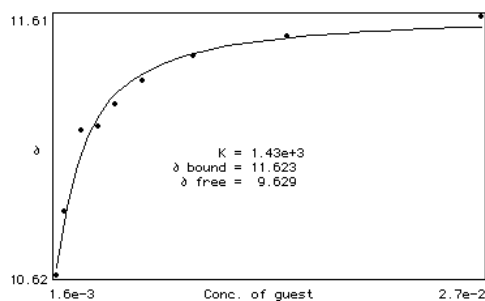
Conc of Host (M)	1.76E-03	Initial volume (μL)	600
Conc of Guest (M)	8.77E-02		

Volume of guest (μL)	δ NH pyrrole (ppm)	δ CONH (ppm)	δ CONH (ppm)
0.00	9.5637	8.1904	7.5439
3.00	9.5763	8.1916	7.5677
6.00	9.5967	8.1954	7.5928
9.00	9.6064	8.1967	7.6117
12.00	9.6403	8.1967	7.633
22.00	9.6604	8.1992	7.697
32.00	9.7043	8.2092	7.7372
52.00	9.7771	8.1967	7.8201
102.00	9.8173	8.2067	7.9795
202.00	10.6496	8.2105	7.0686

**134+ TBA dihydrogen phosphate in DMSO-*d*₆-0.5% water**

Conc of Host (M)	1.37E-03	Initial volume (μL)	600
Conc of Guest (M)	3.84E-02		

Volume of guest (μL)	δ NH pyrrole (ppm)	δ CONH (ppm)	δ CONH (ppm)
0.00	9.5637	8.1904	7.5439
3.00	-	8.1841	-
6.00	-	8.1628	-
9.00	10.6163	8.1678	-
12.00	10.8617	8.1615	8.9976
18.00	11.1718	-	9.3189
24.00	11.1843	8.1628	9.3340
30.00	11.2709	8.1766	9.3867
40.00	11.3613	8.2230	9.4997
60.00	11.4555	8.2770	9.6327
100.00	11.5308	8.3762	9.6905
200.00	11.6111	8.5846	9.8374



134+ NBoc-D-PheOTBA in DMSO- d_6 0.5% water

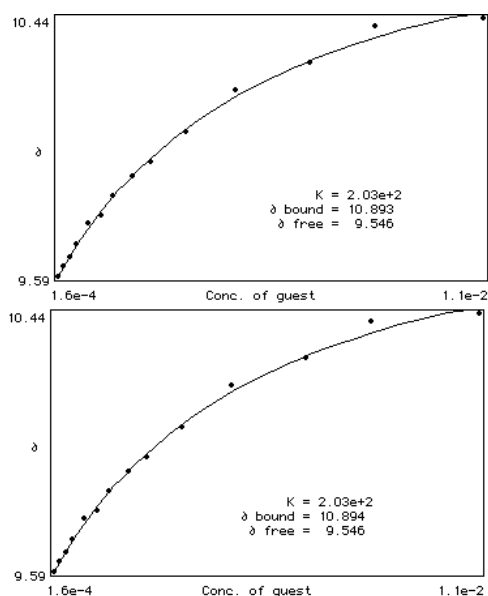
Conc of Host (M)	6.49E-04	Starting volume (μL)	600
Conc of Guest (M)	3.28E-02		

Volume of guest (μL)	δ NH pyrrole (ppm)	δ CONH (ppm)
3.00	9.5863	7.5564
6.00	9.6189	7.0000
9.00	9.6503	9.6240
12.00	9.6917	9.6556
18.00	9.7620	9.6792
24.00	9.7859	9.7181
30.00	9.8512	9.7570
40.00	9.9165	9.8010
50.00	9.9610	9.8374
70.00	10.0590	9.9001
100.00	10.2002	10.0000
150.00	10.2868	10.0922
200.00	10.4098	10.2290
300.00	10.4367	10.3269

134+ NBoc-L-PheOTBA in DMSO- d_6 0.5% water

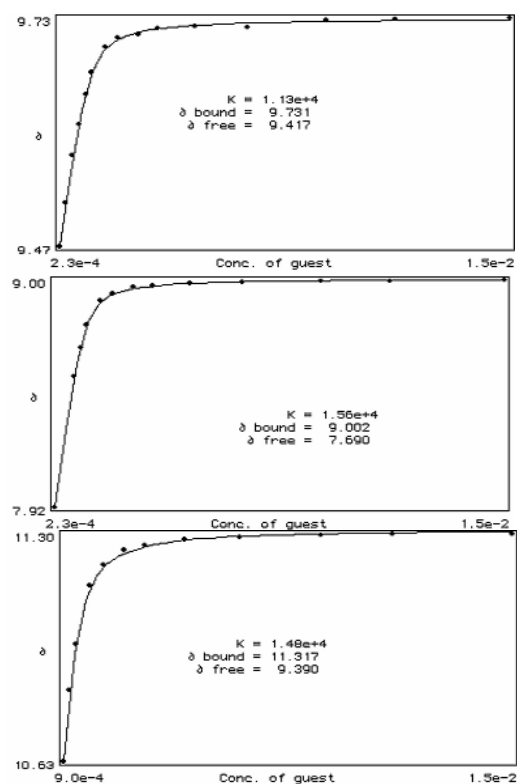
Conc of Host (M)	1.31E-03	Starting volume (μL)	600
Conc of Guest (M)	3.38E-02		

Volume of guest (μL)	δ NH pyrrole (ppm)	δ CONH (ppm)
3	9.5838	7.5640
6	9.6127	7.2665
9	9.2640	7.5715
12	9.6556	7.5740
15	9.6792	7.5878
21	9.7181	7.6067
27	9.7570	7.6217
33	9.8010	7.6192
40	9.8374	7.6343
50	9.9001	7.6694
70	10.0000	7.7200
100	10.0922	7.7485
150	10.2290	7.7950
200	10.3269	7.8301
300	10.4060	7.8627

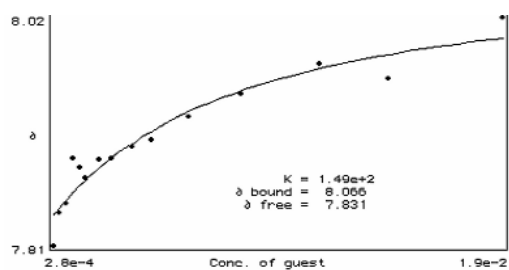
**Macrocycle 150****150 + TBAOAc in DMSO-*d*₆ 0.5 water**

Conc of Host (M)	1.22E-03	Starting volume (μL)	600
Conc of Guest (M)	4.61E-02		

Volume of guest (μL)	δ NH pyrrole (ppm)	δ CONH (ppm)	δ CONH (ppm)
3	9.4721	-	7.9243
6	9.5210	-	-
9	9.5750	-	-
12	9.6102	10.6320	8.5381
15	9.6440	10.8404	8.6743
18	9.6692	10.9759	8.7841
24	9.6980	11.1467	8.8971
30	9.7093	11.2094	8.9310
40	9.7131	11.2534	8.9611
50	9.7156	11.2659	8.9687
70	9.7219	11.2848	8.9797
100	9.7206	11.2898	8.9837
150	9.7282	11.2973	8.9900
200	9.7294	11.3010	8.9875
300	9.7319	11.3023	8.9976

**150 + TBAhydrogen sulphate in DMSO-*d*₆ 0.5 water**

Conc of Host (M)	1.22E-03	Starting volume (μL)	600
Conc of Guest (M)	5.60E-02		
Volume of guest (μL)	δ CONH (ppm)		
3	7.8113		
6	7.8169		
9	7.8502		
15	7.8653		
18	7.8728		
24	8.8904		
30	7.8916		
40	7.9017		
70	7.9507		
100	7.9506		

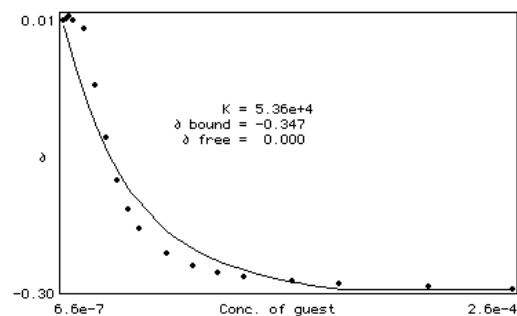


4.8 UV titrations

105 + TBA dihydrogenphosphate in CH_3CN

Conc of Host (M)	1.86E-05	Starting volume (μL)	2500
Conc of Guest (M)	1.59E-03		

Volume of guest (μL)	ΔA (298nm)
1	0.0013
4	0.0024
7	0.0064
10	0.0103
20	-0.0081
30	-0.0733
40	-0.133
50	-0.1801
60	-0.2135
70	-0.236
95	-0.2646
120	-0.2782
145	-0.2857
170	-0.2902
220	-0.2957
270	-0.2979
370	-0.3016
407	-0.3039



105 + TBAOAc in CH_3CN

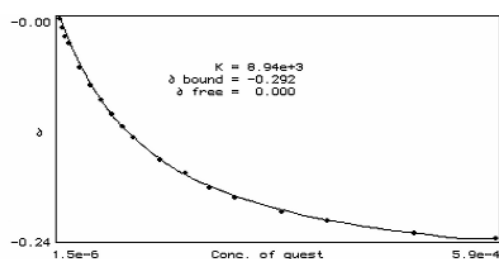
Conc of Host (M)	1.86E-05	Starting volume (μL)	2500
Conc of Guest (M)	3.38E-03		

Volume of guest (μL)	ΔA (298nm)
1	-0.0034
4	-0.0142
7	-0.0229
10	-0.0304
20	-0.0546
30	-0.0753
40	-0.0915
50	-0.1069
60	-0.1206
70	-0.1319
95	-0.1557
120	-0.1709
145	-0.1864
170	-0.1973

106 + TBAOAc in CH_3CN

Conc of Host (M)	1.89E-05	Starting volume (μL)	2500
Conc of Guest (M)	2.93E-03		

Volume of guest (μL)	ΔA (298nm)
4	0.0103
8	0.0236

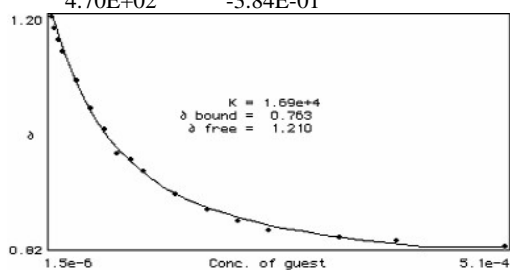


12	0.0375
20	0.0598
30	0.0692
40	0.0687
50	0.0646
60	0.0608
85	0.0514
135	0.0448
160	0.0403
210	0.0372
260	0.0342
360	0.0326
460	0.0283

107 + TBAOAc in CH₃CN

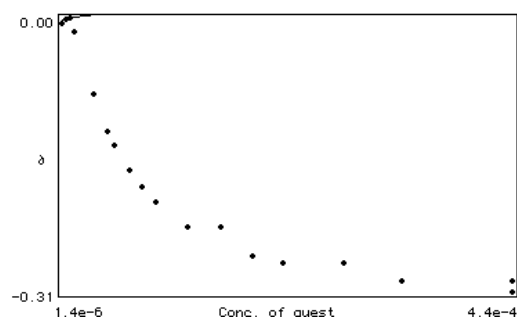
Conc of Host (M)	1.86E-05	Starting volume (μL)	2500
Conc of Guest (M)	3.38E-03		

Volume of guest (μL)	ΔA (298nm)
1.00E+00	0.00E+00
4.00E+00	-1.95E-02
7.00E+00	-3.89E-02
1.00E+01	-5.69E-02
2.00E+01	-1.05E-01
3.00E+01	-1.51E-01
4.00E+01	-1.86E-01
5.00E+01	-2.25E-01
6.00E+01	-2.35E-01
7.00E+01	-2.53E-01
9.50E+01	-2.90E-01
1.20E+02	-3.16E-01
1.45E+02	-3.35E-01
1.70E+02	-3.49E-01
2.20E+02	-3.61E-01
2.70E+02	-3.67E-01
3.80E+02	-3.75E-01
4.70E+02	-3.84E-01

**107 + TBAdihydrogenphosphate in CH₃CN**

Conc of Host (M)	2.93E-05	Starting volume (μL)	2500
Conc of Guest (M)	3.42E-03		

Volume of guest (μL)	ΔA (298nm)
1.00E+00	-3.20E-03
4.00E+00	6.00E-04
7.00E+00	3.20E-03
1.00E+01	-1.38E-02
2.40E+01	-8.47E-02
3.40E+01	-1.28E-01
4.00E+01	-1.44E-01
5.10E+01	-1.73E-01
6.00E+01	-1.93E-01
7.00E+01	-2.09E-01
9.50E+01	-2.39E-01
1.20E+02	-2.39E-01
1.45E+02	-2.71E-01
1.70E+02	-2.80E-01
2.20E+02	-2.80E-01
2.70E+02	-3.01E-01
3.70E+02	-3.01E-01
3.70E+02	-3.13E-01



4.9 NMR Job Plots

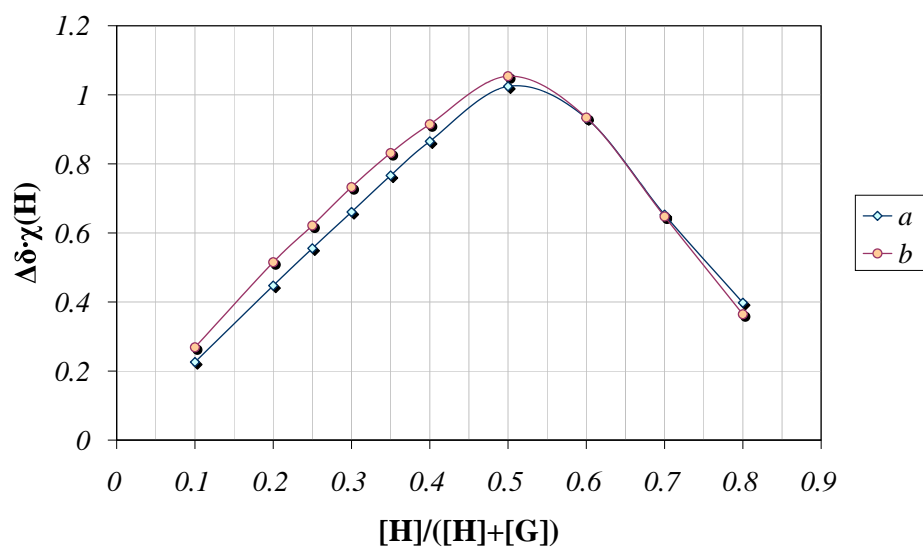
105 + TBAOAc in CD₃CN

NH pyrrole

Number	X	δ	$\Delta\delta$	$\chi \Delta\delta$	
0	0	8.9083			
1	0.1	11.1679	-2.2596	-0.22596	0.22596
2	0.2	11.1453	-2.237	-0.4474	0.4474
3	0.25	11.1302	-2.2219	-0.55548	0.555475
4	0.3	11.1101	-2.2018	-0.66054	0.66054
5	0.35	11.0976	-2.1893	-0.76626	0.766255
6	0.4	11.0712	-2.1629	-0.86516	0.86516
8	0.5	10.957	-2.0487	-1.02435	1.02435
9	0.6	10.4624	-1.5541	-0.93246	0.93246
10	0.7	9.841	-0.9327	-0.65289	0.65289
11	0.8	9.4054	-0.4971	-0.39768	0.39768

NHAmide

Number	χ	δ	$\Delta\delta$	$\chi \Delta\delta$	
0	0	6.6261			
1	0.1	9.3133	-2.6872	-0.26872	0.26872
2	0.2	9.202	-2.5759	-0.51518	0.51518
3	0.25	9.1117	-2.4856	-0.6214	0.6214
4	0.3	9.0677	-2.4416	-0.73248	0.73248
5	0.35	9.0012	-2.3751	-0.83129	0.831285
6	0.4	8.9127	-2.2866	-0.91464	0.91464
8	0.5	8.7338	-2.1077	-1.05385	1.05385
9	0.6	8.1827	-1.5566	-0.93396	0.93396
10	0.7	7.5513	-0.9252	-0.64764	0.64764
11	0.8	7.0818	-0.4557	-0.36456	0.36456



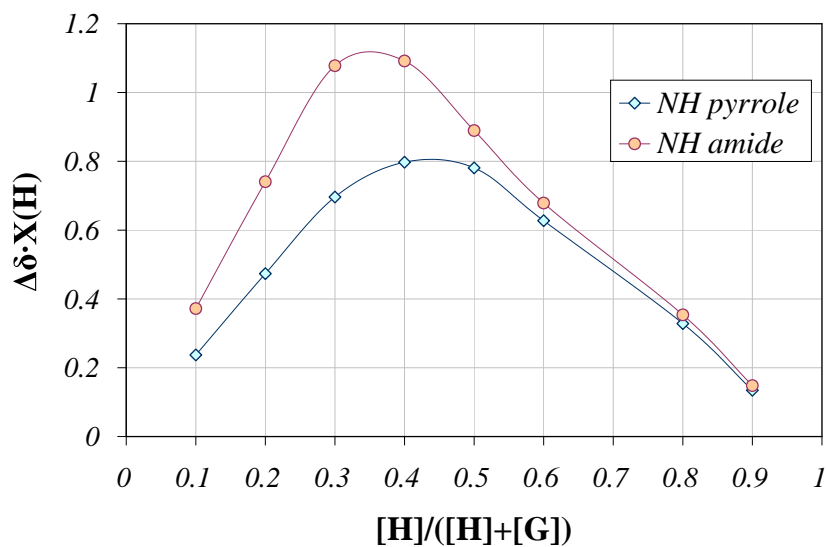
106 + TBAOAc in CD_3CN

NH pyrrole

Number	X	δ	$\Delta\delta$	$\chi \Delta\delta$
0	0	8.9786		
1	0.1	11.3512	2.3726	0.23726
2	0.2	11.3464	2.3678	0.47356
3	0.3	11.2997	2.3211	0.69633
4	0.4	10.9721	1.9935	0.7974
5	0.5	10.5402	1.5616	0.7808
6	0.6	10.0243	1.0457	0.62742
7	0.8	9.3891	0.4105	0.3284
8	0.9	9.128	0.1494	0.13446

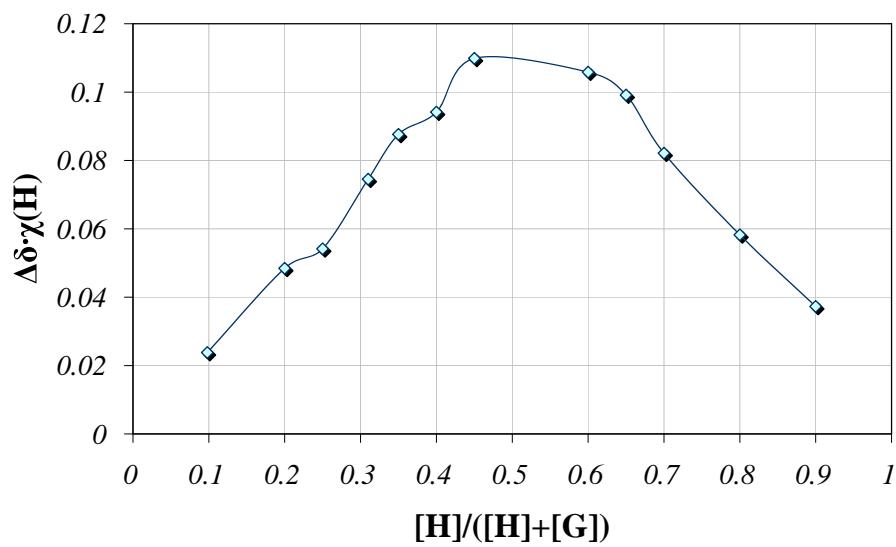
NH amide

Number	X	δ	$\Delta\delta$	$\chi \Delta\delta$
0	0	6.6412		
1	0.1	10.3601	3.71895	0.371895
2	0.2	10.3444	3.70325	0.74065
3	0.3	10.2340	3.5928	1.07784
4	0.4	9.3703	2.72915	1.09166
5	0.5	8.4200	1.77885	0.889425
6	0.6	7.7723	1.1311	0.67866
7	0.8	7.0831	0.44195	0.35356
8	0.9	6.8056	0.16445	0.148005

**107 + TBAOAc in CD₃CN**

CH

Number	X	δ	$\Delta\delta$	$\chi \Delta\delta$
0	0	4.83165		
1	0.098	4.58875	0.2429	0.023804
2	0.2	4.58935	0.2423	0.04846
3	0.25	4.61505	0.2166	0.05415
4	0.31	4.59125	0.2404	0.074524
5	0.35	4.58125	0.2504	0.08764
6	0.4	4.5963	0.23535	0.09414
7	0.45	4.5875	0.24415	0.109868
8	0.5	4.6741	0.15755	0.078775
9	0.55	4.6678	0.16385	0.090118
10	0.6	4.65525	0.1764	0.10584
11	0.65	4.6791	0.15255	0.099157
12	0.7	4.7143	0.11735	0.082145
13	0.8	4.75885	0.0728	0.05824
14	0.9	4.7902	0.04145	0.037305



Appendix A

Software for the determination of association constants from NMR binding studies¹³⁹

NMRTit HG

NMRTit HG fits the data to a 1:1 binding isotherm by solving the equations (1) – (3) in which $[H]_0$ is the total concentration of host; $[G]_0$ is the total concentration of guest; $[H]$ is the concentration of unbound free host; $[HG]$ is the concentration of host + guest complex; K is the association constant for the formation of the host-guest complex; δ_f is the free chemical shift of the host; δ_b is the limiting bound chemical shift of the host-guest complex.

$$[HG] = \frac{1 + K[H]_0[G]_0 - \sqrt{\{(1 + [H]_0[G]_0)^2 - 4K^2[H]_0[G]_0\}}}{2K} \quad (1)$$

$$[H] = [H]_0 - [HG] \quad (2)$$

$$\delta_{obs} = \frac{[HG]}{[H]_0} \delta_b + \frac{[H]}{[H]_0} \delta_f \quad (3)$$

NMRTit HGG

NMRTit HGG fits the data to a 1:2 binding isotherm by an iterative procedure to solve the following simultaneous equations. The method starts by assuming the $[HGG] = 0$, so that Equation (4) can be solved exactly for $[HG]$. This value of $[HG]$ is the used to solve Equation (5) for $[HGG]$. Equation (6) gives the concentration of free host $[H]$. At this point, $[H] + [HG] + [HGG] \neq [H]_0$ so the value of $[HGG]$ from equation (5) is used in equation (4) to re-evaluate $[HG]$.

$$[HG] = \frac{1 + 2K_1[G]_0([H]_0 - [HGG]) - \sqrt{\{(1 + 2K_1[G]_0([H]_0 - [HGG]))^2 - 16K_1^2[G]_0([H]_0 - [HGG])\}}}{4K_1} \quad (4)$$

$$[HGG] = \frac{1 + 0.5K_2[G]_0([H]_0 - [HG]) - \sqrt{\{(1 + 0.5K_2[G]_0([H]_0 - [HG]))^2 - K_2[G]_0([H]_0 - [HG])\}}}{K_2} \quad (5)$$

$$[H] = [H]_0 - [HG] - [HGG] \quad (6)$$

$$\delta_{obs} = \frac{[HGG]}{[H]_0} \delta_{b2} + \frac{[HG]}{[H]_0} \delta_{b1} + \frac{[H]}{[H]_0} \delta_f \quad (7)$$

This procedure is reiterated until $[H] + [HG] + [HGG] = [H]_0$. This allows the set of simultaneous equations [Eq. (4)-(7)] to be solved for the concentrations of all species present where $[HGG]$ is the concentration of host·(guest)₂ complex; K_1 is the microscopic association constant for formation of the host·guest complex; K_2 is the microscopic association constant for formation of the host·(guest)₂ complex; δ_{b2} is the limiting bound chemical shift of the host·(guest)₂ complex. In order to calculate the macroscopic constants, the microscopic values have to be converted as follows: $K_{1mac} = 2 \cdot K_{1mic}$, $K_{2mac} = 0.5 \cdot K_{2mic}$.

References

- (1) Vega, I. E.; Gale, P. A.; Hursthouse, M. B.; Light, M. E. *Org. Biomol. Chem.* **2004**, *2*, 2935-2941.
- (2) Pedersen, C. J. *Angew. Chem. Int. Ed. Eng.* **1988**, *27*, 1021-1027.
- (3) Lehn, J. M. *Angew. Chem. Int. Ed. Eng.* **1988**, *27*, 89-112.
- (4) Wolf, K. L. *Angew. Chem.* **1949**, *61*, 191-201.
- (5) Ehrlich, P. *Studies on Immunity*; Wiley: New York, 1906.
- (6) Fisher, E. *Ber. Deutsch. Chem. Ges.* **1894**, *27*, 2985.
- (7) Lehn, J.-M. *Supramolecular Chemistry- concepts and perspectives*; VCH, 1995.
- (8) Schmidtchen, F. P. *Angew. Chem. Int. Ed. Eng.* **1977**, *16*, 720-721.
- (9) Aakeroy, C. B.; Seddon, K. R. *Chem. Soc. Rev.* **1993**, *22*, 397-407.
- (10) Turner, D. H.; Sugimoto, N.; Kierzek, R.; Dreiker, S. D. *J. Am. Chem. Soc.* **1987**, *109*, 3783-3785.
- (11) Chang, S. K.; Vanengen, D.; Fan, E.; Hamilton, A. D. *J. Am. Chem. Soc.* **1991**, *113*, 7640-7645.
- (12) Lenthall, J. T.; Steed, J. W. *Coord. Chem. Rev.* **2007**, *251*, 1747-1760.
- (13) Harrowfield, J. M.; Ogden, M. I.; Richmond, W. R.; White, A. H. *J. C -Chem. Commun.* **1991**, 1159-1161.
- (14) De Wall, S. L.; Meadows, E. S.; Barbour, L. J.; Gokel, G. W. *J. Am. Chem. Soc.* **1999**, *121*, 5613-5614.
- (15) Hunter, C. A.; Sanders, J. K. M. *J. Am. Chem. Soc.* **1990**, *112*, 5525-5534.
- (16) Cozzi, F.; Cinquini, M.; Annunziata, R.; Dwyer, T.; Siegel, J. S. *J. Am. Chem. Soc.* **1992**, *114*, 5729-5733.
- (17) Carver, F. J.; Hunter, C. A.; Livingstone, D. J.; McCabe, J. F.; Seward, E. M. *Chem. Eur. J.* **2002**, *8*, 2848-2859.
- (18) Aoyama, Y.; Asakawa, M.; Matsui, Y.; Ogoshi, H. *J. Am. Chem. Soc.* **1991**, *113*, 6233-6240.
- (19) Aoyama, Y.; Asakawa, M.; Yamagishi, A.; Toi, H.; Ogoshi, H. *J. Am. Chem. Soc.* **1990**, *112*, 3145-3151.
- (20) Kato, Y.; Conn, M. M.; Rebek, J., Jr. *J. Am. Chem. Soc.* **1994**, *116*, 3279-3284.
- (21) Adams, H.; Carver, F. J.; Hunter, C. A.; Morales, J. C.; Seward, E. M. *Angew. Chem. Int. Ed. Eng.* **1996**, *35*, 1542-1544.
- (22) Smithrud, D. B.; Diederich, F. *J. Am. Chem. Soc.* **1990**, *112*, 339-343.
- (23) Dijkstra, P. J.; Brunink, J. A. J.; Bugge, K. E.; Reinhoudt, D. N.; Harkema, S.; Ungaro, R.; Ugozzoli, F.; Ghidini, E. *J. Am. Chem. Soc.* **1989**, *111*, 7567-7575.
- (24) Stewart, K. D.; Miesch, M.; Knobler, C. B.; Maverick, E. F.; Cram, D. J. *J. Org. Chem.* **1986**, *51*, 4327-4337.
- (25) Cram, D. J. *Angew. Chem. Int. Ed. Eng.* **1986**, *25*, 1039-1057.
- (26) Jonathan W Steed, J. L. A. *Supramolecular Chemistry*; John Wiley & Sons, Ltd, 2000.
- (27) Cabbiness, D. K.; Margerum, D. W. *J. Am. Chem. Soc.* **1969**, *91*, 6540-6541.
- (28) Liu, Y.; Flood, A. H.; Bonvallett, P. A.; Vignon, S. A.; Northrop, B. H.; Tseng, H. R.; Jeppesen, J. O.; Huang, T. J.; Brough, B.; Baller, M.; Magonov, S.; Solares, S. D.; Goddard, W. A.; Ho, C. M.; Stoddart, J. F. *J. Am. Chem. Soc.* **2005**, *127*, 9745-9759.
- (29) Beer, P. D.; Gale, P. A. *Angew. Chem. Int. Ed.* **2001**, *40*, 486-516.
- (30) Yagai, S.; Kinoshita, T.; Higashi, M.; Kishikawa, K.; Nakanishi, T.; Karatsu, T.; Kitamura, A. *J. Am. Chem. Soc.* **2007**, *129*, 13277-13287.
- (31) Pieters, R. J.; Huc, I.; Rebek, J. *Tetrahedron* **1995**, *51*, 485-498.
- (32) Taylor, M. S.; Jacobsen, E. N. *Angew. Chem. Int. Ed.* **2006**, *45*, 1520-1543.
- (33) Vachal, P.; Jacobsen, E. N. *J. Am. Chem. Soc.* **2002**, *124*, 10012-10014.
- (34) Gale, P. A.; Twyman, L. J.; Handlin, C. I.; Sessler, J. L. *Chem. Commun.* **1999**, 1851-1852.

- (35) Patrick, G. L. *An introduction to Medicinal chemistry*; Second edition ed.; Oxford University Press: Oxford, 2002.
- (36) Lehn, J. M. *Pure and Appl. Chem.* **1979**, *51*, 979-997.
- (37) Santacroce, P. V.; Davis, J. T.; Light, M. E.; Gale, P. A.; Iglesias-Sanchez, J. C.; Prados, P.; Quesada, R. *J. Am. Chem. Soc.* **2007**, *129*, 1886-+.
- (38) Fuhrhop, J. H.; Liman, U. *J. Am. Chem. Soc.* **1984**, *106*, 4643-4644.
- (39) Hanan, G. S.; Arana, C. R.; Lehn, J. M.; Fenske, D. *Angew. Chem. Int. Ed. Engl.* **1995**, *34*, 1122-1124.
- (40) Potts, K. T.; Raiford, K. A. G.; Keshavarz, M. *J. Am. Chem. Soc.* **1993**, *115*, 2793-2807.
- (41) Jean-Marie Lehn, M. M., Andre DeCianb, Jean Fischer *JCS Perkin Trans. 2* **1992**, 461-467.
- (42) Joachim Garric, J.-M. L., Ivan Huc *Angew. Chem. Int. Ed.* **2005**, 1954-1959.
- (43) Schalley, C. A.; Weilandt, T.; Bruggemann, J.; Vogtle, F. *Templates in Chemistry I* **2004**, *248*, 141-200.
- (44) Lukin, O.; Vogtle, F. *Ang. Chem. Int. Ed.* **2005**, *44*, 1456-1477.
- (45) Davis, A. P.; Sheppard, D. N.; Smith, B. D. *Chem. Soc. Rev.* **2007**, *36*, 348-357.
- (46) Gale, P. A. *Acc. Chem. Res.* **2006**, *39*, 465-475.
- (47) Sessler, J. L.; Gale, P. A.; Cho, W.-S.; Sessler, J. L.; Gale, P. A.; Cho, W. S. *Monographs in Supramolecular Chemistry* **2006**.
- (48) Gale, P. A.; Garcia-Garrido, S. E.; Garric, J. *Chem. Soc. Rev.* **2008**, *37*, 151-190.
- (49) Gale, P. A.; Quesada, R. *Coord. Chem. Rev.* **2006**, *250*, 3219-3244.
- (50) Bates, G. W.; Gale, P. A. *Structure and Bonding* **2008**, in press.
- (51) Bondy, C. R.; Loeb, S. J. *Coord. Chem. Rev.* **2003**, *240*, 77-99.
- (52) Kang, S. O.; Begum, R. A.; Bowman-James, K. *Angew. Chem. Intern. Ed.* **2006**, *45*, 7882-7894.
- (53) Choi, K. H.; Hamilton, A. D. *J. Am. Chem. Soc.* **2001**, *123*, 2456-2457.
- (54) Chmielewski, M. J.; Jurczak, J. *Chem. Eur. J.* **2005**, *11*, 6080-6094.
- (55) Hunter, C. A.; Purvis, D. H. *Angew. Chem. Int. Ed. Engl.* **1992**, *31*, 792-795.
- (56) Kyne, G. M.; Light, M. E.; Hursthouse, M. B.; de Mendoza, J.; Kilburn, J. D. *JCS-Perkin Trans. 1* **2001**, 1258-1263.
- (57) Brooks, S. L.; Garcia-Garrido, S. E.; Light, M. E.; Cole, P. A.; Gale, P. A. *Chem. Eur. J.* **2007**, *13*, 3320-3329.
- (58) Kang, S. O.; Llinares, J. M.; Powell, D.; VanderVelde, D.; Bowman-James, K. *J. Am. Chem. Soc.* **2003**, *125*, 10152-10153.
- (59) Shionoya, M.; Furuta, H.; Lynch, V.; Harriman, A.; Sessler, J. L. *J. Am. Chem. Soc.* **1992**, *114*, 5714-5722.
- (60) Fitzmaurice, R. J.; Kyne, G. M.; Douheret, D.; Kilburn, J. D. *JCS-Perkin Trans. 1* **2002**, 841-864.
- (61) Brooks, S. J.; Edwards, P. R.; Gale, P. A.; Light, M. E. *New J. Chem.* **2006**, *30*, 65-70.
- (62) Rashdan, S.; Light, M. E.; Kilburn, J. D. *Chem. Commun.* **2006**, 4578-4580.
- (63) Park, C. H.; Simmons, H. E. *J. Am. Chem. Soc.* **1968**, *90*, 2431-2432.
- (64) Frontera, A.; Morey, J.; Oliver, A.; Pina, M. N.; Quinonero, D.; Costa, A.; Ballester, P.; Deya, P. M.; Anslyn, E. V. *J. Org. Chem.* **2006**, *71*, 7185-7195.
- (65) Blondeau, P.; Benet-Buchholz, J.; de Mendoza, J. *New J. Chem.* **2007**, *31*, 736-740.
- (66) Sessler, J. L.; Camiolo, S.; Gale, P. A. *Coord. Chem. Rev.* **2003**, *240*, 17-55.
- (67) Coles, S. J.; Gale, P. A.; Hursthouse, M. B. *Crystengcomm* **2001**, art. no.-53.
- (68) Sessler, J. L.; Cyr, M. J.; Lynch, V.; McGhee, E.; Ibers, J. A. *J. Am. Chem. Soc.* **1990**, *112*, 2810-2813.
- (69) Springs, S. L.; Gosztola, D.; Wasielewski, M. R.; Kral, V.; Andrievsky, A.; Sessler, J. L. *J. Am. Chem. Soc.* **1999**, *121*, 2281-2289.
- (70) Gale, P. A.; Sessler, J. L.; Kral, V.; Lynch, V. *J. Am. Chem. Soc.* **1996**, *118*, 5140-5141.
- (71) Custelcean, R.; Delmau, L. H.; Moyer, B. A.; Sessler, J. L.; Cho, W. S.; Gross, D.; Bates, G. W.; Brooks, S. J.; Light, M. E.; Gale, P. A. *Angew. Chem. Int. Ed.* **2005**, *44*, 2537-2542.
- (72) Cafeo, G.; Kohnke, F. H.; La Torre, G. L.; White, A. J. P.; Williams, D. J. *Angew. Chem. Int. Edition* **2000**, *39*, 1496-+.

- (73) Cafeo, G.; Kohnke, F. H.; La Torre, G. L.; Parisi, M. F.; Nascone, R. P.; White, A. J. P.; Williams, D. J. *Chem. Eur. J.* **2002**, 8, 3148-3156.
- (74) Gale, P. A.; Sessler, J. L.; Kral, V. *Chem. Commun.* **1998**, 1-8.
- (75) Cafeo, G.; White, P.; Garozzo, D.; Messina, A. *Chem. Eur. J.* **2007**, 649-656.
- (76) Schmuck, C. *Chem. Eur. J.* **2000**, 6, 709-718.
- (77) Gale, P. A.; Camiolo, S.; Tizzard, G. J.; Chapman, C. P.; Light, M. E.; Coles, S. J.; Hursthouse, M. B. *J. Org. Chem.* **2001**, 66, 7849-7853.
- (78) Camiolo, S.; Gale, P. A.; Hursthouse, M. B.; Light, M. E. *Tet. Lett.* **2002**, 43, 6995-6996.
- (79) Camiolo, S.; Gale, P. A.; Hursthouse, M. B.; Light, M. E. *Org. Biomol. Chem.* **2003**, 1, 741-744.
- (80) Camiolo, S.; Gale, P. A.; Hursthouse, M. B.; Light, M. E.; Shi, A. J. *Chem. Commun.* **2002**, 758-759.
- (81) Gale, P. A.; Navakhun, K.; Camiolo, S.; Light, M. E.; Hursthouse, M. B. *J. Am. Chem. Soc.* **2002**, 124, 11228-11229.
- (82) Denuault, G.; Gale, P. A.; Hursthouse, M. B.; Light, M. E.; Warriner, C. N. *New Journal of Chemistry* **2002**, 26, 811-813.
- (83) Joseph M. Mahoney, R. A. M., Alicia M. Beatty, Bradley D. Smith, Salvatore Camiolo, Philip A. Gale. *J. Supramol. Chem.* **2001**, 289-292.
- (84) Sessler, J. L.; Pantos, G. D.; Gale, P. A.; Light, M. E. *Org. Lett.* **2006**, 8, 1593-1596.
- (85) Zielinski, T.; Jurczak, J. *Tetrahedron* **2005**, 61, 4081-4089.
- (86) Bates, G. W.; Triyanti; Light, M. E.; Albrecht, M.; Gale, P. A. *J. Org. Chem.* **2007**, 72, 8921-8927.
- (87) Ji-Yeon Lee, M.-H. L., Kyu-Sung Jeong *Supramolecular Chemistry* **2007**, 257-263.
- (88) Sessler, J. L.; Cho, D. G.; Lynch, V. J. *Am. Chem. Soc.* **2006**, 128, 16518-16519.
- (89) Chmielewski, M. J.; Charon, M.; Jurczak, J. *Org. Lett.* **2004**, 6, 3501-3504.
- (90) Buhlmann, P.; Nishizawa, S.; Xiao, K. P.; Umezawa, Y. *Tetrahedron* **1997**, 53, 1647-1654.
- (91) Piatek, P.; Lynch, V. M.; Sessler, J. L. *J. Am. Chem. Soc.* **2004**, 126, 16073-16076.
- (92) Kang, J.; Kim, H. S.; Jang, D. O. *Tet. Lett.* **2005**, 46, 6079-6082.
- (93) Moon, K. S.; Singh, N.; Lee, G. W.; Jang, D. O. *Tetrahedron* **2007**, 63, 9106-9111.
- (94) Duval, R.; Leveque, H.; Prigent, Y.; Aboul-Enein, H. Y. *Biomedical Chromatography* **2001**, 15, 202-206.
- (95) Stibor, I.; Zlatuskova, P. *Anion Sensing* **2005**, 255, 31-63.
- (96) Pirkle, W. H.; Pochapsky, T. C. *Chem. Rev.* **1989**, 89, 347-362.
- (97) Hembury, G. A.; Borovkov, V. V.; Inoue, Y. *Chem. Rev.* **2008**, 108, 1-73.
- (98) Gasparrini, F.; Misiti, D.; Pierini, M.; Villani, C. *Org. Lett.* **2002**, 4, 3993-3996.
- (99) Breccia, P.; Van Gool, M.; Perez-Fernandez, R.; Martin-Santamaria, S.; Gago, F.; Prados, P.; de Mendoza, J. C. *J. Am. Chem. Soc.* **2003**, 125, 8270-8284.
- (100) Qing, G. Y.; He, Y. B.; Wang, F.; Qin, H. J.; Hu, C. G.; Yang, X. *European J. Org. Chem.* **2007**, 1768-1778.
- (101) Kitae, T.; Nakayama, T.; Kano, K. *J C S Perkin Trans. 2* **1998**, 207-212.
- (102) Lara, K. O.; Godoy-Alcantar, C.; Eliseev, A. V.; Yatsimirsky, A. K. *Org. Biomol. Chem.* **2004**, 2, 1712-1718.
- (103) Alfonso, I.; Dietrich, B.; Rebolledo, F.; Gotor, V.; Lehn, J. M. *Helv. Chim. Acta* **2001**, 84, 280-295.
- (104) Muller, G.; Riede, J.; Schmidtchen, F. P. *Angew. Chem. Int. Ed. Eng.* **1988**, 27, 1516-1518.
- (105) Lawless, L. J.; Blackburn, A. G.; Ayling, A. J.; Perez-Payan, M. N.; Davis, A. P. *JCS Perkin Trans. 1* **2001**, 1329-1341.
- (106) Graham M. Kyne, M. E. L., Mike B. Hursthouse, Javier de Mendoza, Jeremy D. Kilburn. *J. Chem. Soc., Perkin Trans. 1* **2001**, 1258-1263.
- (107) Rossi, S.; Kyne, G. M.; Turner, D. L.; Wells, N. J.; Kilburn, J. D. *Angew. Chem. Int. Ed.* **2002**, 41, 4233-4236.
- (108) Schmuck, C. *Chem. Eur. J.* **2000**, 6, 1279-1279.
- (109) Louie, G. V.; Brownlie, P. D.; Lambert, R.; Cooper, J. B.; Blundell, T. L.; Wood, S. P.; Warren, M. J.; Woodcock, S. C.; Jordan, P. M. *Nature* **1992**, 359, 33-39.

- (110) Vega, I. E.; Camiolo, S.; Gale, P. A.; Hursthouse, M. B.; Light, M. E. *Chem. Commun.* **2003**, 1686-1687.
- (111) Katayev, E. A.; Sessler, J. L.; Khrustalev, V. N.; Ustynyuk, Y. A. *J. Org. Chem.* **2007**, 72, 7244-7252.
- (112) Vega, I. E.; Gale, P. A.; Hursthouse, M. B.; Light, M. E. *Org. Biomol. Chem.* **2004**, 2, 2935-2941.
- (113) Lemay, M.; Aumand, L.; Ogilvie, W. W. *Advanced Synthesis & Catalysis* **2007**, 349, 441-447.
- (114) Xie, M. Q.; Lightner, D. A. *Tetrahedron* **1993**, 49, 2185-2200.
- (115) Kleinspehn, G. G. *J. Am. Chem. Soc.* **1955**, 77, 1546-1548.
- (116) *Name Reaction in Heterocyclic Chemistry*; John Wiley and Sons: Hoboken, New jersey, 2005.
- (117) Byun, Y. S.; Lightner, D. A. *J. Org. Chem.* **1991**, 56, 6027-6033.
- (118) Boev, N. V.; Ustynyuk, Y. A. *Russian J. Org. Chem.* **2007**, 43, 297-304.
- (119) Omote, M.; Ando, A.; Takagi, T.; Koyama, M.; Kumadaki, I. *Tetrahedron* **1996**, 52, 13961-13970.
- (120) Chang, K. H.; Liao, J. H.; Chen, C. T.; Mehta, B. K.; Chou, P. T.; Fang, J. M. *J. Org. Chem.* **2005**, 70, 2026-2032.
- (121) Barton, D. H. R.; Kervagoret, J.; Zard, S. Z. *Tetrahedron* **1990**, 46, 7587-7598.
- (122) Gellman, S. H.; Dado, G. P.; Liang, G. B.; Adams, B. R. *J. Am. Chem. Soc.* **1991**, 113, 1164-1173.
- (123) Boger, D. L.; Miyazaki, S.; Kim, S. H.; Wu, J. H.; Castle, S. L.; Loiseleur, O.; Jin, Q. *J. Am. Chem. Soc.* **1999**, 121, 10004-10011.
- (124) Luly, J. R.; Dellaria, J. F.; Plattner, J. J.; Soderquist, J. L.; Yi, N. *J. Org. Chem.* **1987**, 52, 1487-1492.
- (125) Coste, J.; Lenguyen, D.; Castro, B. *Tet. Lett.* **1990**, 31, 205-208.
- (126) Vanoijen, A. H.; Huck, N. P. M.; Kruijtzter, J. A. W.; Erkelens, C.; Vanboom, J. H.; Liskamp, R. M. J. *J. Org. Chem.* **1994**, 59, 2399-2408.
- (127) Baldwin, J. E.; Freeman, R. T.; Schofield, C. *Tet. Lett.* **1989**, 30, 4019-4020.
- (128) Anderson, G. W.; Zimmerman, J. E.; Callahan, F. M. *J. Am. Chem. Soc.* **1963**, 85, 3039-3039.
- (129) Schmidt, U.; Zah, M.; Lieberknecht, A. *J C S Chem. Commun.* **1991**, 1002-1004.
- (130) Pernia, G. J.; Kilburn, J. D.; Essex, J. W.; MortishireSmith, R. J.; Rowley, M. *J. Am. Chem. Soc.* **1996**, 118, 10220-10227.
- (131) Heffner, R. J.; Jiang, J. J.; Joullie, M. M. *J. Am. Chem. Soc.* **1992**, 114, 10181-10189.
- (132) Paul, R.; Anderson, G. W. *J. Am. Chem. Soc.* **1960**, 82, 4596-4600.
- (133) Kataoka, H.; Katagi, T. *Tetrahedron* **1987**, 43, 4519-4530.
- (134) Ye, T.; McKervey, M. A. *Tetrahedron* **1992**, 48, 8007-8022.
- (135) Ward, D. E.; Rhee, C. K. *Tet. Lett.* **1991**, 32, 7165-7166.
- (136) Devos, A.; Remion, J.; Frisquehesbain, A. M.; Colens, A.; Ghosez, L. *J. C.S. Chem. Commun.* **1979**, 1180-1181.
- (137) Enev, V. S.; Drescher, M.; Mulzer, J. *Tetrahedron* **2007**, 63, 5930-5939.
- (138) Wolf, C.; Francis, C. J.; Hawes, P. A.; Shah, M. *Tetrahedron-Asymmetry* **2002**, 13, 1733-1741.
- (139) Hulme, A. N.; Rosser, E. M. *Org. Lett.* **2002**, 4, 265-267.
- (140) Bisson, A. P.; Hunter, C. A.; Morales, J. C.; Young, K. *Chem. Eur. J.* **1998**, 4, 845-851.
- (141) Fielding, L. *Tetrahedron* **2000**, 56, 6151-6170.
- (142) Connors, K. A. *Binding Constants*; John Wiley & sons: New York, 1987.
- (143) Quinonero, D.; Garau, C.; Rotger, C.; Frontera, A.; Ballester, P.; Costa, A.; Deya, P. M. *Angew. Chem. Int. Ed.* **2002**, 41, 3389-3392.
- (144) Schottel, B. L.; Chifotides, H. T.; Dunbar, K. R. *Chem. Soc. Rev.* **2008**, 37, 68-83.
- (145) Berryman, O. B.; Hof, F.; Hynes, M. J.; Johnson, D. W. *Chem. Commun.* **2006**, 506-508.
- (146) Bryantsev, V. S.; Hay, B. P. *J. Am. Chem. Soc.* **2005**, 127, 8282-8283.
- (147) Schneider, H.; Vogelhuber, K. M.; Schinle, F.; Weber, J. M. *J. Am. Chem. Soc.* **2007**, 129, 13022-13026.

- (148) Berryman, O. B.; Bryantsev, V. S.; Stay, D. P.; Johnson, D. W.; Hay, B. P. *J. Am. Chem. Soc.* **2007**, *129*, 48-58.
- (149) Mammoliti, O. PhD Thesis, University of Southampton, 2007.
- (150) James Dowden; Peter D. Edwards; Stephen S. Flack; Kilburn, J. D. *Chem. Eur. J.* **1999**, *5*, 79-89.
- (151) Illuminati, G.; Mandolini, L.; Masci, B. *J. Am. Chem. Soc.* **1983**, *105*, 555-563.
- (152) Vilar, R. *Angew. Chem. Int. Ed.* **2003**, *42*, 1460-1477.
- (153) Katayev, E. A.; Boev, N. V.; Khrustalev, V. N.; Ustynyuk, Y. A.; Tananaev, I. G.; Sessler, J. L. *J. Org. Chem.* **2007**, *72*, 2886-2896.
- (154) Wilcox, C. S.; Cowart, M. D. *Tet. Lett.* **1986**, *27*, 5563-5566.
- (155) Fielding, L. *Tetrahedron* **2000**, *56*, 6151.
- (156) Hynes, M. J. *J.C. Society-Dalton Transactions* **1993**, 311-312.
- (157) Chen, Q.; Wang, T.; Zhang, Y.; Wang, Q.; Jinshi *Synthetic Communications* **2002**, *32*, 1031 - 1040.
- (158) Xie, M. Q.; Holmes, D. L.; Lightner, D. A. *Tetrahedron* **1993**, *49*, 9235-9250.
- (159) Zindel, J.; Lightner, D. A. *Journal of Heterocyclic Chemistry* **1995**, *32*, 1219-1223.
- (160) Dyatkin, A. B.; Gong, Y.; Miskowski, T. A.; Kimball, E. S.; Prouty, S. M.; Fisher, M. C.; Santulli, R. J.; Schneider, C. R.; Wallace, N. H.; Hornby, P. J.; Diamond, C.; Kinney, W. A.; Maryanoff, B. E.; Damiano, B. P.; He, W. *Bioorganic & Medicinal Chemistry* **2005**, *13*, 6693-6702.
- (161) Jackson, R. F. W.; Turner, D.; Block, M. H. *Journal of the Chemical Society-Perkin Transactions I* **1997**, 865-870.
- (162) Hulme, A. N.; Rosser, E. M. *Org. Lett.* **2002**, *4*, 265-267.
- (163) Jurczak, J.; Gryko, D.; Kobrzycka, E.; Gruza, H.; Prokopowicz, P. *Tetrahedron* **1998**, *54*, 6051-6064.
- (164) Cai, W.; Kwock, S. W.; P.Taulane, J.; Goodman, M. *Journal of American Chemical Society* **2004**, *126*, 15030-15031.
- (165) Millet, R.; Urig, S.; Jacob, J.; Amtmann, E.; Moulinoux, J. P.; Gromer, S.; Becker, K.; Davioud-Charvet, E. *Journal of Medicinal Chemistry* **2005**, *48*, 7024-7039.
- (166) Barker, P. L.; Gendler, P. L.; Rapoport, H. *Journal of Organic Chemistry* **1981**, *46*, 2455-2465.